



A National Center of Excellence in Advanced Technology Applications

ISSN 1520-295X

Response Modification Factors for Seismically Isolated Bridges

by

Michael C. Constantinou and Joseph K. Quarshie
University at Buffalo, State University of New York
Department of Civil, Structural and Environmental Engineering
Ketter Hall
Buffalo, New York 14260

Technical Report MCEER-98-0014

November 3, 1998

This research was conducted at the University at Buffalo, State University of New York and was supported by the Federal Highway Administration under contract number DTFH61-92-C-00106.

NOTICE

This report was prepared by the University at Buffalo, State University of New York as a result of research sponsored by the Multidisciplinary Center for Earthquake Engineering Research (MCEER) through a contract from the Federal Highway Administration. Neither MCEER, associates of MCEER, its sponsors, the University at Buffalo, State University of New York, nor any person acting on their behalf:

- a. makes any warranty, express or implied, with respect to the use of any information, apparatus, method, or process disclosed in this report or that such use may not infringe upon privately owned rights; or
- b. assumes any liabilities of whatsoever kind with respect to the use of, or the damage resulting from the use of, any information, apparatus, method, or process disclosed in this report.

Any opinions, findings, and conclusions or recommendations expressed in this publication are those of the author(s) and do not necessarily reflect the views of MCEER or the Federal Highway Administration.

Response Modification Factors for Seismically Isolated Bridges

by

Michael C. Constantinou¹ and Joseph K. Quarshie²

Publication Date: November 3, 1998

Submittal Date: July 9, 1998

Technical Report MCEER-98-0014

Task Number 106-F-4.2.3

FHWA Contract Number DTFH61-92-C-00106

- 1 Professor, Department of Civil, Structural and Environmental Engineering, University at Buffalo, State University of New York
- 2 Engineer, Thornton-Tomasetti Engineers, N.J.; former Graduate Research Assistant, Department of Civil, Structural and Environmental Engineering, University at Buffalo, State University of New York

MULTIDISCIPLINARY CENTER FOR EARTHQUAKE ENGINEERING RESEARCH
University at Buffalo, State University of New York
Red Jacket Quadrangle, Buffalo, NY 14261

Preface

The Multidisciplinary Center for Earthquake Engineering Research (MCEER) is a national center of excellence in advanced technology applications that is dedicated to the reduction of earthquake losses nationwide. Headquartered at the University at Buffalo, State University of New York, the Center was originally established by the National Science Foundation in 1986, as the National Center for Earthquake Engineering Research (NCEER).

Comprising a consortium of researchers from numerous disciplines and institutions throughout the United States, the Center's mission is to reduce earthquake losses through research and the application of advanced technologies that improve engineering, pre-earthquake planning and post-earthquake recovery strategies. Toward this end, the Center coordinates a nationwide program of multidisciplinary team research, education and outreach activities.

MCEER's research is conducted under the sponsorship of two major federal agencies, the National Science Foundation (NSF) and the Federal Highway Administration (FHWA), and the State of New York. Significant support is also derived from the Federal Emergency Management Agency (FEMA), other state governments, academic institutions, foreign governments and private industry.

The Center's FHWA-sponsored Highway Project develops retrofit and evaluation methodologies for existing bridges and other highway structures (including tunnels, retaining structures, slopes, culverts, and pavements), and improved seismic design criteria and procedures for bridges and other highway structures. Specifically, tasks are being conducted to:

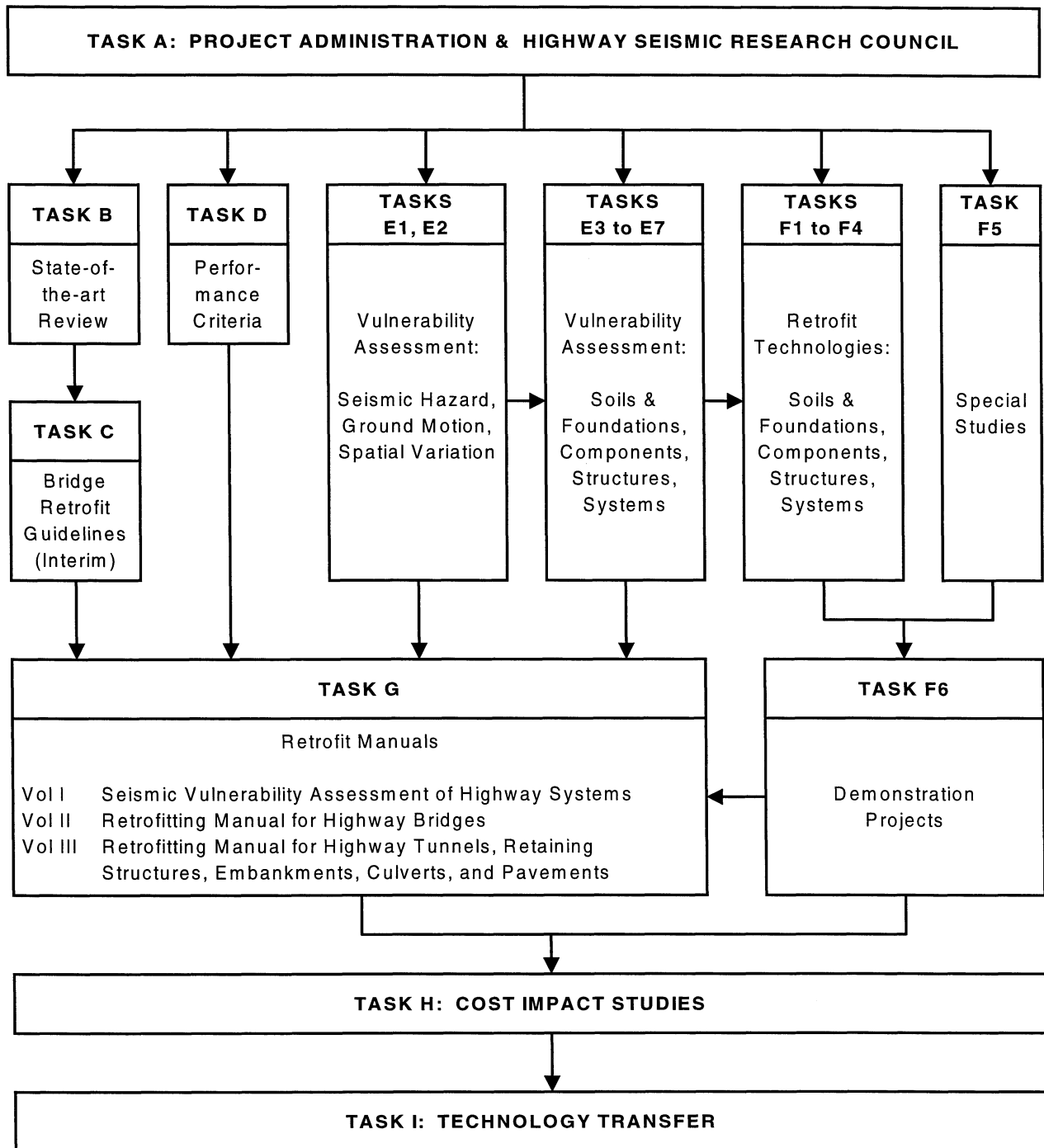
- assess the vulnerability of highway systems, structures and components;
- develop concepts for retrofitting vulnerable highway structures and components;
- develop improved design and analysis methodologies for bridges, tunnels, and retaining structures, which include consideration of soil-structure interaction mechanisms and their influence on structural response;
- review and recommend improved seismic design and performance criteria for new highway systems and structures.

Highway Project research focuses on two distinct areas: the development of improved design criteria and philosophies for new or future highway construction, and the development of improved analysis and retrofitting methodologies for existing highway systems and structures. The research discussed in this report is a result of work conducted under the existing highway structures project, and was performed within Task 106-F-4.2.3, "R-Factors for Isolated Bridges" of that project as shown in the flowchart on the following page.

The overall objective of this task was to provide the basis for selecting and validating appropriate response modification factors (R-factors) for seismically isolated bridges. This report investigates the rationale for the lower R-factors that have been specified for seismically isolated bridges in the 1997 AASHTO "Guide Specifications for Seismic Isolation Design." Dynamic analyses were conducted on a number of simple models of both seismically isolated and non-

isolated bridges for a range of isolation system types, properties and substructure behaviors. Based on the results from these studies, the authors concluded that R-factors for the substructures of seismically isolated bridges should be in the range of 1.5 to 2.5. These recommended values are similar to those presented in the 1997 AASHTO Guide Specifications.

SEISMIC VULNERABILITY OF EXISTING HIGHWAY CONSTRUCTION
FHWA Contract DTFH61-92-C-00106



ABSTRACT

The 1997 AASHTO "Guide Specifications for Seismic Isolation Design" specify response modification factors for the substructures of isolated bridges that are lower than those specified for the substructures of non-isolated bridges. This report presents the rationale behind these specifications and presents research results that lead to the establishment of appropriate response modification factors for isolated bridges.

The research concentrated on the dynamic analysis of simple models of seismic-isolated and non-isolated bridges for a range of isolation system and substructure behaviors, and for seismic excitation characterized by AASHTO ground motion spectra for a range of soil conditions and acceleration coefficients. The study investigated the displacement ductility demand in the substructure of these bridges and established the appropriate value of the ductility-based portion of the response modification factors. This was achieved by comparing the displacement ductility ratio for the substructures of isolated and non-isolated bridges.

The study concludes that response modification factors should be lower in the substructures of isolated bridges than in the substructures of non-isolated bridges because: (a) elastic or nearly elastic substructure behavior is required for proper behavior of the isolation system, and (b) isolated bridges exhibit more sensitivity in the substructure inelastic response due to variability in the seismic input.

ACKNOWLEDGEMENTS

Financial support for this project has been provided by the National Center for Earthquake Engineering Research under Highway Project Task 106-F-4.2.3. The idea for this project originated at the AASHTO T-3 Task Group meetings during the writing of the 1997 AASHTO "Guide Specifications for Seismic Isolation Design."

TABLE OF CONTENTS

SECTION	TITLE	PAGE
1.	INTRODUCTION	1
2.	RESPONSE-MODIFICATION FACTORS FOR SEISMIC-ISOLATED BRIDGES	13
2.1	Response-Modification Factor	13
2.2	Determination of Components of R-Factor	15
2.3	Specified Values of R-Factor	17
2.4	R-Factors for Seismic-Isolated Bridges	18
2.5	Underlying Reasons for Lower R-Factors in Isolated Bridges	20
2.6	Objectives of this Study	28
3.	APPROACH FOR ESTABLISHING THE DUCTILITY-BASED PORTIONS OF THE R-FACTOR FOR SUBSTRUCTURE OF SEISMIC ISOLATED BRIDGES	33
3.1	General Description of Approach	33
3.2	Studied System	35
3.3	Selection of Parameters for Pinched Pier Model	37
3.4	Selection and Scaling of Ground Motions	41
3.5	Application of Uniform Load Method for Analysis of Seismic-Isolated Bridges	46
3.5.1	Isolation System with Bilinear Hysteretic or Sliding Behavior	48
3.5.2	Isolation System with Linear Elastic, Linear Viscous Behavior	49
3.6	Model for Analysis of Non-Isolated Bridge	53
4.	RESULTS AND INTERPRETATION	55
4.1	Non-Isolated Bridge	55

TABLE OF CONTENTS (continued)

SECTION	TITLE	PAGE
4.2	Results for Seismic-Isolated Bridge Obtained by Uniform Load Method of AASHTO Guide Specifications	57
4.3	Results of Nonlinear Dynamic Analysis of Seismic-Isolated Bridge	61
4.4	Pier Displacement Ductility Ratio for Seismic-Isolated Bridges	65
4.5	Concluding Remarks	75
5.	OVERSTRENGTH AND RESPONSE MODIFICATION FACTORS	77
5.1	Introduction	77
5.2	Overstrength Factor of Non-Isolated Bridges	78
5.3	Overstrength Factor of Seismic-Isolated Bridges	81
5.4	Concluding Remarks	84
6.	CONCLUSIONS	87
7.	REFERENCES	91
APPENDIX A	Equations of motion of analyzed system	A-1
APPENDIX B	Data on Motions Used for Dynamic Analysis and Response Spectra of Scaled Components	B-1
APPENDIX C	Calculated Values of Pier Displacement Ductility ratio of non-isolated bridge	C-1

TABLE OF CONTENTS (continued)

APPENDIX D	Results of Analysis of Seismic-Isolated Bridge by the Uniform Load Method of the 1997 AASHTO Guide Specifications for Seismic Isolation Design	D-1
APPENDIX E	Results of Nonlinear Analysis of Seismic-Isolated Bridge with Perfect Bilinear Hysteretic Pier and Bilinear Hysteretic Isolation System for AASHTO, $A=0.4$, Soil Profile Type II Input	E-1
APPENDIX F	Results of Nonlinear Dynamic Analysis of Seismic-Isolated Bridge with Perfect Bilinear Hysteretic Pier and Sliding Isolation System for AASHTO, $A=0.4$, Soil Profile Type II Input	F-1
APPENDIX G	Results of Nonlinear Dynamic Analysis of Seismic-Isolated Bridge with Perfect Bilinear Hysteretic Pier and Linear Elastic/Viscous Isolation System for AASHTO, $A=0.4$, Soil Profile Type II Input	G-1
APPENDIX H	Results of Nonlinear Dynamic Analysis of Seismic-Isolated Bridge with Perfect Bilinear Hysteretic Pier and Bilinear Hysteretic Isolation System for AASHTO, $A=0.2$, Soil Profile Type II Input	H-1
APPENDIX I	Results of Nonlinear Dynamic Analysis of Seismic-Isolated Bridge with Perfect Bilinear Hysteretic Pier and Bilinear	

TABLE OF CONTENTS (continued)

	Hysteretic Isolation System for AASHTO, $A=0.4$, Soil Profile Type III Input	I-1
APPENDIX J	Results of Nonlinear Dynamic Analysis of Seismic-Isolated Bridge with Pinched Hysteretic Pier and Bilinear Hysteretic Isolation System for AASHTO, $A=0.4$, Soil Profile Type II Input	J-1

LIST OF ILLUSTRATIONS

FIGURE	TITLE	PAGE
1-1	Typical Lateral Force-Displacement Relation of Seismic Isolation Bearing	2
1-2	Pushover Curve of Non-Isolated Bridge and Calculation of Inelastic Response by Use of Design Demand Spectra and Nonlinear Static Analysis Procedures	4
1-3	Pushover Curves of Seismic-Isolated Bridge (note that isolation bearings are not used at the abutment locations so that redistribution of the inertia force is not considered).	6
1-4	Calculation of Inelastic Response of Seismic-Isolated Bridge by Use of Design Demand Spectra and Nonlinear Static Analysis Procedures	8
1-5	Effect of Redistribution of Inertia Force on Design Forces for Elements of the Substructure of Non-Isolated and Seismic-Isolated Bridges	9
2-1	Structural Response of Inelastic System	14
2-2	Behavior of Isolated Bridge with Elastoplastic Pier	21
2-3	Model of Isolated Bridge Used in Analysis	22
2-4	Calculated Response of Isolated Bridge Model With $T_p=0.1$ sec and $R_\mu=1.0$ (elastic pier)	24
2-5	Calculated Response of Isolated Bridge Model With $T_p=0.1$ sec and $R_\mu=2.0$	25
2-6	Calculated Response of Isolated Bridge Model With $T_p=0.5$ sec and $R_\mu=1.0$ (elastic pier)	26

LIST OF ILLUSTRATIONS (continued)

FIGURE	TITLE	PAGE
2-7	Calculated Response of Isolated Bridge Model With $T_p=0.5$ sec and $R_\mu=2.0$	27
2-8	Calculated Response of Isolated Bridge Model With $T_p=0.5$ sec and $R_\mu=4.0$	29
2-9	Analyzed System and Illustration of Utilized Force-Displacement Relations for Isolation System and Pier	34
3-2	Comparison of Experimental and Analytical Force-Displacement Loops of Reinforced Concrete Columns with Pinched Hysteretic Behavior	39
3-3	Calculated Pier Shear Force-Drift Loops of Isolated Bridge with Perfect Bilinear Hysteretic and with Pinched Hysteretic Behavior ($T_p=0.5$ sec, $T_b=2.0$ sec, $\nu=10$, $\delta=0.06$, $R_\mu=1.5$, Earthquake EQ20 per Appendix B)	42
3-4	Maximum, Average and Minimum Spectral Acceleration Values of Scaled Motions for AASHTO A=0.4, Soil Profile Type II Spectrum	44
3-5	Maximum, Average and Minimum Spectral Acceleration Values of Scaled Motions for AASHTO A=0.4, Soil Profile Type III Spectrum	47
3-6	Plot of Base Shear versus Drift Loop of Highly Damped Single-Degree-of-Freedom System Undergoing Harmonic Displacement of Frequency ω	52

LIST OF ILLUSTRATIONS (continued)

FIGURE	TITLE	PAGE
3-7	Model Used in Analysis of Non-Isolated Bridge	54
4-1	Average Pier Displacement Ductility Ratio of Non-Isolated Bridge	56
4-2	Variability in Pier Displacement Ductility Ratio of Non-Isolated Bridge for the Case of Bilinear Hysteretic Pier and Soil Profile Type II Input 4-4	58
4-3	Variability in Pier Displacement Ductility Ratio of Non-Isolated Bridge for the Case of Bilinear Hysteretic Pier and Soil Profile Type III Input	59
4-4	Variability in Pier Displacement Ductility Ratio of Non-Isolated Bridge for the case of Pinched Hysteretic Pier Behavior and $A=0.4$, Soil Profile Type II Input	60
4-5	Variability in Pier Displacement Ductility Ratio of Isolated Bridge for $A=0.4$, Soil Profile Type II Input and Bilinear Hysteretic Pier Behavior. Cases $\delta=0.06$, $\xi=0.2$	66
4-6	Variability in Pier Displacement Ductility Ratio of Isolated Bridge for $A=0.2$, Soil Profile Type II Input and Bilinear Hysteretic Pier Behavior. Cases $\delta=0.06$, $\xi=0.2$	67
4-7	Variability in Pier Displacement Ductility Ratio of Isolated Bridge for $A=0.4$, Soil Profile Type III Input and Bilinear Hysteretic Pier Behavior. Cases $\delta=0.06$, $\xi=0.2$	68

LIST OF ILLUSTRATIONS (continued)

FIGURE	TITLE	PAGE
4-8	Variability in Pier Displacement Ductility Ratio of Isolated Bridge for A=0.4, Soil Profile Type II Input and Bilinear Hysteretic Pier Behavior. Cases $\delta=0.10$, $\xi=0.3$	70
4-9	Variability in Pier Displacement Ductility Ratio of Isolated Bridge for A=0.4, Soil Profile Type III Input and Bilinear Hysteretic Pier Behavior. Cases $\delta=0.10$, $\xi=0.3$	71
4-10	Variability in Pier Displacement Ductility Ratio of Isolated Bridge for A=0.4, Soil Profile Type II Input and Pinched Hysteretic Pier Behavior. Cases $\delta=0.06$, $\xi=0.10$	72
5-1	Non-Isolated Bridge and Force-Displacement Relations in Longitudinal Direction for Rigid Superstructure	79
5-2	Seismic-Isolated Bridge and Force-Displacement Relations in Longitudinal Direction for Rigid Superstructure	82

LIST OF TABLES

TABLE	TITLE	PAGE
3-1	Parameters Describing the Analyzed System and Range of Values (see Fig. 3-1 and Appendix A)	38
3-2	Motions Used to Represent AASHTO, Soil Profile Type II, $A=0.4$ and 0.2 Spectra, and Scale Factors	43
3-3	Motions Used to Represent AASHTO, Soil Profile Type III, $A=0.4$ Spectra, and Scale Factors	46
4-1	Average Pier Displacement Ductility Ratio of Non-Isolated Bridge With $T=0.5$ sec	73
4-2	Average Pier Displacement Ductility Ratio of Non-Isolated Bridge With $T_p=0.25$ sec, $\nu=10$	74
5-1	Appropriate Values of R-factor for Substructures of Seismic-Isolated Bridges	85

SECTION 1

INTRODUCTION

Earthquakes cause significant loss of life and property damage. In an attempt to mitigate the effects of earthquakes, engineers have developed various aseismic construction techniques and technologies. Of these, seismic isolation has rapidly evolved in the last twenty years, has been extensively tested in the laboratory and, in a few cases so far, has successfully withstood the effects of strong earthquakes in the field.

The technology of seismic isolation is used to decouple a structure from the horizontal components of earthquake ground motion. It has been used in seismic protection of bridges, buildings and special structures, and equipment. In bridges, it involves the separation of the superstructure from the substructure, typically at the bent cap level. In most bridge applications, the primary intent is to protect the vulnerable substructure by reducing the inertia forces transmitted from the massive superstructure.

The decoupling of the bridge superstructure from the damaging components of earthquake motions is achieved by the use of seismic isolation bearings which are characterized by horizontal flexibility to reduce sufficiently the transmission of shear force and by energy dissipation capability to reduce the relative displacements across the isolation bearings to tolerate levels. A number of bridge seismic isolation design strategies have been developed. They may be grouped into three main categories: (a) the strategy championed by engineers in New Zealand and the United States which requires strong restoring force capability in the isolation system, (b) the Italian strategy in which the isolation system exhibits essentially elastoplastic behavior, and (c) the Japanese strategy, otherwise known as Menshin, in which seismic isolation bearings are used as

elements to enhance the energy dissipation capability of the bridge rather than to increase its flexibility.

Figure 1-1 illustrates a typical lateral force-displacement relation of a seismic

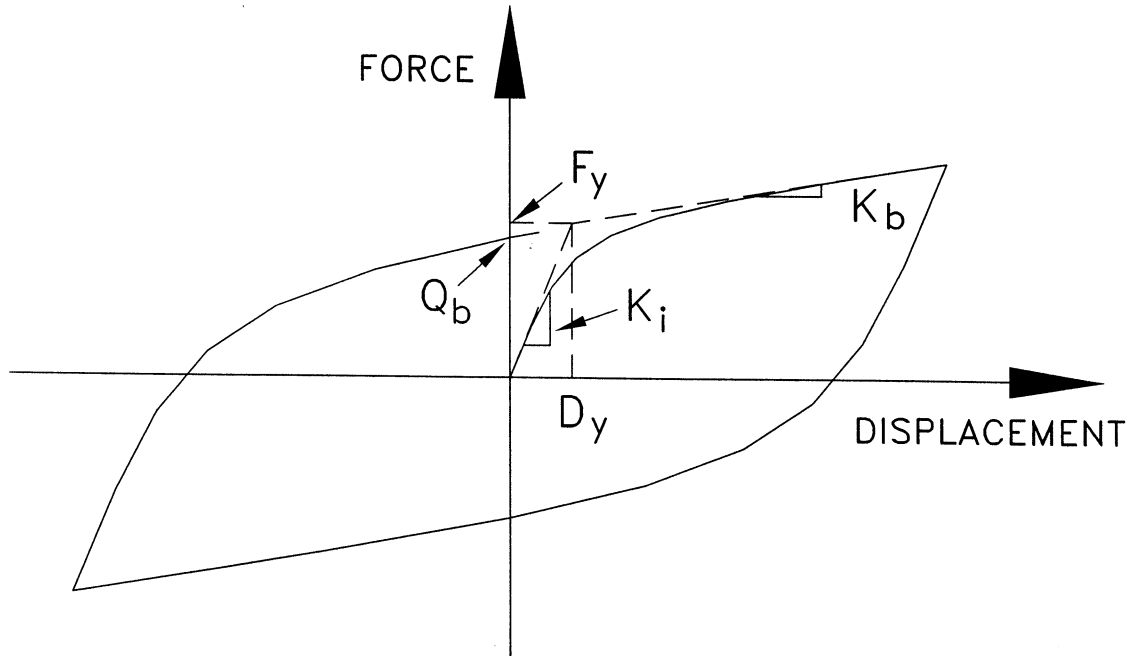


Figure 1-1 Typical Lateral Force-Displacement Relation of Seismic Isolation Bearing

isolation bearing. It is characterized by the strength (Q_b) and the post-yielding stiffness (K_b). In the strong restoring force approach favored in the United States, the post-yielding stiffness K_b is sufficiently large to reduce the uncertainty in the peak seismic displacement and to prevent the development of cumulative permanent displacements. By contrast, the use of a very low post-yielding stiffness, as favored in Italy, results in a bounded force transmitted by the bearing to the substructure for a wide range of bearing displacements. This desirable performance is achieved at the expense of uncertainty in the resulting maximum bearing displacements and the possibility of significant

permanent displacements. Regardless of the design strategy, seismic isolation can result in reduction of both the design force and damage in the bridge substructure.

The typical approach to demonstrating the effectiveness of seismic isolation is through the use of the response spectrum which very well illustrates the effects of increased flexibility and energy absorption capability. The interested reader is referred to Skinner et al. (1993), Kelly (1993), Soong and Constantinou (1994), and Constantinou et al. (1998a) for more general expositions of the technologies of seismic isolation and energy dissipation. However, in order to fully understand the benefits of bridge seismic isolation, it is best to consider the nonlinear behavior of the system. Such behavior is caused by yielding of the substructure (in non-isolated bridges) or by inelastic action in the isolation system (in isolated bridges). We choose to present an example, in which we utilize nonlinear static analysis procedures (or pushover analysis) and obtain the nonlinear response by comparing the pushover curve of the system to the design demand. This approach is termed Nonlinear Static Procedure Method 2 in Federal Emergency Management Agency (1997).

Figure 1-2 shows a simple representation of a two-span non-isolated bridge and its push-over curve. The seismic input is described by the AASHTO, $A=0.4$, soil profile type II response spectrum (American Association of State Highway and Transportation Officials, 1995). Shown also in the same figure are the design demand spectra for this seismic input. They are plots of the spectral acceleration (that is, acceleration at the instant of peak displacement) versus the spectral displacement (that is, peak displacement) of a viscously damped linear elastic system for a range of values of the damping ratio. These spectra were constructed from scaled ground motion histories to

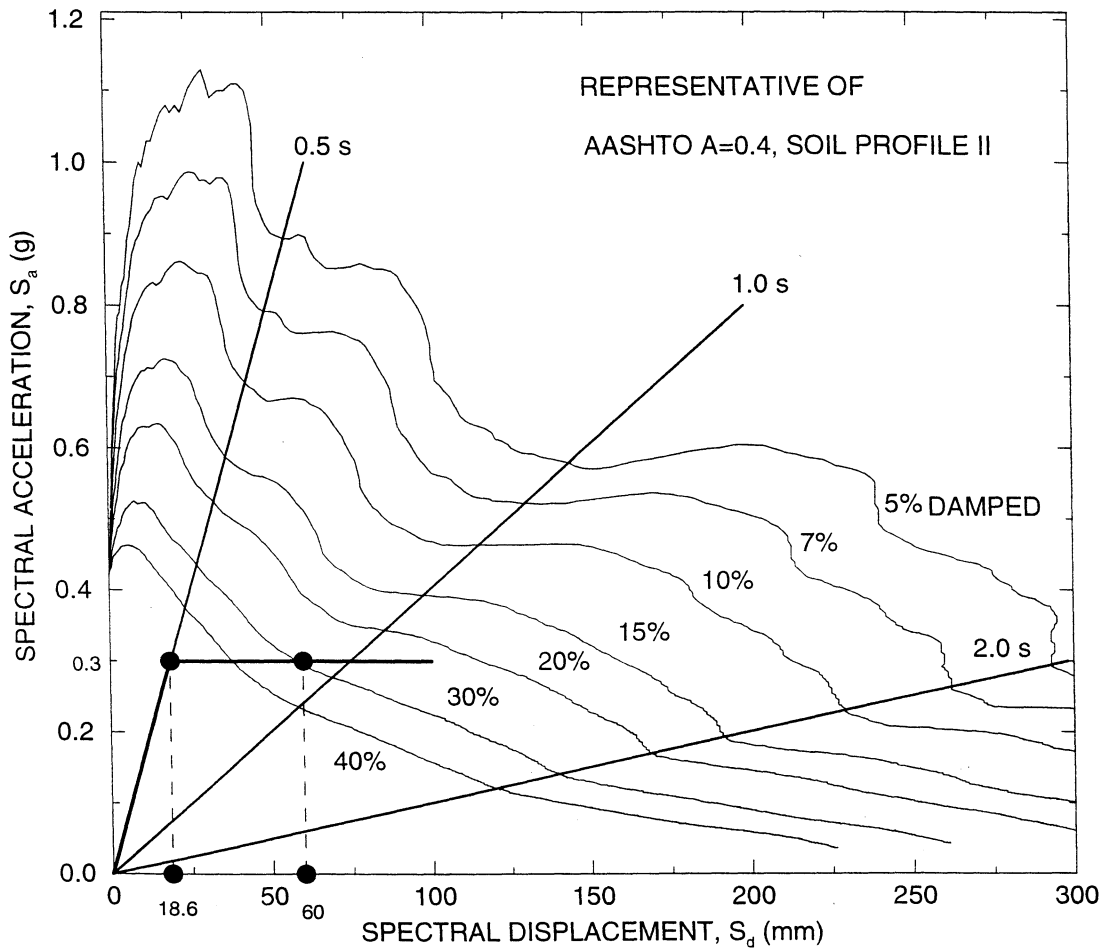
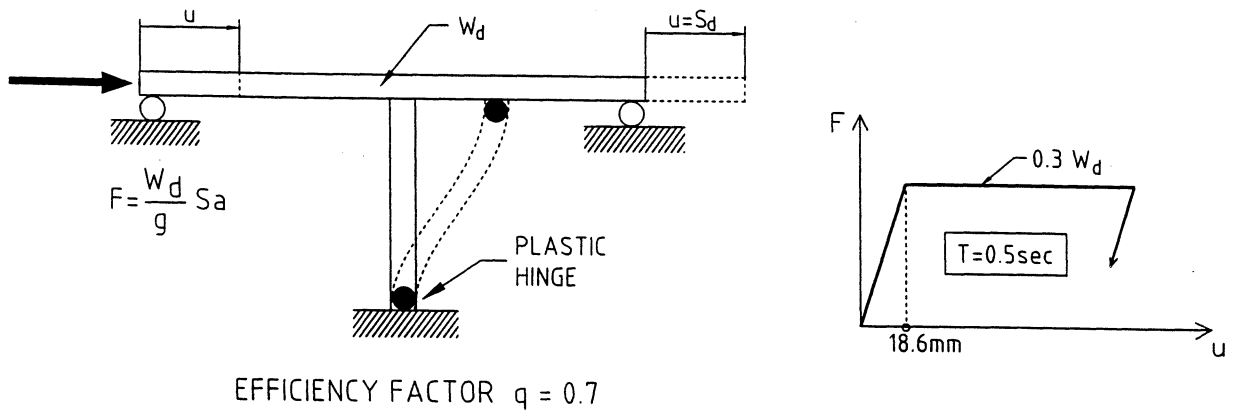


Figure 1-2 Pushover Curve of Non-Isolated Bridge and Calculation of Inelastic Response by Use of Design Demand Spectra and Nonlinear Static Analysis Procedures

represent, on the average, the applicable response spectrum. Details are provided in Section 3. Note that, in the demand spectra, straight lines radiating from the origin correspond to systems with the same period.

The non-isolated bridge has initial period $T=0.5$ sec and has been designed to have an actual strength of $0.3W_d$, where W_d =effective weight (or weight of deck in this case). This corresponds to a design with a ductility-based portion of the response modification factor $R_\mu=3.3$. In this case of a single-degree-of freedom representation of the structure, the spectral capacity curve (S_a vs. S_d) is identical to the normalized pushover curve (Fg/W_d vs. U). The intersection of this curve with the design demand spectrum at the appropriate level of effective damping determines the peak response. In this case the effective damping is determined on the assumption of elastoplastic behavior with imperfect hysteresis loop so that the area enclosed by the loop is 70-percent of that of the perfect loop (efficiency factor $q=0.7$ per Federal Emergency Management Agency, 1997). It is a case of good hysteretic behavior. The calculated response is $U=60$ mm with the effective damping being 30-percent and the effective period being 0.9 sec. The substructure (pier) displacement ductility ratio is $60/18.6 = 3.2$, which is consistent with the used R-factor. The substructure needs to be detailed for a force of $0.3W_d$ (which will much affect the design of the foundation) and for the calculated ductility of 3.2.

When seismically isolated, the bridge pier is designed to have an actual strength of $0.17W_d$ in order to avoid inelastic action in the substructure. Isolation bearings are placed only on top of the pier and not at the abutments. It is an atypical situation which is used herein to demonstrate the effect of isolation without the added benefit of redistribution of the inertia force. This subject is discussed later in this section. Figure 1-3

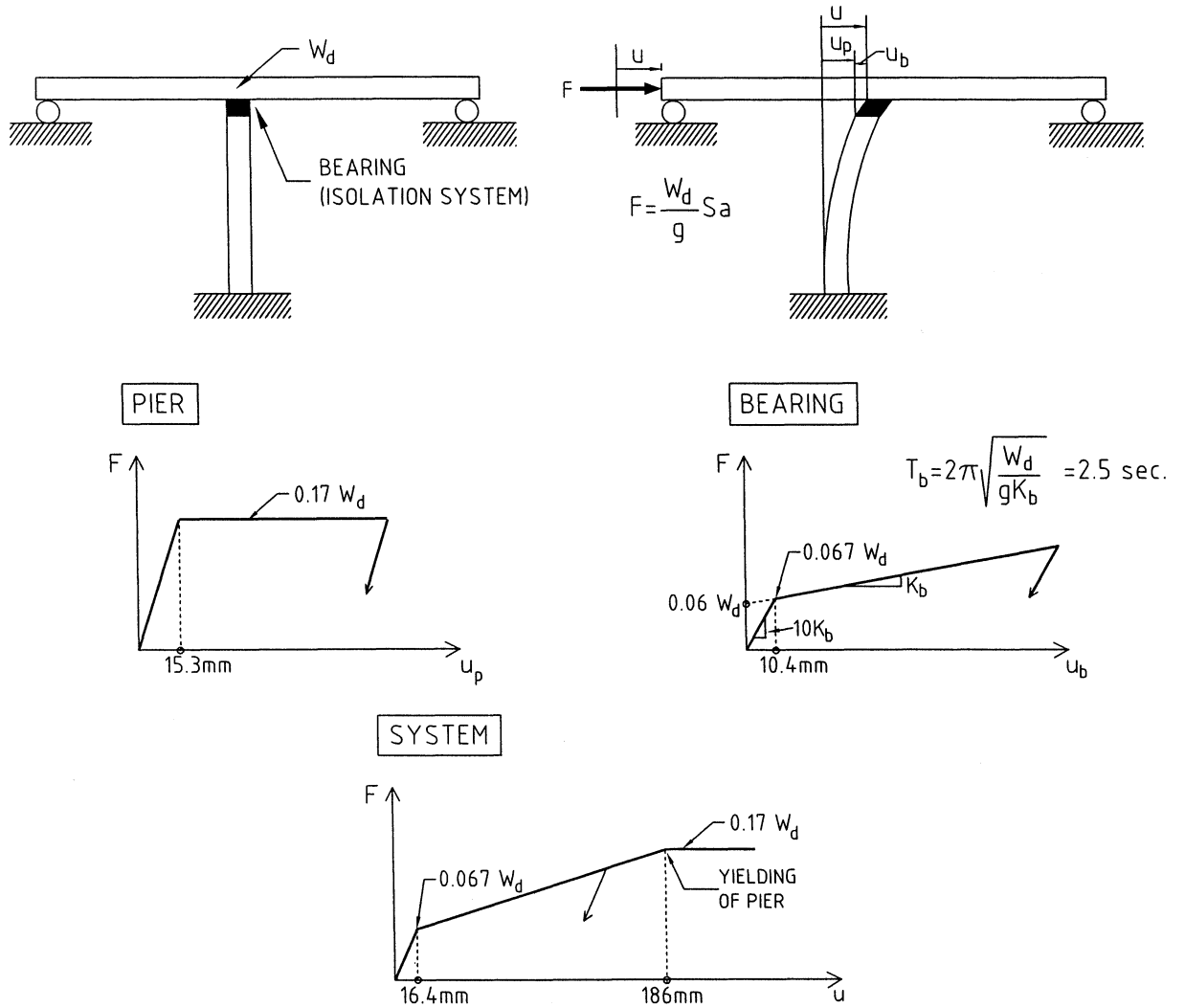


Figure 1-3 Pushover Curves of Seismic-Isolated Bridge
 (note that isolation bearings are not used at the abutment locations so that redistribution of the inertia force is not considered)

shows the force-displacement curves for each of the elements of system and of the system itself. The isolation bearings are designed to have a characteristic strength of $0.06W_d$ and a post-yielding stiffness such that the corresponding period is 2.5 sec. The system can accommodate a displacement (U of the deck with respect to the ground) of 186 mm, after which inelastic action in the pier occurs.

The response of the isolated bridge is determined by the nonlinear static procedure as shown in Figure 1-4. The calculated displacement $U=163$ mm, of which 149 mm is the bearing displacement and 14 mm is the pier displacement. The effective period is 2.05 sec and the effective damping is 23-percent. The shear force on the pier equals $0.156W_d$. In this case the effective damping was estimated on the assumption of perfect bilinear hysteretic behavior as being a realistic representation of the behavior of the seismic isolation bearings. Actually, the assumed bearing behavior is typical of a lead-rubber bearing design, although similar behavior can be achieved with friction pendulum bearings (Skinner et al. , 1993, Soong and Constantinou, 1994). The important conclusion of this example is that seismic isolation can eliminate damage to the substructure with a simultaneous reduction in the design force. In this realistic example the design force of the pier of the isolated bridge could be reduced to half of that of the non-isolated bridge.

Seismic-isolated bridges will not, in general, be constructed as shown in Figure 1-3. Rather, isolation bearings will be placed at both the pier and abutment locations. The behavior will be the same but the already reduced inertia force will be distributed to all elements of the substructure, not just the pier. This important aspect in isolated bridge

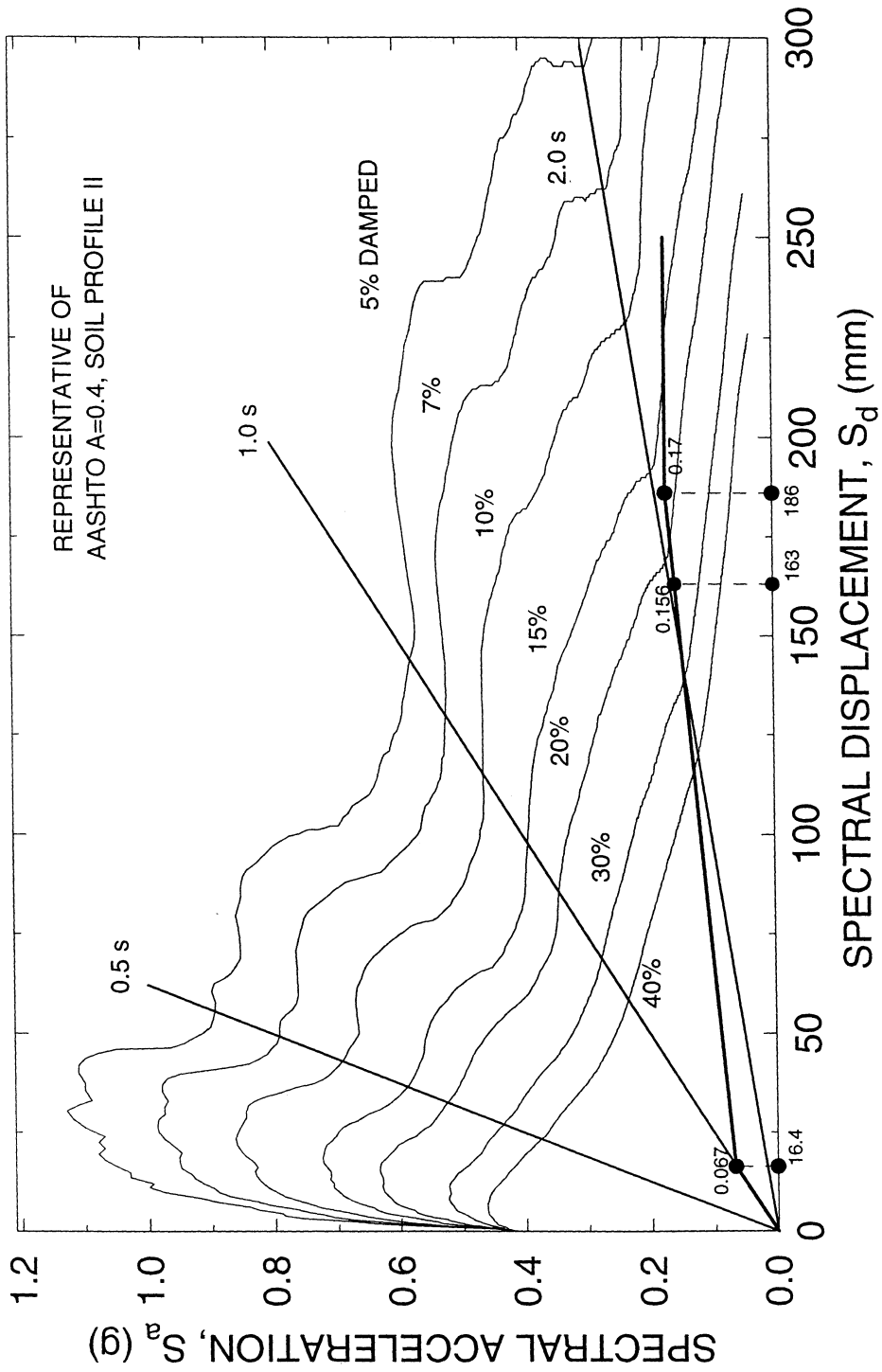


Figure 1-4 Calculation of Inelastic Response of Seismic-Isolated Bridge by Use of Design Demand Spectra and Nonlinear Static Analysis Procedures

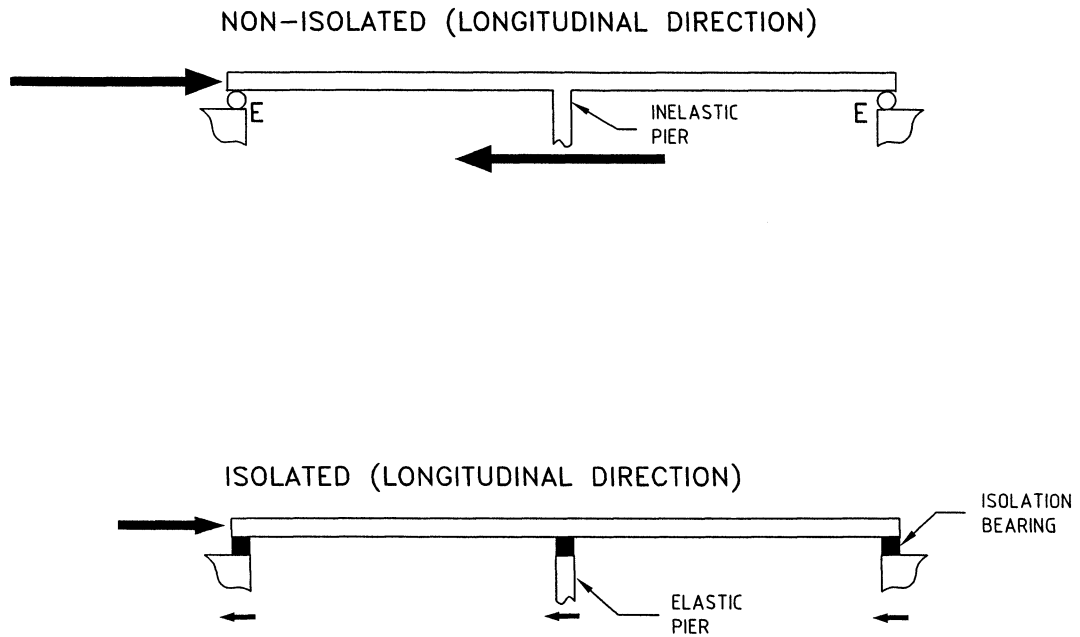


Figure 1-5 Effect of Redistribution of Inertia Force on Design Forces for Elements of the Substructure of Non-Isolated and Seismic-Isolated Bridges

design is illustrated in Figure 1-5. If the isolation system design is such that the distribution of inertia force is in accordance with the tributary weight, then the pier can be designed for a force of $0.08W_d$ and each of the abutments for a force of $0.04W_d$. That is, the combined effects of isolation and redistribution of force can eliminate damage to the pier and reduce the pier design force by 3.75 times. This exceptional performance is achieved at the expense of a bearing displacement of 149 mm which is very easily accommodated within standard seismic isolation bearings.

Over 500 bridges, varying in size from single-span to monumental structures, are currently seismic-isolated, or are in the construction or design phase. An account of these

structures and some information on their isolation system may be found in the database of the Earthquake Engineering Research Center at the University of California, Berkeley on the World Wide Web at <http://www.eerc.berkeley.edu/prosys.html> .

An interesting aspect of the behavior of seismic-isolated bridges may be presented through the example illustrated in Figures 1-3 and 1-4. The force demand on the pier for elastic pier behavior is $0.156W_d$. Had the pier been designed with the same response modification factor that was used in the non-isolated bridge ($R_\mu=3.3$), the strength of the pier would have been less than the strength of the isolation bearing. Accordingly, all inelastic action would have occurred in the pier with the isolation system rendered totally ineffective. The ductility demand on the pier would have been excessive. To demonstrate this consider the case of the isolated bridge with the yield strength of the pier being equal to $0.05W_d$ and the yield displacement being 15.3 mm. The force-displacement of the system is also elastoplastic with strength equal to $0.05W_d$ and yield displacement equal to 23 mm. The response is calculated by the procedure illustrated in Figure 1-3 and is found to be $U=178$ mm, $U_b=8.7$ mm, $U_p=169.3$ mm, whereas the effective period is 3.8 sec and the effective damping is 40-percent (again the assumption of $q=0.7$ was made). The pier displacement ductility ratio is $169.3/15.3 = 11.1$, which is excessive.

It is evident that response modification factors for the substructures of seismic-isolated bridges cannot be as high as those for the substructures of non-isolated bridges. This fact has been recently recognized in the 1997 AASHTO "Guide Specifications for Seismic Isolation Design" (American Association of State Highway and Transportation Officials, 1997) which, unlike its 1991 predecessor (American Association of State Highway and Transportation Officials, 1991), specifies low R-factors for the

substructures of seismic-isolated bridges. The underlying reasons for this specification are the proper performance of the isolation system and the sensitivity of the substructure inelastic response to the inherent variability in the seismic input. The objective of the study reported herein is to investigate the substructure response of seismic-isolated bridges and establish appropriate values of the response modification factor for these substructures.

SECTION 2

RESPONSE-MODIFICATION FACTORS FOR SEISMIC-ISOLATED BRIDGES

2.1 Response-Modification Factor

Response-modification factors (or R-factors) are used to calculate the design forces in structural components from the elastic force demand. That is, the demand is calculated on the assumption of elastic structural behavior and subsequently the design forces are established by dividing the elastic force demand by the R-factor. Illustrated in Figure 2-1 is the structural response of an inelastic system. The elastic force demand is F_e , whereas the yield force of an idealized representation of the system is F_y . The design force is F_D so that

$$F_D = \frac{F_e}{R} \quad (2-1)$$

where R = response modification factor.

The response modification factor contains two components. That is,

$$R = \frac{F_e}{F_D} = \frac{F_e}{F_y} \cdot \frac{F_y}{F_D} = R_\mu \cdot R_o \quad (2-2)$$

where R_μ = ductility-based portion of the factor and R_o = overstrength factor. The ductility-based portion is the result of inelastic action in the structural system. The overstrength factor is the result of reserve strength that exists between the design force and actual yield strength of the system (this is the strength that corresponds to the structural collapse level).

When a strength design approach is followed, the design force corresponds to the level at which the first plastic hinge develops and the structural response deviates from

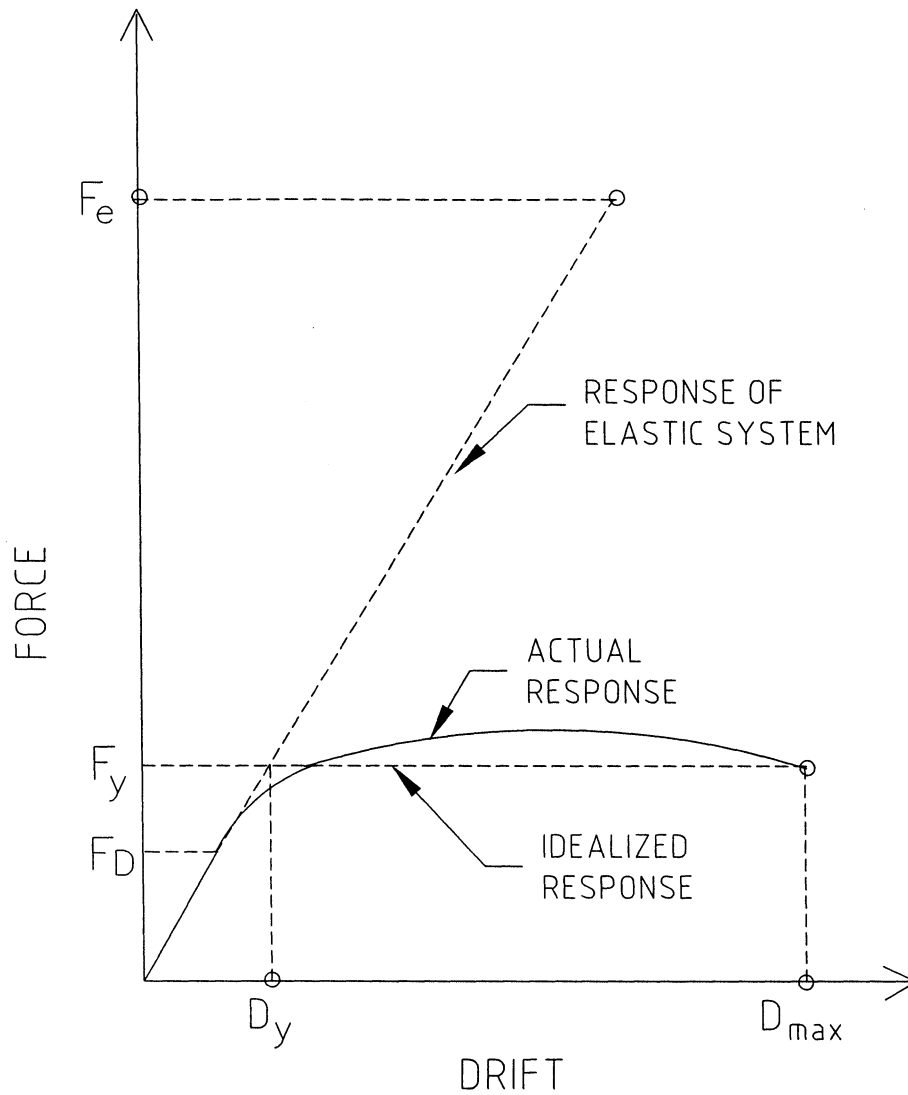


Figure 2-1 Structural Response of Inelastic System

linearity (as illustrated in Figure 2-1). In this case the overstrength factor results from structural redundancies, material overstrength, oversize of members, strain hardening, strain rate effects and code-specified minimum requirements related to drift, detailing, etc.

When an allowable stress design approach is followed, the design force corresponds to a level of stress which is less than the nominal yield stress of the material.

Accordingly, the R-factor (which is designated as R_w) contains an additional component which is the product of the ratio of the yield stress to the allowable stress and the shape factor (ratio of the plastic moment to moment at initiation of yield). This factor is often called the allowable stress factor, R_y , and has a value of about 1.5 . That is ,

$$R_w = R_\mu \cdot R_o \cdot R_y \quad (2-3)$$

There are numerous sources of information on response modification factors, such as Uang (1991), Uang (1993), Miranda and Bertero (1994), Applied Technology Council (1995), and Rojahn et al. (1997).

2.2 Determination of Components of R-Factor

While R-factors are specified without separating their components, the components are established by analysis. The ductility-based portion of the R-factor for a particular earthquake excitation is defined as the ratio of the elastic strength demand (that is, the strength required to avoid yielding of the system) and the yield strength required to maintain the displacement ductility ratio below a specified target ductility. That is,

$$R_\mu = \frac{F_e}{F_y(\mu = \mu_i)} \quad (2-4)$$

where μ_i = specified target ductility and μ =displacement ductility ratio given by (with references to Figure 2-1):

$$\mu = \frac{D_{\max}}{D_y} \quad (2-5)$$

Accordingly, the establishment of the ductility-based portion of the R-factor requires first the construction of inelastic response spectra for various levels of displacement ductility ratio, and then knowledge of the permissible ductility ratio for a particular structural system.

Miranda and Bertero (1994) presented a review of studies conducted to establish expressions for the ductility-based portion of the R-factor. These studies are based on analyses of single-degree-of-freedom inelastic systems in which a variety of behavioral models and collections of earthquake motions are used. In general, the results of these studies are expressions relating R_{μ} to the period of the system (initial period under elastic conditions), the displacement ductility ratio and some parameter (or parameters) that describes the ground motion.

The establishment of the ductility-based portion of the R-factor on the basis of analyses of single-degree-of-freedom systems is problematic for buildings given that the distribution of drift over the height depends on the characteristics of the structural system (that is, it does not solely depend on the period). On the other hand for bridges, which essentially behave as single-degree-of-freedom systems, the so-established R_{μ} factors should be valid.

Overstrength factors can be obtained by pushover analysis of the structural system and the construction of a representative force-displacement relation for the structure, such as the base shear versus deck displacement relation for a bridge or the base shear versus roof displacement relation for a building (Federal Emergency Management Agency, 1997). An analytical approach in establishing the overstrength factor can not account for the contributions of material overstrength and strain rate effects (and other effects depending on the complexity of the model), and it is limited to the particular structure that is analyzed.

2.3 Specified Values of R-Factor

Model codes (such as the Uniform Building Code), Specifications (such as the AASHTO Standard Specification for Highway Bridges) and Resource Documents (such as the NEHRP Provisions) specify values of the R or R_w factor which are empirical in nature. In general, the specified factor is dependent only on the structural system without consideration of the other affecting factors such as the period, framing layout, height, ground motion characteristics, etc. As noted in Applied Technology Council (1978), where R -factors were introduced, the specified R -factors are justified on the basis of risk assessment, economics, and nonlinear behavior.

In reality, the R -factors of today are, with only a few additions, equivalent to the K -factor which was introduced in 1959 in the SEAOC Blue Book (Structural Engineers Association of California, 1959).

R -factors, or their equivalent, are used for the design of structures in countries other than the United States. Particularly, in Mexico the 1987 Mexico City Building Code and in Europe the 1988 Eurocode (Commission of the European Communities, 1988) utilize factors which are dependent on the period and other affecting parameters.

In a drastic departure from force-based procedures (and the R -factor) the recently released Federal Emergency Management Agency (1997) resource document introduces systematic displacement-oriented and displacement-based procedures for evaluation of the seismic response. Although developed for seismic rehabilitation, they are equally applicable to new construction. They are eminently suitable for implementing performance-based design.

2.4 R-Factors for Seismic-Isolated Bridges

The American Association of State Highway and Transportation Officials (1991) "Guide Specifications for Seismic Isolation Design" specify the response modification factors for isolated bridges to be the same as those for non-isolated bridges. For substructures (piers, columns and column bents) this factor has values in the range of 2 to 5 (American Association of State Highway and Transportation Officials, 1996).

While not explicitly stated in the 1991 AASHTO "Guide Specifications" it is implied that the use of the same R-factors would result in comparable seismic performance of the substructure of isolated and non-isolated bridges. Accordingly, the "Guide Specifications" recommend the use of lower R-factors when lower ductility demand on the substructure of the isolated bridge is desired. The assumption that the use of the same R-factor would result in comparable substructure seismic performance in isolated and non-isolated bridges appears rational. However, it can be demonstrated by simple analysis that when inelastic action commences in the substructure, the effectiveness of the isolation system diminishes and larger displacement demands are imposed on the substructure.

New "Guide Specifications for Seismic Isolation Design" have been developed and approved in 1998 by the AASHTO states (American Association of State Highway and Transportation Officials, 1997). One significant change in the 1997 "Guide Specifications" over the 1991 predecessor is the specification for lower R-factor values for substructures of isolated bridges. These values are in the range of 1.5 to 2.5 . The following statements from the new "Guide Specifications" provide the rationale for the changes:

(1) In the Preface:

“The response modification factors (R-Factors) have been reduced to values between 1.5 and 2.5 . This implies that the ductility-based portion of the R-Factor is unity or close to unity. The remainder of the factor accounts for material overstrength and structural redundancies that are inherent in most structures. The specification of lower R-Factors has been based on the following considerations:

- (i) Proper performance of the isolation system, and
- (ii) Variability in response given the inherent variability in the characteristics of the design basis earthquake.

The lower R-Factors ensure, on the average, essentially elastic substructure response in the design basis earthquake. However, they do not necessarily ensure either proper behavior of the isolation system or acceptable substructure performance in the maximum capable earthquake (e.g., described as an event with 10% probability of being exceeded in 250 years). Owners may opt to consider this earthquake for the design of important bridges. This approach is currently utilized for the design of isolated bridges by the California Department of Transportation.”

(2) In Section C6. Response Modification Factor:

“The specified R-Factors are in the range of 1.5 to 2.5, of which the ductility based portion is near unity and the remainder accounts for material overstrength and structural redundancy that are inherent in most structures. That is, the lower R-Factors ensure, on the average, essentially elastic substructure behavior in the design basis earthquake. It should be noted that the calculated response by the procedures described in this document

represents an average value, which may be exceeded given the inherent variability in the characteristics of the design basis earthquake.”

There is, thus, a clear intention in the new "Guide Specifications" to essentially eliminate inelastic action in the substructure of seismic-isolated bridges. It is the objective of the work presented herein to provide, on the basis of analysis, justification for this change.

2.5 Underlying Reasons for Lower R-Factors in Isolated Bridges

We provide in this subsection results which demonstrate the necessity for lower R-factors in isolated bridges. The first example is sufficiently simple to allow for the establishment of a relation between the system displacement ductility ratio and the substructure displacement ductility ratio. We consider the pier-bearing-deck model of Figure 2-2. The pier has elastoplastic behavior with initial stiffness K_p , yield strength F_{yp} and yield displacement Y_p . The bearing (isolation system) is assumed to have linear-elastic behavior with stiffness K_b (it may be assumed to be the effective stiffness of the bearing). In general, K_b is much less than K_p . When a force F acts on the system (consider this to be a pushover analysis), the force-displacement relations for the pier, bearing and system are easily derived and shown in Figure 2-2 (for the particular case of $K_p = 4K_b$ and $U_{pmax}=5Y_p$). Of importance is to note that upon yielding of the pier no further deformations of the bearing occur. That is, further deformation takes place only in the pier. The pier displacement ductility ratio is

$$\mu_p = \frac{U_{pmax}}{Y_p} \quad (2-6)$$

and the system displacement ductility ratio is

$$\mu = \frac{U_{\max}}{U_y} \quad (2-7)$$

It may be easily shown that

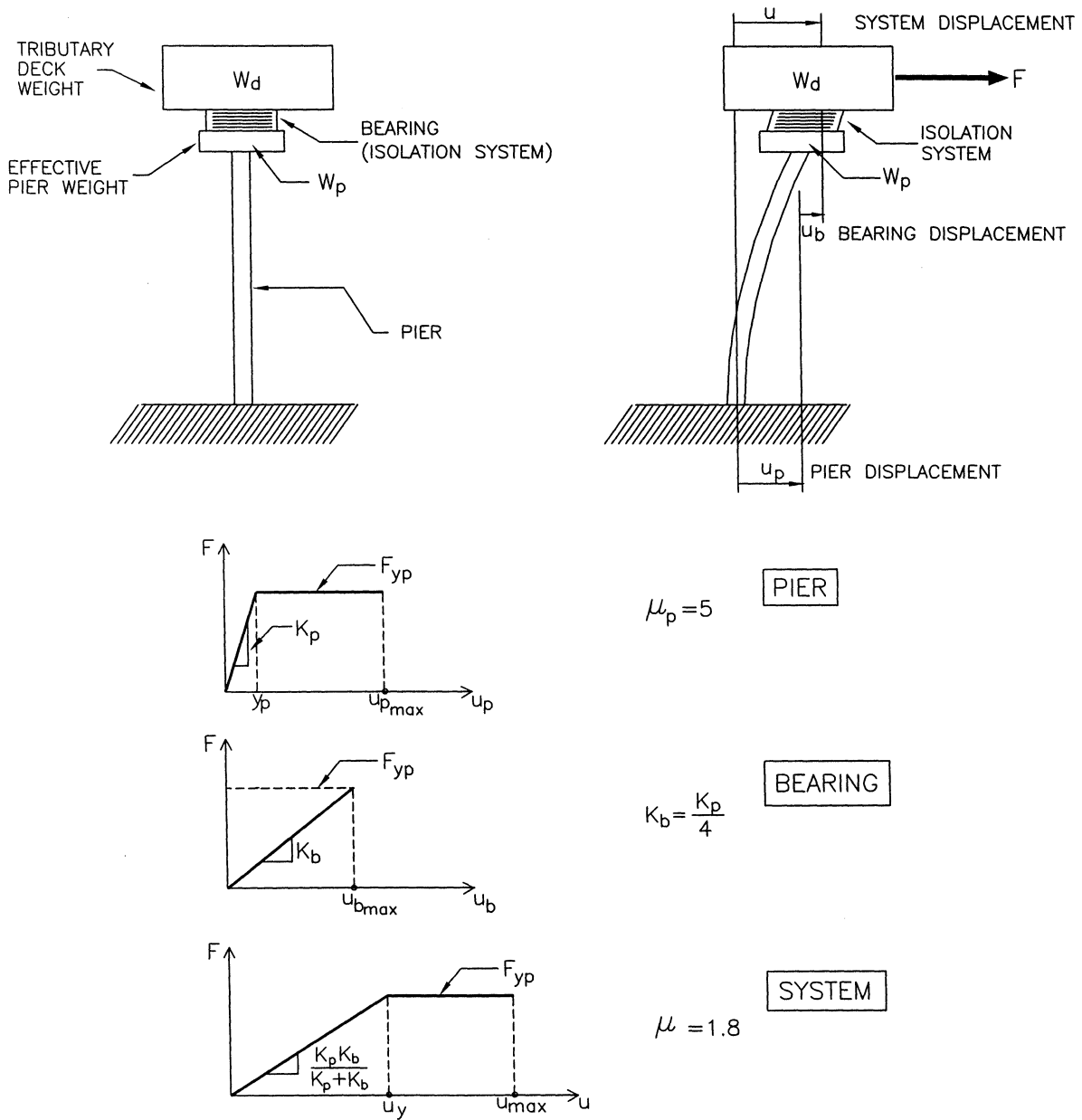


Figure 2-2 Behavior of Isolated Bridge with Elastoplastic Pier

$$U_y = Y_p \left(1 + \frac{K_p}{K_b} \right) \quad (2-8)$$

and

$$\mu_p = \mu + (\mu - 1) \left(\frac{K_p}{K_b} \right) \quad (2-9)$$

Equation (2-9) clearly demonstrates that the pier displacement ductility ratio is larger than the system ductility ratio (except for the case of elastic response). Given that quantity K_p/K_b is large, significant inelastic action in the pier will occur even when the system ductility ratio is low. The underlying reason for this behavior is the low strength of the pier.

To further demonstrate this behavior we present a second example in which dynamic nonlinear analysis is performed. Figure 2-3 illustrates the analyzed system. Both

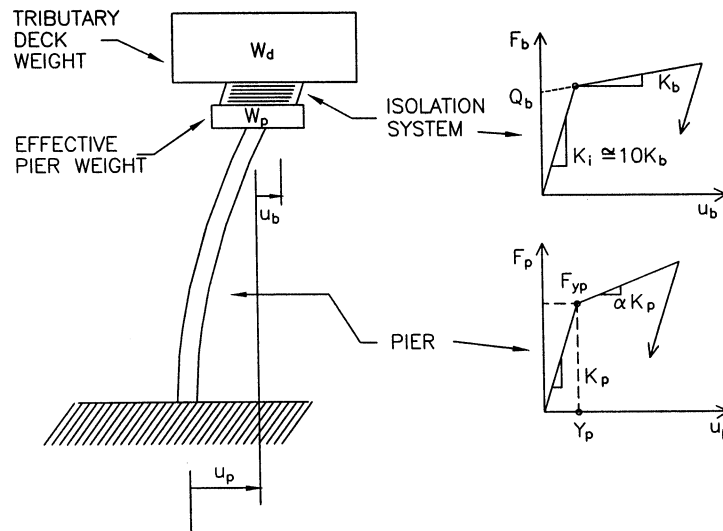


Figure 2-3 Model of Isolated Bridge Used in Analysis Example

the isolation system and the pier are assumed to have ideal smooth bilinear hysteretic behavior with the parameters indicated in the figure. Note that the system lacks structural

redundancy so that the overstrength factor is unity. The following parameters are selected: $W_d/W_p=5$, $Q_b/W_d=0.06$, $T_b=2.5$ sec, $\alpha=0.05$, and $T_p=0.1$ and 0.5 sec, where T_b = isolation system period on the basis of the post-elastic stiffness of the isolation system:

$$T_b = 2\pi \left(\frac{W_d}{gK_b} \right)^{1/2} \quad (2-10)$$

and T_p = initial period of the pier in its free cantilever position:

$$T_p = 2\pi \left(\frac{W_p}{gK_p} \right)^{1/2} \quad (2-11)$$

Two analyses are performed:

- (a) One in which the pier is assumed elastic (but with small viscous damping), as it would have been in the case of a design with ductility-based R-factor $R_\mu=1.0$.
- (b) Another in which the pier has yield strength $F_{yp}=F_e/R_\mu$ where $R_\mu=2.0$ and F_e = elastic demand calculated in the first analysis.

Figures 2-4 to 2-7 present the calculated histories of bearing displacement and pier drift, and the calculated loops of bearing force versus bearing displacement and pier shear force versus pier drift in the following four cases: (i) $T_p=0.1$ sec, $R_\mu=1.0$, (ii) $T_p=0.1$ sec, $R_\mu=2.0$, (iii) $T_p=0.5$ sec, $R_\mu=1.0$, and (iv) $T_p=0.5$ sec, $R_\mu=2.0$. The ground motion is one of the scaled acceleration histories used to represent the AASHTO A=0.4, soil profile type II ground motion spectrum in the analyses reported in Sections 3 and 4.

The following observations can be made from the results of these figures:

- (1) The elastic force demand is about $0.2W_d$. Accordingly, when the $R_\mu=2.0$ factor is applied the yield strength of the pier is $0.1W_d$. That is the strength of the pier is higher

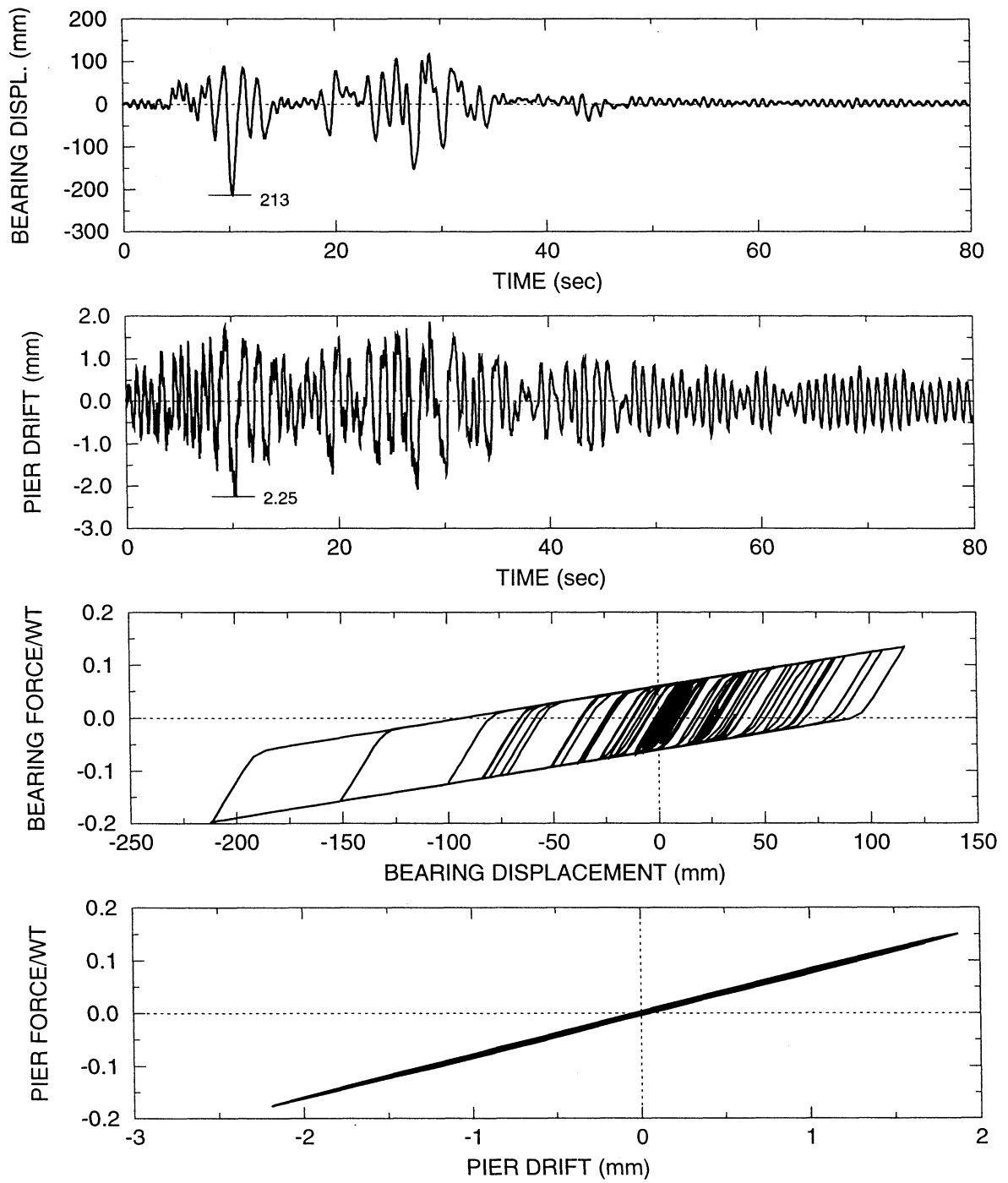


Figure 2-4 Calculated Response of Isolated Bridge Model
With $T_p=0.1$ sec and $R_{\mu}=1.0$ (elastic pier)

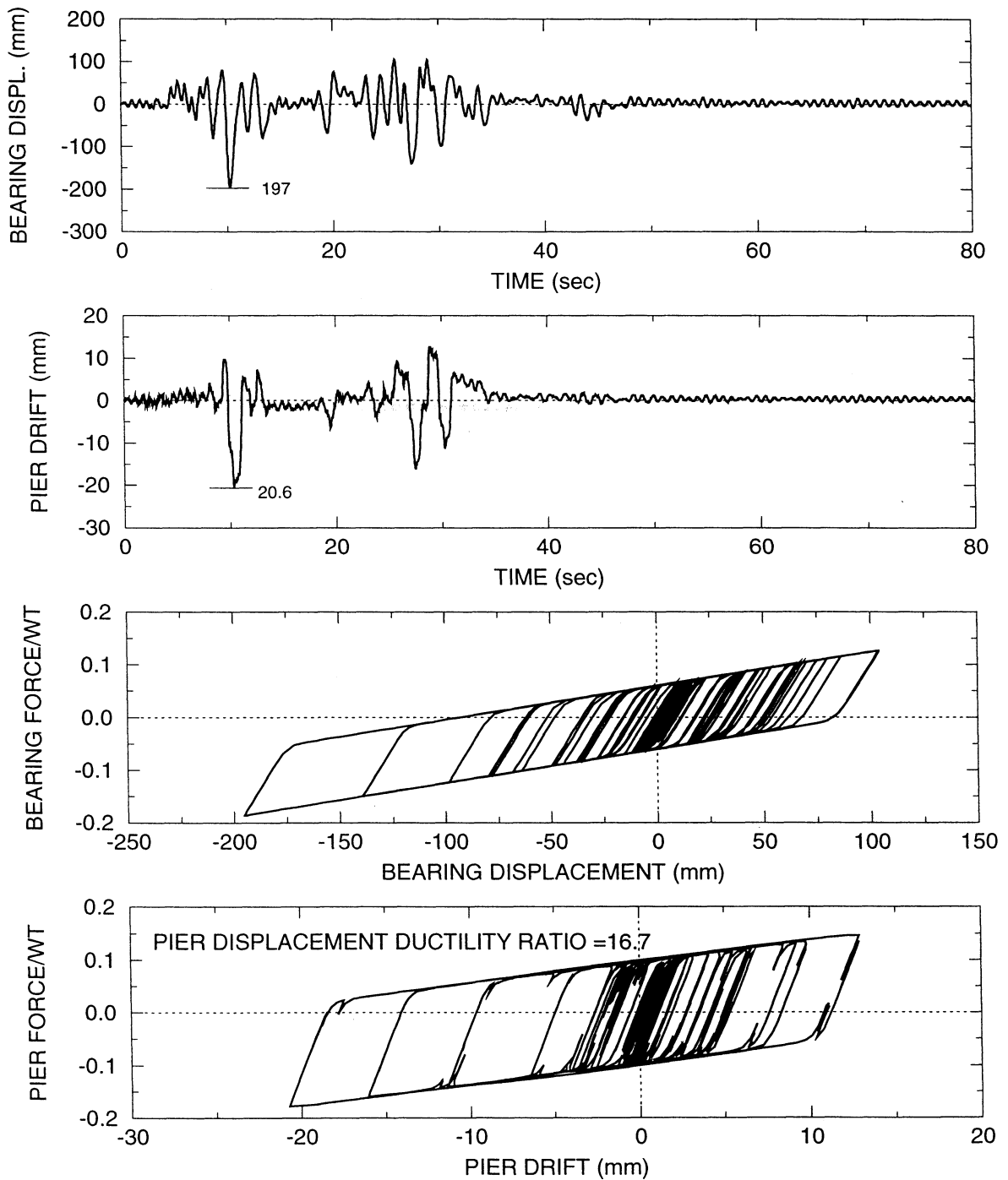


Figure 2-5 Calculated Response of Isolated Bridge Model
With $T_p=0.1$ sec and $R_\mu=2.0$

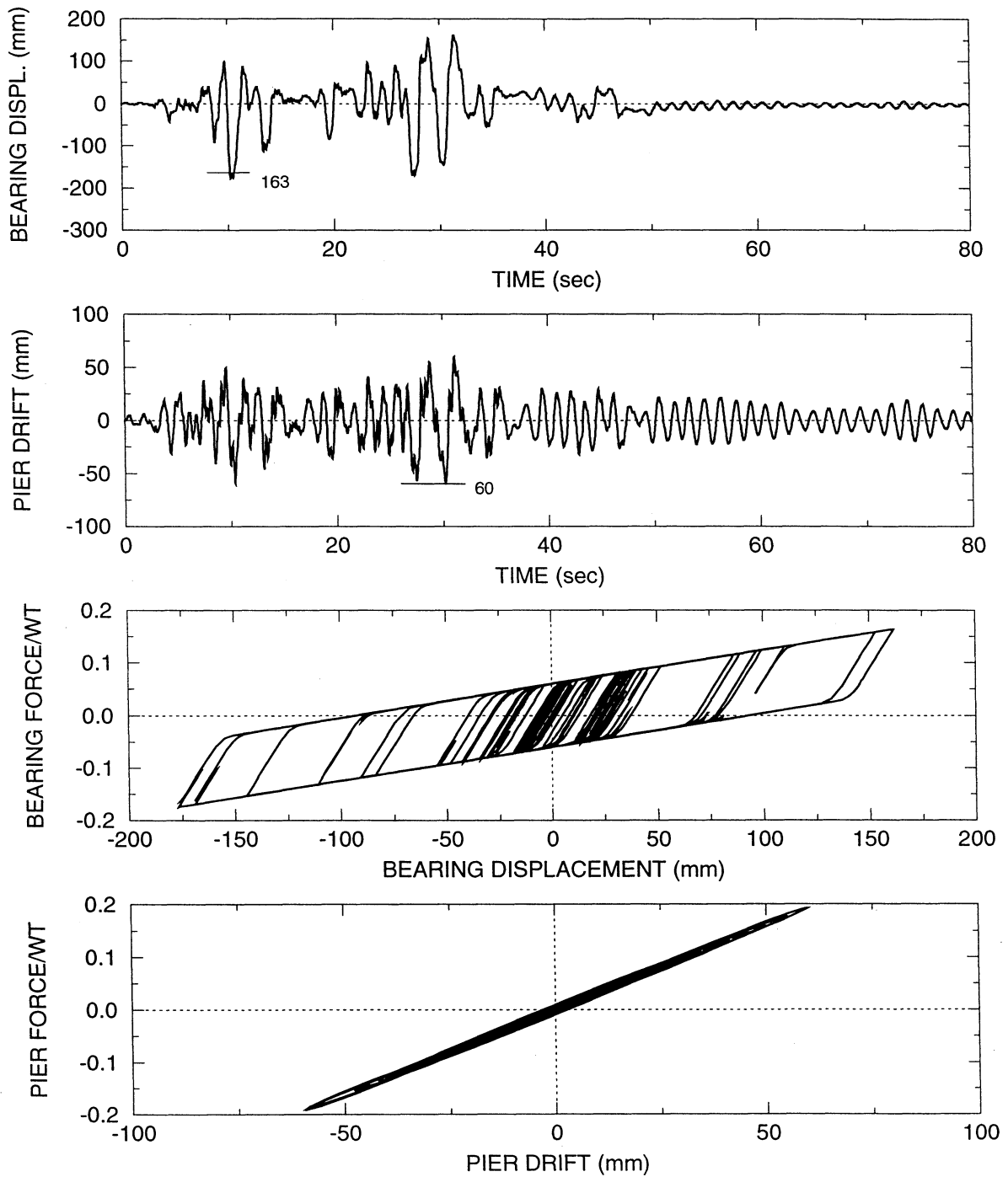


Figure 2-6 Calculated Response of Isolated Bridge Model
With $T_p=0.5$ sec and $R_\mu=1.0$ (elastic pier)

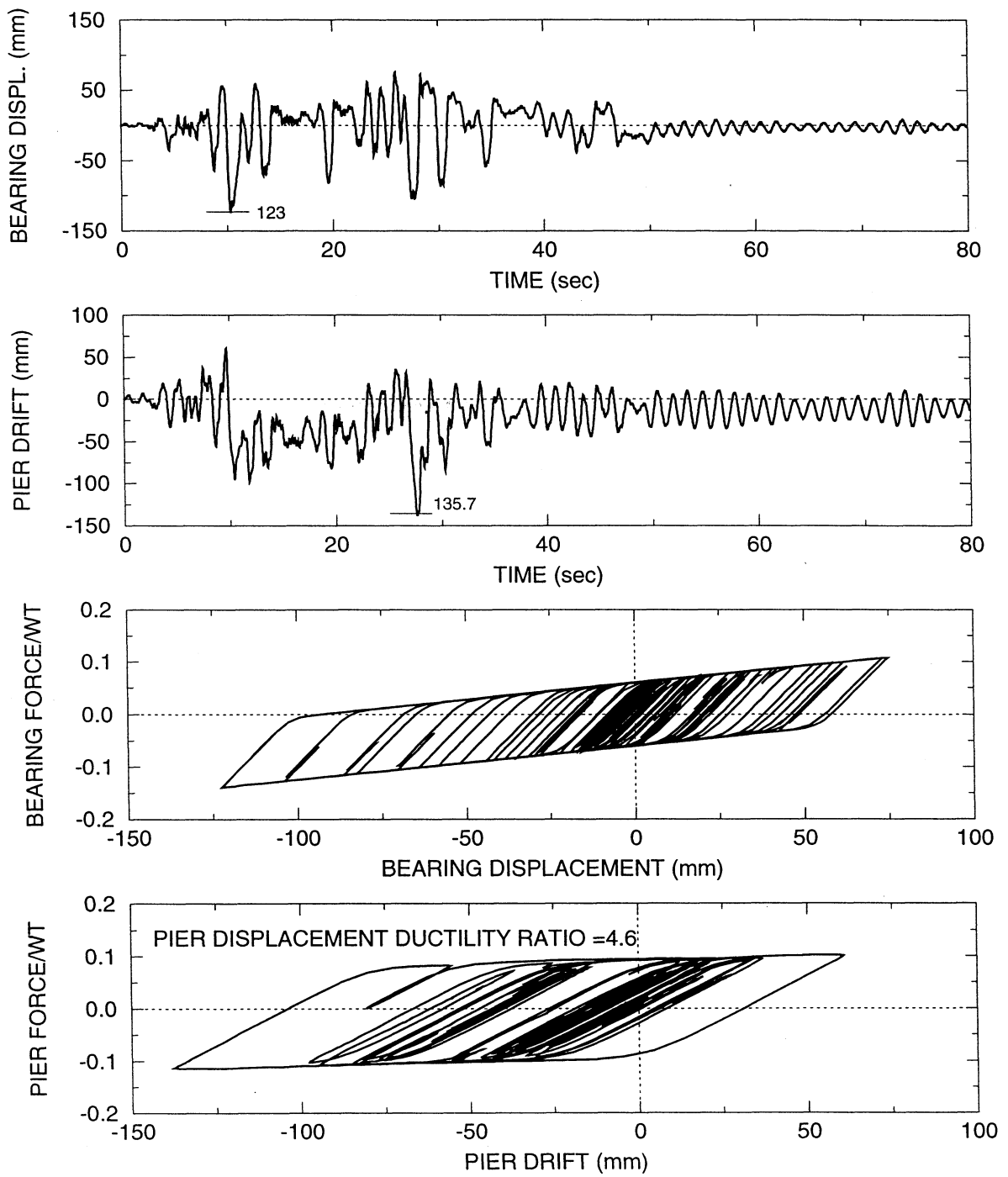


Figure 2-7 Calculated Response of Isolated Bridge Model
With $T_p=0.5$ sec and $R_\mu=2.0$

than the strength of the isolation system, which is equal to $0.06W_d$. Accordingly, inelastic action occurs first in the isolation system and inelastic action in the pier commences when bearing displacements exceed 62.1 mm.

- (2) Despite the higher strength of the pier by comparison to that of the isolation system significant inelastic action occurs in the pier, for which the displacement ductility ratio greatly exceeds R_μ . Analyses of a system with elastoplastic pier behavior resulted in even larger ductility ratio.
- (3) With the onset of inelastic action in the pier, the bearing displacement decreases. This reduction depends on the strength of the pier by comparison to that of the bearing, and on the deformational characteristics of the two beyond the elastic limit.

To further illustrate the effect of inelastic action in the pier, we analyze the case of $T_p=0.5$ sec with $R_\mu=4.0$. In this case the pier strength is $0.05W_d$, that is, less than the strength of the isolation system. Accordingly, inelastic action occurs first in the pier and the isolation system becomes totally ineffective. Figure 2-8 presents the calculated response in this case.

2.6 Objectives of this Study

Based on the few results presented in Section 2.5 it is clear that the ductility-based portion of the R-factor for isolated bridges should be lower than that of non-isolated bridges. Ideally, R_μ should be unity or very close to unity. Accordingly, the R-factor values of 1.5 to 2.5 in the 1997 AASHTO "Guide Specifications" (American Association of State Highway and Transportation Officials, 1997) are appropriate.

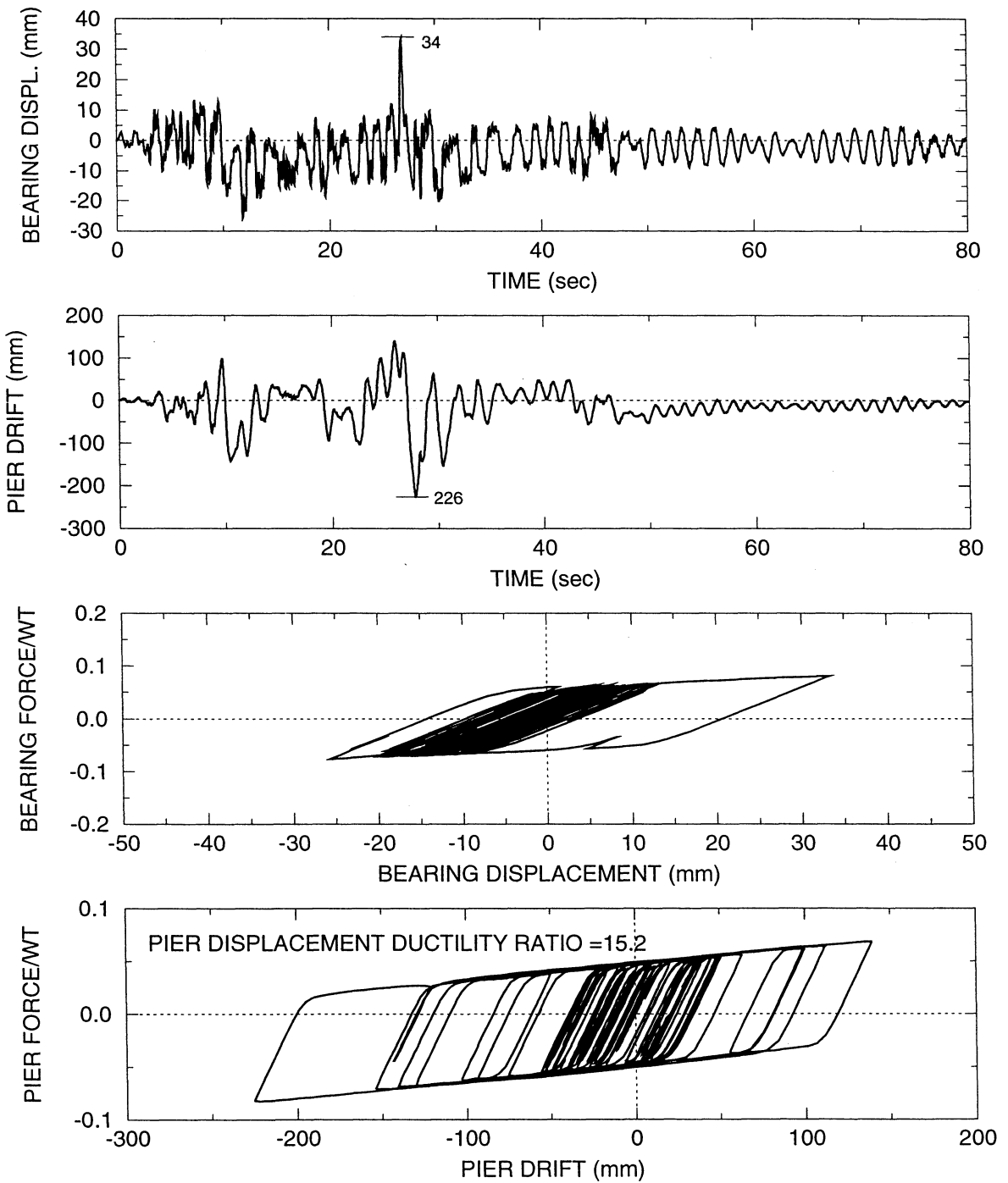


Figure 2-8 Calculated Response of Isolated Bridge Model
With $T_p=0.5$ sec and $R_{\mu}=4.0$

This study started in early 1996 with the objective of providing analytical justification for the reduced R-factor values for isolated bridges in the 1997 AASHTO "Guide Specifications." Options for achieving the objective were:

- (1) To proceed with an approach along the lines described in Section 2.2 and determine expressions of the ductility-based portion of the R-factor as function of the characteristics of the system (which include, in addition to period, the properties of the isolation system), the pier displacement ductility and the characteristics of the seismic excitation. These expressions would have to be compared to those that are applicable to non-isolated bridges (for example, those reviewed in Miranda and Bertero, 1994).
- (2) To proceed with a modified approach in which a large number of simple models, representing a range of substructure conditions and isolation system properties, is analyzed for a large number of scaled ground motions which are representative of specific AASHTO ground motion spectra. The result of these analyses would be average values (or other statistical quantity) of the pier displacement ductility ratio for given values of the ductility-based portion of the R-factor, and parameters of the isolation system and bridge substructure. This average ductility ratio is then compared to the average pier displacement ductility ratio calculated for the same ground motions of models which are representative of non-isolated bridges. Acceptable values of R_{μ} are those for which comparable substructure ductility ratios are calculated for the isolated and non-isolated bridge models.

The second approach is essentially the reverse of the first approach. That is, instead of establishing R_{μ} as a function of the ductility ratio and other parameters, it determines the

ductility ratio as a function of R_{μ} and the other parameters. It is also simpler than the first approach, which is of significance given the great number of analyses needed and the large number of parameters. As a result, the second approach is followed herein. It is supplemented by some simple results from pushover analysis of idealized models of non-isolated and isolated bridge models in order to establish the differences in the overstrength factors in the two types of models.

SECTION 3

APPROACH FOR ESTABLISHING THE DUCTILITY-BASED PORTION OF THE R-FACTOR FOR SUBSTRUCTURES OF SEISMIC-ISOLATED BRIDGES

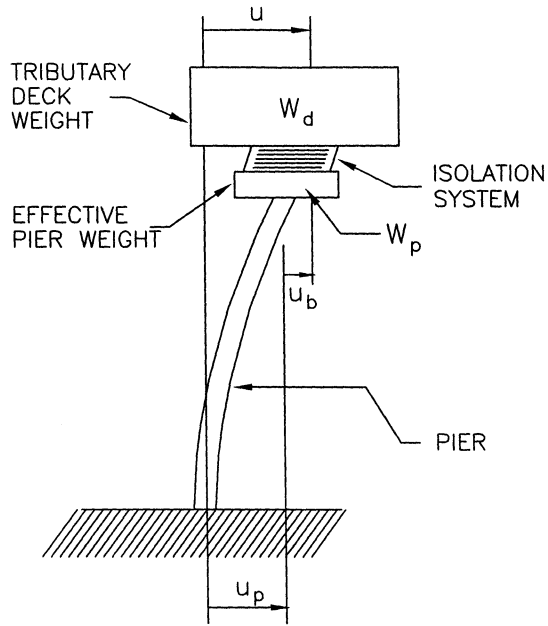
3.1 General Description of Approach

The approach is based on the study of simple systems which lack structural redundancy. Figure 3-1 shows the studied system, which consists of two degrees of freedom: the displacement of the isolation system and the displacement of the substructure (pier). A number of models for the isolator system and pier behavior were considered as illustrated in Figure 3-1 and explained later in this section.

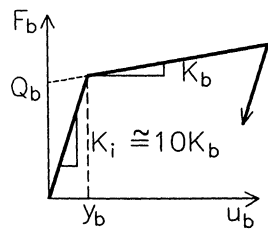
This system was analyzed with earthquake motions which were consistently scaled to represent a particular response spectrum. Specifically, motions representative of the AASHTO, soil profile type II, $A=0.4$, and 0.2 , and AASHTO, soil profile III, $A=0.4$ were used. An ensemble of either 14 or 20 scaled ground acceleration histories were developed to consistently represent each of these response spectra in an average sense.

For each response spectrum, isolation system model and substructure (pier) models, the following steps were completed:

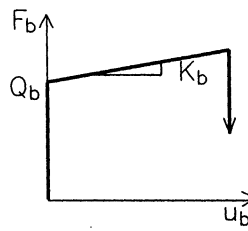
- (1) The Uniform Load Method of the 1997 AASHTO "Guide Specifications for Seismic Isolation Design" (American Association of State Highway and Transportation Officials, 1997) was applied and the statically equivalent seismic force, F_{pe} , was calculated on the assumption of elastic substructure.



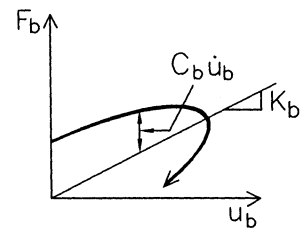
ISOLATION SYSTEM



BILINEAR HYSTERETIC
(a)

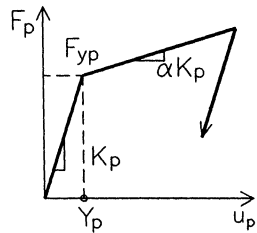


SLIDING
(b)

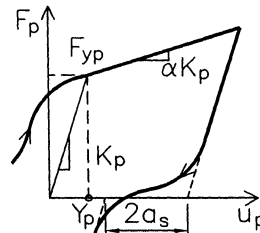


LINEAR ELASTIC-LINEAR VISCOUS
(c)

PIER



PERFECT BILINEAR HYSTERETIC
(d)



PINCHED WITH SLIP
(e)

Figure 3-1 Analyzed System and Illustration of Utilized Force-Displacement Relations for Isolation System and Pier

- (2) The statically equivalent seismic force was divided by the ductility-based portion of the response modification factor, R_{μ} , to arrive at the actual strength of the pier ($F_{yp}=F_{pe}/R_{\mu}$).
- (3) Nonlinear time history analysis of the system was performed with seismic input being the ensemble of scaled ground acceleration histories.
- (4) The calculated peak response was processed to obtain statistical measures of the response (e.g., average values) in terms of the isolation system displacement, pier displacement ductility ratio, and pier shear force.
- (5) A set of similar analyses were performed for the case of non-isolated bridges, which resulted in average values of the pier displacement ductility ratio for a range of values of parameters and R_{μ} .
- (6) Comparison of plots of the pier displacement ductility ratio for various values of the ductility-based portion of the response modification factor, R_{μ} , of isolated and non-isolated bridges provided information on :
 - (a) Values of R_{μ} for isolated bridges that result in comparable pier displacement ductility ratio with non-isolated bridges designed with different R_{μ} value.
 - (b) Information on the sensitivity of the pier displacement ductility ratio of isolated and non-isolated bridges due to the inherent variability in seismic input.

3.2 Studied System

The studied system is shown in Figure 3-1. It consists of the pier (substructure), which is modeled as an inelastic single-degree-of freedom system, the isolation system and the tributary deck weight on top of the isolation system. The system has two degrees

of freedom: the pier displacement U_p and the isolation system (or bearing) displacement U_b .

A variety of isolation system and pier force-displacement relations were considered. For the isolation system the following relations were considered.

- (1) Bilinear hysteretic behavior as shown in Figure 3-1(a). This behavior is typical of lead-rubber bearings and can be used to approximate the behavior of high damping rubber bearings. The behavior is described by the characteristic strength Q_b and the post-yielding stiffness K_b .
- (2) Sliding behavior as shown in Figure 3-1(b). This behavior is typical of sliding bearings with restoring force capability, such as in the Friction Pendulum System bearings. The behavior is described by the characteristic strength Q_b (the friction force, which is assumed to be constant) and the stiffness K_b . This behavior is essentially the same as that of the bilinear hysteretic model except for the very high initial stiffness.
- (3) Linear elastic and linear viscous behavior as shown in Figure 3-1(c). The model consists of a linear spring of stiffness K_b and a linear viscous damper of constant C_b . It is an appropriate model for an isolation system consisting of low damping elastomeric bearings and fluid viscous dampers (Kasalanati, 1998).

For the pier the following relations were considered:

- (1) Perfect bilinear hysteretic behavior as shown in Figure 3-1(d). This behavior is described by the initial stiffness K_p , the yield force F_{yp} and the ratio of post-yielding stiffness to initial stiffness α .

(2) Pinched hysteretic behavior as shown in Figure 3-1(e). This behavior is more realistic than the perfect bilinear hysteretic because it allows for slip ($2a_s$ as shown in Fig. 3-1(e)) and results in less energy dissipation in the pier.

The equations of motion of the studied system are presented in detail in Appendix A. The parameters describing the analyzed system and the range of values used are presented in Table 3-1.

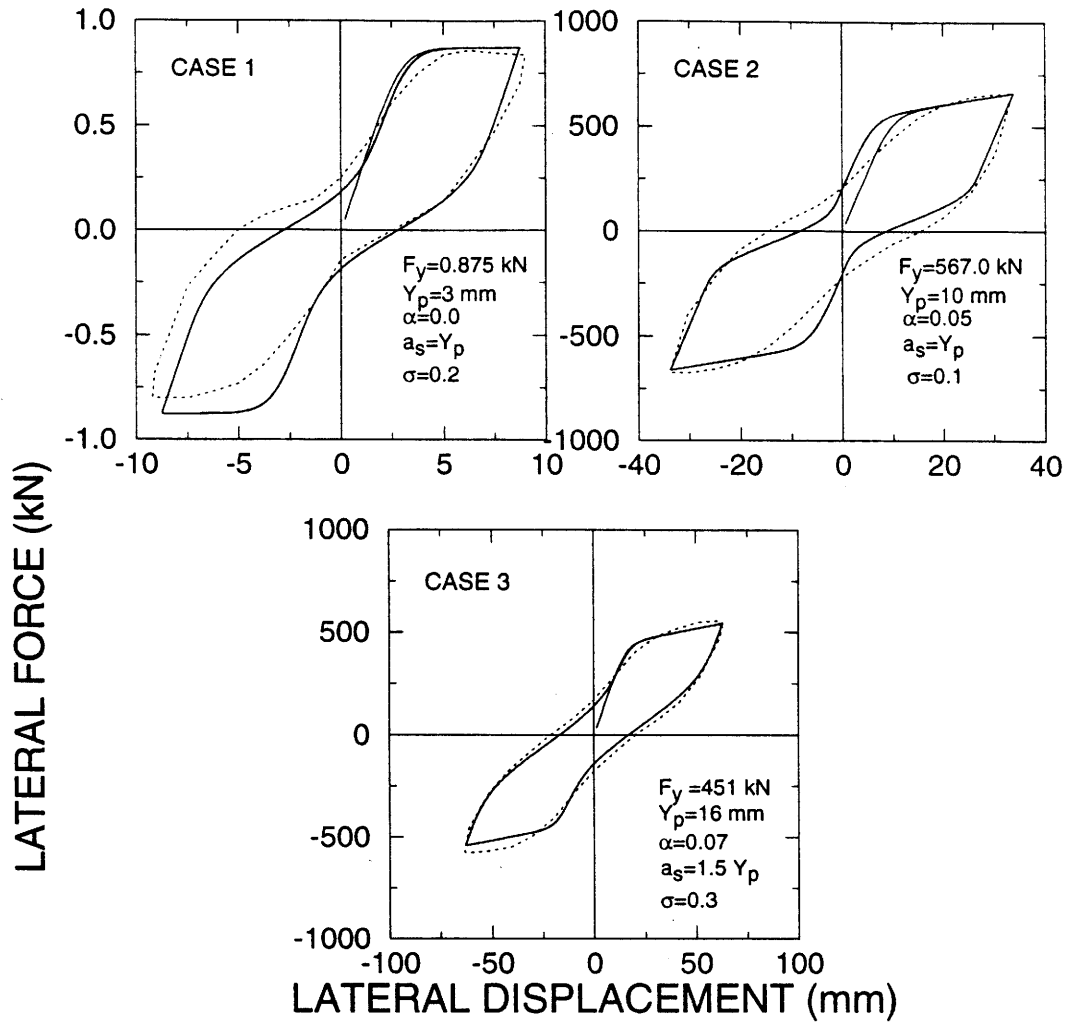
3.3 Selection of Parameters for Pinched Pier Model

The model used to represent pinched hysteretic behavior for the pier (see Appendix A) may be regarded as a mathematical construction that modifies the bilinear hysteretic model which has direct physical interpretation. The two additional parameters, a_s and σ , represent the half slip and the sharpness of transition from hysteretic to pinched behavior, respectively. Of interest is to know how well this model represents the actual behavior and how to select values of the parameters.

In order to provide some insight into the behavior of this model, experimental results from cyclic testing of reinforced concrete columns were selected from data compiled in the National Institute of Standards and Technology report No. NISTIR 5984 (Taylor et al., 1997) and from Gilbertsen et al. (1980). A number of force-displacements loops from these experimental results exhibit clear pinching behavior. The model of equations (A-14) to (A-17) was used to reproduce the tested behavior in three cases. Figure 3-2 presents a comparison of the experimental and analytical results. The three cases represent a case from Gilbertsen et al. (1980) (case 1), and the specimens denoted with filenames “Gill79S1” and “TANAKA90OU7” in Taylor et al. (1997) (cases 2 and 3, respectively).

**Table 3-1 Parameters Describing the Analyzed System and Range of Values
(see Fig. 3-1 and Appendix A)**

Parameter	Definition	Description	Value
ν	W_d/W_p	Deck to pier effective weight ratio	5,10
T_p	$2\pi(W_p/gK_p)^{1/2}$	Initial pier period when free standing (without deck)	0.1 to 0.5 sec
γ	F_{yp}/W_d	Pier strength/deck weight	Depends on spectrum and R_μ value
α	--	Pier post-yielding stiffness to elastic stiffness	0.05
a_s	--	Slip parameter for pinched pier behavior	Equal to Y_p
σ	--	Lock to slip transition parameter for pinched pier behavior	0.2
η	--	Parameter controlling sharpness of transition between elastic and inelastic ranges	5
T_b	$2\pi(W_d/gK_b)^{1/2}$	Period of isolation system on the basis of its post-yielding stiffness (or actual stiffness)	1.5 to 3.0 sec
δ	Q_b/W_d	Ratio of isolation system strength to deck weight (= friction coeff. for sliding system)	0.04, 0.06, 0.08, 0.10
ξ	$C_b g T_b / (4\pi W_d)$	Damping ratio of linear elastic, linear viscous isolation system	0.1, 0.2, 0.3, 0.4
β_i	--	Inherent viscous damping ratio of pier	0.05



Solid line indicates theoretical; dashed line indicates experimental

Figure 3-2 Comparison of Experimental and Analytical Force-Displacement Loops of Reinforced Concrete Columns with Pinched Hysteretic Behavior

The procedure followed to calibrate the model was as follows:

- (1) The experimental loops were used to reconstruct by graphical means the corresponding perfect bilinear hysteretic loops. This enabled the determination of parameters F_{yp} (yield strength), Y_p (yield displacement) and α (post-yielding to elastic stiffness ratio). Moreover, parameter η was fixed at 5.
- (2) Values for parameters σ and a_s were assumed, with the latter being a portion of the yield displacement.

The experiment was analytically simulated by specifying the displacement as a sinusoidal function (note that the amplitude is known, whereas the frequency is not an important parameter since the model is nearly rate-independent). Comparison of the analytical and experimental loops established the appropriate values of the parameters σ and a_s .

The results in Figure 3-2 provide evidence for the applicability of the model. Moreover, it may be observed that use of $a_s=Y_p$ and $\sigma=0.2$ results in significant pinching with a loop having an area approximately 60 to 70-percent of the area enclosed by the perfect bilinear hysteretic loop provided that the displacement ductility ratio is of the order of 3.

It may be observed in the analytical loops of the Figure 3-2 that the model does not exhibit the pinching behavior during the initial ascending branch of the loop. The model, as described in Appendix A and in Baber and Noori (1985), does not have this realistic behavior. The model has been modified as follows:

- (a) Parameter a_s was set equal to zero and maintained so until the first reversal of motion.

(b) At the instant of first reversal of motion and provided that the displacement exceeded $1.5Y_p$ the value of parameter a_s was set to the actual value.

Thus, the pinching behavior in the modified model is activated only when the displacement exceeds $1.5Y_p$. As an example, Figure 3-3 presents the calculated pier shear force-drift loops in the analysis of an isolated bridge configuration for one of the scaled motions (motion EQ20, representative of AASHTO $A=0.4$, soil type II – Appendix B) and for parameters $T_p=0.5$ sec, $\nu=10$, $T_b=2.0$ sec, $\delta=0.06$ and $R_\mu=1.5$. The figure includes two loops, one for the case of perfect bilinear hysteretic pier behavior and one for pinched hysteretic pier behavior.

3.4 Selection and Scaling of Ground Motions

The selection and scaling of the ground motions followed the approach presented in Tsopelas et al. (1997). In this approach N pairs of recorded horizontal components of ground acceleration histories are selected from earthquakes having a magnitude greater than 6.5, an epicentral distance between 10 and 20 km (that is near-fault motions are excluded), and with site conditions representative of the soil profile of the applicable response spectrum.

The motions are scaled by the following procedure:

- (1) Each pair of ground accelerations is normalized by the SRSS (square root of the sum of squares) of the peak ground velocities of the two components. The normalization produces N pairs of ground accelerations with the same SRSS peak ground velocity.
- (2) The SRSS spectra of each normalized pair are constructed.
- (3) The average of the N SRSS spectra is constructed and raised by factor f to match at the period of 1.0 sec the 1.4 times the target response spectrum.

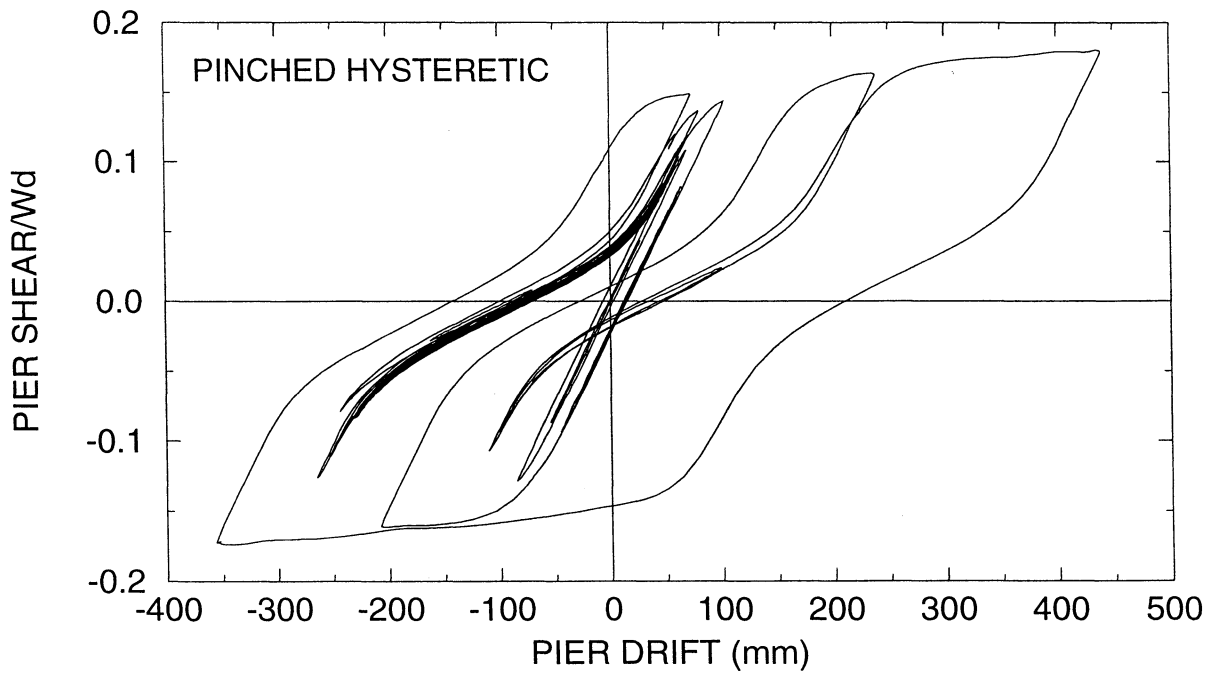
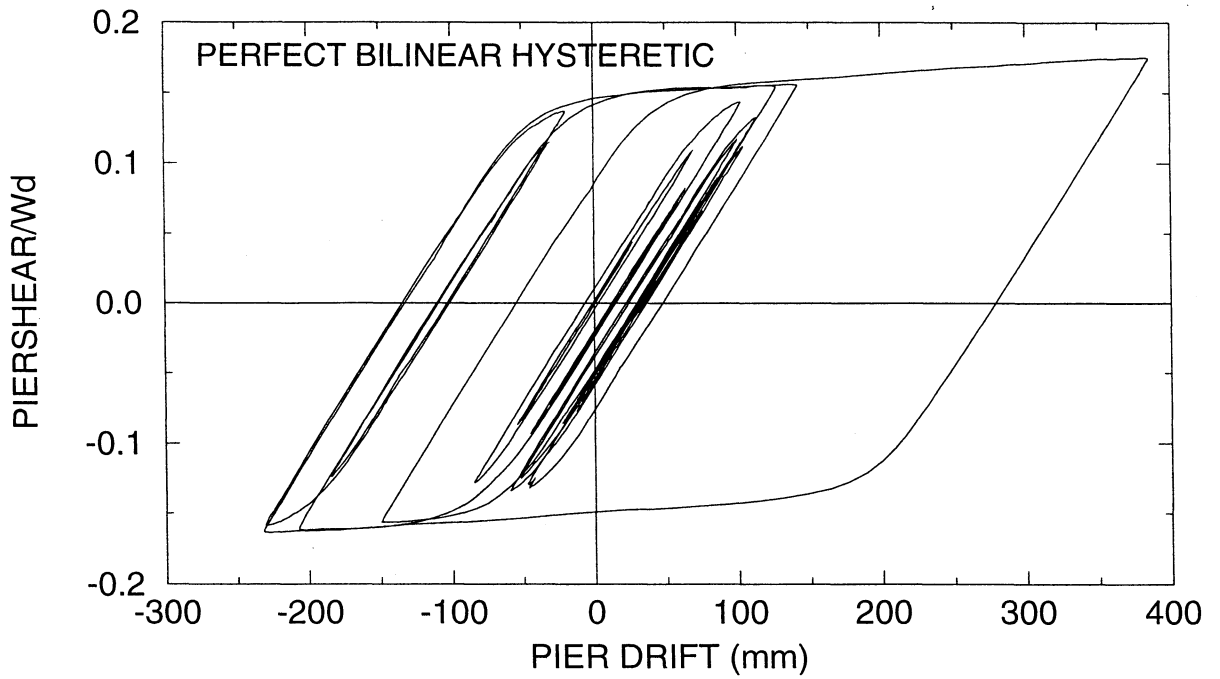


Figure 3-3 Calculated Pier Shear Force – Drift Loops of Isolated Bridge with Perfect Bilinear Hysteretic and with Pinched Hysteretic Behavior ($T_p=0.5$ sec, $T_b=2.0$ sec, $v=10$, $\delta=0.06$, $R_\mu=1.5$, earthquake EQ20 per Appendix B)

(4) The scaled factor for each pair (applied to the unscaled pair prior to normalization) is then determined as f times the SRSS of the peak ground velocities of the pair (from step (1)). This scaling process preserves the frequency content of the records and ensures an equal contribution of the normalized records to the average response spectrum.

For the case of the AASHTO $A=0.4$ and $A=0.2$, and soil profile type II (American Association of State Highway and Transportation Officials, 1996) response spectra, ten pairs of ground acceleration histories were selected from sites classified as soft rock to stiff soil. Table 3-2 presents these motions and the scale factors. Figure 3-4 presents the average, maximum and minimum spectral acceleration values of the 20 scaled motions for the case of the $A=0.4$, soil profile type II spectrum. It may be observed that, on the average, the scaled motions represent on the average well the AASHTO spectrum over a wide range of period values. Moreover, the figure demonstrates the variability in the characteristics of the scaled motions. Such variability is implicit in the definition of seismic hazard.

Table 3-2 Motions Used to Represent AASHTO, Soil Profile Type II, $A = 0.4$ and 0.2 Spectra and Scale Factors

Earthquake	Station	Components	Scale Factor, $A=0.4$	Scale Factor, $A=0.2$
1949 W. Washington	325 (USGS)	N04W, N86E	2.74	1.37
1954 Eureka	022 (USGS)	N11W, N79E	1.74	0.87
1971 San Fernando	241 (USGS)	N00W, S90W	1.96	0.98
1971 San Fernando	458 (USGS)	S00W, S90W	2.22	1.11
1989 Loma Prieta	Gilroy 2 (CDMG)	90, 0	1.07	0.54
1989 Loma Prieta	Hollister (CDMG)	90, 0	1.46	0.73
1992 Landers	Yermo (CDMG)	360,270	1.28	0.64
1992 Landers	Joshua (CDMG)	90,0	1.48	0.74
1994 Northridge	Moorpark (CDMG)	180,90	2.61	1.31
1994 Northridge	Century (CDMG)	90,360	2.27	1.14

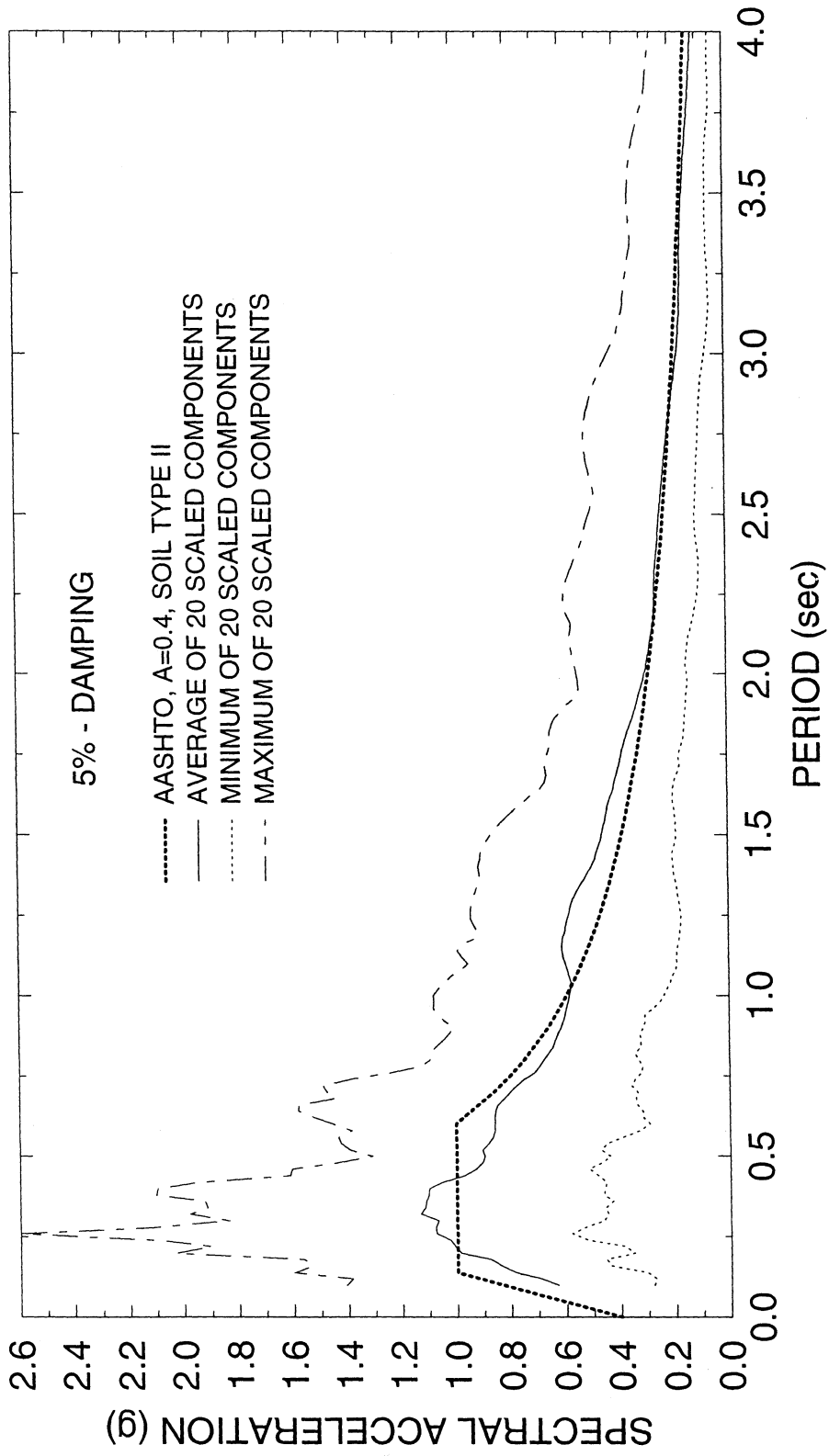


Figure 3-4 Maximum, Average and Minimum Spectral Acceleration Values of Scaled Motions for AASHTO A=0.4, Soil Profile Type II Spectrum

Considerable difficulties were encountered in the selection of acceleration histories for soil profile type III. It was not possible to select 10 pairs of histories from earthquakes having epicentral distance of 10 to 20 km. Moreover, many earthquake records from sites classified as soft soil did not exhibit strong spectral accelerations at long periods. Accordingly, the selection and scaling process was modified. Seven pairs of earthquake records were selected from sites classified as soft soil or alluvium. For some of these motions the site conditions were unknown, however, their spectra contained strong long period components. The magnitude of the earthquakes ranged from 6.7 to 7.5 but the epicentral distances varied from 16 to 166 km.

The scaling process treated the 14 components as being independent and was applied as follows:

- (1) Each component was normalized by the peak ground velocity of the component.
- (2) The response spectrum of each normalized component was constructed.
- (3) The average of the response spectra was constructed and raised by factor f to obtain a good fit of the average spectrum with the target response spectrum.
- (4) The scale factor for each (applied to the unscaled component prior to normalization) was then determined as ' f ' times the peak ground velocity of the component.

Table 3-3 presents the motions selected to represent the AASHTO $A=0.4$, soil profile type III spectrum and the scale factors.

Table 3-3 Motions Used to Represent AASHTO, Soil Profile Type III, A= 0.4 Spectra and Scale Factors

Earthquake	Station	Components	Scale Factors*
1992 Landers	Barstow-Vineyard (CDMG)	90,0	3.03, 3.46
1989 Loma Prieta	Gilroy 3 (CDMG)	90,0	1.74, 2.20
1992 Landers	Amboy (CDMG)	90,0	4.26,3.79
1992 Landers	Hotsprings (CDMG)	90,0	4.01, 3.65
1989 Loma Prieta	Hollister & Pine (CDMG)	90,0	2.46, 1.21
1994 Northridge	Sylmar (CDMG)	90,0	0.99, 0.59
1979 Southern Alaska	Yakutat	90,270	3.20, 2.45

*Scale Factors Apply to Indicated Components

Furthermore, Figure 3-5 presents the average, maximum, and minimum spectral values of the scaled 14 components. Again the scaled motions represent on the average well the AASHTO spectrum and demonstrate the variability in their characteristics. However, it should be noted that the scaled components represent well the AASHTO spectrum for periods above 1.0 sec, and that they are conservative for shorter periods. That is, the use of these scaled motions will provide conservative estimates of the response of bridges with effective period less than 1.0 sec. This case is encountered only in some of the analyzed non-isolated configurations. Appendix B presents details on the motions used and response spectra for each scaled motion

3.5 Application of Uniform Load Method for Analysis of Seismic-Isolated Bridges

The Uniform Load Method of the 1997 AASHTO "Guide Specifications" (American Association of State Highway and Transportation Officials, 1997) provides estimates of the isolation system and substructure displacements, and the statically equivalent seismic force on the basis of the assumption of elastic substructure response. The isolation system is represented by an equivalent linear elastic and linear viscous representation which is dependent on the actual displacement of the isolation system.

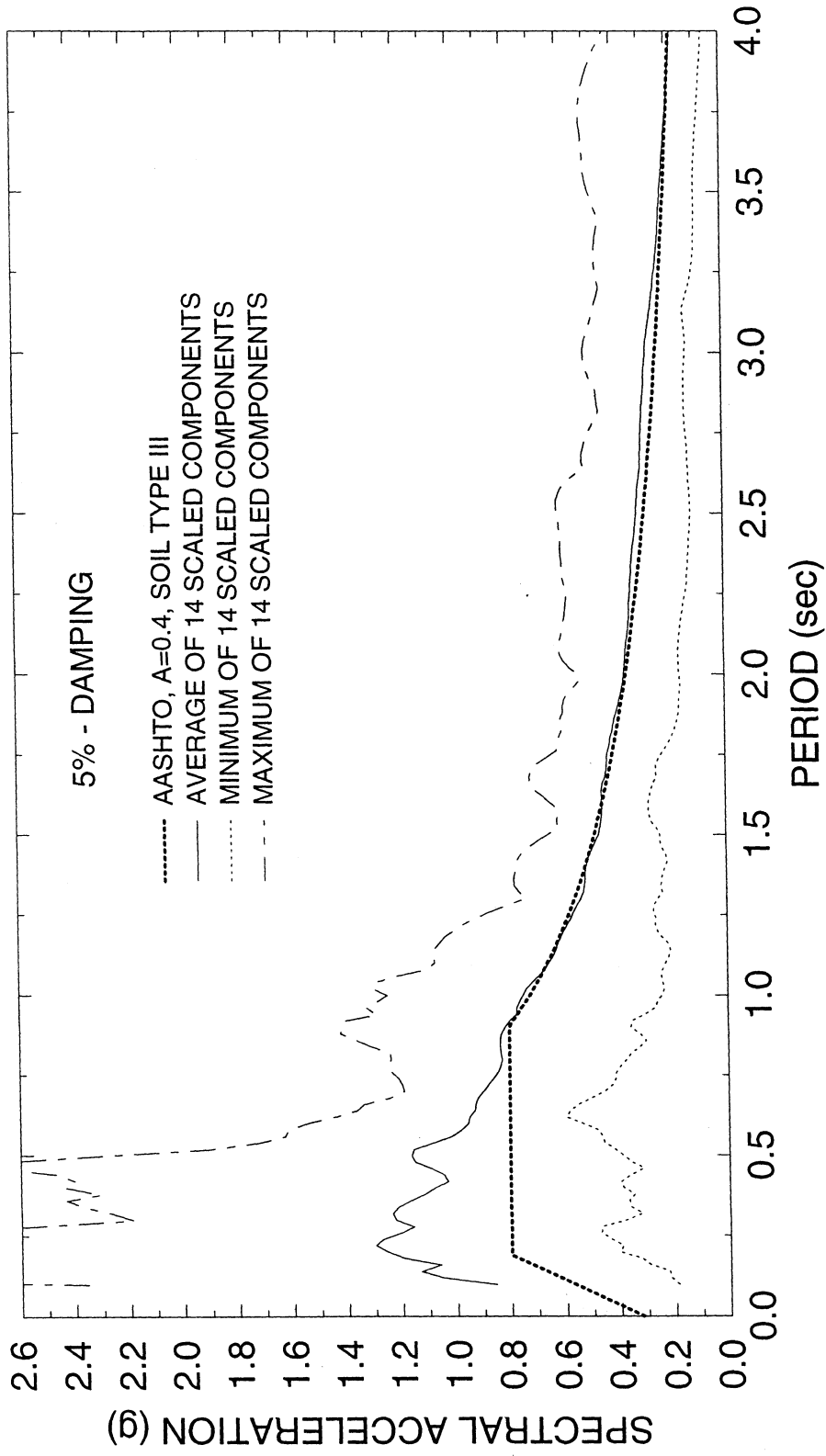


Figure 3-5 Maximum, Average and Minimum Spectral Acceleration Values of Scaled Motions for AASHTO A=0.4, Soil Profile Type III Spectrum

3.5.1 Isolation System with Bilinear Hysteretic or Sliding Behavior

The parameters describing the system (see Appendix A) are: pier period T_p , weight ratio ν , isolation system period T_b and strength to weight ratio (or friction coefficient) δ .

Let the isolation system displacement be U_b . The period of the system including the effect of the flexibility of the substructure (this is the effective period) may be easily determined and cast into the following form:

$$T_{eff} = T_p \nu^{1/2} \left[1 + \left(\frac{\nu T_p^2}{T_b^2} + \frac{\delta \nu g T_p^2}{4\pi^2 U_b} \right)^{-1} \right]^{1/2} \quad (3-1)$$

The equivalent damping of the system is calculated as

$$\beta = \frac{\text{Energy Dissipated per Cycle}}{4\pi(\text{Maximum Kinetic Energy})} \quad (3-2)$$

Equation (3-2) is in a more convenient form than the one in the 1997 AASHTO "Guide Specifications" which utilizes the potential rather than the kinetic energy (the maxima of the two are equal). The dissipated energy is calculated as $4Q_b U_b$, thus neglecting the small additive contribution from the pier and also the small term $(-4Q_b Y_b)$ due to the bilinear behavior of the isolation system. The result is

$$\beta = \frac{\delta g T_{eff}^2 U_b}{2\pi^3 \left[(U_b + U_p)^2 + \frac{U_p^2}{\nu} \right]} \quad (3-3)$$

where U_p = pier displacement (see Fig. 3-1). The displacement of the system (that is, displacement $U = U_p + U_b$ per Fig. 3-1) is given by

$$U = \frac{250AS_iT_{eff}}{B} \quad (\text{in mm}) \quad (3-4)$$

where A = acceleration coefficient, S_i = site coefficient and B = damping coefficient (related to β), which are prescribed in the 1997 "AASHTO Guide Specifications" (note that in the Guide Specifications the system displacement is denoted as d).

The pier displacement is related to the system displacement by

$$U_p = \left(\frac{\delta v g T_p^2}{4\pi^2} + \frac{v T_p^2 U}{T_b^2} \right) \left(1 + v \frac{T_p^2}{T_b^2} \right)^{-1} \quad (3-5)$$

Finally, the isolation system displacement is given by

$$U_b = U - U_p \quad (3-6)$$

and the equivalent seismic force, which is the elastic force on the pier, is given by

$$\frac{F_{pe}}{W_d} = \frac{4\pi^2 U_b}{g T_b^2} + \delta \quad (3-7)$$

The procedure for calculating displacement U_b and force F_{pe} is iterative. It involves the following steps:

- (1) Assume U_b
- (2) Use (3-1) to (3-6) to calculate U_b
- (3) Repeat steps (1) and (2) until satisfactory convergence is reached.
- (4) Use (3-7) to calculate the pier elastic force.

3.5.2 Isolation System with Linear Elastic, Linear Viscous Behavior

The parameters describing the system (see Appendix A) are: pier period T_p, weight ratio v, isolation system period T_b and isolation system damping ratio ξ.

The period of the system is given by

$$T_{eff} = T_b \left[1 + \nu \left(\frac{T_p}{T_b} \right)^2 \right]^{1/2} \quad (3-8)$$

The energy dissipated per cycle is given by $2\pi^2 C_b U_b^2 / T_{eff}$ so that the equivalent damping of the system is determined by (use of eq. 3-2):

$$\beta = \frac{\xi T_{eff} U_b^2}{T_b (U^2 + U_p^2 / \nu)} \quad (3-9)$$

Equation (3-4) for the system displacement is valid, whereas the pier displacement is given by:

$$U_p = \nu \left(\frac{T_p}{T_b} \right)^2 U_b \quad (3-10)$$

Moreover, equation (3-6) is valid. The procedure for determining displacements could follow the following steps:

- (1) Assume U_b
- (2) Calculate U_p using (3-10)
- (3) Use (3-8), (3-9), (3-4) and (3-6) to calculate U_b
- (4) Repeat steps (1) to (3) until satisfactory convergence is reached.

However, this is not necessary since the system is linear. Combination of (3-8), (3-9), (3-10) and (3-6) results in

$$\beta = \frac{\xi \left[1 + \nu \left(\frac{T_p}{T_b} \right)^2 \right]^{1/2}}{\left[1 + \nu \left(\frac{T_p}{T_b} \right)^2 \right]^2 + \nu \left(\frac{T_p}{T_b} \right)^4} \quad (3-11)$$

Accordingly, the procedure requires use of (3-8) and (3-11) to evaluate the effective period and equivalent damping, and then use of (3-4), (3-6) and (3-10) to determine the displacements.

Either procedure will yield the peak displacements of the pier and the isolation system. The calculation of the peak elastic pier force requires further analysis because this force does not occur at the instant of peak displacement. The concept is briefly described in American Association of State Highway and Transportation Officials (1997), and more elaborately in Federal Emergency Management Agency (1997) and Tsopelas et al. (1997). Considering the harmonic response of a single-degree-of-freedom viscous system as shown in Figure 3-6, three instants are recognized for which the force is easily calculated: (a) the instant of maximum velocity at which the displacement is zero, (b) the instant of maximum displacement at which the velocity is zero, and (c) the instant of maximum acceleration. It is easily shown that the maximum force is equal to f_1 times the force at the instant of maximum displacement plus f_2 times the force at the instant of maximum velocity, where:

$$f_1 = \cos[\tan^{-1}(2\xi)] \quad (3-12)$$

$$f_2 = \sin[\tan^{-1}(2\xi)] \quad (3-13)$$

and ξ = viscous damping ratio.

Accordingly, the elastic force for the pier is given by

$$\frac{F_{pe}}{W_d} = f_1 \left(\frac{4\pi^2 U_b}{gT_b^2} \right) + f_2 \left(\frac{8\pi^2 \xi U_b}{gT_b T_{eff}} \right) \quad (3-14)$$

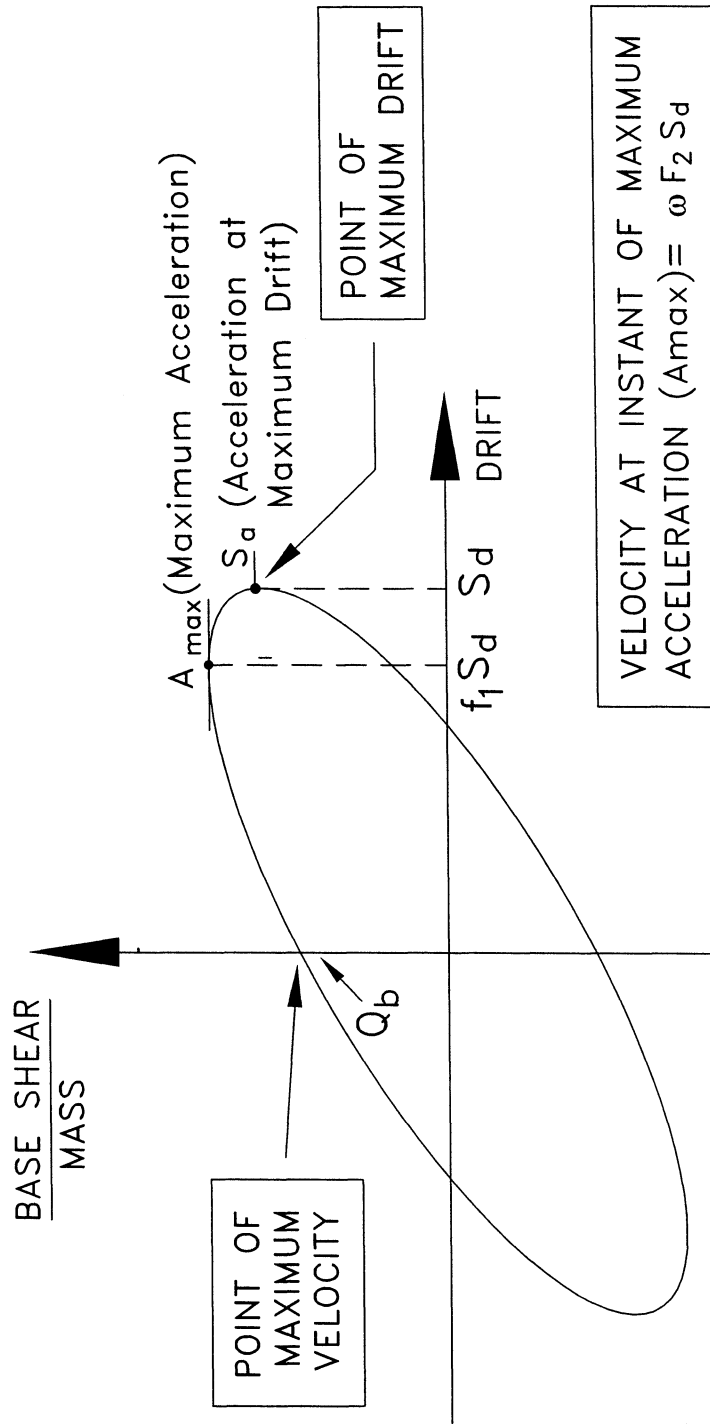


Figure 3-6 Plot of Base Shear versus Drift Loop of Highly Damped Single-Degree-of-Freedom System Undergoing Harmonic Displacement of Frequency ω

3.6 Model for Analysis of Non-isolated Bridge

The model used is the single-degree-of-freedom inelastic system shown in Figure 3-7. The behavior of this system was assumed to be either perfect bilinear hysteretic or pinched hysteretic. The parameters describing this system are the initial period

$$T = 2\pi \left(\frac{W}{gK_p} \right)^{1/2} \quad (3-15)$$

and the pinched behavior parameters a_s and σ . Moreover, viscous damping was included as described in Appendix A with an inherent viscous damping ratio of $\beta_i = 0.05$.

Analysis of this system involves first analysis in accordance with the Elastic Seismic Response Coefficient Procedure (American Association of State Highway and Transportation Officials, 1996). The elastic force for the pier is given by:

$$\frac{F_{pe}}{W} = \frac{1.2AS}{T^{2/3}} \quad (3-16)$$

where A = acceleration coefficient, T = period and S = site coefficient. It should be noted that coefficient S is not the same as coefficient S_i (for isolated bridges). Specifically, for soil profile type II : $S=1.2$ and $S_i=1.5$, and for soil profile type III : $S=1.5$ and $S_i=2.0$. Moreover, (3-16) has an upper bound of $2.5A$ in all cases and an upper bound of $2.0A$ for $A \geq 0.3$ and soil profile type III.

Having established the elastic pier force, the actual strength of the pier was determined by dividing F_{pe} by the ductility-based portion of the R-factor, R_{μ} . This established F_{yp} and Y_p . Subsequently, nonlinear time history analysis were performed with the ensemble of scaled motions and values of the pier displacement ductility ratio were determined as function of period T and factor R_{μ} .

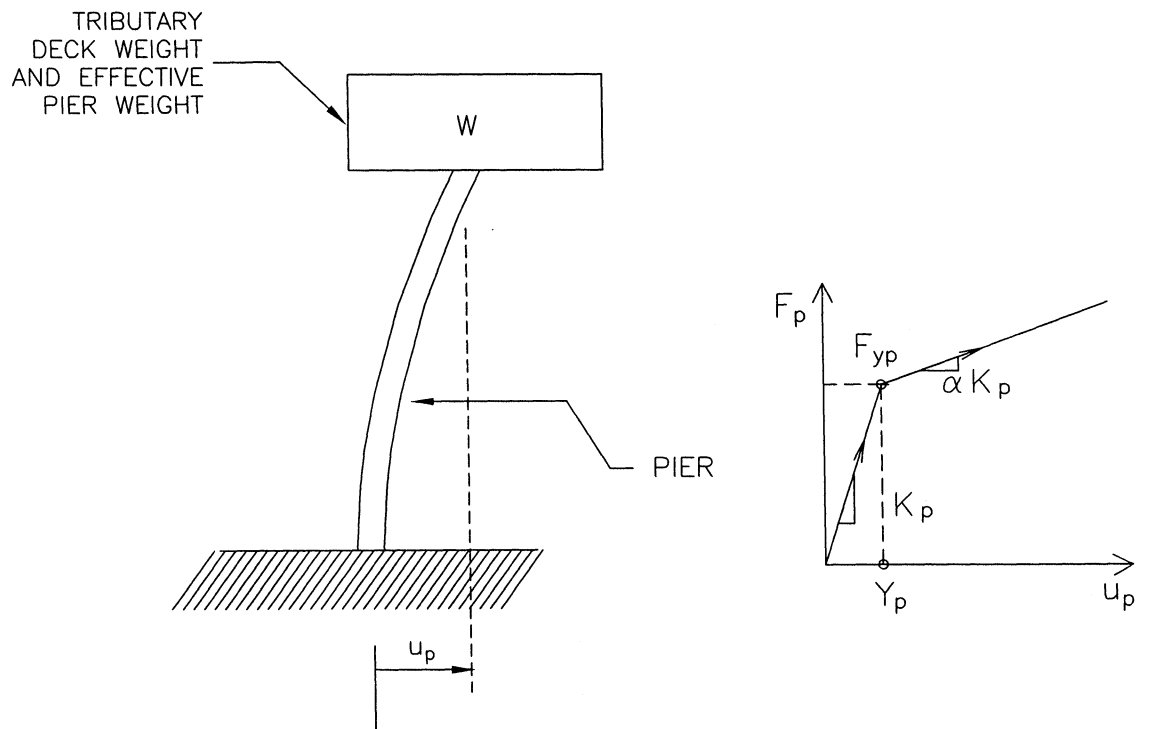


Figure 3-7 Model Used in Analysis of Non-isolated Bridge

SECTION 4

RESULTS AND INTERPRETATION

4.1 Non-Isolated Bridge

Figure 4-1 presents the calculated average pier displacement ductility ratio of the non-isolated bridge for the four considered cases. Note that the cases $A = 0.2$ and $A = 0.4$, soil profile type II result in exactly the same response (however, this is not the case in the isolated bridge). Appendix C presents the calculated ductility ratios for each of the scaled earthquake components in the three cases with $A = 0.4$: bilinear hysteretic pier, soil profile type II and III, and pinched hysteretic pier, soil profile type II.

The results in Figure 4-1 reveal the following:

- (1) There is a general consistency between these results and results obtained on the inverse relation (R_{μ} vs period for various values of ductility ratio) by many investigators and reviewed in Miranda and Bertero (1994). That is, the displacement ductility ratio is approximately equal to R_{μ} for large periods and it is larger than R_{μ} in the short period range. It may be seen in Figure 4-1 that this increase occurs at a period of about 0.4 sec for soil profile type II and at about 0.8 sec for soil profile type III. Both these period values are related to the cut-off period below which the elastic force to weight ratio is bounded by the limits of either $2.5A$ or $2.0A$ (see Section 3.6).
- (2) For soil profile type III there is a substantial increase in the displacement ductility ratio in the short period range. It is related to the used scaled motions which, on the average, have substantially stronger spectral acceleration values than the AASHTO spectrum in the short period range (see Figure 3-5). That is, the results on the

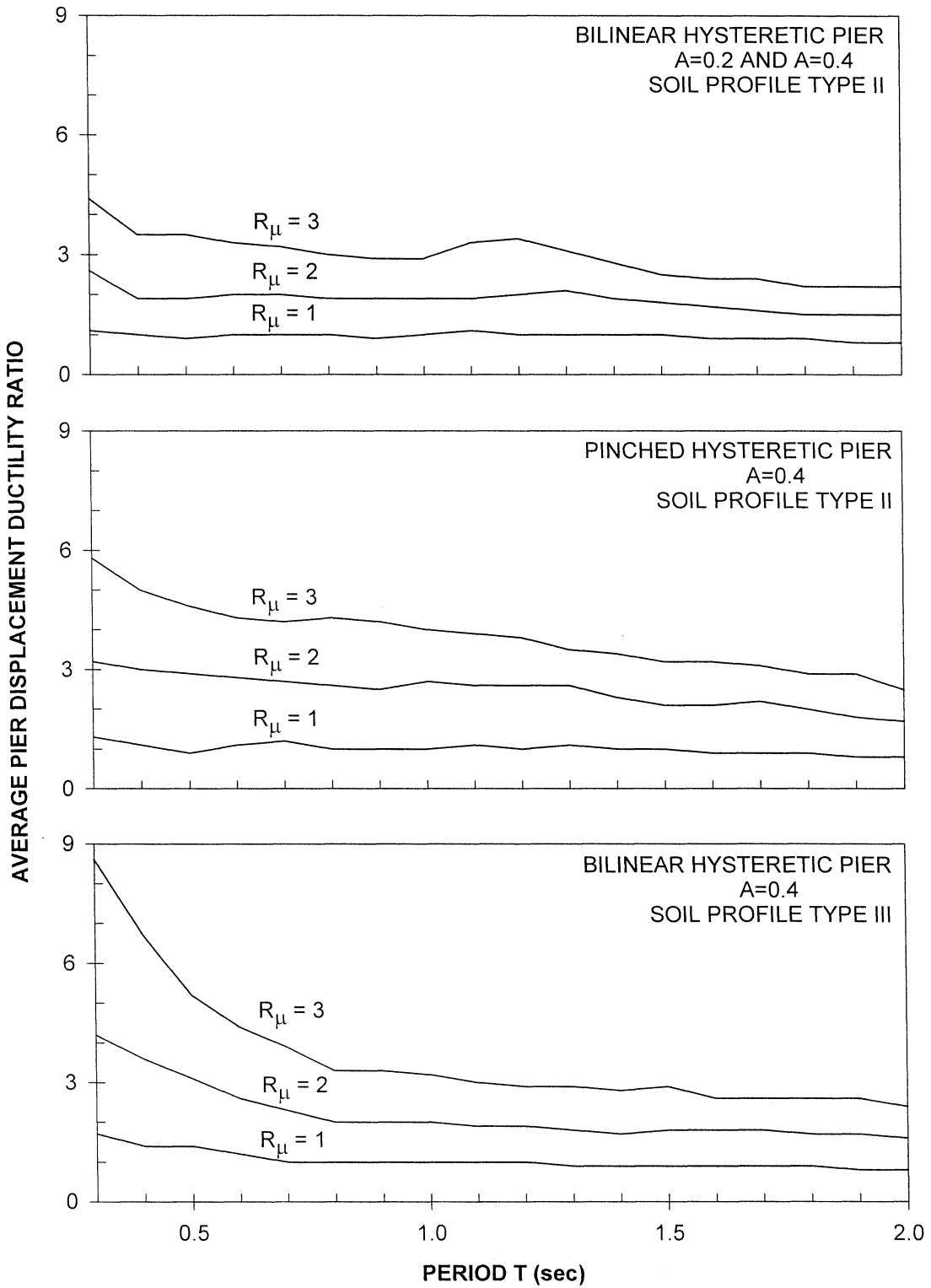


Figure 4-1 Average Pier Displacement Ductility Ratio of Non-isolated Bridge

displacement ductility ratio for soil profile type III should be viewed as conservative in the short period range.

- (3) There is a noticeable increase in the displacement ductility ratio when pinched hysteretic pier behavior is considered.

In addition to the average displacement ductility ratio, of interest is the variability of the substructure response about this average ratio. Compiled from the data in Appendix C, Figures 4-2 to 4-4 present the calculated maximum, average and minimum displacement ductility ratio for each considered value of period and R_{μ} . It may be observed that the variability in the response is consistent with the variability in the seismic input as illustrated in the response spectra of Figures 3-4 and 3-5.

4.2 Results for Seismic-Isolated Bridge Obtained by Uniform Load Method of AASHTO Guide Specifications

Results obtained on the response of the isolated bridge by the Uniform Load Method of the 1977 AASHTO "Guide Specifications for Seismic Isolation Design" (see Section 3.5) are used only for establishing the actual strength of the pier (upon division by R_{μ}) prior to performing nonlinear dynamic analysis. Nevertheless, the results are useful and are presented in graphical form in Appendix D. These results are in terms of the peak isolation system (or bearing) displacement and the peak shear force at the top of the pier. It should be noted that these results are based on the assumption of elastic pier behavior and were obtained by equivalent linearization of the nonlinear isolation system. It is of interest to note that in some of the results of Appendix D for the case of linear elastic-linear viscous isolation system there is only a small difference between the results on

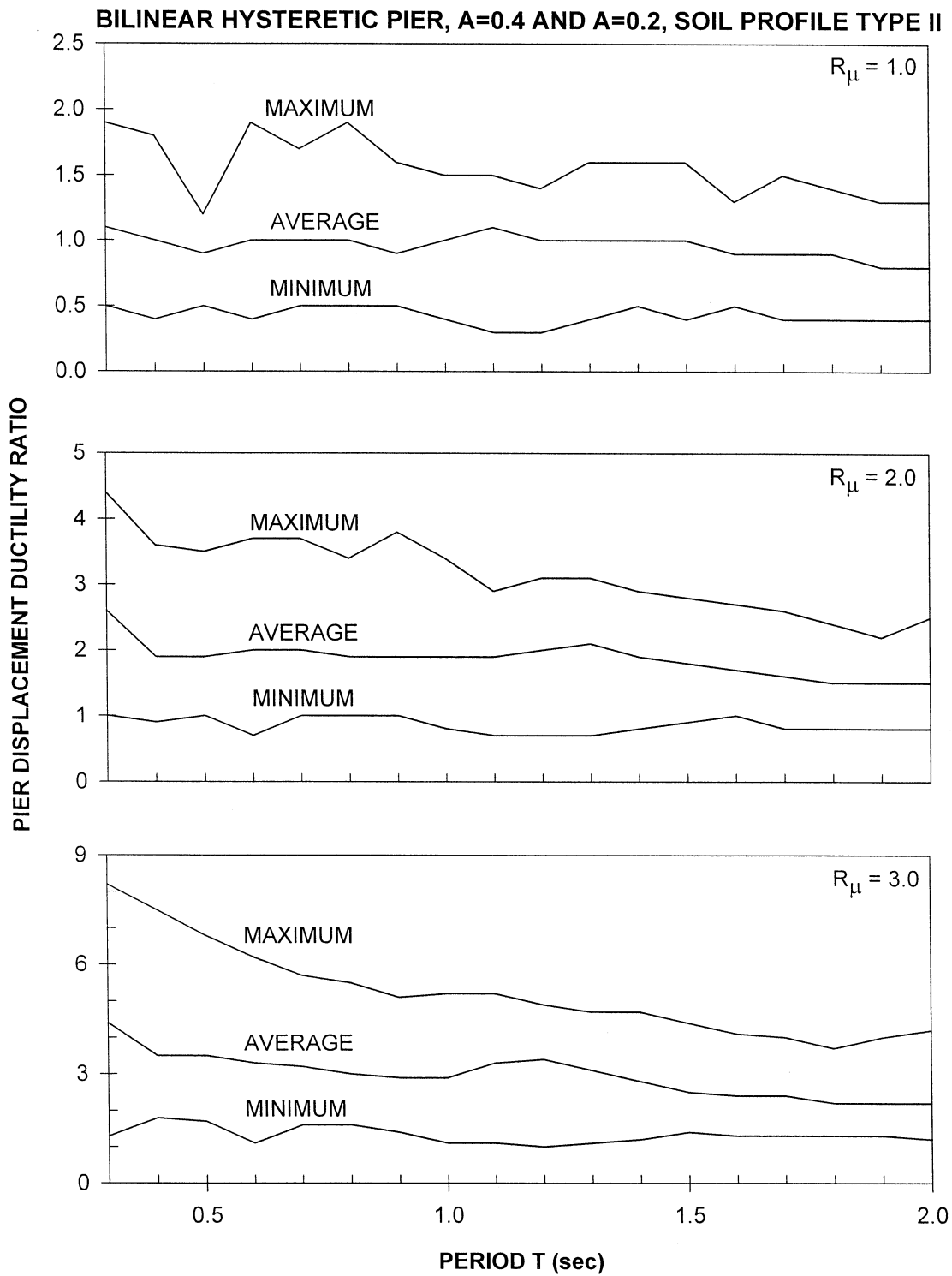


Figure 4-2 Variability in Pier Displacement Ductility Ratio of Non-isolated Bridge for the Case of Bilinear Hysteretic Pier and Soil Profile Type II Input

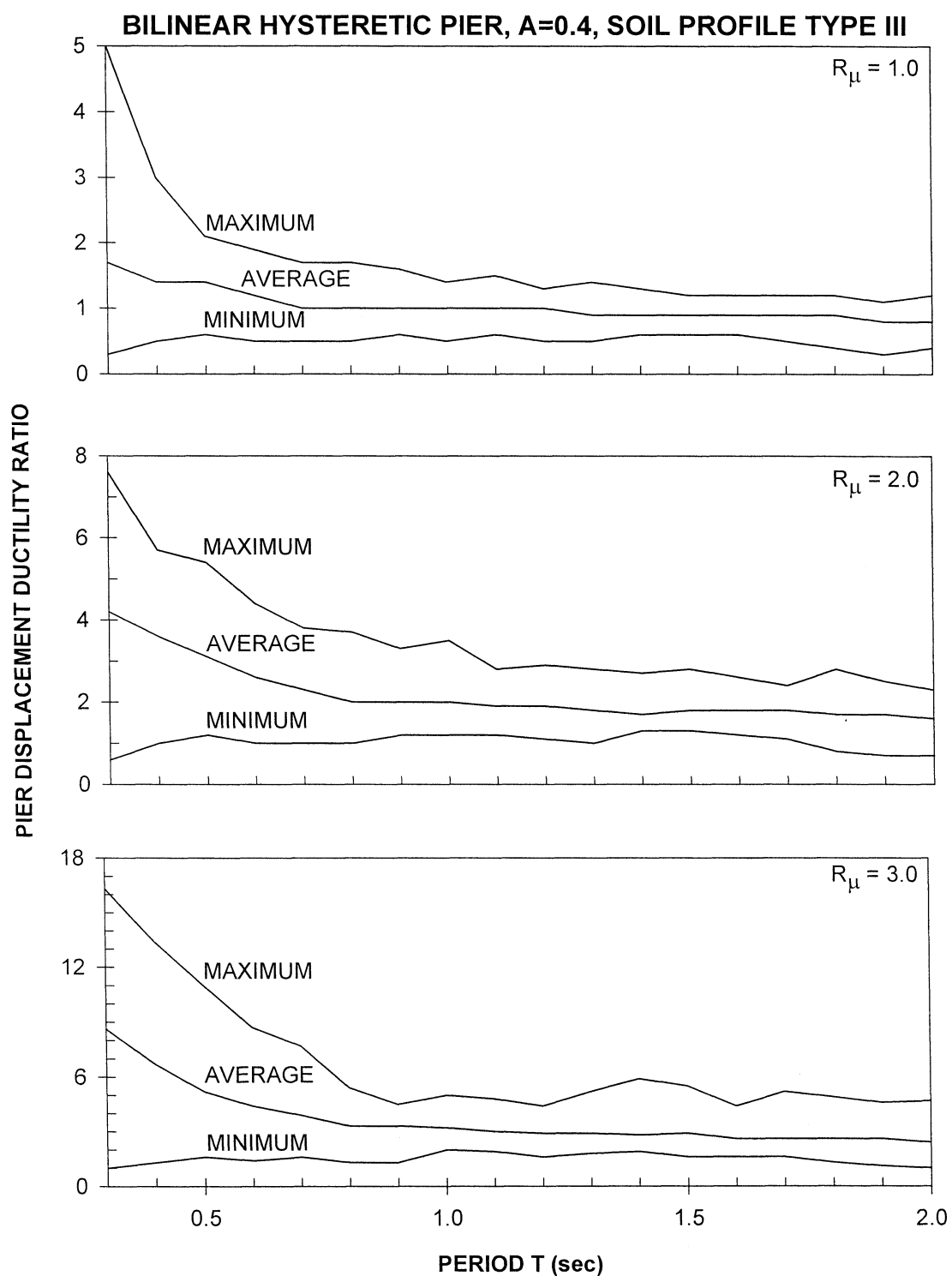


Figure 4-3 Variability in Pier Displacement Ductility Ratio of Non-isolated Bridge for the Case of Bilinear Hysteretic Pier and A = 0.4, Soil Profile Type III Input

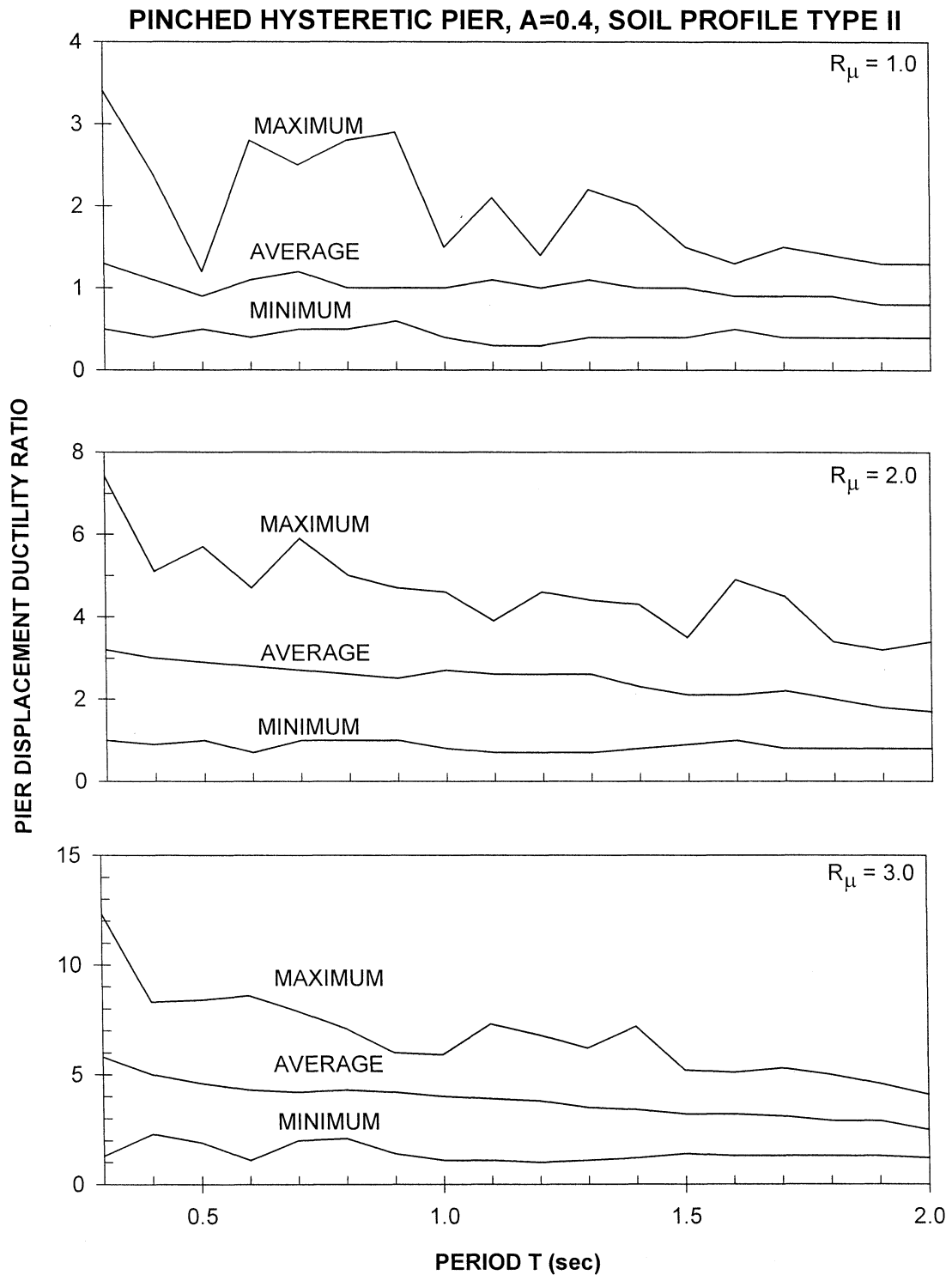


Figure 4-4 Variability in Pier Displacement Ductility Ratio of Non-isolated Bridge for Case of Pinched Hysteretic Pier Behavior and $A = 0.4$, Soil Profile Type II Input

displacements for damping ratio, ξ , of 0.3 and 0.4. The reason is that for the latter case the effective damping, β , exceeded the limit of 0.3. Accordingly, the damping related coefficient B was set at 1.7, resulting in a larger displacement in the isolation system.

4.3 Results of Nonlinear Dynamic Analysis of Seismic-Isolated Bridge

Results of the nonlinear dynamic analysis of the seismic-isolated bridge are presented in Appendices E to J. These appendices contain several graphs on a single page. Each page corresponds to a specific combination of pier behavior and isolation system behavior, a specific AASHTO response spectrum, and specific values of weight ratio $v = W_d/W_p$, pier period T_p and factor R_μ .

Each graph contains four curves that correspond to four different values of the isolation system characteristic strength or four values of the viscous damping ratio in the isolation system. Four graphs are presented on each page. Each presents the **average value** of the following response quantities as function of period T_b of the isolation system:

- (a) Pier displacement ductility ratio,
- (b) Peak bearing (or isolation system) displacement,
- (c) Peak shear force at the pier top (this is the force transmitted by the isolation system), and
- (d) Peak shear force at the base of the pier (this force differs from the force at the pier top due to acceleration of the pier).

A review of these results produces the following observations on the influence of various parameters on the average pier displacement ductility ratio:

(1) For bilinear hysteretic or sliding isolation systems the average pier ductility ratio is markedly affected by the pier period T_p . Particularly, the average ductility ratio is large for low values of this period. In discussing the significance of period T_p it is important to note that this period is the initial (elastic) period of the pier as if the pier were standing free, without the deck on top of it.

To relate the pier period T_p to period T of a non-isolated bridge we consider that the pier of the non-isolated bridge has the same stiffness as that of the seismic-isolated bridge. It can be easily shown that the initial period of the non-isolated bridge (model of Figure 3-7) T is given by

$$T = T_p (1 + \nu)^{1/2} \quad (4-1)$$

where $\nu = W_d/W_p$. In reality period T will be less than what (4-1) predicts given that the piers of non-isolated bridges are typically stiffer than those of seismic-isolated bridges. We may approximately write

$$T \approx T_p (1 + \nu)^{1/2} \left(\frac{F_{pis}}{F_{pni}} \right)^{0.7} \quad (4-2)$$

where F_{pis} = pier strength of isolated bridge and F_{pni} = pier strength non-isolated bridge. Equation (4-2) was derived on the assumption that the pier strength is proportional to the maximum stress under elastic conditions, which is proportional to the pier plan dimension to some power between 2 and 3. Moreover, the pier stiffness was assumed proportional to the pier plan dimension to some power between 3 and 4 (power 0.7 is the average of 2/3 and 3/4).

The ratio F_{pis}/F_{pni} is less than unity and its value depends on the soil conditions, period, response modification factor R , isolation system strength and isolation system period T_b . If we assume $F_{pis}/F_{pni} = 0.5$ then a value of $T_p = 0.1$ sec corresponds to a value of T equal to approximately 0.2 sec, thus a very stiff system. Moreover, a value $T_p = 0.5$ sec corresponds to a value T of the order of 1.0 sec. Therefore, the case $T_p = 0.1$ sec should be regarded as a lower bound, whereas the case $T_p = 0.5$ sec should be regarded as an upper bound on the pier period.

(2) For bilinear hysteretic or sliding isolation systems the average pier ductility ratio is affected by the characteristic strength and period T_b of the isolation system. Particularly, the ductility ratio is larger for the combination of large characteristic strength and large period T_b . This is due to the fact that large period T_b (flexible isolation system) and large characteristic strength (large equivalent damping) result in significant isolation effect for elastic substructure response. Accordingly, this increase in the ductility ratio is caused by the combination of low pier yield strength and large characteristic strength of the isolation system.

Reviewing the results of Appendix D we observe that for $A = 0.4$ the elastic pier shear force is, in general, larger than $0.15W_d$. Accordingly, the actual pier strength in the analyses was larger than $0.10 W_d$ (after division by $R_\mu = 1.5$, the largest value considered). Therefore, in all analyzed cases for $A = 0.4$ the strength of the strength of the pier was larger than (or at worst nearly the same as) the strength of the isolation system. The large displacement ductility ratio resulted for those cases in which the two strengths were close and has been primarily caused by some of the used seismic

motions which had significant demand for inelastic action in the pier. This brings up the issue of variability in the response which will be discussed later.

It is of interest to note in relation to the calculated large pier displacement ductility ratios the following. In the application of the Uniform Load Method of AASHTO (Section 3.5) a bound on the damping coefficient B of 1.7 was used (see eq. (3-4)) when the equivalent damping exceeded 0.3. Accordingly, for some of the analyzed cases (particularly large values of period T_b and strength Q_b/W_d) the isolation system displacement and the elastic pier force were conservatively estimated, that is, overestimated. Therefore, the ductility ratio has been underestimated by comparison to a system in which the true elastic pier force has been used to establish the yield strength of the pier.

- (3) The average pier displacement ductility for sliding isolation systems is less, but marginally so, than that for bilinear hysteretic isolation systems. There are two reasons for this difference. The first is related to the behavior of the two systems. Sliding isolation systems have slightly less isolation system displacements than comparable (same characteristic strength and period T_b) bilinear hysteretic isolation systems due to differences in the yield displacement. The second reason is related to the application of the Uniform Load Method of AASHTO. For the bilinear hysteretic isolation systems (see Section 3.5.1) the equivalent damping was slightly overestimated, resulting in a slightly lower elastic pier force than it should be.
- (4) The average pier displacement ductility ratio for linear elastic/linear viscous isolation systems is, in general, noticeably less dependent on the isolation system period T_b

than in the case of either bilinear hysteretic or sliding isolation systems. Specifically, the ductility ratio is about the same for the entire considered range of period T_p (1.5 to 3.0 sec) for soil profile type II. However, there is some dependency on period T_p for soil profile type III.

4.4 Pier Displacement Ductility Ratio for Seismic-Isolated Bridges

We concentrate on the pier displacement ductility ratio and present the results in a form that will allow comparison with the results for the case of the non-isolated bridge (Figs. 4-1 to 4.4). We choose to present results for the particular case of weight ratio $v = W_d/W_p = 10$ and pier period $T_p = 0.25s$ as being representative of the typical situation and with the understanding that lower values of the pier period T_p result in higher ductility ratio and vice versa. Moreover, we present results for the case of the bilinear hysteretic and the linear elastic and viscous isolation systems. It should be noted that sliding isolation systems exhibit a behavior similar to that of bilinear hysteretic isolation systems.

Figures 4-5 to 4-7 present graphs of maximum, average and minimum pier displacement ductility ratio calculated for the bilinear hysteretic isolation system with $\delta = Q_b/W_d = 0.06$ and for the linear elastic and viscous system with $\xi = 0.2$. The latter system is characterized by an equivalent damping of 0.2 or less, whereas in the former the equivalent damping varies depending primarily on the input and the period T_b . In general, it is in the range of 0.10 to 0.25 for $A = 0.4$, soil profile type II input, in the range of 0.25 to 0.40 for $A = 0.2$, soil profile type II input, and in the range of 0.08 to 0.18 for $A = 0.4$, soil profile type III input.

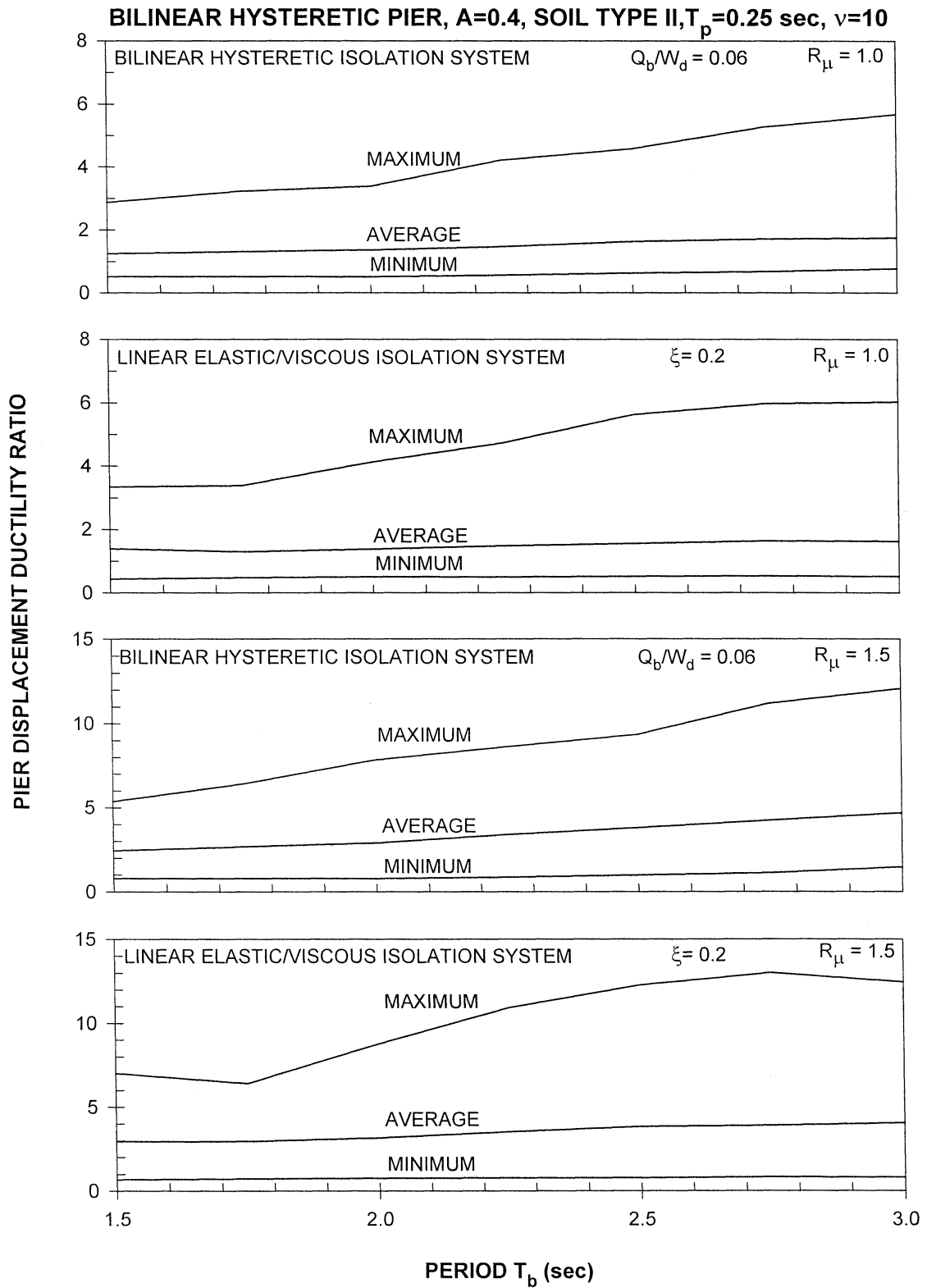


Figure 4-5 Variability in Pier Displacement Ductility Ratio of Isolated Bridge for $A = 0.4$, Soil Profile Type II Input and Bilinear Hysteretic Pier Behavior. Cases $\delta = 0.06$, $\xi = 0.2$

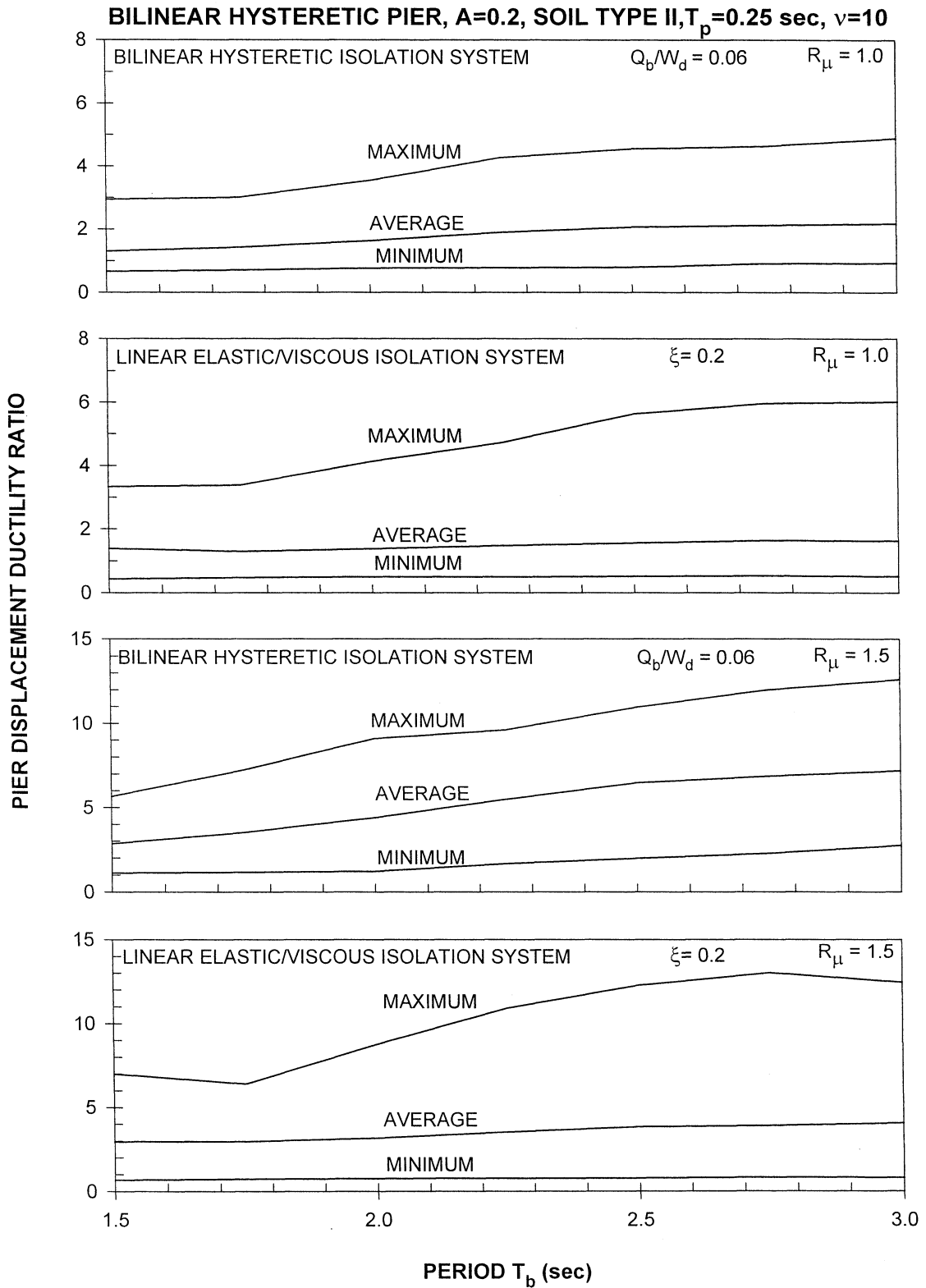


Figure 4-6 Variability in Pier Displacement Ductility Ratio of Isolated Bridge for $A = 0.2$, Soil Profile Type II Input and Bilinear Hysteretic Pier Behavior. Cases $\delta = 0.06$, $\xi = 0.2$

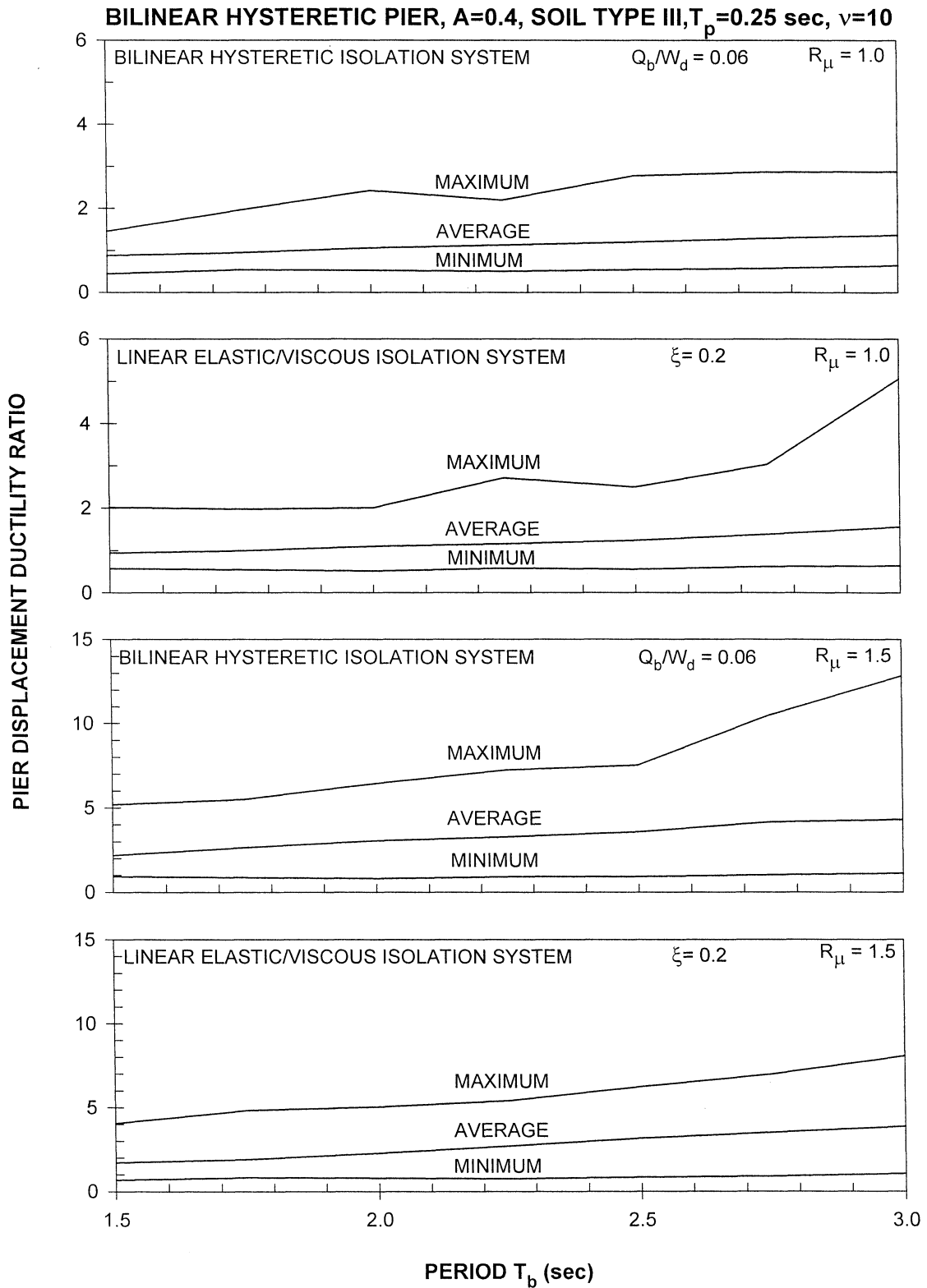


Figure 4-7 Variability in Pier Displacement Ductility Ratio of Isolated Bridge for $A = 0.4$, Soil Profile Type III Input and Bilinear Hysteretic Pier Behavior. Cases $\delta = 0.06$, $\xi = 0.2$

Similarly Figures 4-8 and 4-9 present graphs of the maximum, average and minimum pier displacement ductility ratio calculated for the bilinear hysteretic isolation system with $\delta = Q_b/W_d = 0.10$ and for the linear elastic and viscous isolation system with $\xi = 0.3$. In the latter case the equivalent damping was 0.3 or less. In the former case the equivalent damping varied in the range of 0.20 to 0.37 for $A = 0.4$, soil profile type II input, and in the range of 0.15 to 0.30 for $A = 0.4$, soil profile type III input.

Finally, Figure 4-10 presents graphs of the maximum average and minimum pier displacement ductility ratio calculated for the case of the pinched hysteretic pier and for the bilinear hysteretic isolation system with $\delta = Q_b/W_d = 0.06$ and 0.10.

A comparison of the results in Figures 4-5 to 4-10 to those in Figures 4-2 to 4-4 for the non-isolated bridge reveals a wider spread of ductility ratio values around the average value for the isolated than for the non-isolated bridge. For a more meaningful comparison we have to select an appropriate period of the non-isolated bridge to be comparable to the pier period in the isolated bridge. On the basis of (4-2) for $T_p = 0.25$ sec, $\nu = 10$ and $F_{pis}/F_{pni} \approx 0.5$ a period of the non-isolated bridge $T \approx 0.5$ sec is calculated.

Accordingly, the results of Figures 4-5 to 4-10 are compared to those of the non-isolated bridge (Fig. 4-1 to 4-4) at a period of about 0.5 sec. At this period, the maximum pier displacement ductility ratio in the non-isolated bridge is approximately twice or less than the average ductility ratio. For the isolated bridge the maximum pier displacement ductility ratio is about two to three times the average ductility ratio. In general, this wider spread of ductility ratio values indicates more sensitivity of the substructure inelastic response of isolated bridges to the details of the seismic input.

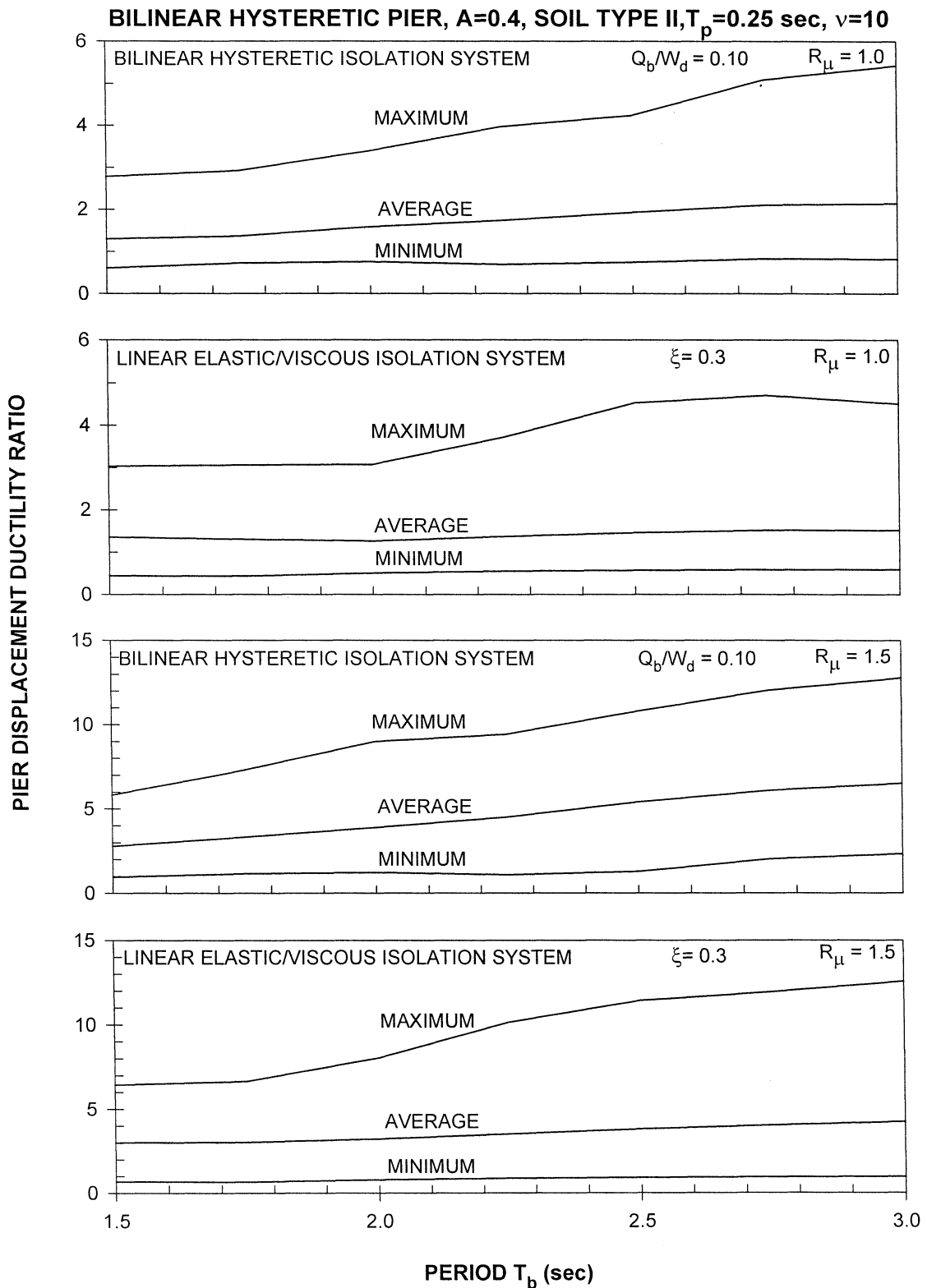


Figure 4-8 Variability in Pier Displacement Ductility Ratio of Isolated Bridge for $A = 0.4$, Soil Profile Type II Input and Bilinear Hysteretic Pier Behavior. Cases $\delta = 0.10$, $\xi = 0.3$

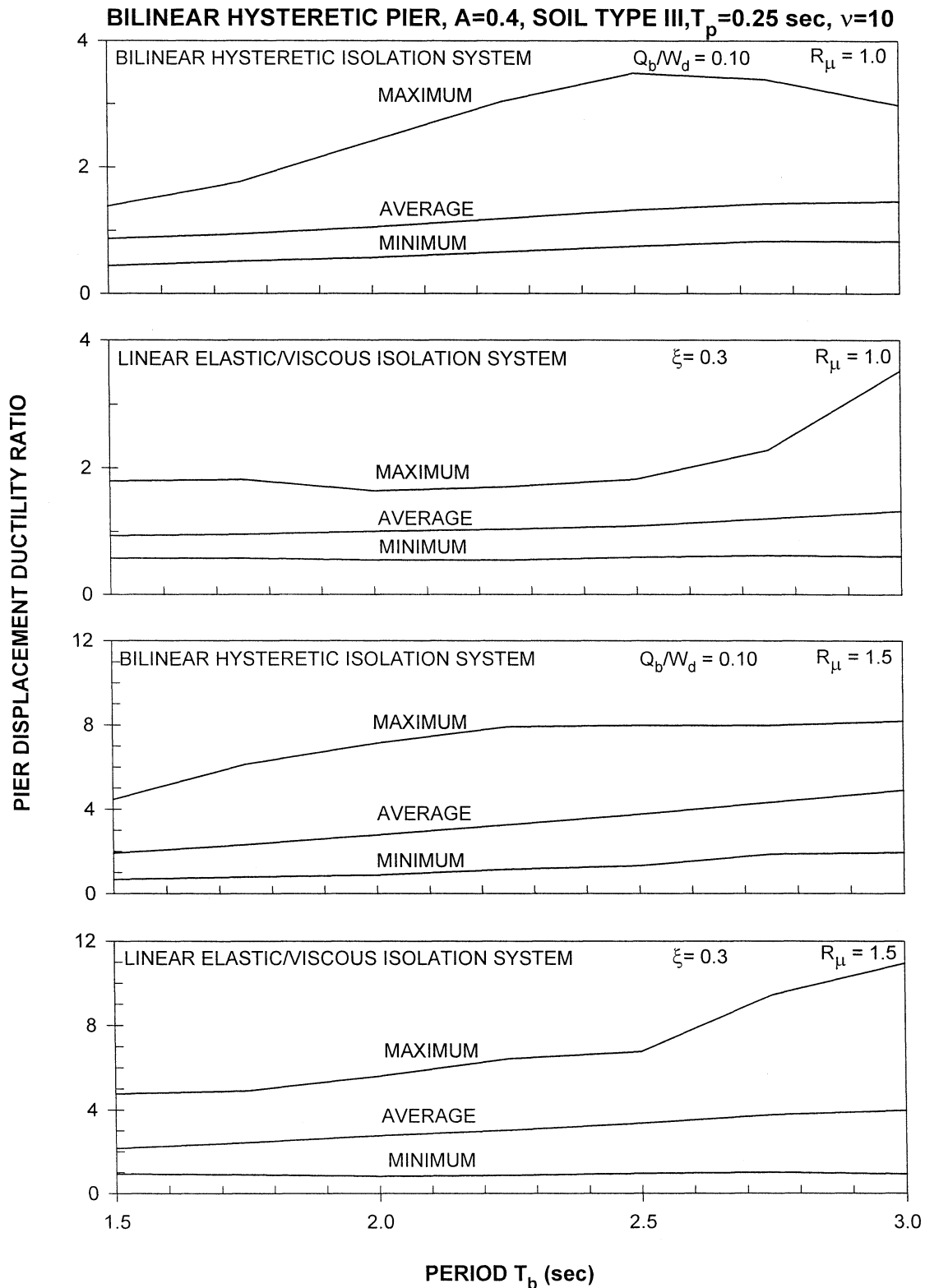


Figure 4-9 Variability in Pier Displacement Ductility Ratio of Isolated Bridge for $A = 0.4$, Soil Profile Type III Input and Bilinear Hysteretic Pier Behavior. Cases $\delta = 0.10$, $\xi = 0.3$

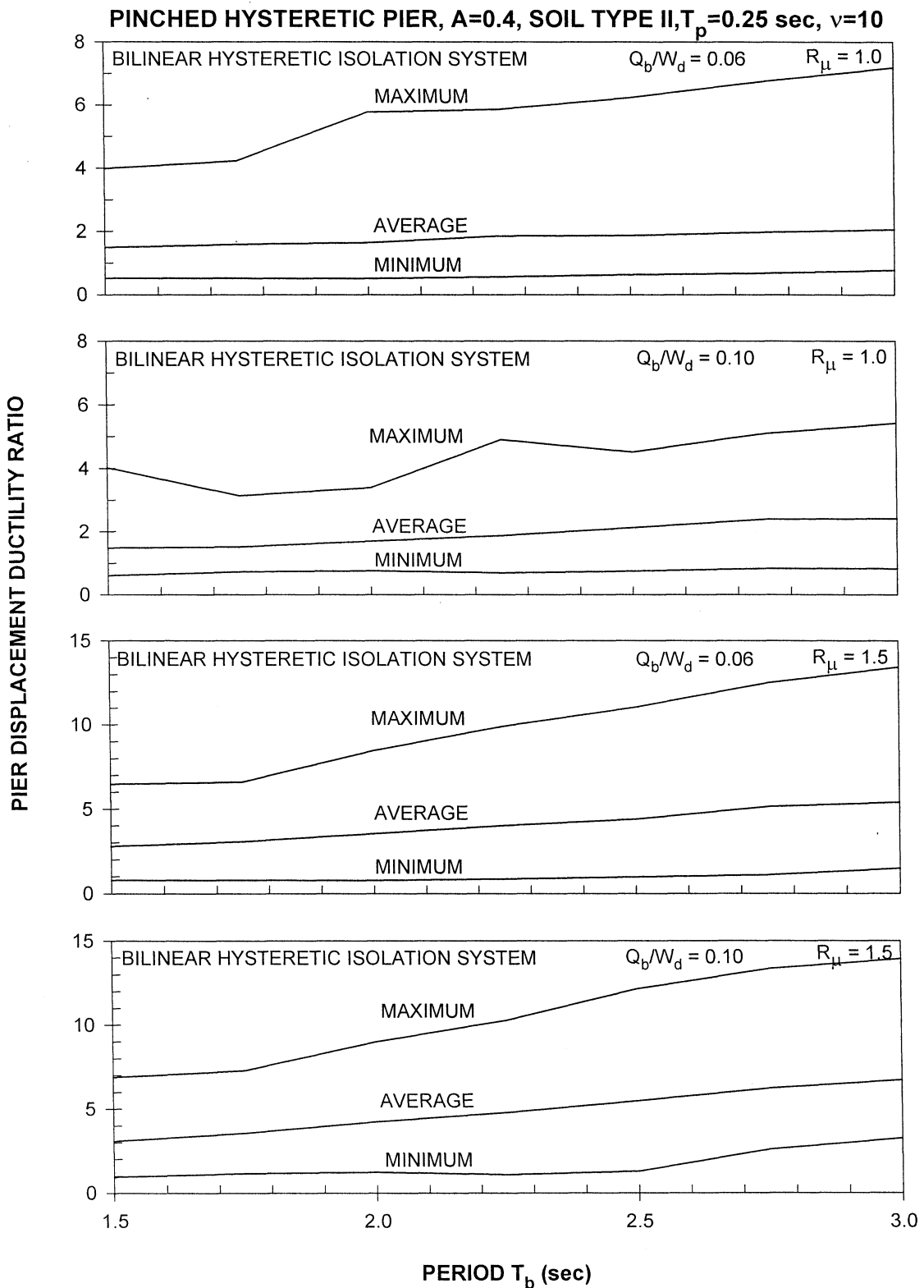


Figure 4-10 Variability in Pier Displacement Ductility Ratio of Isolated Bridge for $A = 0.4$, Soil Profile Type II Input and Pinched Hysteretic Pier Behavior. Cases $\delta = 0.06$, $\xi = 0.10$

Concentrating now on the average pier displacement ductility ratio, Tables 4-1 and 4-2 include the range of calculated values for the isolated bridge and for the comparable non-isolated bridge of $T = 0.5$ sec. For the isolated bridge the range of values is due to the isolation system period T_b varying between 1.5 and 3.0 sec. A comparison of values indicates that the isolated bridge with $R_\mu = 1.5$ has comparable values of the average pier displacement ductility ratio with the non-isolated bridge with $R_\mu = 3.0$. Similarly, the isolated bridge with $R_\mu = 1.0$ has comparable values of the ductility ratio with the non-isolated bridge designed for R_μ in the range 1.0 to 2.0.

Table 4-1 Average Pier Displacement Ductility Ratio of Non-Isolated Bridge with $T = 0.5$ sec

System	$R_\mu = 1.0$	$R_\mu = 2.0$	$R_\mu = 3.0$
Bilinear Hysteretic Pier $A = 0.4$, Soil Type II	0.9	1.9	3.5
Bilinear Hysteretic Pier $A = 0.4$, Soil Type III*	1.4	3.1	5.2
Pinched Hysteretic Pier $A = 0.4$, Soil Type II	0.9	2.9	4.6

*Conservative values (see Fig. 3-5 and related commentary)

Based on these results, the demonstrated sensitivity of the substructure inelastic response of isolated bridges to the details of the seismic input, and the increased pier displacement ductility ratio when the pier is stiff or when the isolation system is of low stiffness and of high characteristic strength, it is appropriate to design the substructure of isolated bridges with a R_μ -factor of 1.5 or less.

Ideally and considering that current specifications specify R-values on the basis of the type of substructure without consideration of the influences of the pier period and isolation system properties, the R_{μ} value for isolated bridges should be unity.

Table 4-2 Average Pier Displacement Ductility Ratio of Isolated Bridge with $T_p = 0.25$ sec, $\nu = 10$

System	$R_{\mu} = 1.0$	$R_{\mu} = 1.5$
Bilinear Hysteretic Pier, A = 0.4, Soil Type II, Bilinear Hysteretic Isolation System $\delta = 0.06$	1.2 - 1.8	2.4 - 4.7
Bilinear Hysteretic Pier, A = 0.4, Soil Type II, Bilinear Hysteretic Isolation System $\delta = 0.10$	1.3 - 2.1	2.8 - 6.5
Bilinear Hysteretic Pier, A = 0.4, Soil Type II, Linear Elastic/Viscous Isolation System $\xi = 0.2$	1.4-1.6	3.0 - 4.0
Bilinear Hysteretic Pier, A = 0.4, Soil Type II, Linear Elastic/Viscous Isolation System $\xi = 0.3$	1.4 - 1.5	3.0 - 4.2
Bilinear Hysteretic Pier, A = 0.4, Soil Type III, Bilinear Hysteretic Isolation System $\delta = 0.06$	0.9 - 1.4	2.2 - 4.3
Bilinear Hysteretic Pier, A = 0.4, Soil Type III, Bilinear Hysteretic Isolation System $\delta = 0.10$	0.9 - 1.5	1.9 - 4.9
Bilinear Hysteretic Pier, A = 0.4, Soil Type III, Linear Elastic/Viscous Isolation System $\xi = 0.2$	0.9 - 1.6	1.7 - 3.9
Bilinear Hysteretic Pier, A = 0.4, Soil Type III, Linear Elastic/Viscous Isolation System $\xi = 0.3$	0.9 - 1.3	2.2 - 4.0
Pinched Hysteretic Pier, A = 0.4, Soil Type II, Bilinear Hysteretic Isolation System $\delta = 0.06$	1.5 - 2.1	2.8 - 5.4
Pinched Hysteretic Pier, A = 0.4, Soil Type II, Bilinear Hysteretic Isolation System $\delta = 0.10$	1.5 - 2.4	3.1 - 6.7

4.5 Concluding Remarks

Isolated bridges exhibit a sensitivity in the substructure inelastic response due to the variability in the seismic input. This sensitivity of the response is more pronounced than that in non-isolated bridges.

Design of the substructure of isolated bridges for an R_{μ} factor of 1.5 or less results in a comparable average substructure displacement ductility ratio with non-isolated bridges for which the substructure is designed for an R_{μ} -factor of 3.0 or less. However, for certain substructure and isolation system configurations, such as stiff pier and low stiffness/high characteristic strength isolation system configurations, it may be appropriate to design for an R_{μ} value of 1.0.

The R-factor for an isolated bridge should thus be the product of the R_{μ} -factor (range 1.0 to 1.5) and the overstrength factor. The latter is, in general, the same or slightly larger in isolated bridges than in non-isolated bridges. This will be demonstrated in Section 5. If we accept a value of about 1.5 for the overstrength factor of isolated bridges, then R-factors in the range of 1.5 to 2.5 are calculated. This range of values is specified in the 1997 "AASHTO Guide Specifications" (American Association of State Highway and Transportation Officials, 1997).

SECTION 5

OVERSTRENGTH AND RESPONSE MODIFICATION FACTORS

5.1 Introduction

The overstrength factor is defined as the ratio of the lateral force on the system when a collapse mechanism develops to the lateral force on the system when the first plastic hinge develops. It can be calculated by pushover analysis on the basis of nominal properties for the materials. The actual overstrength factor can then be obtained by increasing the calculated value due to known or assumed effects of strain hardening, rate effects and actual material properties.

It may be inferred from the AASHTO "Standard Specifications" (American Association of State Highway and Transportation Officials, 1996) that the assumed overstrength factor for bridge substructures is in the range of about 1.0 to over $5/3 = 1.67$. For example, single columns which lack redundancy are assigned an R-factor of 3.0. This figure includes the ductility based portion and likely a multiplier of just above unity for material overstrength, etc. Well-detailed multiple column bents are assigned an R-value of 5.0. Since both types of substructures are considered to have similar ductility capacity, the difference is entirely due to redundancy. That is, the overstrength due to structural redundancy is $5/3 = 1.67$. Therefore, the overstrength factor for multiple column bents is larger than 1.67. This observation is sufficient to conclude that appropriate values of R-factor for the substructures of isolated bridges are in the range of 1.5 to 2.5 (assuming appropriate values of R_{μ} of 1.0 for substructures with minimal

ductility capacity, 1.5 for substructures with good ductility capacity, and R_o values of just over 1.0 for substructures without redundancy and 1.67 for substructures with redundancy).

Therefore, the appropriate values of R-factor for the substructures of isolated bridges are exactly as currently specified in the 1997 AASHTO "Guide Specifications" (American Association of State Highway and Transportation, 1997). Accordingly, further work related to the establishment of overstrength factors for isolated bridges is unnecessary. Nevertheless, it is of interest to provide at least a rudimentary analysis of overstrength. Accordingly, we obtain herein expressions for the overstrength factor of simple non-isolated and isolated bridges for the single purpose of demonstrating that this factor is, in general, the same or slightly higher in isolated bridges than in non-isolated bridges.

5.2 Overstrength Factor of Non-isolated Bridges

Consider the simple bridge model of Figure 5-1. The superstructure (deck) is assumed rigid, and each pier is assumed to have elastic stiffness K_i and to simultaneously form plastic hinges at its two ends. The latter assumption implies that the inflection point is in the middle of each pier, a situation that is affected by the distribution of stiffness and strength in the pier, and the deck and foundation flexibilities. The assumption of simultaneous formation of plastic hinges at both ends leads to a larger level of force F_F at which the first plastic hinge develops and accordingly to lower value of the overstrength factor.

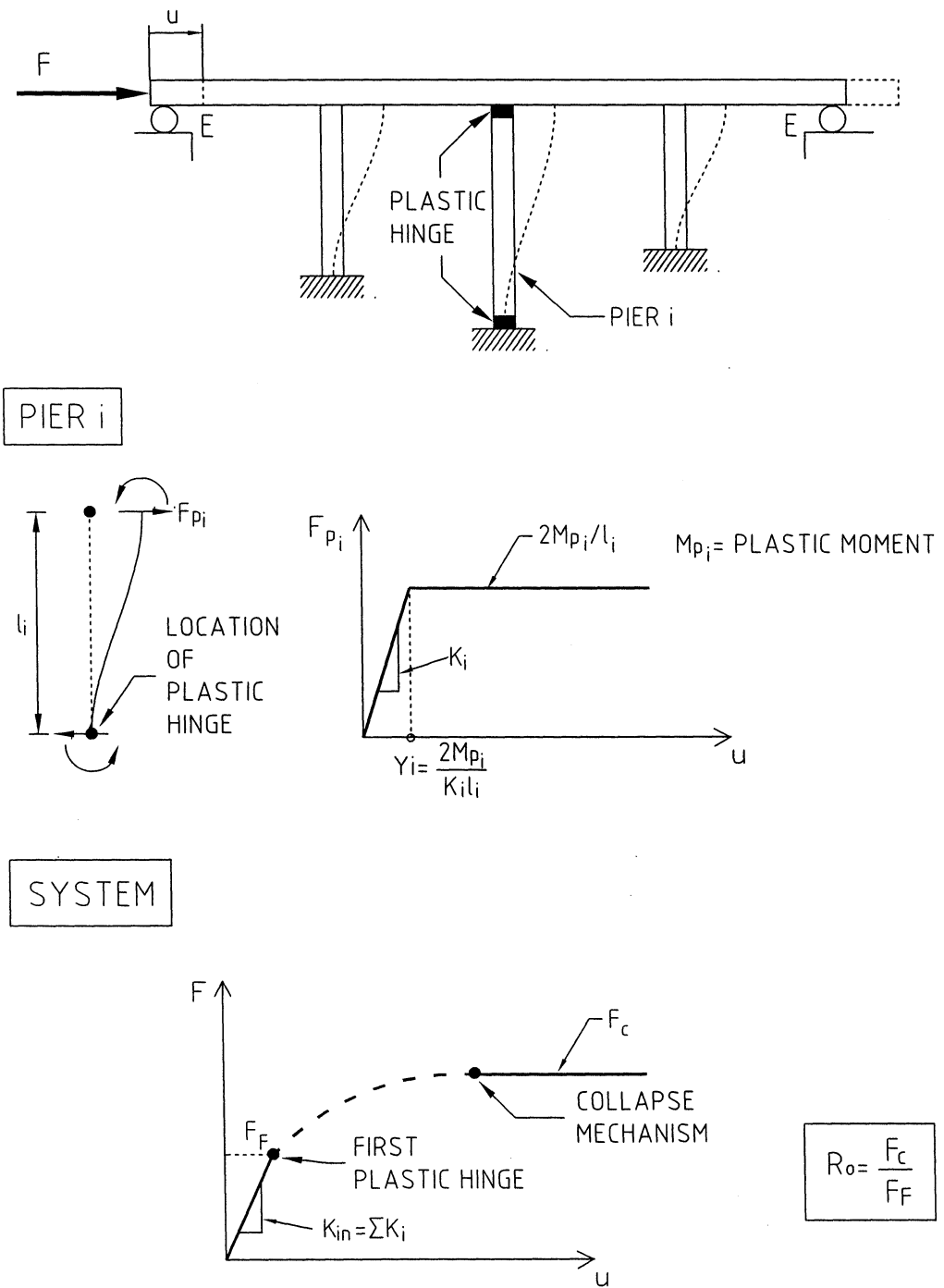


Figure 5-1 Non-isolated Bridge and Force-Displacement Relations in Longitudinal Direction for Rigid Superstructure

The force-displacement relations for each pier and of the system are shown in Figure 5-1 where M_{pi} = plastic moment at both ends of pier i , F_F = force at which the first plastic hinge develops, and F_c = force at which a collapse mechanism develops. The first plastic hinge develops when the displacement of the deck reaches the limit

$$U = \min_i \left(\frac{2M_{pi}}{K_i l_i} \right) \quad (5-1)$$

that is, the minimum yield displacement among the N piers. Accordingly, the force at formation of the first plastic hinge is

$$F_F = \min_i \left(\frac{2M_{pi}}{K_i l_i} \right) \cdot \sum_{i=1}^N K_i \quad (5-2)$$

where $\sum_{i=1}^N K_i$ denotes the sum of the elastic stiffness of all piers.

The collapse mechanism develops when plastic hinges develop at both ends of all piers. Accordingly,

$$F_c = \sum_{i=1}^N \left(\frac{2M_{pi}}{l_i} \right) \quad (5-3)$$

The overstrength factor is the ratio F_c/F_F :

$$R_o = \frac{\sum_{i=1}^N \left(\frac{2M_{pi}}{l_i} \right)}{\min_i \left(\frac{2M_{pi}}{K_i l_i} \right) \cdot \sum_{i=1}^N K_i} \quad (5-4)$$

Note that (5-4) produces a conservative estimate of the overstrength factor due to the assumption of simultaneous plastic hinge formation at both ends. However, it derived without consideration of P- Δ moment effects, consideration of which would have resulted

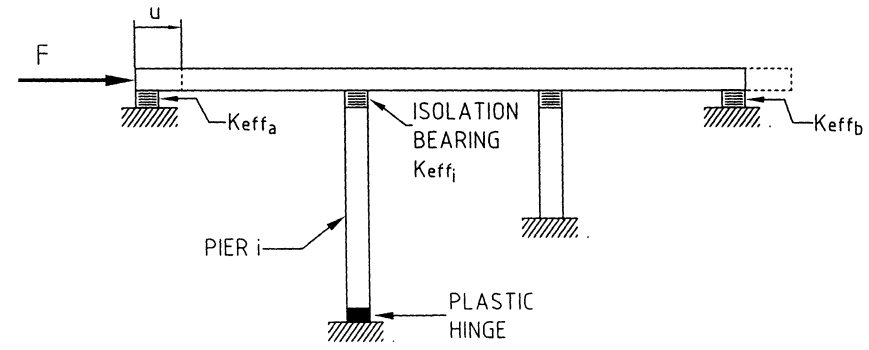
in a lower R_o value. Consideration of these effects requires that systematic pushover analysis is performed. Nevertheless, (5-4) provides insight into the factors affecting overstrength and produces quick estimates of the overstrength factor. As an example, consider the case of a two-span continuous deck with a single pier. Equation (5-4) produces the obvious result $R_o = 1.0$. The actual value will be higher due to the aforementioned effects of strain rate, material overstrength, strain hardening, etc.

5.3 Overstrength Factor of Seismic-Isolated Bridges

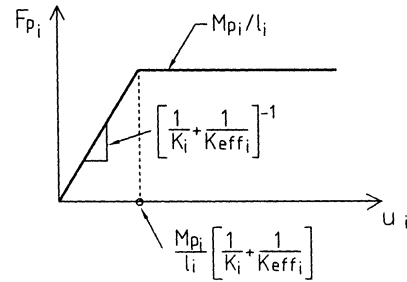
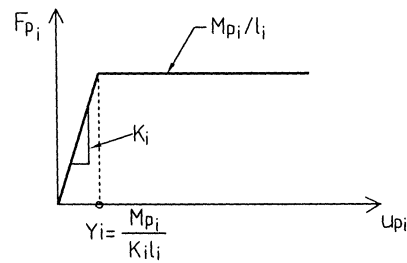
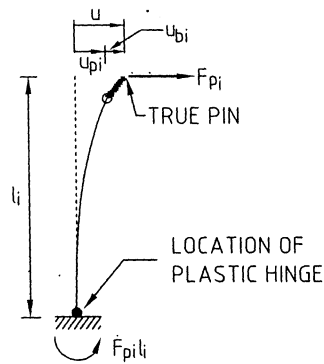
Figure 5-2 shows the considered simple seismic-isolated bridge model. The isolation bearings on top of each pier have effective stiffness K_{effi} , whereas those at the two abutments have effective stiffnesses K_{effa} and K_{effb} , respectively. Each pier has elastic stiffness K_i (which is not the same as that of the piers of the non-isolated bridge) and the assumption is made that plastic hinges form at the base of each pier. That is, each pier is treated as a vertical cantilever. Moreover, P- Δ moment effects are neglected. These effects include a component due to the pier top deformation (which was also neglected in the case of the non-isolated bridge) and a component due to the isolation bearing deformation. This component depends on the type of isolation bearing. In particular, it is zero only for the case of sliding bearings (e.g., FPS bearings) when placed with the sliding surface facing up.

The force F_F at first plastic hinge formation is determined as follows. The initial stiffness of the system is given by

$$K_{in} = K_{effa} + K_{effb} + \sum_{i=1}^N \left[\frac{1}{K_i} + \frac{1}{K_{effi}} \right]^{-1} \quad (5-5)$$



PIER i



SYSTEM

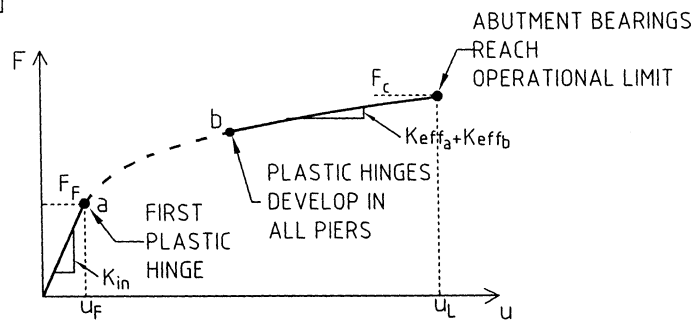


Figure 5-2 Seismic-isolated Bridge and Force-Displacement Relations in Longitudinal Direction for Rigid Superstructure

The displacement of the system at first plastic hinge formation (see Fig. 5-2) is

$$U_F = \min_i \left\{ \frac{M_{pi}}{l_i} \left(\frac{l}{K_i} + \frac{l}{K_{effi}} \right) \right\} \quad (5-6)$$

The force F_F is then given by

$$F_F = K_{in} U_F \quad (5-7)$$

The force beyond the stage of plastic hinge formation in all piers at which the abutment bearings can safely operate is given by:

$$F_c = \sum_{i=1}^N \left(\frac{M_{pi}}{l_i} \right) + (K_{effa} K_{effb}) U_L \quad (5-8)$$

where U_L = maximum deck displacement with respect to ground at which the abutment bearings operate safely. It should be noted that the effective stiffnesses K_{effa} , K_{effb} and K_{effi} in (5-5) are established at the displacement U_F , whereas the effective stiffnesses K_{effa} and K_{effb} in (5-8) are established at the displacement U_L .

The overstrength factor is obtained as

$$R_o = \frac{F_c}{F_F} \quad (5-9)$$

Equations (5-5) to (5-9) determine the overstrength factor. They also reveal the effect of various aspects of isolation system design. For example, the first two terms in (5-5) and the last term in (5-8) describe the effect of redistribution of the inertia force to the isolation elements at the abutment locations. This redistribution affects both the force at the formation of the first plastic hinge and force F_c . Moreover, these equations and Figure 5-2 demonstrate that isolated bridges may have higher overstrength than non-

isolated bridges due to the fact that the force F_c occurs at some displacement larger than that at which plastic hinges develop in all piers. That is when point b is reached on the force-displacement (pushover) curve of the system (see Fig. 5-2), there is further capacity to resist force until the abutment bearings reach their operational limit. This limit, which corresponds to displacement U_L , is not the ultimate force but some lesser force at which the abutment bearings still have positive stiffness. This implies, of course, that the isolation system is designed with a displacement capacity larger than the design displacement.

5.4 Concluding Remarks

The overstrength factor for seismic-isolated bridges is either the same as that of non-isolated bridges or slightly higher. The former case occurs in multi-span bridges in which the abutment bearings may be assumed to contribute little to the redundancy of the system. The latter case occurs in bridges with a small number of spans in which the abutment bearings contribute to the redundancy of the system.

Considering that the overstrength factor for isolated bridges is the same as that for non-isolated bridges, its value ranges between something above unity for substructures without structural redundancy (e.g., single columns) and 1.67 for substructures with redundancy (e.g., multiple column bents). Moreover, considering R_{μ} values in the range of 1.0 to 1.5 (depending on the ductility capacity), Table 5-1 has been prepared to include appropriate values of R-factor for substructures of isolated bridges. These values are identical, or slightly larger than those in the 1997 AASHTO "Guide Specifications" (American Association of State Highway and Transportation Officials, 1997).

Table 5-1 Appropriate Values of R-factor for Substructures of Seismic-Isolated Bridges

Substructure	R_{μ}	R_o	R
Wall-Type Pier (Strong Direction)	1.0	1.67	1.67
Wall-Type Pier (Weak Direction, Designed as a Column)	1.5	1.0	1.5
Single Columns	1.5	1.0	1.5
Multiple Column Bent	1.5	1.67	2.5

SECTION 6

CONCLUSIONS

This study has been concerned with establishing appropriate response modification factors for the substructures of seismic-isolated bridges. The study had two specific objectives:

- (a) To establish R-factors for isolated bridges on the basis of the assumption that the currently specified R-factors in the "AASHTO Standard Specifications" (American Association of State Highway and Transportation Officials, 1996) for the substructures of non-isolated bridges are appropriate. That is, the study has been concerned with the evaluation of the seismic demand on the substructures of isolated bridges and not the evaluation of their seismic capacity. Rather, the latter was presumed known.
- (b) To present the conceptual framework, the underlying reasons and analysis results that necessitate the use of lower R-factors for isolated bridges as they are specified in the 1997 AASHTO "Guide Specifications" (American Association of State Highway and Transportation Officials, 1997).

An analysis of simple models of non-isolated and of seismic-isolated bridges has been performed. A range of isolation system types, isolation system properties and of substructure behaviors has been considered. Moreover, seismic excitation representative of the AASHTO $A = 0.4$ and 0.2 , soil profile type II and III response spectra were considered. The analysis resulted in values of the substructure displacement ductility

ratio, isolation system displacement and other relevant response quantities for particular configurations of the isolation system and/or substructure, and for a range of values of the ductility factor R_{μ} . On the basis of these results the following have been observed:

- (1) The average substructure displacement ductility ratio of seismic-isolated bridges is markedly affected by the substructure elastic period T_p , isolation system period T_b and ratio of characteristic strength of the isolation system to deck weight. Particularly, the displacement ductility ratio is highest when the strength ratio is large and the isolation system period is long (Table 4-2 provides information on the range of calculated values of the average ductility ratio). That is, the average displacement ductility ratio is highest for isolation systems configured for highest performance. The reason for this behavior is that in these systems the strength of the isolation system is marginally larger than that of the substructure.
- (2) The substructure displacement ductility ratio in isolated bridges having isolation systems with bilinear hysteretic and with sliding behaviors is essentially the same. However, the substructures of bridges with isolation systems having linear elastic/linear viscous behavior have displacement ductility ratios which are noticeably less dependent on the isolation system period T_b . This difference may be best observed in the data of Table 4-2. It is likely the result of the characteristic strength of these systems being velocity dependent rather than constant (like in the bilinear hysteretic or sliding isolation systems).
- (3) In general, seismic-isolated bridges exhibit greater sensitivity in their substructure inelastic response than non-isolated bridges. This sensitivity of response is due to the

variability in the seismic input. Figures 4-1 to 4-7 demonstrate this difference by presenting maximum, minimum and average values of the substructure displacement ductility ratio.

- (4) Design of the substructure of seismic-isolated bridges for an R_{μ} -factor in the range of 1.0 to 1.5 results in comparable average substructure displacement ductility with non-isolated bridges designed for an R_{μ} in the range of 1.0 to 3.0.
- (5) Seismic-isolated bridges exhibit overstrength that is the same or slightly higher than that of non-isolated bridges. The overstrength may be higher as result of increased structural redundancy due to redistribution (e.g., existence of isolation bearings with stiffness at the abutment locations).
- (6) The overstrength factor, R_o , for non-isolated bridges may be inferred from the specified R-factor values in the American Association of State Highway and Transportation Officials (1996). Values of this factor are presented in Table 5-1.

Based on these results it was concluded that R-factor values for the substructures of seismic-isolated bridges should be in the range of 1.5 to 2.5. Values for specific substructures are presented in Table 5-1. The recommended values are identical to or slightly higher than those in the 1997 AASHTO "Guide Specifications" (American Association of State Highway and Transportation Officials, 1997).

SECTION 7

REFERENCES

- American Association of State Highway and Transportation Officials (1991), "Guide Specifications for Seismic Isolation Design", Washington, D.C.
- American Association of State Highway and Transportation Officials (1996), "Standard Specifications for Highway Bridges", 16th Edition, Washington, D.C.
- American Association of State Highway and Transportation Officials (1997), "Guide Specifications for Seismic Isolation Design", Washington, D.C.
- Applied Technology Council (1978), "Tentative Provisions for the Development of Seismic Regulations for Buildings", Report No. ATC-3-06, Redwood City, California.
- Applied Technology Council (1995), "Structural Response Modification Factors", Report No. ATC-19, Redwood City, California.
- Baber, T. T., and Noori, M. N. (1985), "Random Vibration of Degrading, Pinching, Systems", Journal of Engineering Mechanics, ASCE, Vol. 111, No. 8, pp. 1010-1026.
- Commission of the European Communities (1988), "Structures in Seismic Regions – Design Part 1," Eurocode No. 8, Luxembourg.
- Constantinou, M. C., Soong, T. T., Dargush, G. F. (1998a), "Passive Energy Dissipation Systems for Structural Design and Retrofit", NCEER Monograph Series No. 1, National Center for Earthquake Engineering Research, Buffalo, NY.
- Constantinou, M. C., Tsopeles, P., Kasalanati, A. (1998b), "Property Modification Factors for Seismic Isolation Bearings", Technical Report NCEER-98 (to be published), Final Report on NCEER Highway Project Task 106-F-4.2.1(a), National Center for Earthquake Engineering Research, Buffalo, NY.
- Federal Emergency Management Agency (1997), "NEHRP Guidelines and Commentary for the Seismic Rehabilitation of Buildings", Reports FEMA 273 and FEMA 274, Washington, D.C.
- Gilbertsen, N. D., Moehle, J. P., Sozen, M. A. (1980), "Experimental Study of Small-Scale R/C Columns Subjected to Axial and Shear Force Reversals", Report NSF/RA-800495, National Science Foundation, Washington, D.C.
- Kasalanati, A. (1998), "Experimental Study of Bridge Elastomeric and other Isolation and Energy Dissipation Systems with Emphasis on Uplift Prevention and High Velocity Near-Source Seismic Excitation". Ph.D. Dissertation, State University of New York, Buffalo, NY.

- Kelly, J. M. (1993), "Earthquake-Resistant Design with Rubber" Springer-Verlag, London.
- Miranda, E., Bertero, V. V. (1994), "Evaluation of Strength Reduction Factors for Earthquake-Resistant Design", *Earthquake Spectra*, 10 (2), pp. 357-379.
- Reinhorn, A. M., Nagarajaiah, S., Constantinou, M. C., Tsopelas, P., Li, R. (1994), "3D-BASIS-TABS: Version 2.0 Computer Program for Nonlinear Dynamic Analysis of Three Dimensional Base Isolated Structures", Technical Report NCEER-94-0018, National Center for Earthquake Engineering Research, Buffalo, NY.
- Rojahn, C., Mayes, R., Anderson, D. G., Clark, J., Hom, J. H., Nutt, R. V., O'Rourke, M. J. (1997), "Seismic Design Criteria for Bridges and Other Highway Structures", Technical Report NCEER-97-0002, National Center for Earthquake Engineering Research, Buffalo, NY.
- Skinner, R. I., Robinson, W. H., and McVerry, G. H. (1993), "An Introduction to Seismic Isolation", J. Wiley, Chichester, UK.
- Soong, T. T., Constantinou, M. C. (1994), "Passive and Active Structural Vibration Control in Civil Engineering", Springer-Verlag, Wien-New York.
- Structural Engineers Association of California (1959), "Recommended Lateral Force Requirements and Commentary", Seismology Committee, Sacramento, California.
- Taylor, A. W., Kuo, C., Wellenius, K., Chung, D. (1997). "A Summary of Cyclic Lateral Load Tests on Rectangular Concrete Columns", Report NISTIR 5984, National Institute of Standards and Technology, Gaithersburg, Maryland.
- Tsopelas, P. C., Constantinou, M. C., Reinhorn, A. M. (1994), "3D-BASIS-ME: Computer Program for Nonlinear Dynamic Analysis of Seismically Isolated Single and Multiple Structures and Liquid Storage Tanks", Technical Report NCEER-94-0010, National Center for Earthquake Engineering Research, Buffalo, NY.
- Tsopelas, P., Constantinou, M. C., Kircher, C.A., Whittaker, A.S. (1997), "Evaluation of Simplified Methods of Analysis for Yielding Structures", Technical Report NCEER-97-0012, National Center for Earthquake Engineering Research, Buffalo, NY.
- Uang, Chia-Ming (1991), "Establishing R (or R_w) and C_d Factors for Building Seismic Provisions", *Journal of Structural Engineering*, ASCE, 117, (1), pp. 19-28.
- Uang, Chia-Ming (1993), "An Evaluation of Two-Level Seismic Design Procedure", *Earthquake Spectra*, 9(1), pp. 121-135.
- Wen, Y. K., (1976), "Method of Random Vibration of Hysteretic Systems", *J. Engineering Mechanics Division*, ASCE, 102, (EM2), pp. 249-263.

APPENDIX A

EQUATIONS OF MOTION OF ANALYZED SYSTEM

With reference to Figure 3-1 the equations of motion of the system are:

$$\left(\frac{W_d}{g}\right)\left(\ddot{U}_b + \ddot{U}_p + \ddot{U}_g\right) + F_b = 0 \quad (\text{A-1})$$

$$\left(\frac{W_d}{g}\right)\left(\ddot{U}_b + \ddot{U}_p + \ddot{U}_g\right) + \left(\frac{W_p}{g}\right)\left(\ddot{U}_p + \ddot{U}_g\right) + F_p = 0 \quad (\text{A-2})$$

where \ddot{U}_g = horizontal component of ground acceleration, g = acceleration of gravity,

F_b = force in the isolation system and F_p = shear force in the pier. A dot denotes differentiation with respect to time.

A.1 MODELING OF ISOLATION SYSTEM

(1) Bilinear Hysteretic Behavior

$$F_b = K_b U_b + Q_b Z_b \quad (\text{A-3})$$

$$Y_b \dot{Z}_b + 0.5 \dot{U}_b \left| Z_b |Z_b|^{\eta-1} + 0.5 \dot{U}_b |Z_b|^{\eta} - \dot{U}_b = 0 \quad (\text{A-4})$$

where Z_b = dimensionless variable with values in the range $[-1,1]$, η = parameter with value 5, Y_b = yield displacement, and $|\cdot|$ = absolute value. Equations (A-3) and (A-4) describe the behavior shown in Figure 3-1 (a). The model represents a slight modification of the Bouc-Wen model (Wen, 1976) as it has been implemented in computer codes 3D-BASIS (Reinhorn et al., 1994, Tsopelas et al., 1994).

The yield displacement is related to the characteristic strength, Q_b , and stiffnesses K_b and K_i (see Figure 3-1). The latter was assumed to be $K_i = 10 K_b$, so that

$$Y_b = \frac{Q_b}{9K_b} \quad (\text{A-5})$$

(2) Sliding Behavior

Equations (A-3) and (A-4) describe this behavior (Reinhorn et al., 1994, Tsopelas et al., 1994) except that the yield is very small. It has been assumed to be $Y_b = 0.25$ mm.

Moreover, the characteristic strength Q_b is expressed as

$$Q_b = \delta W_d \quad (\text{A-6})$$

where δ = coefficient of sliding friction, which is assumed to be constant. More appropriately, δ should be assumed to be of the form

$$\delta = f_{\max} - (f_{\max} - f_{\min}) \exp\left(-a \left| \dot{U}_b \right| \right) \quad (\text{A-7})$$

which describes the velocity dependence of the coefficient of sliding friction (Constantinou et al., 1998b). Since the velocity of sliding is large, the use of $\delta = f_{\max}$ produces nearly identical results with the case when (A-7) is used. Accordingly, δ is the coefficient of friction at large velocity of sliding.

(3) Linear Elastic and Linear Viscous Behavior.

$$F_b = K_b U_b + C_b \dot{U}_b \quad (\text{A-8})$$

A.2 MODELING OF PIER

(1) Perfect Bilinear Hysteretic Behavior

$$F_p = \alpha K_p U_p + (1 - \alpha) F_{yp} Z_p + F_{VD} \quad (\text{A-9})$$

$$Y_p \dot{Z}_p + 0.5 \left| \dot{U}_p \right| Z_p \left| Z_p \right|^{\eta-1} + 0.5 \dot{U}_p \left| Z_p \right|^{\eta} - \dot{U}_p = 0 \quad (\text{A-10})$$

where $\eta = 5$. Note that these equations are practically the same as (A-3) and (A-4) but expressed in terms of different parameters. Analyses were performed only for the case $\alpha = 0.05$, which describes a pier with very low post-yielding stiffness (but not elastoplastic behavior for which $\alpha = 0$).

Quantity F_{VD} represents a viscous force in order to account for energy dissipation under elastic conditions. This force was expressed as

$$F_{VD} = 2\beta_i \left(\frac{W_p}{g} \right) \omega_{p,eff} \dot{U}_p \quad (\text{A-11})$$

where β_i = inherent damping ratio in the pier when standing alone without the deck on top of it (assumed equal to 0.05) and ω_{peff} = effective frequency of the free standing pier.

For elastic pier conditions ($F_p \leq F_{yp}$), quantity ω_{peff} is equal to

$$\omega_{peff} = \left(\frac{K_p g}{W_p} \right)^{1/2} \quad (A-12)$$

which is the frequency of the pier under elastic conditions. The use of (A-12) for inelastic pier conditions results in overestimation of the damping provided by this force and results in substantial reduction of the pier displacement response (Tsopelas et al., 1997). Accordingly, quantity ω_{peff} is defined as

$$\omega_{peff} = \left(\frac{K_{peff} g}{W_p} \right)^{1/2} \quad (A-13)$$

where K_{peff} is the effective pier stiffness, which is the peak shear force in the pier divided by the peak pier displacement.

Calculation of K_{peff} and ω_{peff} required an iterative analysis. However, a two-step analysis produced acceptable results. In the first step a dynamic analysis was performed with $\omega_{peff} = 0$ and the peak pier displacement and force were calculated. K_{peff} was then calculated, (A-13) was used to calculate ω_{peff} and a new dynamic analysis was performed.

This procedure ensured that the contribution to the effective damping ratio of the free standing pier from the viscous force F_{VD} was not more than 0.05.

(2) Pinched Behavior

The pier displacement is split into the hysteretic component, U_{p1} , and the slip component, U_{p2} :

$$U_p = U_{p1} + U_{p2} \quad (\text{A-14})$$

Equations (A-9) and (A-10) apply for the total pier displacement and the hysteretic component of the pier displacement, respectively:

$$F_p = \alpha K_p U_p + (1 - \alpha) F_{yp} Z_p + F_{VD} \quad (\text{A-15})$$

$$Y_p \dot{Z}_p + 0.5 \dot{U}_{p1} \left| Z_p \right| \left| Z_p \right|^{\eta-1} + 0.5 \dot{U}_{p1} \left| Z_p \right|^{\eta} - \dot{U}_{p1} = 0 \quad (\text{A-16})$$

in which F_{VD} is given by (A-11) and (A-13).

The slip component of displacement is described by the following equation which was proposed by Baber and Noori (1985):

$$\dot{U}_{p2} = \left(\frac{2}{\pi}\right)^{1/2} \frac{a_s}{\sigma} \exp\left(\frac{-Z_p^2}{2\sigma^2}\right) \dot{Z}_p \quad (\text{A-17})$$

where $2a_s$ = the slip as shown in Figure 3-1(e) and σ = dimensionless parameter that controls the transition between the slip and lock phases.

A.3 PARAMETRIC FORM OF EQUATIONS OF MOTION

The equations of motion were normalized by the deck weight (W_d) in order to reduce the number of parameters and to arrive at parameters with direct physical interpretation. The equations were then reduced to first order form for numerical integration.

(1) System with Perfect Bilinear Hysteretic Pier and Bilinear Hysteretic or Sliding Behavior of the Isolation System

The equations of motion are:

$$\ddot{U}_p = \left(\frac{4\pi^2\nu}{T_b^2}\right)U_b + \delta\nu gZ_b - \left(\frac{4\pi^2\alpha}{T_p^2}\right)U_p - (1-\alpha)\gamma\nu gZ_p - 2\beta_i\omega_{peff}\dot{U}_p - \ddot{U}_g \quad (\text{A-18})$$

$$\ddot{U}_b = -\frac{4\pi^2(1+\nu)}{T_b^2}U_b - \delta(1+\nu)gZ_b + \frac{4\pi^2\alpha}{T_p^2}U_p + (1-\alpha)\gamma g\nu Z_p + 2\beta_i\omega_{peff}\dot{U}_p \quad (\text{A-19})$$

where

$$T_p = 2\pi \left(\frac{W_p Y_p}{g F_{yp}} \right)^{1/2} = 2\pi \left(\frac{W_p}{g K_p} \right)^{1/2} \quad (\text{A-20})$$

$$\gamma = \frac{F_{yp}}{W_d} \quad (\text{A-21})$$

$$T_b = 2\pi \left(\frac{W_d}{g K_b} \right)^{1/2} \quad (\text{A-22})$$

$$\delta = \frac{Q_b}{W_d} \quad (\text{A-23})$$

$$\nu = \frac{W_d}{W_p} \quad (\text{A-24})$$

and ω_{peff} is given by (A-13) with $\beta_i = 0.05$. Quantity T_p is the initial period of the pier if it is free standing (i.e., without the deck on top of it). Moreover, quantity T_b is period of the isolation system on the basis of the post-yielding stiffness (this is not the effective period per definition of the 1997 AASHTO Guide Specifications).

Furthermore, equations (A-4) and (A-10) are needed to fully describe the system. In these equations $\eta = 5$ and the yield displacements are as follows:

(a) For the pier

$$Y_p = \frac{\gamma \nu T_p^2 g}{4\pi^2} \quad (\text{A-25})$$

(b) For the isolation system

$$Y_b = \frac{\delta g T_b^2}{36\pi^2} \quad (\text{A-26})$$

when the behavior is bilinear hysteretic. For sliding behavior, $Y_b = 0.25$ mm.

The variables are quantities $U_b, \dot{U}_b, U_p, \dot{U}_p, Z_b, Z_p$.

(2) System with Perfect Bilinear Hysteretic Pier and Linear Elastic / Linear Viscous Behavior of the Isolation System

The equations of motion are:

$$\ddot{U}_p = \left(\frac{4\pi^2 \nu}{T_b^2} \right) U_b + \left(\frac{4\pi \nu \xi}{T_b} \right) \dot{U}_b - \left(\frac{4\pi^2 \alpha}{T_p^2} \right) U_p - (1-\alpha) \gamma \nu g Z_p - 2\beta_i \omega_{peff} \dot{U}_p - \ddot{U}_g \quad (\text{A-27})$$

$$\ddot{U}_b = -\frac{4\pi^2(1+\nu)}{T_b^2} U_b - \frac{4\pi \xi(1+\nu)}{T_b} \dot{U}_b + \frac{4\pi^2 \alpha}{T_p^2} U_p + (1-\alpha) \gamma \nu g Z_p + 2\beta_i \omega_{peff} \dot{U}_p \quad (\text{A-28})$$

in which

$$\xi = \frac{C_b g T_b}{4\pi W_d} \quad (\text{A-29})$$

Moreover, equations (A-10) and (A-20) to (A-25) apply.

The variables are quantities $U_b, \dot{U}_b, U_p, \dot{U}_p, Z_p$.

(3) Systems with Pinched Pier Behavior and Bilinear Hysteretic Behavior of the Isolation System

Equations (A-16), and (A-18) to (A-25) apply. Moreover, equations (A-14), (A-16) and (A-17) with the condition $\text{sign}(\dot{U}_p) = \text{sign}(\dot{U}_{p1})$ yield:

$$\dot{U}_{p1} = \frac{Y_p \dot{U}_p}{Y_p + \left(\frac{2}{\pi}\right)^{1/2} \frac{a_s}{\sigma} \exp\left(-\frac{Z_p^2}{2\sigma^2}\right) \left[1 - 0.5|Z_p|^n - 0.5\text{sign}(\dot{U}_p) Z_p |Z_p|^{n-1}\right]} \quad (\text{A-30})$$

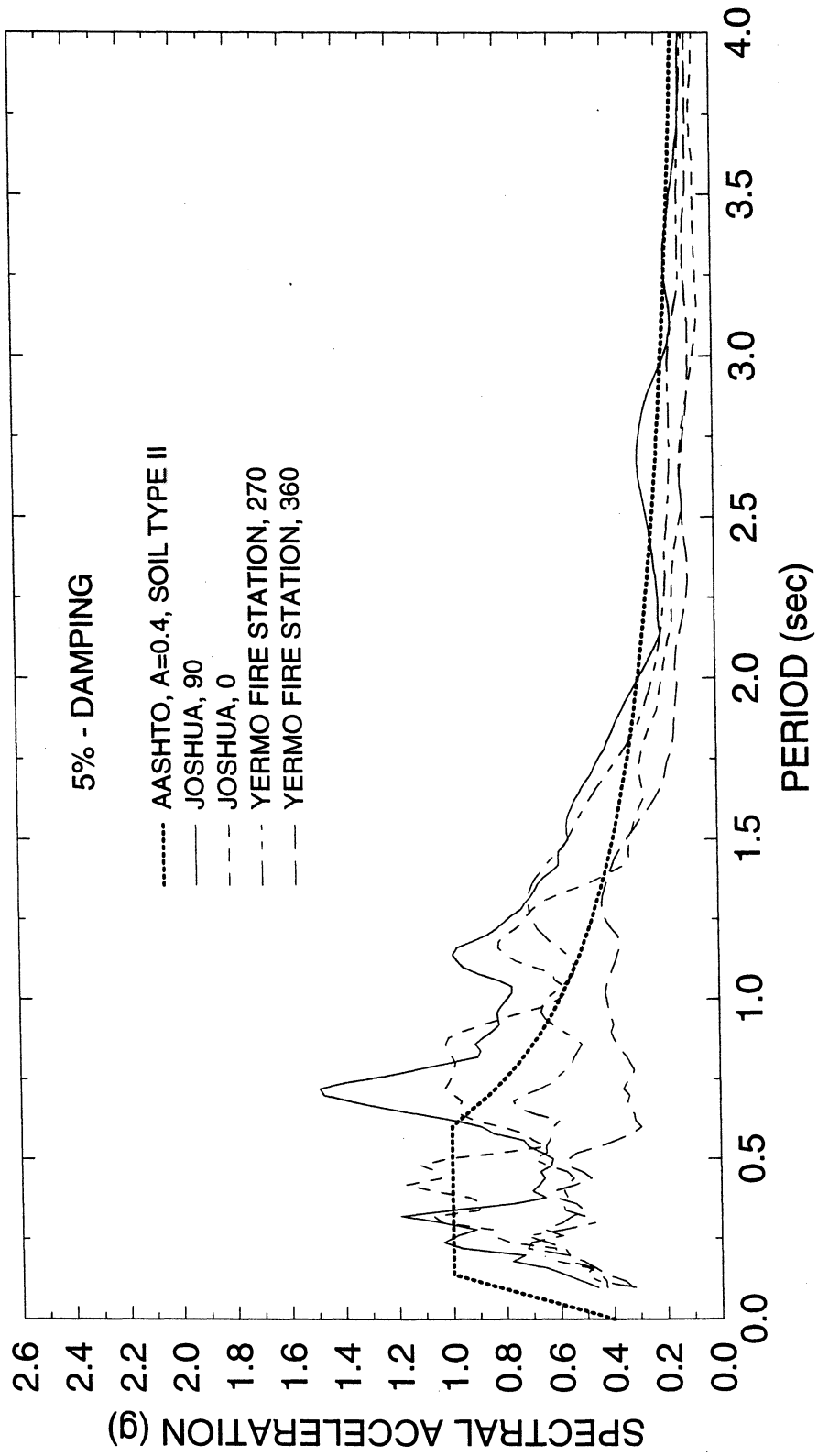
The variables are quantities $U_b, \dot{U}_b, U_p, \dot{U}_p, Z_b, Z_p$.

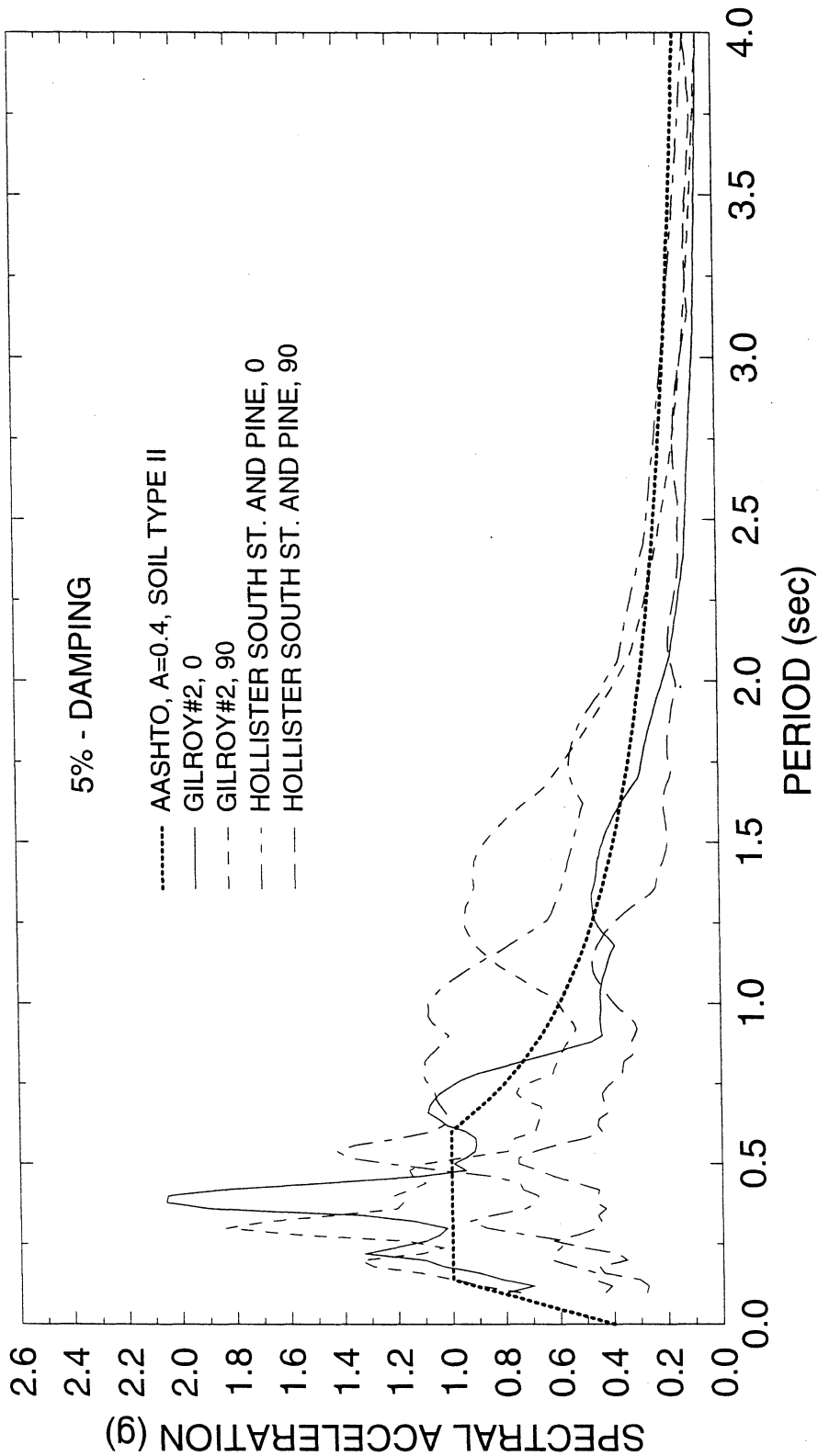
APPENDIX B

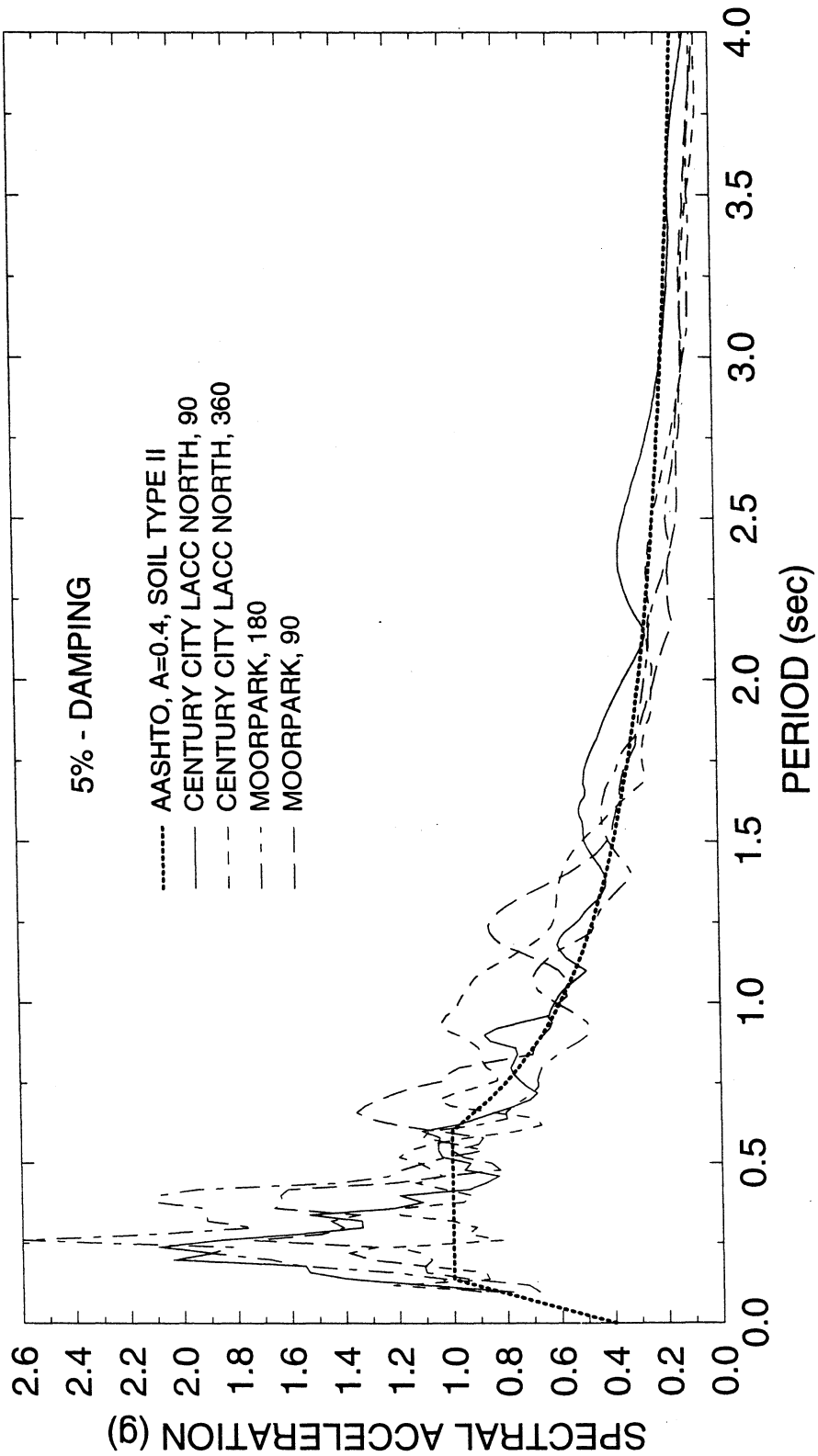
**DATA ON MOTIONS USED FOR DYNAMIC ANALYSIS AND
RESPONSE SPECTRA OF SCALED COMPONENTS**

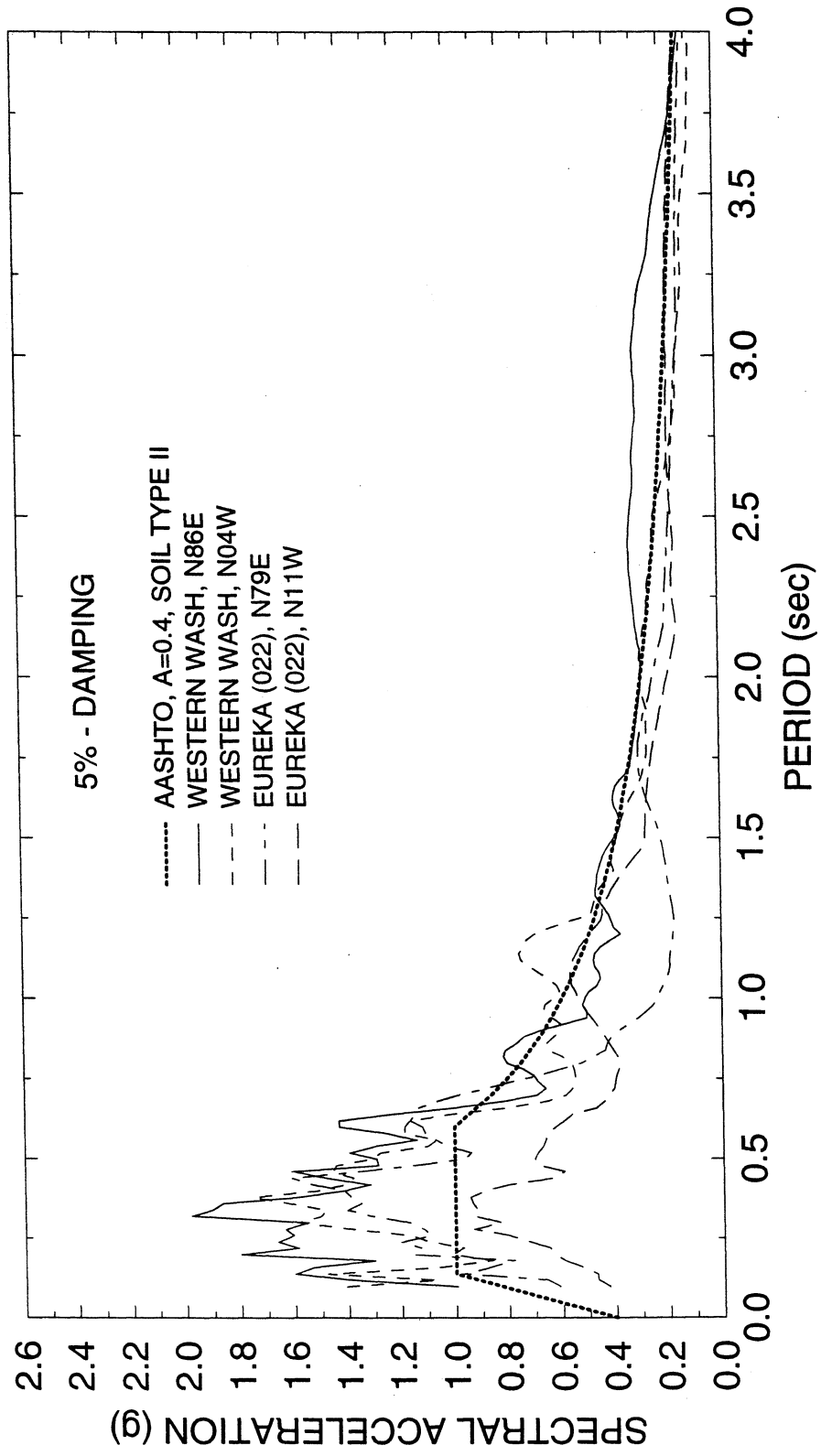
Motions for Soil Profile Type II

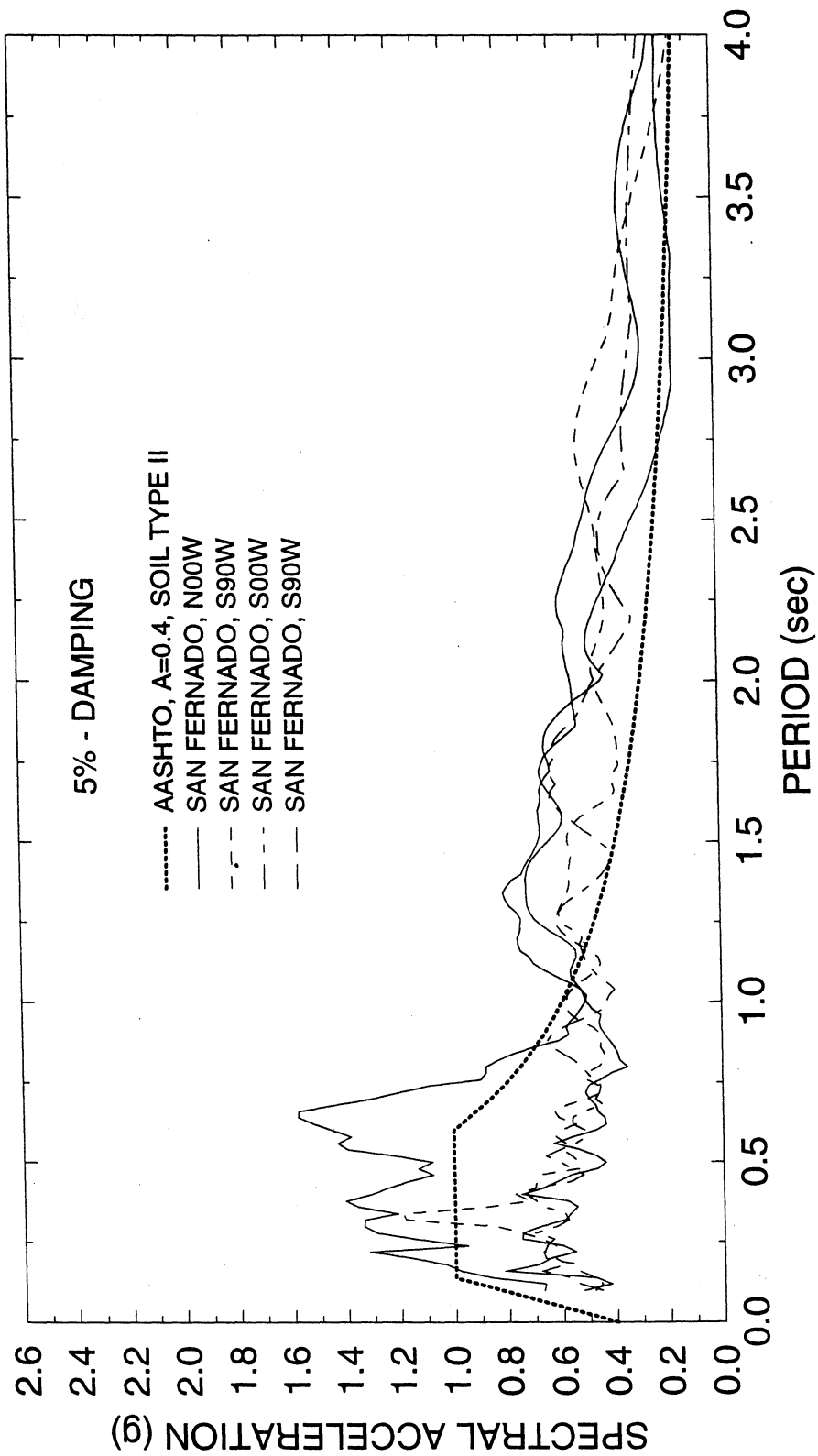
1992 LANDERS (MAG= 7.5)					
		Jhoshua Tree (EPICENT. DIST.=15Km)		Yermo Fire Station(EPICENT. DIST.=84Km)	
		T	L	L	T
COMPONENT	90	0	360	270	
PGA(cm/s/s)=	278	268	149	240	
PGV(cm/s)=	42.71	27.08	29	50.8	
SRSS Acc	386.15		282.49		
SRSS Veloc	50.57		58.49		
Final Scale Factor	1.48	1.48	1.28	1.28	
File Name	EQ01	EQ02	EQ04	EQ03	
1989 LOMA PRIETA (MAG=7.1)					
		Gilroy#2 (EPICENT. DIST.=31Km)		Hollister-SouthStreet and Pine (EPIC.DIST.=50Km)	
		L	T	T	
COMPONENT	90	0	90	0	
PGA(cm/s/s)=	316	344	175	362	
PGV(cm/s)=	39.23	33.34	30.89	62.78	
SRSS Acc	467.11		402.08		
SRSS Veloc	51.48		69.97		
Final Scale Factor	1.46	1.46	1.07	1.07	
File Name	EQ06	EQ05	EQ08	EQ07	
1994 NORTHRIDGE (MAG= 6.8)					
		Century City LACC North (EPIC. DIST.=19.8Km)		Moorpark (EPICENT. DIST.=32.6Km)	
		T	L	T	L
COMPONENT	90	360	180	90	
PGA(cm/s/s)=	265	235	294	186	
PGV(cm/s)=	21.4	25.1	20.3	20.4	
SRSS Acc	354.19		347.90		
SRSS Veloc	32.98		28.78		
Final Scale Factor	2.27	2.27	2.61	2.61	
File Name	EQ09	EQ10	EQ11	EQ12	
		1949 WESTERN WASH (MAG=7.1) Olympia Hwy Test Lab (EPIC. DIST.=39Km)		1954 EUREKA (022) (MAG= 6.5) Eureka Federal Bldg. (EPIC.DIST.=5Km)	
		301	302	303	304
		L	T	L	T
COMPONENT	N04W	N86E	N11W	N79E	
PGA(cm/s/s)=	162	275	165	253	
PGV(cm/s)=	21.4	17.1	31.6	29.4	
SRSS Acc	319.17		302.05		
SRSS Veloc	27.39		43.16		
Final Scale Factor	2.74	2.74	1.74	1.74	
File Name	EQ14	EQ13	EQ16	EQ15	
		1971 SAN FERNANDO (241) (MAG= 6.6) L.A. 8244 Orion Blvd 1 st fl. (EPIC. DIST.=21Km)		1971 SAN FERNANDO (458) (MAG=6.6) 616 S Normandie St, bsmt (EPIC. DIST.=40Km)	
		309	310	311	312
		T	L	T	L
COMPONENT	N00W	S90W	S00W	S90W	
PGA(cm/s/s)=	250	132	114	103	
PGV(cm/s)=	30	23.9	17.6	28.8	
SRSS Acc	282.71		153.64		
SRSS Veloc	38.36		33.75		
Final Scale Factor	1.96	1.96	2.22	2.22	
File Name	EQ17	EQ18	EQ19	EQ20	





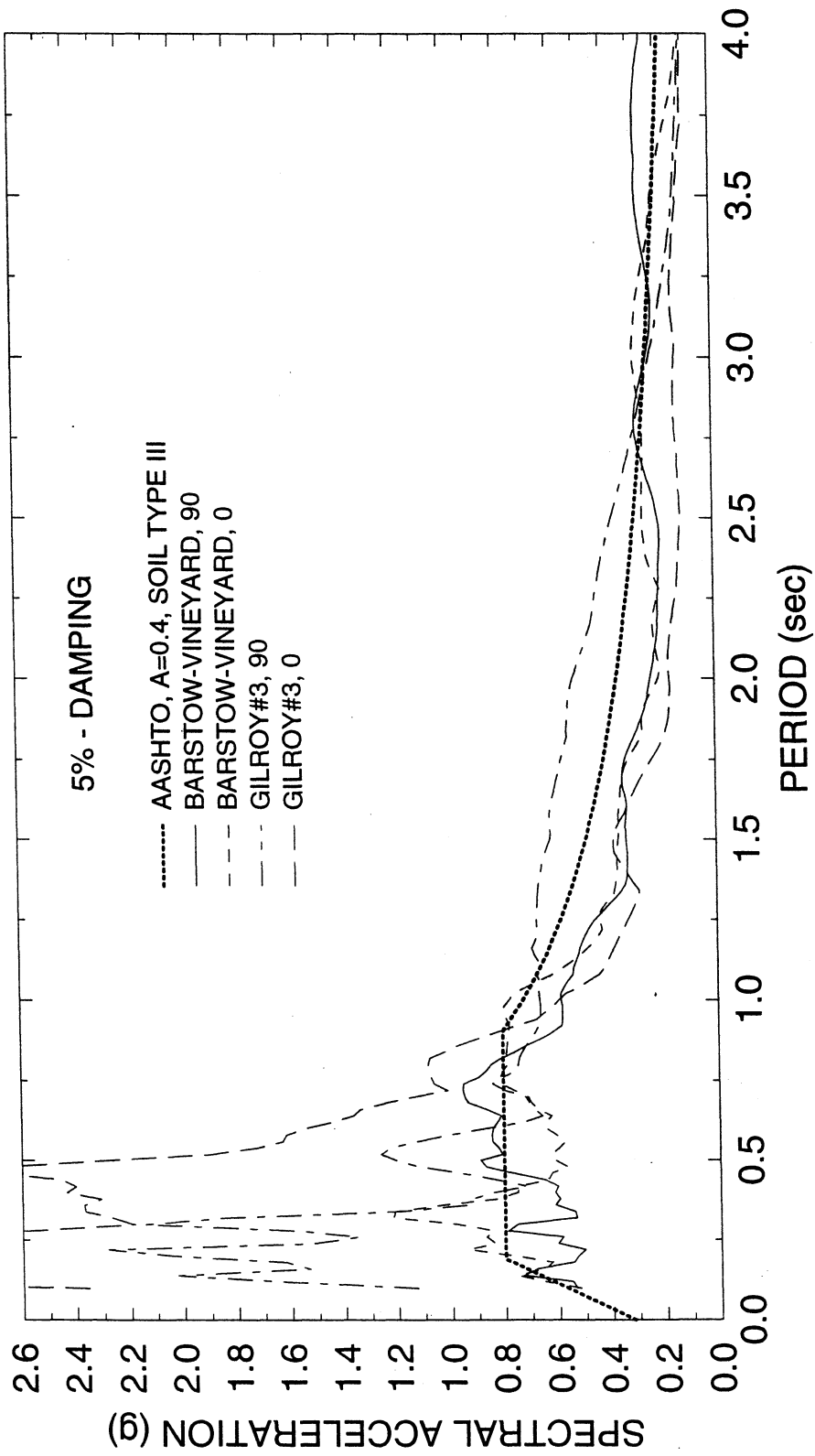


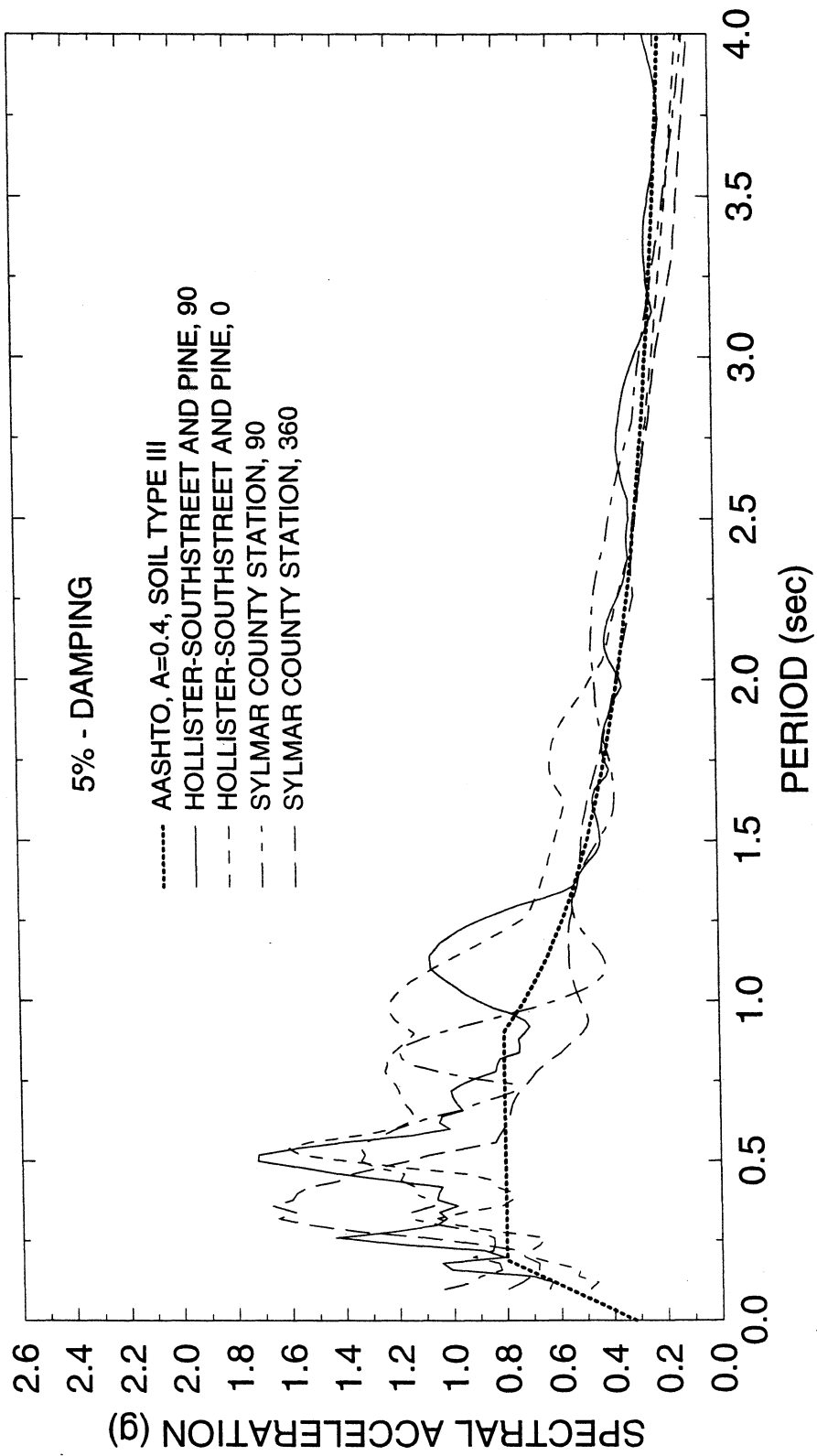


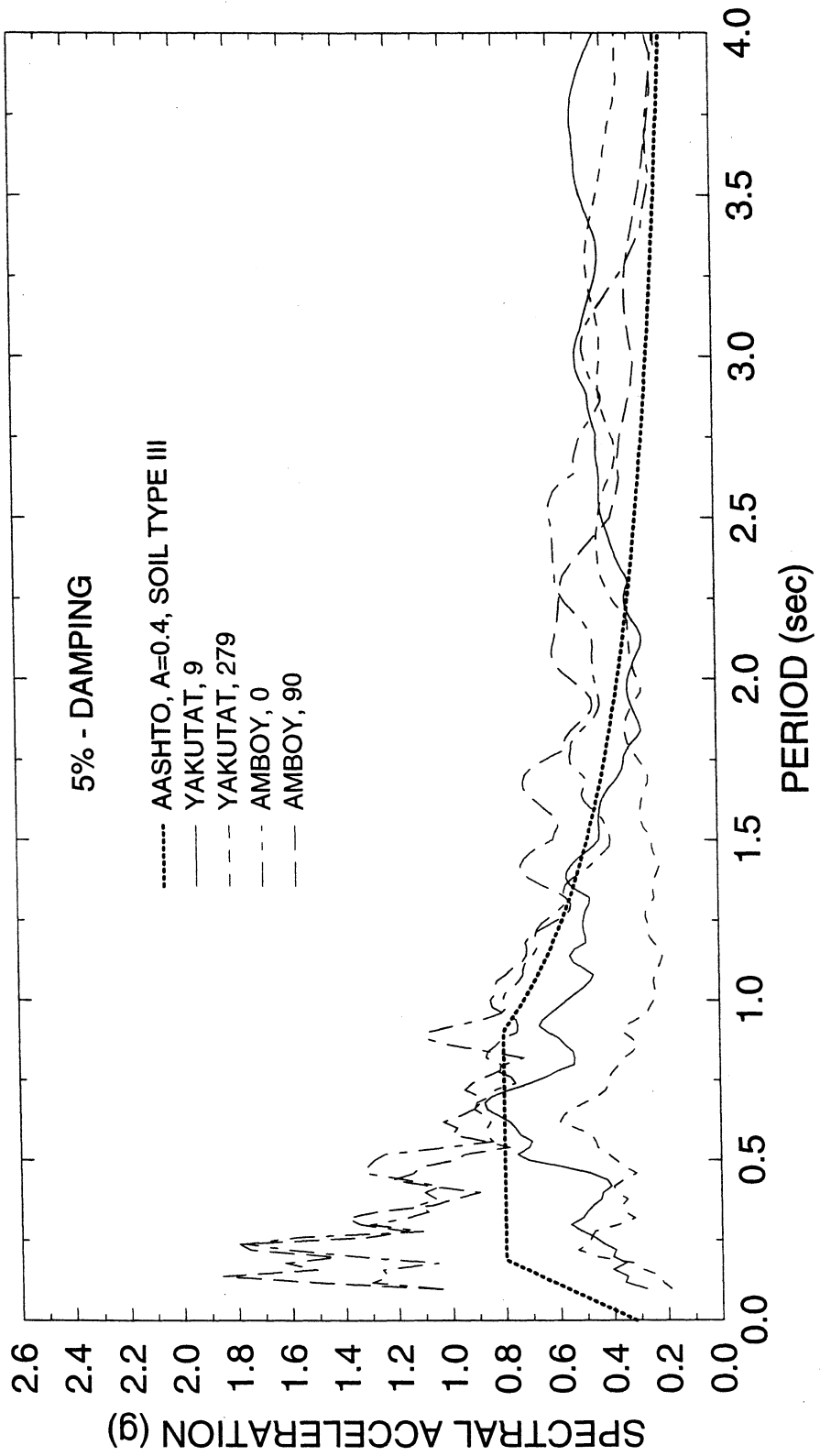


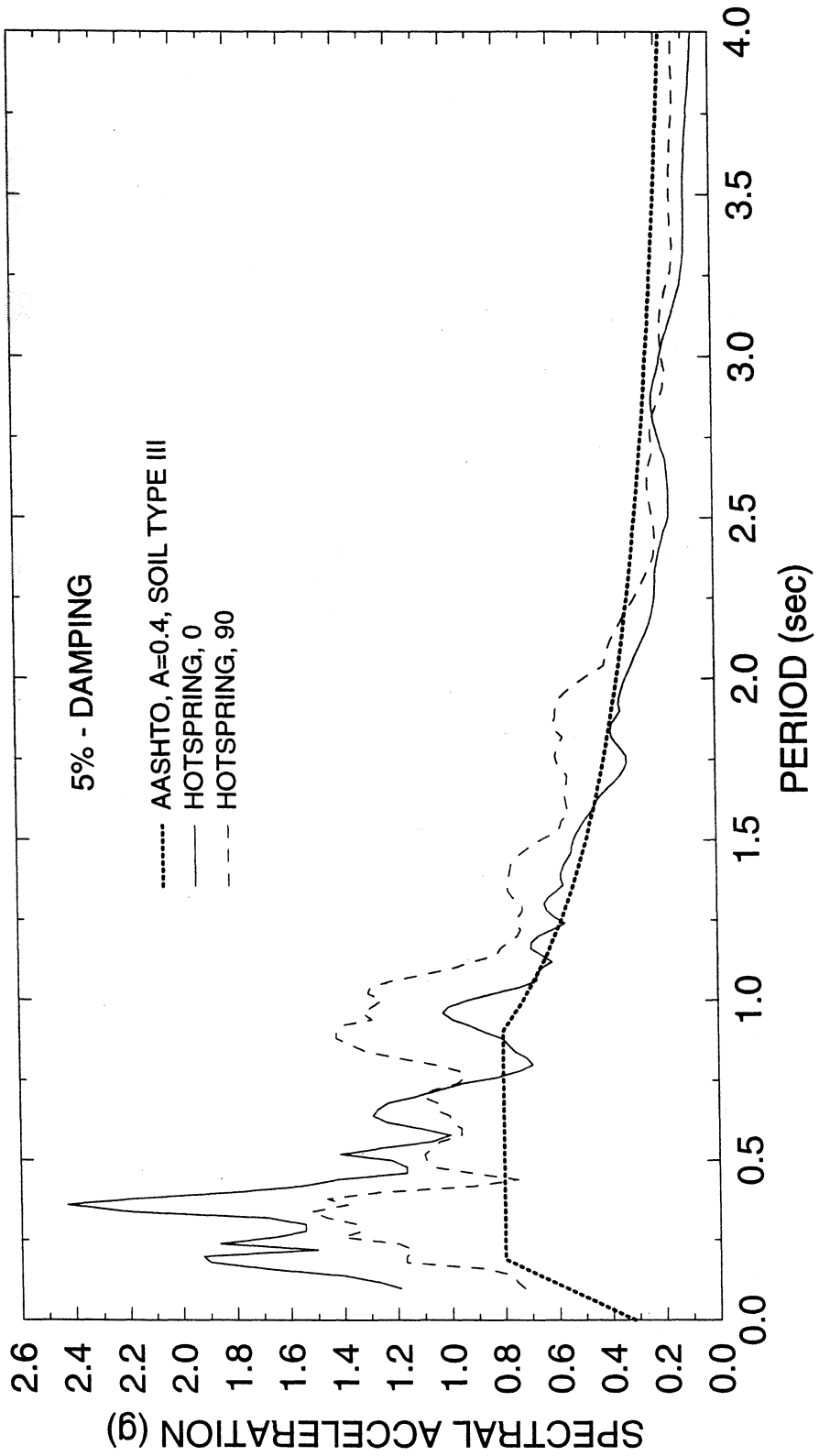
Motions for Soil Profile Type III

COMPONENT: PGA(cm/s/s)= PGV(cm/s)= SRSS Acc SRSS Veloc Final Scale Factor File Name	1992 LANDERS (MAG=7.5)		1989 LOMA PRIETA (MAG=7.1)	
	Barstow-Vineyard (EPICENT.DIST.=93.5Km)		Gilroy #3 (EPICENT.DIST.=32.5Km)	
	T	L	L	T
	90	0	90	0
	133	129	362	532
	25.12	21.95	43.77	34.48
	185.28		643.48	
	33.36		55.71	
	3.03	3.46	1.74	2.20
EQ31	EQ32	EQ33	EQ34	
COMPONENT: PGA(cm/s/s)= PGV(cm/s)= SRSS Acc SRSS Veloc Final Scale Factor File Name	1992 LANDERS (MAG=7.5)		1992 LANDERS (MAG=7.5)	
	Amboy (EPICENT.DIST.=74.2Km)		HotSpring (EPICENT.DIST.=29.1Km)	
	L	T	L	T
	0	90	0	90
	113	143	167	151
	17.86	20.07	18.96	20.80
	182.26		225.14	
	26.87		28.14	
	4.26	3.79	4.01	3.65
EQ51	EQ52	EQ53	EQ54	
COMPONENT: PGA(cm/s/s)= PGV(cm/s)= SRSS Acc SRSS Veloc Final Scale Factor File Name	1989 LOMA PRIETA (MAG=7.1)		1994 NORTHRIDGE (MAG=6.8)	
	Hollister-SouthStreet and Pine (EPIC.DIST.=49.6Km)		Sylmar County Hosp.(EPIC.DIST.=16 Km)	
	L	T	T	L
	90	0	90	360
	175	362	593	827
	30.89	62.78	76.94	128.88
	402.08		1017.63	
	69.97		150.10	
	2.46	1.21	0.99	0.59
EQ39	EQ40	EQ45	EQ46	
COMPONENT: PGA(cm/s/s)= PGV(cm/s)= SRSS Acc SRSS Veloc Final Scale Factor File Name	1979 SOUTHERN ALASKA (MAG=7.3)			
	Yakutat (EPICENT.DIST.=166Km)			
	9	279		
	82	61		
	23.76	31.08		
	102.20			
	39.12			
	3.20	2.45		
EQ47	EQ48			









APPENDIX C

**CALCULATED VALUES OF PIER DISPLACEMENT
DUCTILITY RATIO OF NON-ISOLATED BRIDGE**

A=0.4, SOIL TYPE II, SI=1.2, BILINEAR NON-ISOLATED PIER ALPHA=0.05 R=1.0

MAXIMUM PIER DUCTILITY, YIELD (Yp) in mm

EQ	0.3	0.4	0.5	0.6	0.7	0.8	0.9	1.0	1.1	1.2	1.3	1.4	1.5	1.6	1.7	1.8	1.9	2.0
TP(sec)	22.4	39.8	56.8	72.4	89.0	106.3	124.4	143.1	162.5	182.5	203.1	224.2	245.8	267.9	290.4	313.4	336.8	360.7
Yp(mm)	1.1	0.7	0.7	1.2	1.7	1.2	1.3	1.3	1.4	1.2	1.1	1.2	1.2	1.1	1.1	1.1	0.9	0.8
eq01	1.0	1.2	1.0	1.0	1.1	1.3	1.2	1.0	1.2	1.2	1.2	0.8	0.7	0.7	0.7	0.7	0.6	0.5
eq02	0.5	0.6	0.8	0.8	1.1	0.8	0.9	1.1	1.0	1.1	1.2	1.4	1.3	1.2	1.0	0.8	0.7	0.6
eq03	0.6	0.6	0.6	0.4	0.5	0.5	0.7	0.7	0.7	0.7	0.8	0.8	0.7	0.6	0.5	0.4	0.4	0.4
eq04	1.1	1.3	1.0	1.1	1.5	1.2	0.7	0.7	0.8	0.8	1.0	1.0	0.9	0.8	0.7	0.7	0.6	0.5
eq05	1.9	1.2	1.2	0.8	1.0	0.9	0.9	1.0	1.5	1.4	1.4	1.5	1.5	1.3	1.2	1.1	1.0	1.0
eq06	0.9	0.7	1.1	1.5	1.6	1.8	1.6	1.5	1.4	1.3	1.2	1.1	1.1	1.1	1.2	1.2	1.1	1.0
eq07	0.5	0.4	0.8	0.5	0.6	0.5	0.5	0.7	0.9	0.9	0.6	0.5	0.4	0.5	0.4	0.5	0.5	0.4
eq08	1.4	1.2	1.0	1.3	1.0	1.0	1.1	1.0	1.0	1.1	1.0	0.9	1.0	1.1	1.1	1.0	0.9	0.9
eq09	0.9	1.0	1.1	0.9	1.3	1.2	1.5	1.2	1.3	1.1	1.1	1.1	1.1	0.9	0.6	0.7	0.6	0.6
eq10	1.7	1.8	1.0	1.1	1.0	0.9	0.8	1.0	1.1	0.9	0.9	0.7	0.9	1.0	0.9	0.8	0.7	0.7
eq11	1.3	1.3	0.9	1.3	1.3	1.2	1.0	1.0	1.2	1.3	1.6	1.2	0.9	0.9	0.9	0.7	0.7	0.6
eq12	1.6	1.4	1.2	1.9	1.0	1.1	1.0	0.9	0.9	0.7	0.9	0.9	0.9	0.9	0.8	0.8	0.8	0.8
eq13	1.7	1.3	1.1	1.2	0.8	0.8	0.9	1.0	1.2	1.1	0.9	0.8	0.8	0.8	0.7	0.7	0.7	0.8
eq14	1.3	1.5	1.0	1.3	1.1	0.8	0.6	0.4	0.3	0.3	0.4	0.4	0.5	0.6	0.7	0.7	0.7	0.7
eq15	0.8	0.9	0.8	0.8	0.6	0.6	0.7	0.9	1.1	1.0	0.8	0.7	0.6	0.6	0.6	0.6	0.6	0.5
eq16	1.4	1.2	1.2	1.7	1.5	1.4	1.1	1.0	1.5	1.3	1.3	1.6	1.4	1.3	1.2	1.3	1.2	1.1
eq17	0.8	0.8	0.6	0.8	0.7	0.7	0.7	1.0	0.8	1.1	1.1	1.1	1.1	0.9	0.9	0.9	1.0	1.1
eq18	0.6	0.7	0.7	0.6	0.7	0.8	0.9	0.8	1.0	1.1	1.1	0.9	1.0	1.2	1.5	1.4	1.3	1.2
eq19	0.7	0.8	0.5	0.6	0.7	0.5	0.7	0.9	1.0	1.0	1.3	1.4	1.2	1.2	1.5	1.4	1.2	1.3
eq20	1.1	1.0	0.9	1.0	1.0	1.0	0.9	1.0	1.1	1.0	1.0	1.0	1.0	0.9	0.9	0.9	0.8	0.8
MEAN:	0.4	0.4	0.2	0.4	0.4	0.3	0.3	0.2	0.3	0.3	0.3	0.3	0.3	0.3	0.3	0.3	0.3	0.3
S.DEV.:	1.0	1.1	1.0	1.0	1.0	0.9	0.9	1.0	1.0	1.1	1.1	1.0	1.0	0.9	0.9	0.8	0.7	0.7
MEDIAN:	1.0	1.1	1.0	1.0	1.0	0.9	0.9	1.0	1.0	1.1	1.1	1.0	1.0	0.9	0.9	0.8	0.7	0.7

A=0.4, SOIL TYPE II, SI=1.2, BILINEAR NON-ISOLATED PIER ALPHA=0.05 R=2.0

MAXIMUM PIER DUCTILITY, YIELD (Yp) in mm

EQ	11.2	19.9	0.3	0.4	0.5	0.6	0.7	0.8	0.9	1.0	1.1	1.2	1.3	1.4	1.5	1.6	1.7	1.8	1.9	2.0
TP(sec)	0.3	0.4	0.5	0.6	0.7	0.8	0.9	1.0	1.1	1.2	1.3	1.4	1.5	1.6	1.7	1.8	1.9	2.0	2.1	2.2
EQ	2.3	1.8	1.5	2.7	2.7	2.7	2.1	2.5	2.3	2.0	2.1	2.6	2.7	2.6	2.3	2.6	2.3	1.7	1.4	1.2
EQ01	3.0	2.4	1.6	1.8	1.9	1.9	2.1	1.9	2.0	2.3	2.2	1.8	1.3	1.1	1.3	1.1	1.3	1.1	1.1	1.0
EQ02	1.0	1.2	1.8	1.7	2.4	1.4	1.6	1.8	1.5	2.4	2.9	2.7	2.4	2.0	1.7	2.0	1.7	1.5	1.4	1.3
EQ03	1.1	1.3	1.2	0.7	1.0	1.0	1.1	1.4	1.5	1.6	1.5	1.4	1.3	1.0	0.9	1.0	0.9	0.8	0.8	0.8
EQ04	3.9	2.9	2.1	2.6	3.0	2.4	1.5	1.4	1.5	2.1	2.3	2.1	1.6	1.4	1.3	1.4	1.3	1.2	1.1	1.0
EQ05	3.7	2.1	1.7	2.3	2.9	2.7	2.8	2.6	2.9	3.0	3.0	2.9	2.7	2.5	2.3	2.5	2.3	2.2	2.0	1.9
EQ06	3.0	1.5	3.1	3.7	3.7	2.9	2.7	2.7	2.7	2.5	1.9	1.5	1.7	2.3	2.1	2.3	2.1	1.7	1.8	1.8
EQ07	1.0	0.9	1.6	1.1	1.2	1.1	1.0	1.2	1.6	1.4	1.1	0.9	0.9	1.0	0.8	0.9	0.9	0.9	0.9	0.8
EQ08	2.7	2.2	2.2	2.5	2.2	2.1	1.5	1.9	1.9	1.8	1.9	2.1	2.3	1.9	1.6	1.5	1.6	1.6	1.5	1.5
EQ09	2.3	2.3	1.9	2.2	2.9	2.9	2.1	2.0	2.2	2.2	2.2	2.0	1.6	1.5	1.4	1.3	1.2	1.2	1.1	1.1
EQ10	3.3	3.6	2.4	1.5	1.9	1.9	1.7	1.5	1.9	1.5	1.8	1.7	1.7	1.7	1.6	1.4	1.2	1.4	1.2	1.2
EQ11	3.4	2.4	2.1	2.3	2.3	2.4	2.7	2.2	2.0	3.1	2.9	2.1	1.8	1.7	1.4	1.3	1.4	1.3	1.4	1.3
EQ12	4.2	2.2	3.5	2.7	2.4	2.0	1.8	1.8	1.5	1.7	1.9	1.4	1.5	1.5	1.6	1.5	1.6	1.6	1.6	1.7
EQ13	4.4	2.1	1.5	2.0	1.6	1.8	2.0	1.9	1.8	1.9	1.6	1.2	1.3	1.3	1.3	1.3	1.4	1.4	1.6	1.3
EQ14	2.4	2.4	2.2	1.9	1.8	1.1	1.0	0.8	0.7	0.7	0.7	0.8	1.0	1.1	1.2	1.2	1.2	1.2	1.2	1.2
EQ15	2.2	1.4	1.2	1.3	1.1	1.2	1.7	1.9	1.9	1.8	1.5	1.3	1.3	1.3	1.3	1.3	1.3	1.2	1.1	1.0
EQ16	2.8	1.8	2.9	3.5	2.4	3.4	3.8	3.4	2.2	2.2	3.1	2.7	2.4	1.9	2.4	2.4	2.4	2.4	2.1	1.9
EQ17	1.8	1.6	1.1	1.5	1.2	1.1	1.4	1.6	1.8	1.6	1.6	1.7	1.5	1.4	1.6	1.4	1.6	1.7	2.0	2.1
EQ18	1.3	1.5	1.6	1.7	1.2	1.6	1.7	1.7	2.3	2.3	2.6	2.6	2.8	2.7	2.6	2.7	2.6	2.4	2.2	2.4
EQ19	1.5	1.3	1.0	1.1	1.3	1.2	1.5	1.9	2.3	2.4	2.5	2.6	2.6	2.6	2.6	2.6	2.3	2.1	2.2	2.5
EQ20	2.6	1.9	1.9	2.0	2.0	1.9	1.9	1.9	1.9	2.0	2.1	1.9	1.8	1.7	1.6	1.7	1.6	1.5	1.5	1.5
MEAN:	1.1	0.6	0.7	0.8	0.8	0.7	0.7	0.6	0.5	0.6	0.6	0.6	0.6	0.6	0.5	0.6	0.5	0.4	0.4	0.5
S.DEV.:	2.5	2.0	1.8	2.0	2.0	1.9	1.7	1.9	1.9	2.0	2.0	1.9	1.7	1.6	1.6	1.6	1.6	1.5	1.4	1.3
MEDIAN:																				

A=0.4, SOIL TYPE II, SI=1.2, BILINEAR NON-ISOLATED PIER ALPHA=0.05 R=3.0

MAXIMUM PIER DUCTILITY, YIELD (Yp) in mm

Eq	0.3	0.4	0.5	0.6	0.7	0.8	0.9	1.0	1.1	1.2	1.3	1.4	1.5	1.6	1.7	1.8	1.9	2.0
Eq01	4.7	4.0	3.4	4.7	4.2	4.0	3.8	3.6	3.5	3.3	3.5	4.1	3.8	3.3	2.6	2.1	1.7	1.6
Eq02	5.6	3.5	2.6	3.1	2.7	3.7	3.0	2.5	3.4	3.6	3.0	2.2	1.7	1.9	1.7	1.5	1.3	1.3
Eq03	1.5	1.9	2.7	3.8	4.1	2.5	2.3	1.9	3.7	4.7	4.3	3.7	3.1	2.6	2.1	1.8	1.8	1.9
Eq04	1.8	1.9	1.8	1.1	1.6	1.8	1.6	1.8	2.2	2.3	2.0	1.9	1.8	1.6	1.3	1.3	1.3	1.2
Eq05	6.2	4.4	5.1	5.0	4.6	3.5	3.0	2.9	3.5	4.1	3.7	2.9	2.4	2.2	2.0	1.8	1.6	1.4
Eq06	6.1	4.0	3.3	4.7	4.8	4.9	5.1	5.2	5.2	4.9	4.4	3.9	3.4	3.0	2.7	2.5	2.3	2.2
Eq07	5.9	6.1	5.9	6.2	5.7	4.8	4.7	4.7	4.6	4.4	3.7	3.0	3.0	2.8	3.0	3.0	3.1	3.1
Eq08	1.3	1.8	2.4	1.6	1.7	1.6	1.4	1.7	2.1	1.6	1.3	1.2	1.4	1.3	1.4	1.3	1.3	1.3
Eq09	3.9	2.5	3.7	3.7	3.3	2.8	2.2	2.9	3.6	3.7	3.7	3.4	2.4	2.3	2.6	2.6	2.5	2.5
Eq10	4.5	3.4	3.9	3.0	4.3	3.6	2.7	2.7	3.2	3.2	2.7	2.1	2.2	2.7	2.6	1.8	1.5	1.5
Eq11	8.0	5.0	4.3	2.9	2.8	2.7	2.6	2.6	2.3	2.2	2.8	3.0	2.7	2.4	2.1	1.7	1.8	1.9
Eq12	5.1	3.2	3.8	3.4	4.7	2.9	2.3	3.1	4.5	4.5	4.0	3.3	2.6	2.1	1.9	2.1	2.1	2.0
Eq13	8.2	7.5	6.8	3.9	3.4	2.4	3.4	3.0	3.2	3.2	2.5	2.3	2.1	2.0	2.0	2.1	2.2	2.2
Eq14	5.7	3.1	2.6	2.8	2.5	3.0	3.4	2.7	2.6	2.8	2.5	1.9	1.8	1.7	1.9	1.9	1.6	1.5
Eq15	4.0	3.7	3.2	3.4	2.1	1.9	1.5	1.1	1.1	1.0	1.1	1.2	1.4	1.7	1.8	1.9	1.9	1.9
Eq16	4.7	2.1	1.8	1.5	2.1	2.4	2.8	2.8	2.8	2.6	2.4	2.1	1.8	1.6	1.5	1.4	1.3	1.2
Eq17	4.4	5.1	5.6	4.0	3.7	5.5	4.0	3.4	3.8	4.6	4.3	4.0	3.2	4.0	4.0	3.6	3.2	3.0
Eq18	3.0	2.4	2.0	2.3	1.9	1.8	2.3	2.9	2.5	2.5	2.5	2.1	2.1	2.2	2.8	3.5	3.9	3.9
Eq19	2.3	3.2	2.9	3.1	1.7	3.2	2.4	2.8	3.6	4.5	4.7	4.7	4.4	4.1	3.8	3.7	4.0	4.2
Eq20	2.0	1.8	1.7	1.5	2.0	2.0	3.4	3.4	3.8	3.8	3.3	3.1	3.4	3.6	3.8	3.3	3.4	3.3
MEAN:	4.4	3.5	3.5	3.3	3.2	3.0	2.9	2.9	3.3	3.4	3.1	2.8	2.5	2.4	2.4	2.2	2.2	2.2
S-DEV.:	2.0	1.5	1.4	1.3	1.2	1.1	1.0	0.9	1.0	1.1	1.0	1.0	0.8	0.8	0.8	0.8	0.9	0.9
MEDIAN:	4.6	3.3	3.3	3.2	3.0	2.9	2.8	2.8	3.4	3.4	3.1	2.9	2.4	2.3	2.1	2.0	1.9	1.9

A=0.4, SOIL TYPE II, SI=1.2, PINCHED PIER ALPHA=0.05 R=1.0

MAXIMUM PIER DUCTILITY, YIELD (Yp) in mm

TP(sec)	0.3	0.4	0.5	0.6	0.7	0.8	0.9	1.0	1.1	1.2	1.3	1.4	1.5	1.6	1.7	1.8	1.9	2.0
Yp(mm)	22.4	39.8	56.8	72.4	89.0	106.3	124.4	143.1	162.5	182.5	203.1	224.2	245.8	267.9	290.4	313.4	336.8	360.7
EQ																		
eq01	1.1	0.7	0.7	1.2	2.1	1.2	1.3	1.3	1.4	1.2	1.1	1.2	1.2	1.1	1.1	1.1	0.9	0.8
eq02	1.0	1.2	1.0	1.0	1.1	1.3	1.2	1.0	1.2	1.3	1.2	0.8	0.7	0.7	0.7	0.7	0.6	0.5
eq03	0.5	0.6	0.8	0.8	1.1	0.8	0.9	1.1	1.0	1.1	1.2	1.4	1.3	1.2	1.0	0.8	0.7	0.6
eq04	0.6	0.6	0.6	0.4	0.5	0.5	0.7	0.7	0.7	0.7	0.8	0.8	0.7	0.6	0.5	0.4	0.4	0.4
eq05	1.1	1.3	1.0	1.1	2.1	1.2	0.9	0.7	0.8	0.8	1.0	1.0	0.9	0.8	0.7	0.7	0.6	0.5
eq06	2.7	1.2	1.2	0.8	1.0	0.9	0.9	1.0	1.5	1.4	1.4	1.5	1.5	1.3	1.2	1.1	1.0	1.0
eq07	0.9	0.7	1.2	2.3	2.5	2.8	2.9	1.5	1.4	1.3	1.2	1.1	1.1	1.1	1.2	1.2	1.1	1.0
eq08	0.5	0.4	0.8	0.5	0.6	0.5	0.5	0.7	0.9	0.9	0.6	0.5	0.4	0.5	0.4	0.5	0.5	0.4
eq09	1.4	1.2	1.0	1.3	1.0	1.0	1.1	1.0	1.0	1.1	1.0	0.9	1.0	1.1	1.1	1.0	0.9	0.9
eq10	0.9	1.0	1.1	0.9	1.3	1.2	1.5	1.2	1.3	1.1	1.1	1.1	1.1	0.9	0.6	0.7	0.6	0.6
eq11	2.2	2.4	1.0	1.1	1.0	1.0	0.8	1.0	1.1	0.9	0.9	0.7	0.9	1.0	0.9	0.8	0.7	0.7
eq12	1.3	1.3	0.9	1.3	1.3	1.2	1.0	1.0	1.2	1.3	2.2	1.2	0.9	0.9	0.9	0.7	0.7	0.6
eq13	3.4	1.4	1.2	2.0	1.0	1.1	1.0	0.9	0.9	0.7	0.9	0.9	0.8	0.9	0.8	0.8	0.8	0.8
eq14	3.0	1.4	1.1	1.2	0.8	0.8	0.9	1.0	1.1	1.1	0.9	0.8	0.8	0.8	0.7	0.7	0.7	0.8
eq15	1.3	1.5	1.0	1.3	1.1	0.8	0.6	0.4	0.3	0.3	0.4	0.4	0.5	0.6	0.7	0.7	0.7	0.8
eq16	0.8	0.9	0.8	0.8	0.6	0.6	0.7	0.9	1.1	1.0	0.8	0.7	0.6	0.6	0.6	0.6	0.6	0.5
eq17	1.4	1.2	1.2	2.8	2.5	1.4	1.1	1.0	2.1	1.3	1.3	2.0	1.4	1.3	1.2	1.3	1.2	1.1
eq18	0.9	0.8	0.6	0.8	0.7	0.7	0.7	0.8	0.8	1.1	1.1	1.1	1.1	0.9	0.9	0.9	1.0	1.1
eq19	0.6	0.7	0.7	0.6	0.7	0.8	0.9	0.7	0.9	1.1	1.1	0.9	1.0	1.3	1.5	1.4	1.3	1.2
eq20	0.7	0.8	0.5	0.6	0.7	0.5	0.7	0.9	1.0	1.0	1.3	1.4	1.2	1.2	1.5	1.4	1.2	1.3
MEAN:	1.3	1.1	0.9	1.1	1.2	1.0	1.0	1.0	1.1	1.0	1.1	1.0	1.0	0.9	0.9	0.9	0.8	0.8
S.DEV.:	0.8	0.4	0.2	0.6	0.6	0.5	0.5	0.2	0.4	0.3	0.4	0.4	0.3	0.3	0.3	0.3	0.3	0.3
MEDIAN:	1.1	1.1	1.0	1.0	1.0	0.9	0.9	1.0	1.0	1.1	1.1	1.0	1.0	0.9	0.9	0.8	0.7	0.7

A=0.4, SOIL TYPE II, SI=1.2, PINCHED PIER ALPHA=0.05 R=2.0

MAXIMUM PIER DUCTILITY, YIELD (Yp) in mm

	0.3	0.4	0.5	0.6	0.7	0.8	0.9	1.0	1.1	1.2	1.3	1.4	1.5	1.6	1.7	1.8	1.9	2.0	
TP(sec)	11.2	19.9	28.4	36.2	44.5	53.1	62.2	71.6	81.3	91.3	101.5	112.1	122.9	133.9	145.2	156.7	168.4	180.3	
Yp(mm)	2.7	3.0	1.5	3.6	4.1	3.2	2.9	2.9	2.9	2.4	2.4	2.6	2.6	2.8	2.7	2.0	1.4	1.3	
EQ	eq01	eq02	eq03	eq04	eq05	eq06	eq07	eq08	eq09	eq10	eq11	eq12	eq13	eq14	eq15	eq16	eq17	eq18	eq19
MEAN:	3.2	3.0	2.9	2.8	2.7	2.6	2.5	2.7	2.6	2.6	2.6	2.3	2.2	2.2	2.0	1.4	1.1	1.0	0.8
S.DEV.:	1.6	1.3	1.2	1.1	1.1	1.2	1.1	1.1	0.7	0.8	0.8	0.8	0.8	0.9	0.8	0.9	0.9	0.8	0.8
MEDIAN:	3.4	3.4	3.2	3.1	2.9	3.0	2.5	2.6	2.7	2.6	2.6	2.2	2.3	1.7	2.1	1.7	1.4	1.3	1.3

A=0.4, SOIL TYPE II, SI=1.2, PINCHED PIER ALPHA=0.05 R=3.0

MAXIMUM PIER DUCTILITY, YIELD (Yp) in mm

	0.3	0.4	0.5	0.6	0.7	0.8	0.9	1.0	1.1	1.2	1.3	1.4	1.5	1.6	1.7	1.8	1.9	2.0
TP(sec)	7.5	13.3	18.9	24.1	29.7	35.4	41.5	47.7	54.2	60.8	67.7	74.7	81.9	89.3	96.8	104.5	112.3	120.2
Yp(mm)	7.2	5.8	5.4	5.4	5.3	4.9	4.8	5.3	5.5	5.1	5.0	3.9	4.3	3.9	3.7	3.7	3.5	3.1
EQ	6.4	4.9	4.3	5.2	4.7	4.2	4.7	2.9	3.8	2.7	2.9	2.4	2.3	2.5	2.6	1.5	1.3	1.3
eq02	1.5	3.6	6.1	3.5	4.1	3.2	5.7	5.7	3.7	4.0	3.4	3.2	3.1	3.6	3.1	2.9	2.6	2.4
eq03	3.3	2.3	2.9	1.1	2.8	3.3	2.6	3.8	2.7	2.9	2.5	2.3	2.2	2.3	1.3	1.3	1.3	1.2
eq04	9.0	7.7	6.4	3.4	2.5	3.2	3.8	4.0	2.9	2.7	2.7	2.6	2.4	2.2	2.0	1.8	1.6	1.4
eq05	5.8	5.3	6.3	6.1	4.9	7.1	5.1	5.2	7.3	6.8	6.2	5.5	4.9	4.3	3.9	3.6	3.3	3.1
eq06	8.9	8.3	8.4	8.6	7.9	6.9	5.0	4.6	4.3	4.4	3.6	3.2	3.0	2.8	2.8	3.0	3.1	3.1
eq07	1.3	2.3	2.5	2.7	3.2	3.2	1.4	3.5	2.5	2.4	1.3	1.2	1.4	1.3	1.4	1.3	1.3	1.3
eq08	5.6	6.2	4.4	3.7	4.4	4.6	5.3	4.0	4.5	4.5	3.6	3.2	3.4	3.2	3.4	2.8	2.9	2.7
eq09	5.4	4.8	5.9	5.0	4.9	4.6	4.7	4.6	2.9	3.2	3.9	3.1	2.6	2.9	2.9	2.3	3.4	1.5
eq10	7.4	4.3	4.2	3.6	3.6	3.7	3.7	3.5	3.5	3.0	3.1	2.6	2.8	2.2	2.5	2.2	2.7	2.4
eq11	6.6	5.4	6.0	5.6	5.1	6.2	6.0	4.9	3.4	3.1	2.9	2.4	2.5	2.7	2.5	2.4	2.5	2.2
eq12	12.3	6.9	5.6	3.6	3.5	4.1	3.7	3.0	3.2	3.7	3.6	3.8	3.9	3.8	3.9	4.0	4.0	4.0
eq13	6.1	4.5	3.8	5.2	4.0	4.0	3.5	2.7	3.5	2.8	2.5	3.3	3.8	3.1	3.5	3.4	3.4	1.5
eq14	6.1	5.4	3.1	2.7	2.6	2.1	1.5	1.1	1.1	1.0	1.1	1.2	1.4	2.8	2.9	3.0	3.0	2.8
eq15	4.1	2.9	1.9	1.7	2.0	2.4	2.8	2.7	2.3	2.6	2.5	2.4	2.0	2.1	1.5	1.4	1.3	1.2
eq16	8.4	7.9	6.6	7.3	5.5	5.7	5.7	5.5	4.5	5.5	4.7	4.5	3.7	3.2	3.2	3.2	3.0	2.8
eq17	4.5	3.4	3.1	3.0	3.5	4.0	4.5	3.7	4.9	4.3	5.1	4.8	4.6	4.7	4.4	4.1	3.7	4.1
eq18	3.8	4.7	3.4	4.4	4.4	4.1	4.1	4.3	6.3	6.3	4.7	7.2	5.2	4.3	4.3	4.7	4.6	3.9
eq19	3.0	3.2	2.4	4.7	4.5	5.1	5.4	5.9	4.8	5.0	4.8	5.1	4.9	5.1	5.3	5.0	4.4	4.1
eq20	5.8	5.0	4.6	4.3	4.2	4.3	4.2	4.0	3.9	3.8	3.5	3.4	3.2	3.2	3.1	2.9	2.9	2.5
MEAN:	2.7	1.8	1.8	1.8	1.3	1.4	1.3	1.2	1.5	1.4	1.3	1.5	1.2	1.0	1.1	1.1	1.0	1.0
S.DEV.:	5.9	4.9	4.4	4.1	4.2	4.1	4.6	4.0	3.6	3.4	3.5	3.2	3.0	3.0	3.0	2.9	3.0	2.6
MEDIAN:																		

A=0.4, SOIL TYPE III, SI=1.5, BILINEAR NON-ISOLATED PIER ALPHA=0.05 R=1.0

MAXIMUM PIER DUCTILITY, YIELD (Yp) in mm

EQ	17.9	31.8	49.7	71.6	97.4	127.2	155.5	178.9	203.2	228.1	253.8	280.2	307.2	334.8	363.0	391.7	421.0	450.8
TP(sec)	0.3	0.4	0.5	0.6	0.7	0.8	0.9	1.0	1.1	1.2	1.3	1.4	1.5	1.6	1.7	1.8	1.9	2.0
EQ	1.0	0.8	1.1	1.0	1.1	1.0	0.8	0.8	0.8	0.8	0.7	0.6	0.6	0.6	0.7	0.6	0.6	0.5
eq31	1.1	0.9	0.8	0.8	0.9	0.9	0.9	1.0	0.9	0.7	0.7	0.6	0.6	0.7	0.7	0.6	0.6	0.5
eq32	1.8	1.0	1.6	1.0	1.0	1.0	0.9	0.9	1.0	1.1	1.2	1.2	1.2	1.2	1.1	1.1	1.1	1.0
eq33	5.0	3.0	1.9	1.6	1.1	1.3	1.1	0.8	0.6	0.5	0.5	0.6	0.7	0.6	0.5	0.4	0.3	0.4
eq34	1.3	1.6	2.1	1.3	1.2	1.0	0.9	1.1	1.5	1.3	1.0	0.8	0.8	0.9	0.8	0.8	0.8	0.8
eq39	1.5	1.0	1.6	1.9	1.7	1.7	1.5	1.4	1.4	1.2	1.1	1.0	1.0	1.0	1.1	1.1	1.0	0.9
eq40	1.4	1.2	2.1	1.8	1.0	1.5	1.3	0.8	0.6	0.8	0.9	0.9	0.8	0.7	0.7	0.8	0.9	0.9
eq45	2.0	2.0	1.5	1.0	1.0	0.8	0.7	0.7	0.8	0.9	0.9	0.9	0.9	0.9	0.8	0.8	0.8	0.8
eq46	0.7	0.5	1.0	0.9	1.0	0.7	0.8	0.8	0.7	0.8	0.8	1.0	0.8	0.9	0.7	0.7	0.6	0.7
eq47	0.5	0.5	0.7	0.6	0.6	0.5	0.5	0.3	0.3	0.4	0.4	0.4	0.4	0.5	0.5	0.7	0.7	0.6
eq48	1.9	1.3	1.5	1.1	1.1	0.9	1.2	1.0	1.0	1.0	0.9	0.9	0.7	0.9	1.0	1.1	0.9	0.9
eq51	1.5	1.2	1.3	1.2	1.0	1.0	1.0	1.0	1.0	1.1	1.0	1.1	1.2	1.2	1.1	1.1	1.0	1.2
eq52	2.7	2.1	1.5	1.6	1.2	0.8	1.0	1.0	1.0	1.0	1.0	0.9	1.0	0.9	0.7	0.7	0.8	0.7
eq53	1.4	1.8	1.5	1.3	1.3	1.2	1.6	1.4	1.4	1.1	1.3	1.2	1.0	1.0	1.2	1.1	1.1	0.9
eq54	1.7	1.4	1.4	1.2	1.1	1.0	1.0	0.9	0.9	0.9	0.9	0.9	0.8	0.8	0.8	0.8	0.8	0.8
MEAN:	1.1	0.7	0.5	0.4	0.3	0.3	0.3	0.3	0.3	0.3	0.2	0.2	0.2	0.2	0.2	0.2	0.2	0.2
S.DEV.:	1.4	1.2	1.5	1.2	1.1	1.0	1.0	1.0	0.9	0.9	0.9	0.9	0.8	0.8	0.8	0.8	0.8	0.8
MEDIAN:	1.4	1.2	1.5	1.2	1.1	1.0	1.0	1.0	0.9	0.9	0.9	0.9	0.8	0.8	0.8	0.8	0.8	0.8

A=0.4, SOIL TYPE III, SI=1.5, BILINEAR NON-ISOLATED PIER ALPHA=0.05 R=2.0

MAXIMUM PIER DUCTILITY, YIELD (Yp) in mm

EQ	0.3	0.4	0.5	0.6	0.7	0.8	0.9	1.0	1.1	1.2	1.3	1.4	1.5	1.6	1.7	1.8	1.9	2.0
Yp(sec)	8.9	15.9	24.8	35.8	48.7	63.6	77.7	89.5	101.6	114.1	126.9	140.1	153.6	167.4	181.5	195.9	210.5	225.4
EQ	2.1	1.8	2.0	1.9	1.9	1.4	1.3	1.5	1.8	1.7	1.4	1.3	1.4	1.4	1.3	1.2	1.0	1.0
eq31	2.6	1.8	1.4	2.0	1.6	2.0	1.9	2.0	1.8	1.5	1.3	1.4	1.5	1.5	1.3	1.1	1.0	1.0
eq32	3.4	2.7	2.8	1.8	2.3	2.3	2.1	2.4	2.7	2.8	2.8	2.7	2.6	2.5	2.3	2.2	2.1	1.9
eq33	7.2	4.7	2.7	2.9	2.4	2.4	2.4	1.9	1.2	1.1	1.0	1.3	1.3	1.2	1.1	0.8	0.7	0.7
eq34	4.3	4.9	4.2	2.2	2.0	1.9	2.0	2.3	2.3	1.7	1.4	1.4	1.7	1.6	1.8	1.6	1.6	1.6
eq39	5.6	5.3	4.7	4.4	3.8	2.8	2.4	2.4	2.4	2.2	1.7	1.5	1.6	2.1	2.0	1.6	1.6	1.6
eq40	3.4	5.0	4.9	4.1	3.5	2.8	2.1	1.7	1.3	1.8	2.3	2.1	1.7	1.4	1.6	1.8	1.8	1.9
eq45	6.4	5.0	3.8	2.3	1.8	1.3	1.2	1.3	1.5	1.7	1.8	1.8	1.8	1.8	1.7	1.7	1.6	1.6
eq46	1.8	1.1	2.5	2.1	1.6	1.5	1.4	1.3	1.8	1.6	2.0	2.0	2.3	2.1	1.3	1.2	1.2	1.4
eq47	1.0	1.0	1.0	1.3	1.1	0.9	1.0	0.7	0.7	0.8	0.8	0.8	0.9	1.2	1.0	1.2	1.2	1.3
eq48	4.3	3.8	3.4	2.1	2.1	2.2	2.9	1.6	1.4	1.7	2.0	1.5	1.5	2.0	2.3	2.6	2.3	2.3
eq51	3.8	3.2	2.2	2.7	2.6	1.8	1.6	1.6	1.8	1.6	1.9	2.2	2.4	2.6	2.3	2.0	2.5	2.2
eq52	6.9	4.4	3.7	3.3	2.5	1.9	1.6	1.7	1.5	1.9	1.6	1.5	1.7	1.7	1.4	1.3	1.7	1.5
eq53	7.6	5.7	5.4	4.2	3.3	3.7	3.3	3.5	2.2	2.6	2.3	1.7	2.0	2.3	2.2	2.0	1.9	1.4
eq54	4.3	3.6	3.2	2.7	2.3	2.1	1.9	1.8	1.7	1.8	1.7	1.7	1.7	1.8	1.7	1.6	1.6	1.5
MEAN:	2.1	1.7	1.3	1.0	0.8	0.7	0.7	0.7	0.5	0.5	0.5	0.5	0.4	0.5	0.5	0.5	0.5	0.4
S.DEV.:	4.1	4.1	3.1	2.2	2.2	1.9	2.0	1.7	1.8	1.7	1.7	1.5	1.7	1.8	1.6	1.6	1.6	1.6
MEDIAN:																		

A=0.4, SOIL TYPE III, SI=1.5, BILINEAR NON-ISOLATED PIER ALPHA=0.05 R=3.0

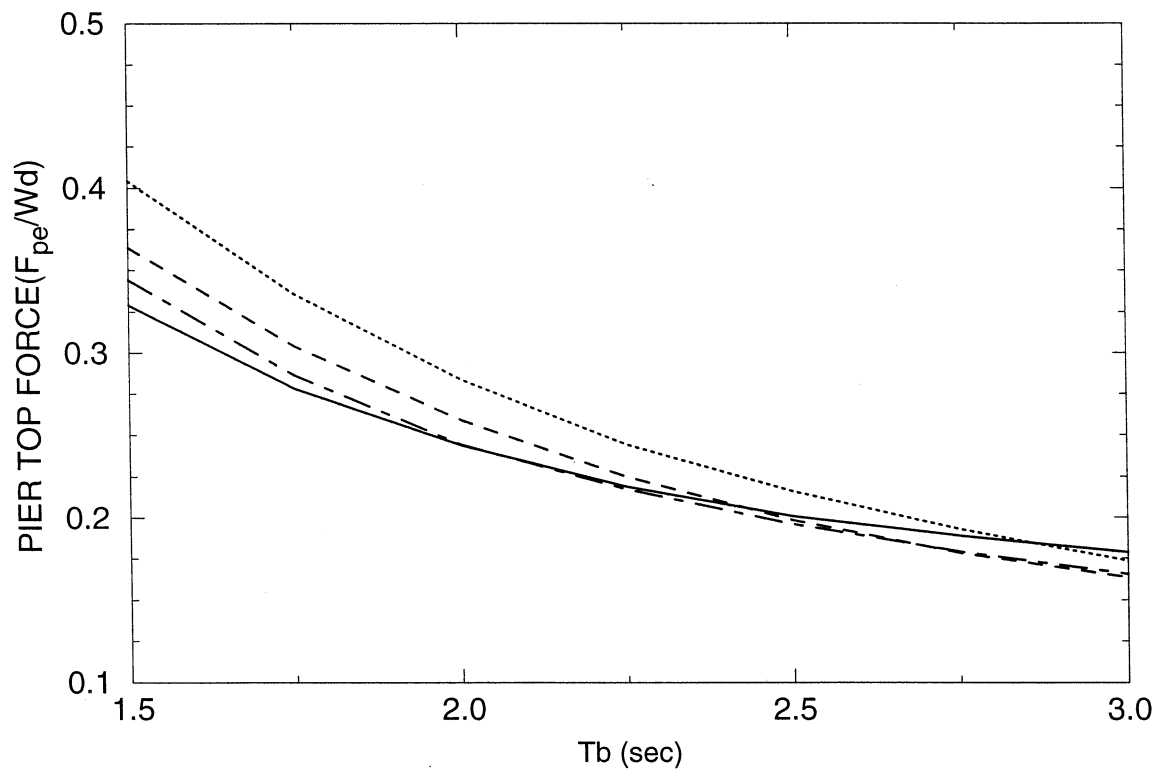
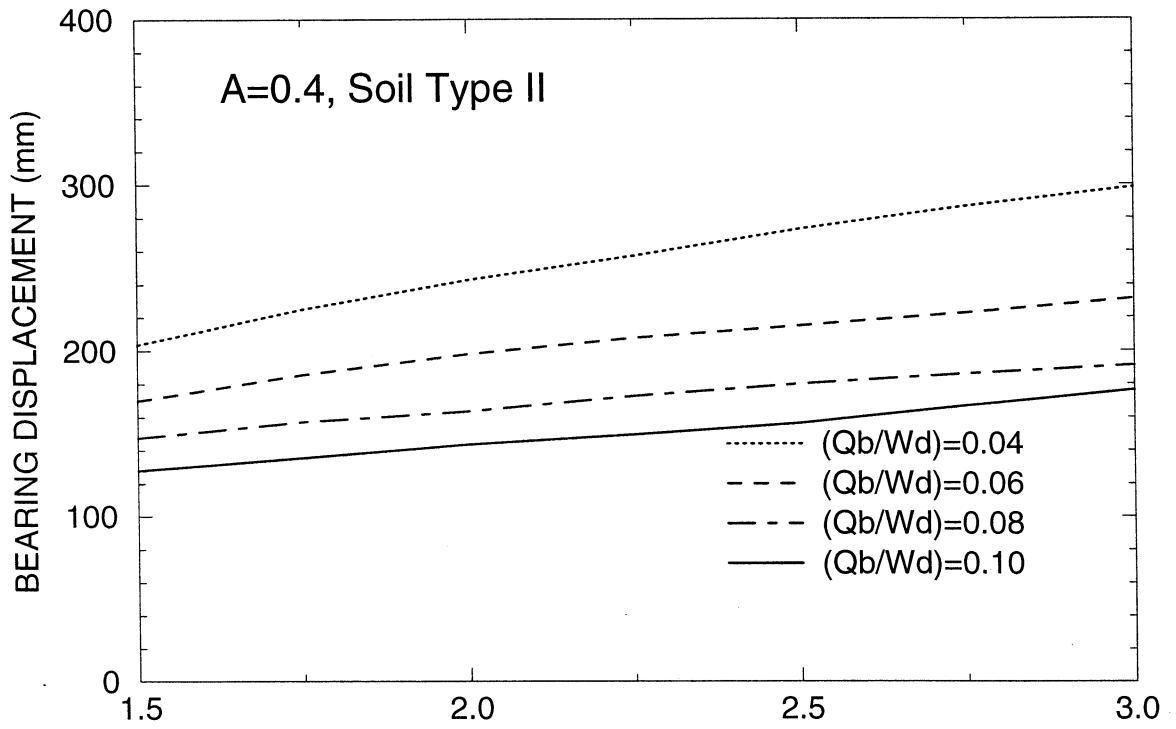
MAXIMUM PIER DUCTILITY, YIELD (Yp) in mm

EQ	0.3	0.4	0.5	0.6	0.7	0.8	0.9	1.0	1.1	1.2	1.3	1.4	1.5	1.6	1.7	1.8	1.9	2.0
TP(sec)	6.0	10.6	16.6	23.9	32.5	42.4	51.8	59.6	67.7	76.0	84.6	93.4	102.4	111.6	121.0	130.6	140.3	150.3
EQ31	4.1	2.8	2.8	2.7	2.9	2.7	2.2	2.8	2.5	2.4	2.5	2.2	2.3	2.3	2.2	1.7	1.5	1.4
EQ32	5.7	3.6	2.9	3.5	2.8	3.0	3.0	2.4	2.6	2.4	2.3	2.3	2.5	2.3	1.7	1.5	1.6	1.4
EQ33	7.2	6.5	3.8	3.8	4.3	4.6	4.5	4.6	4.6	4.4	4.1	3.7	3.2	2.9	2.7	2.5	2.4	2.3
EQ34	11.6	6.1	4.7	5.0	3.9	3.9	4.0	3.0	2.0	1.6	1.8	1.9	1.6	1.6	1.6	1.3	1.1	1.0
EQ39	11.1	8.7	6.5	3.7	3.5	3.4	3.5	3.5	3.2	2.4	2.0	2.2	2.1	2.4	2.7	2.5	2.6	2.9
EQ40	15.9	11.8	8.9	7.6	5.9	4.4	4.0	4.0	4.0	3.8	3.1	2.5	2.7	2.7	2.4	2.6	2.7	2.8
EQ45	9.7	9.9	8.1	7.1	5.5	3.8	3.4	3.1	2.8	3.5	4.0	3.7	3.2	3.1	3.2	3.2	3.0	2.2
EQ46	11.6	8.9	4.9	2.8	2.3	2.3	2.1	2.0	1.9	2.1	2.2	2.3	2.4	2.4	2.4	2.4	2.3	2.2
EQ47	4.4	1.8	4.4	3.5	3.0	2.4	2.5	2.1	3.3	2.4	3.3	3.6	3.9	3.0	2.3	1.7	1.9	2.0
EQ48	1.4	1.3	1.7	1.7	1.5	1.3	1.4	1.1	1.0	1.2	1.5	1.1	1.4	1.7	1.5	1.6	2.5	2.9
EQ51	7.5	6.9	4.8	3.3	3.7	4.0	3.8	3.0	2.7	3.2	2.9	2.0	2.7	3.0	3.4	3.8	3.7	3.3
EQ52	6.5	4.6	4.1	4.0	3.2	2.6	2.3	2.5	2.3	2.6	3.2	3.8	3.9	2.9	2.9	3.1	3.0	3.1
EQ53	10.7	6.6	6.2	3.7	3.7	2.6	2.8	2.3	2.5	2.8	1.9	2.0	2.4	1.8	2.0	2.4	2.7	2.2
EQ54	16.3	13.4	11.0	8.7	7.7	5.4	4.5	3.9	3.2	3.6	2.9	3.1	3.7	3.4	2.7	2.6	2.5	2.2
MEAN:	8.8	6.6	5.4	4.4	3.9	3.3	3.1	2.9	2.8	2.7	2.7	2.6	2.7	2.5	2.4	2.4	2.4	2.3
S.DEV.:	4.4	3.7	2.6	2.0	1.6	1.1	1.0	0.9	0.9	0.9	0.8	0.8	0.8	0.6	0.6	0.7	0.7	0.7
MEDIAN:	8.6	6.5	4.8	3.7	3.6	3.2	3.2	2.9	2.7	2.5	2.7	2.3	2.6	2.6	2.4	2.4	2.5	2.2

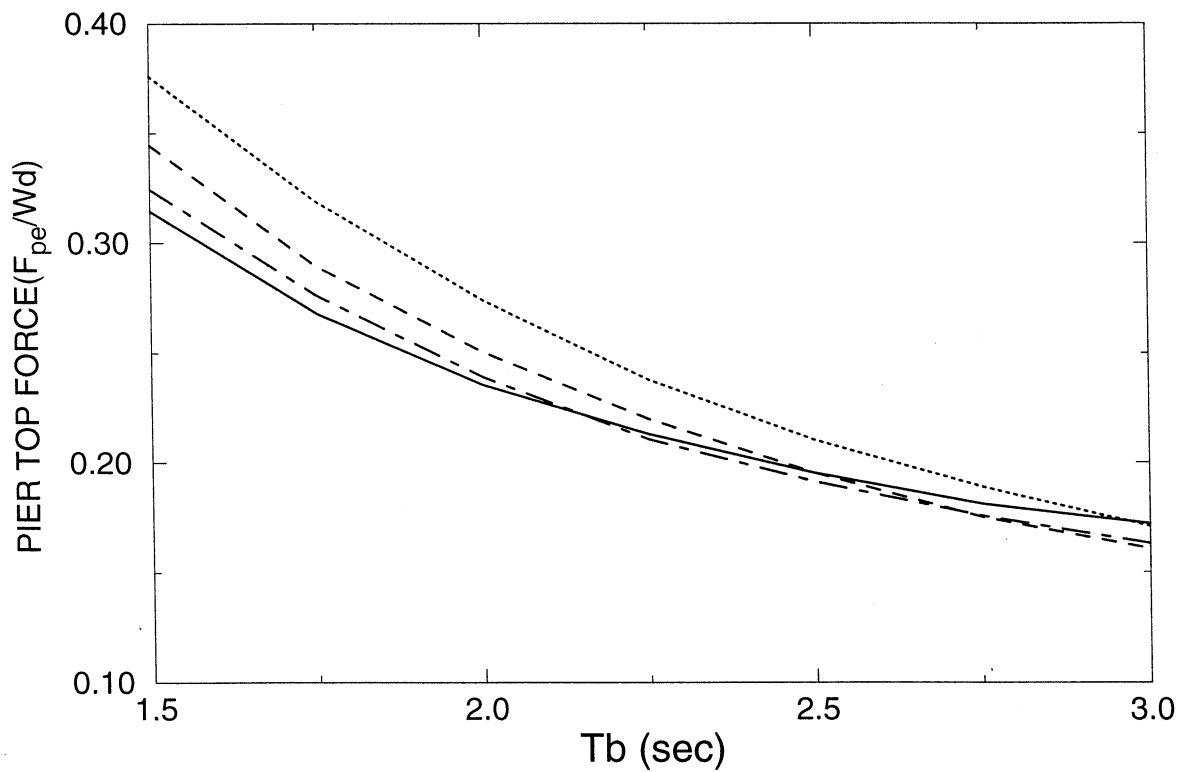
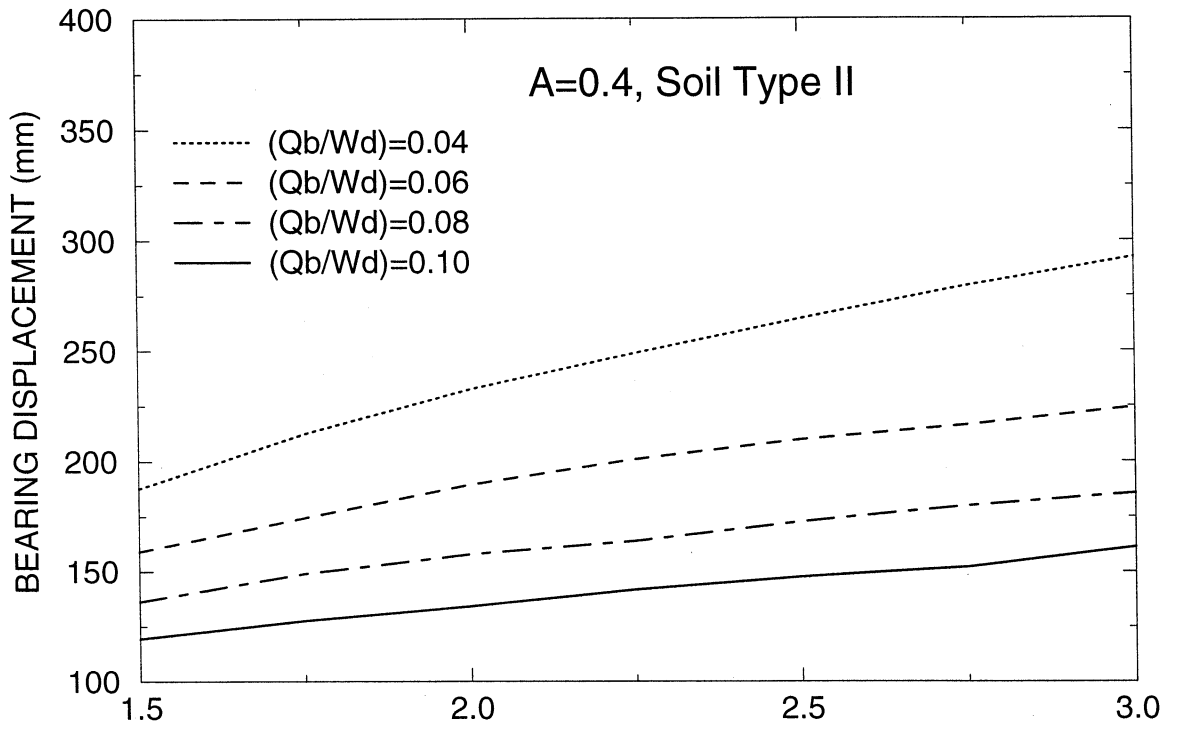
APPENDIX D

**RESULTS OF ANALYSIS OF SEISMIC-ISOLATED
BRIDGE BY THE UNIFORM LOAD METHOD
OF THE 1997 AASHTO GUIDE SPECIFICATIONS
FOR SEISMIC ISOLATION DESIGN**

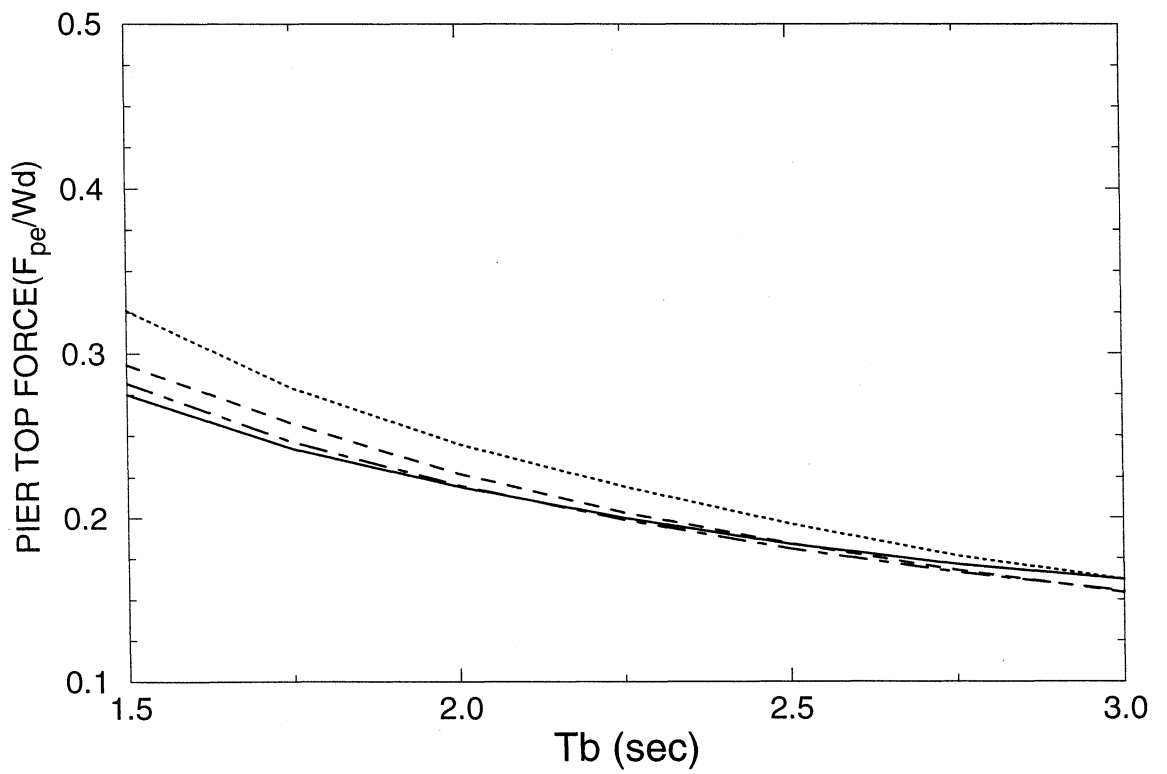
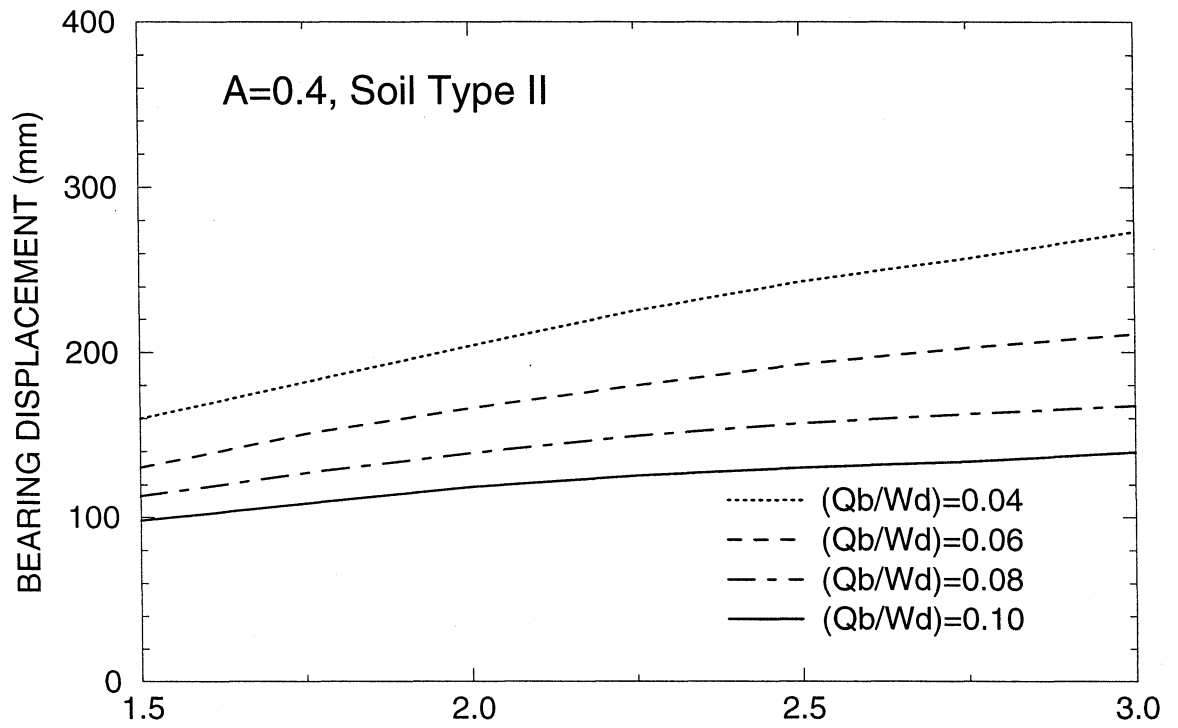
Wd/Wp=10, Tp=0.1 s, AASHTO UNIFORM LOAD METHOD
BILINEAR HYSTERETIC OR SLIDING ISOLATION SYSTEM



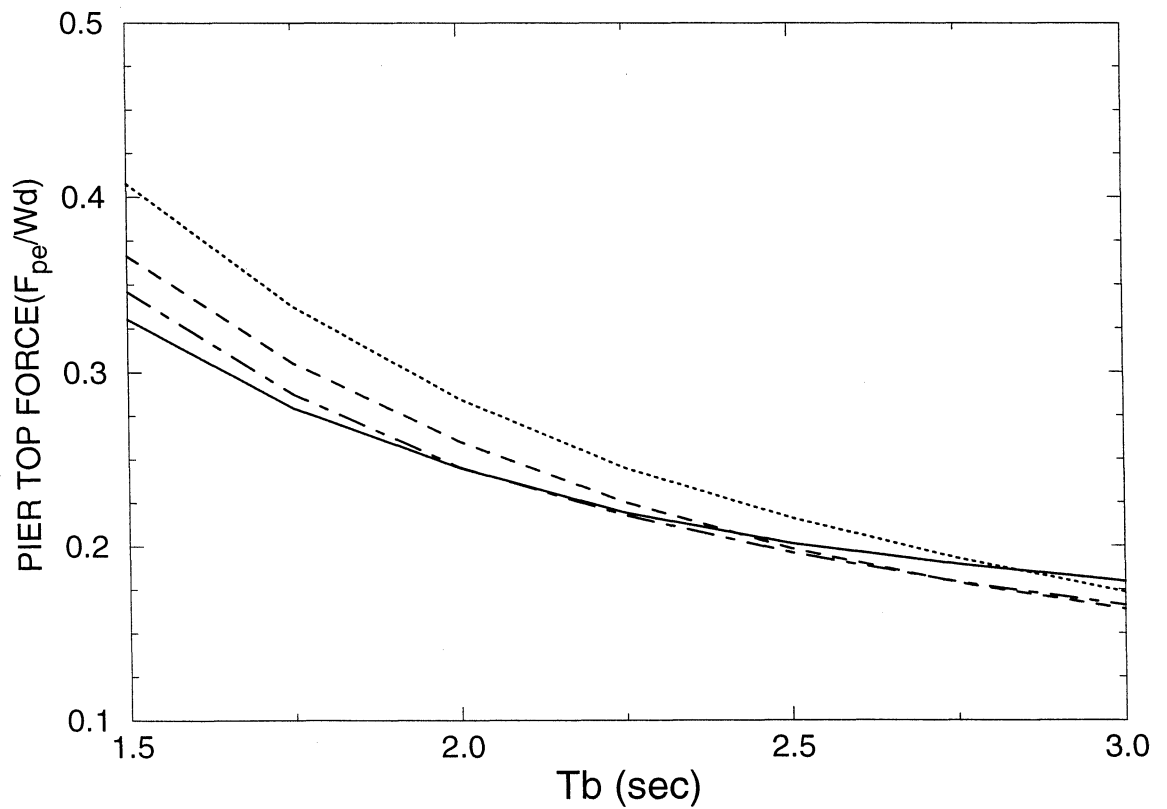
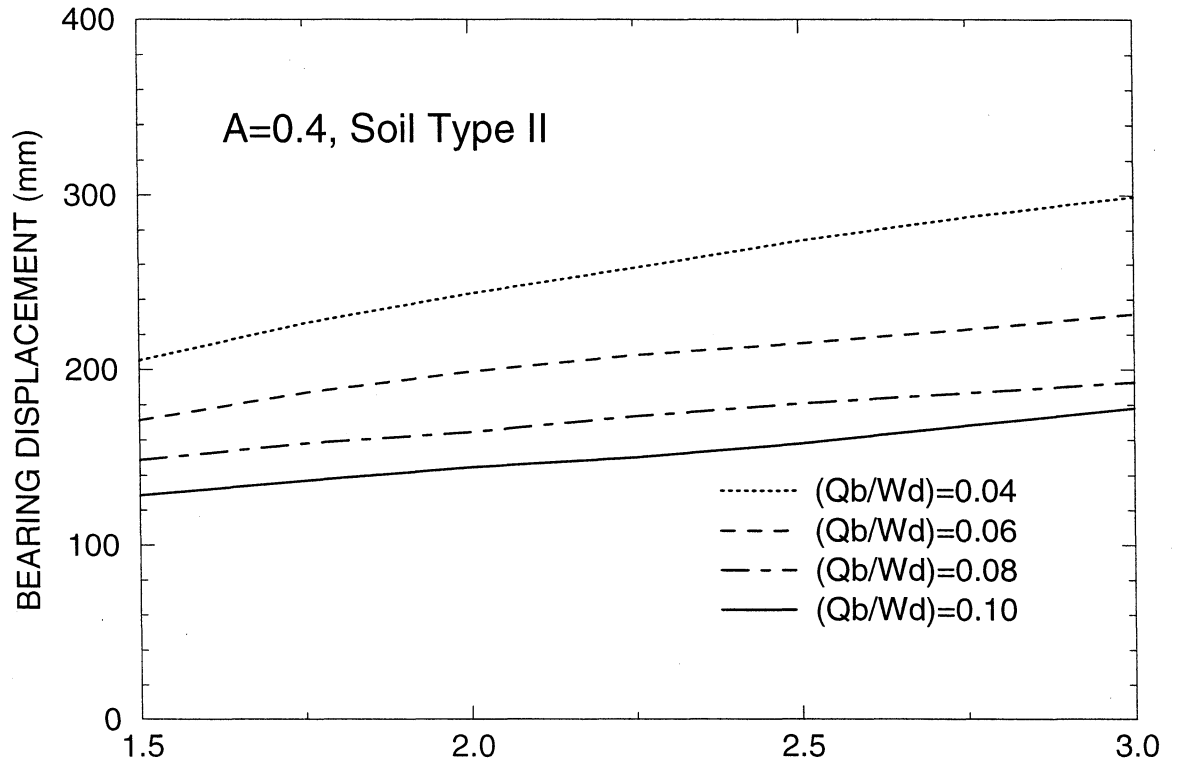
Wd/Wp=10, Tp=0.25 s, AASHTO UNIFORM LOAD METHOD
BILINEAR HYSTERETIC OR SLIDING ISOLATION SYSTEM



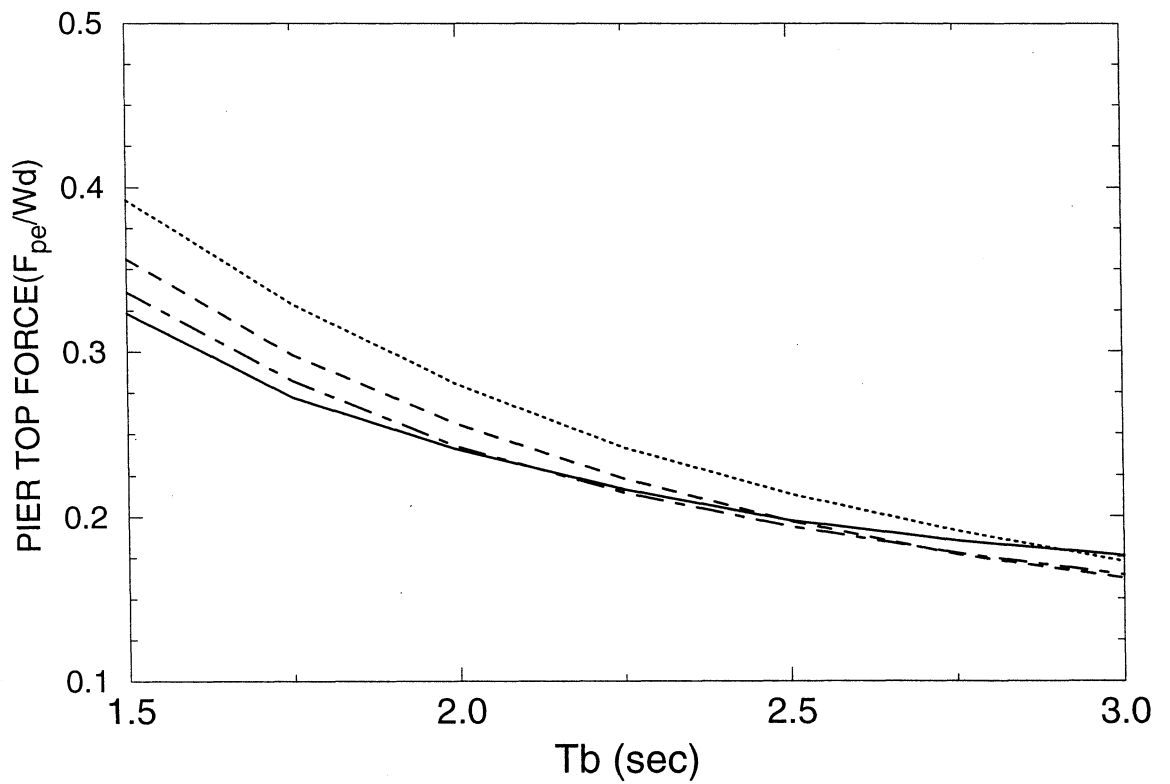
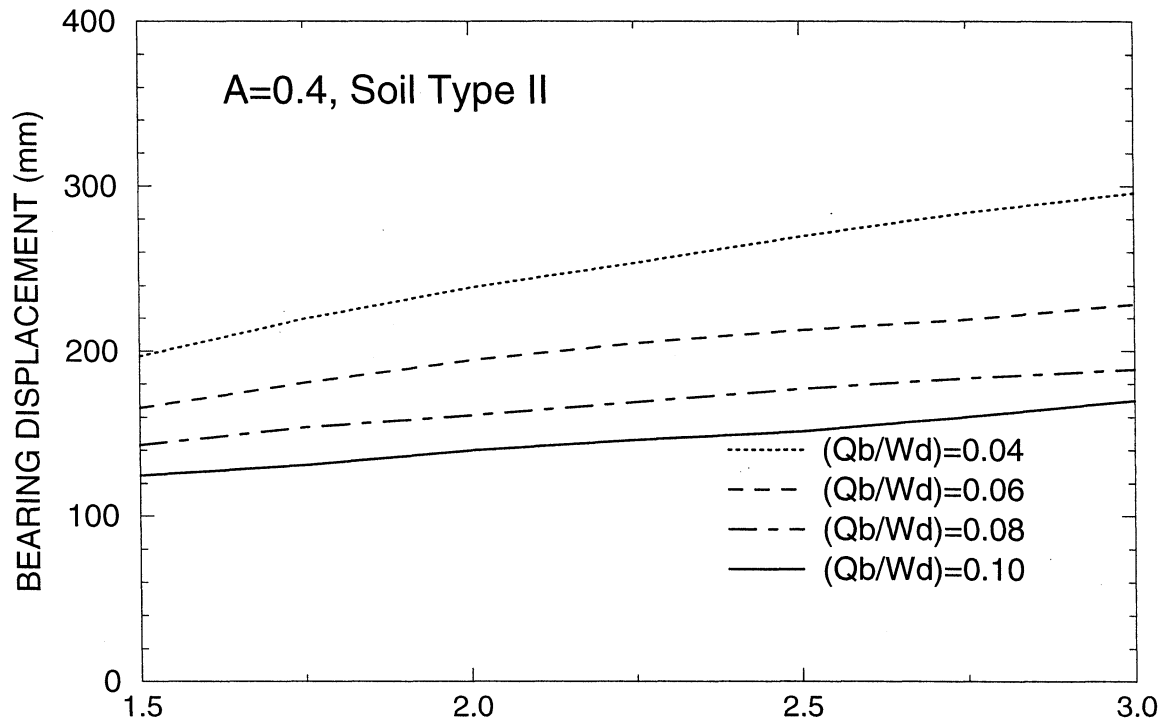
Wd/Wp=10, Tp=0.5 s, AASHTO UNIFORM LOAD METHOD
BILINEAR HYSTERETIC OR SLIDING ISOLATION SYSTEM



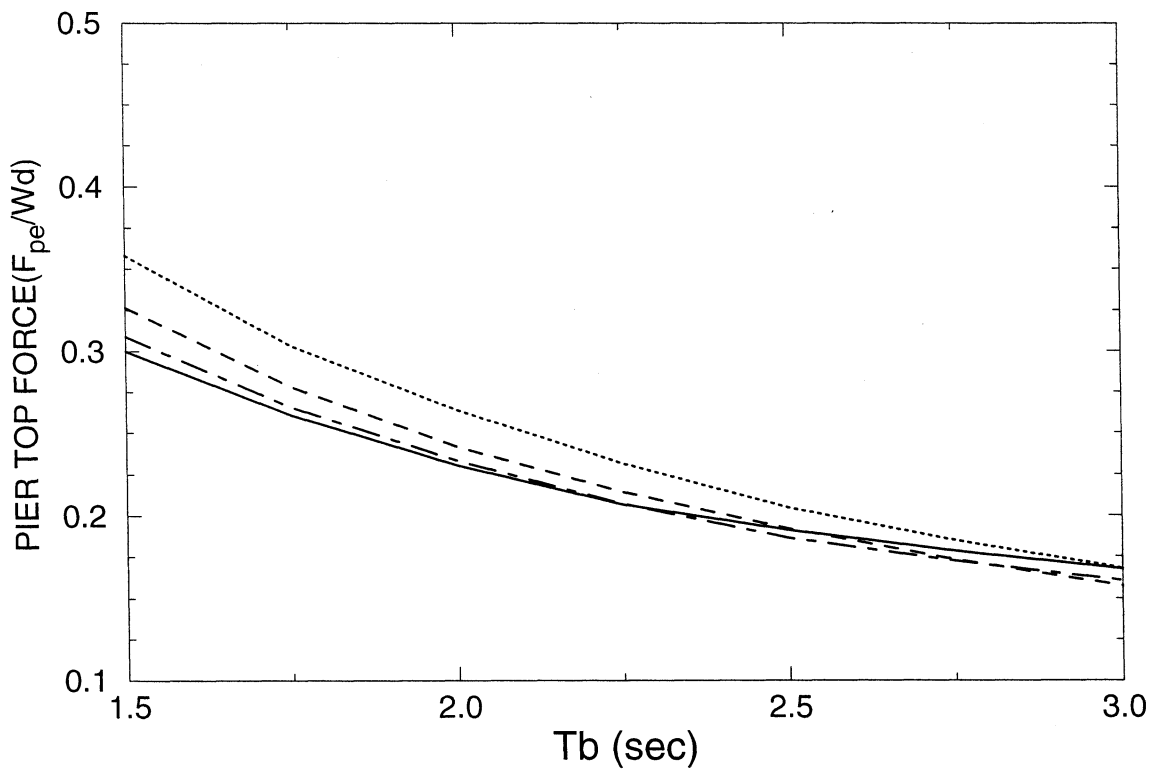
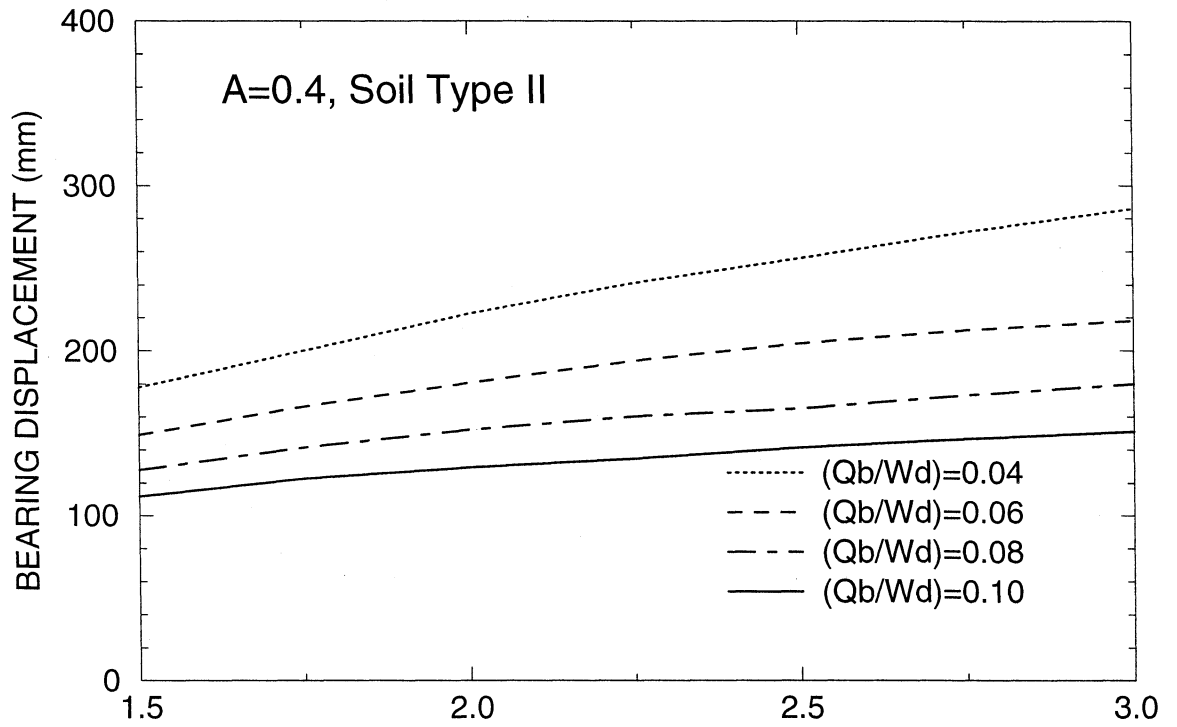
Wd/Wp=5, Tp=0.1 s, AASHTO UNIFORM LOAD METHOD
BILINEAR HYSTERETIC OR SLIDING ISOLATION SYSTEM



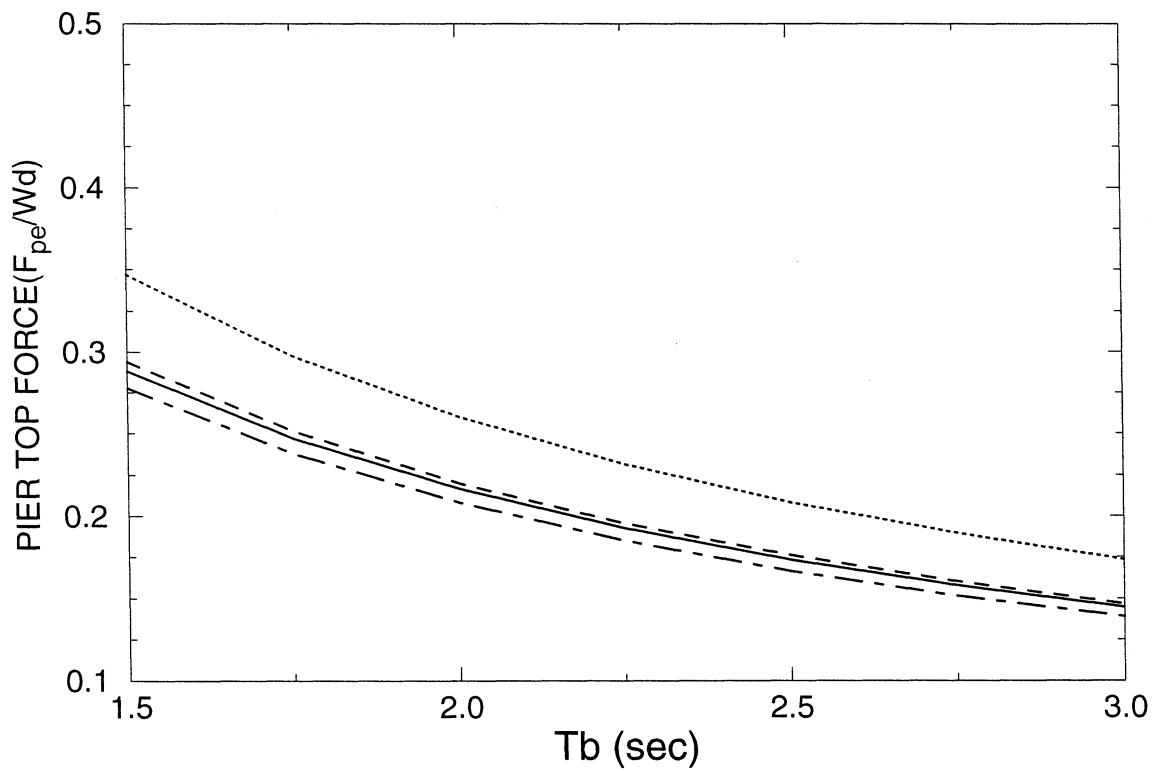
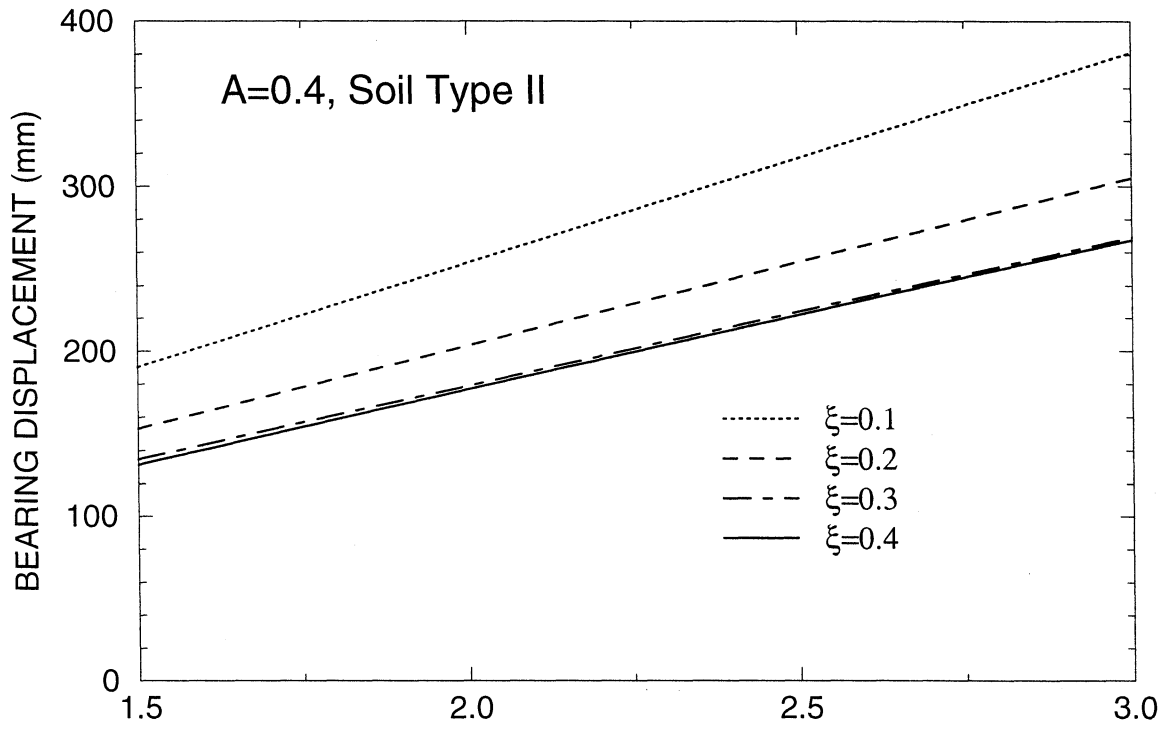
Wd/Wp=5, Tp=0.25 s, UNIFORM LOAD METHOD
BILINEAR HYSTERETIC OR SLIDING ISOLATION SYSTEM



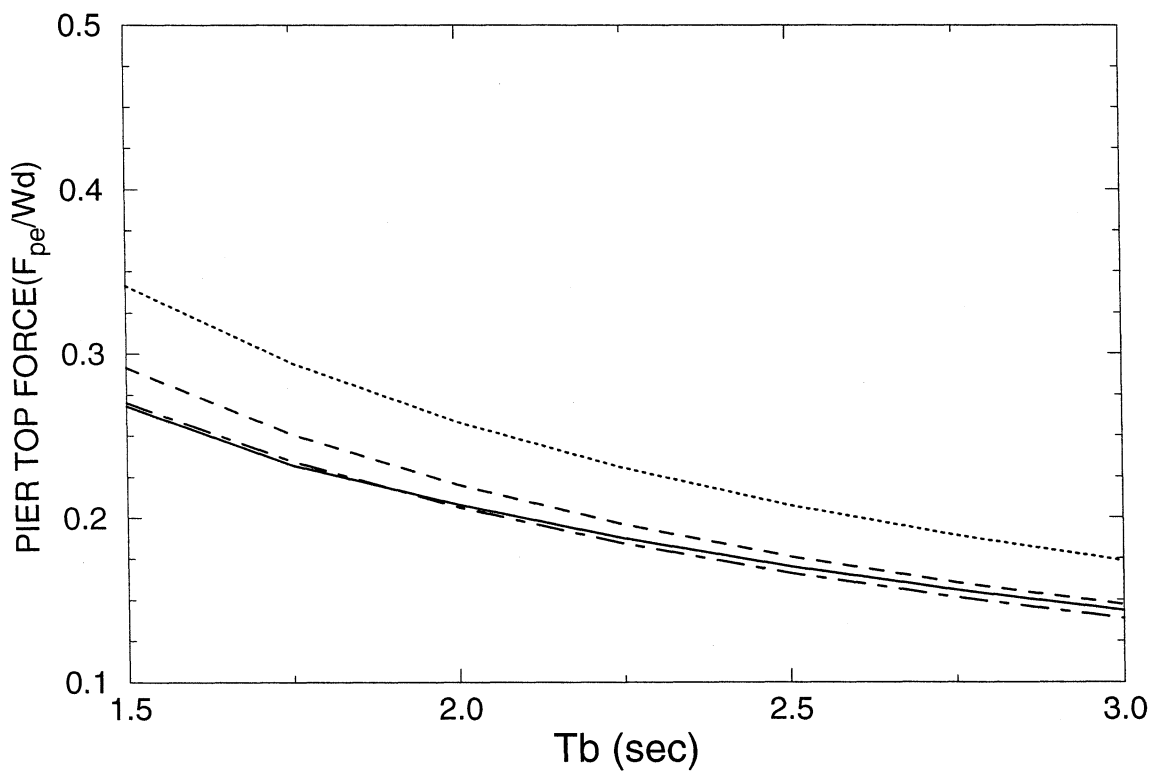
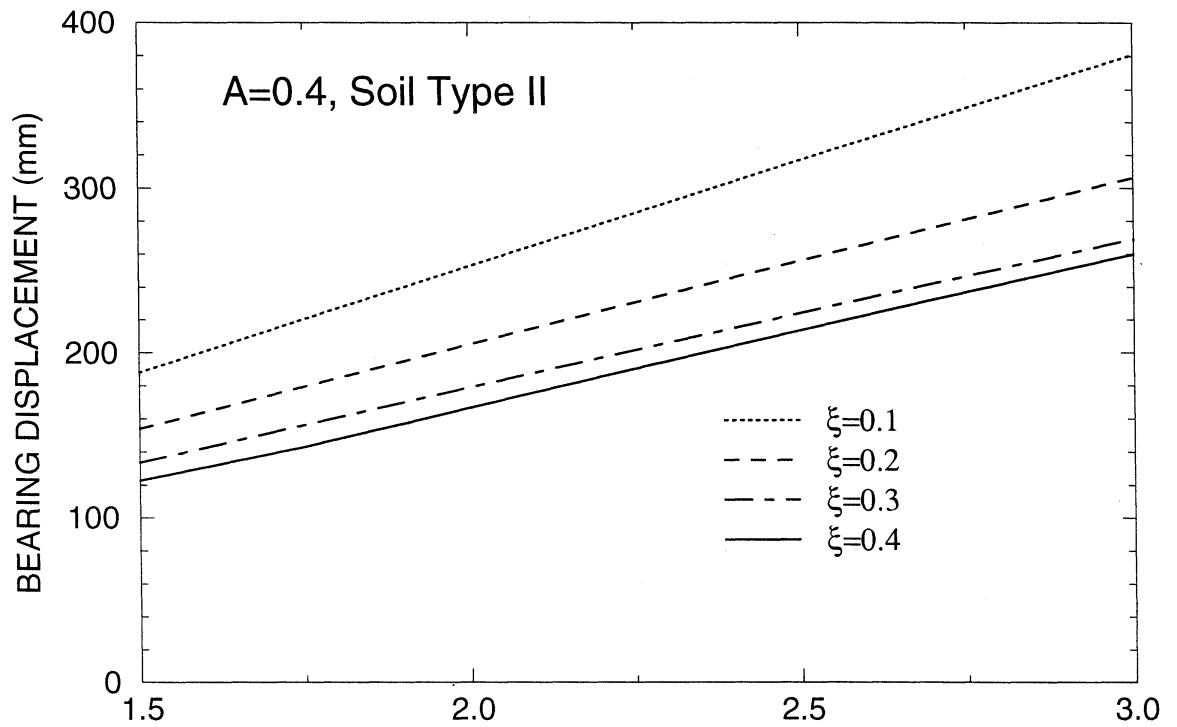
Wd/Wp=5, Tp=0.5 s, UNIFORM LOAD METHOD
BILINEAR HYSTERETIC OR SLIDING ISOLATION SYSTEM



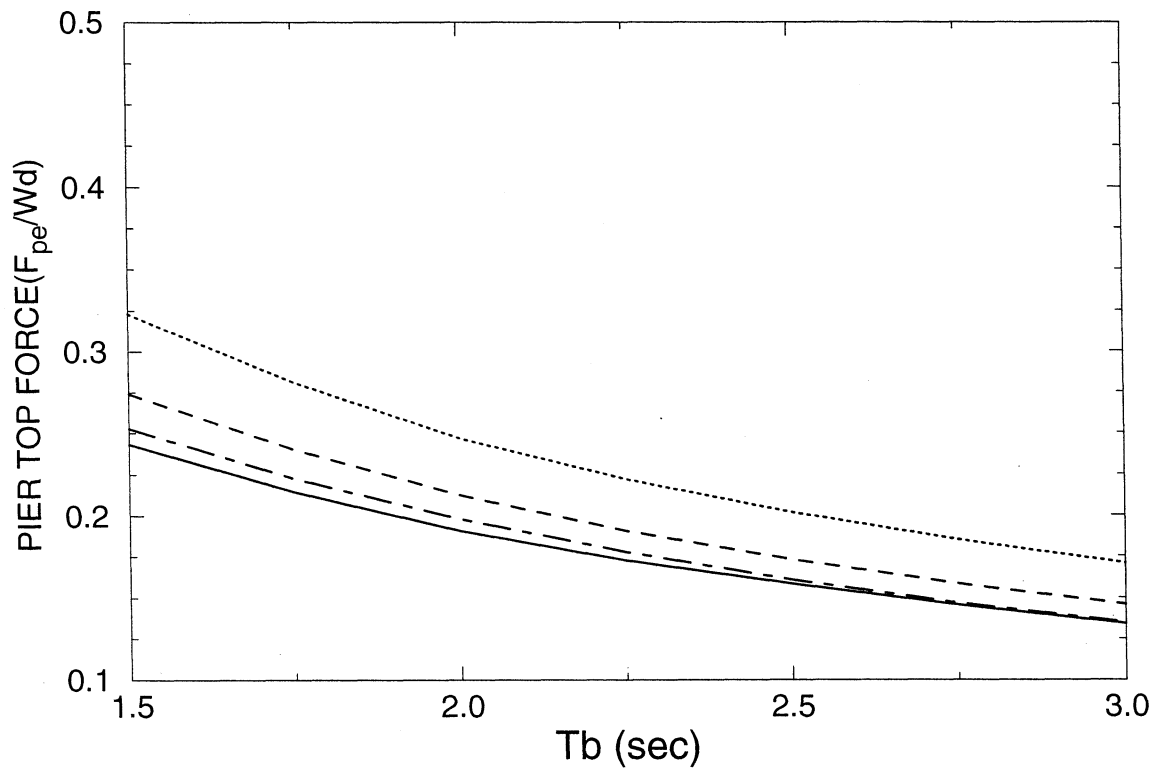
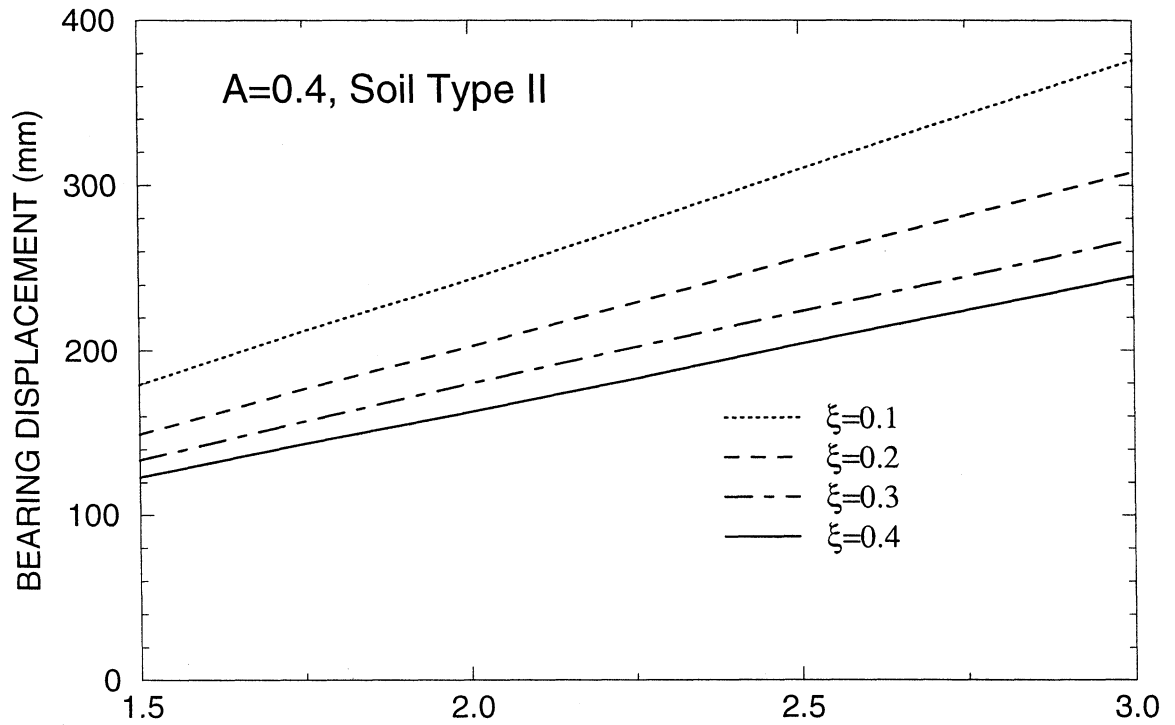
Wd/Wp=10, Tp=0.1 s, AASHTO UNIFORM LOAD METHOD
LINEAR ELASTIC/VISCOUS ISOLATION SYSTEM



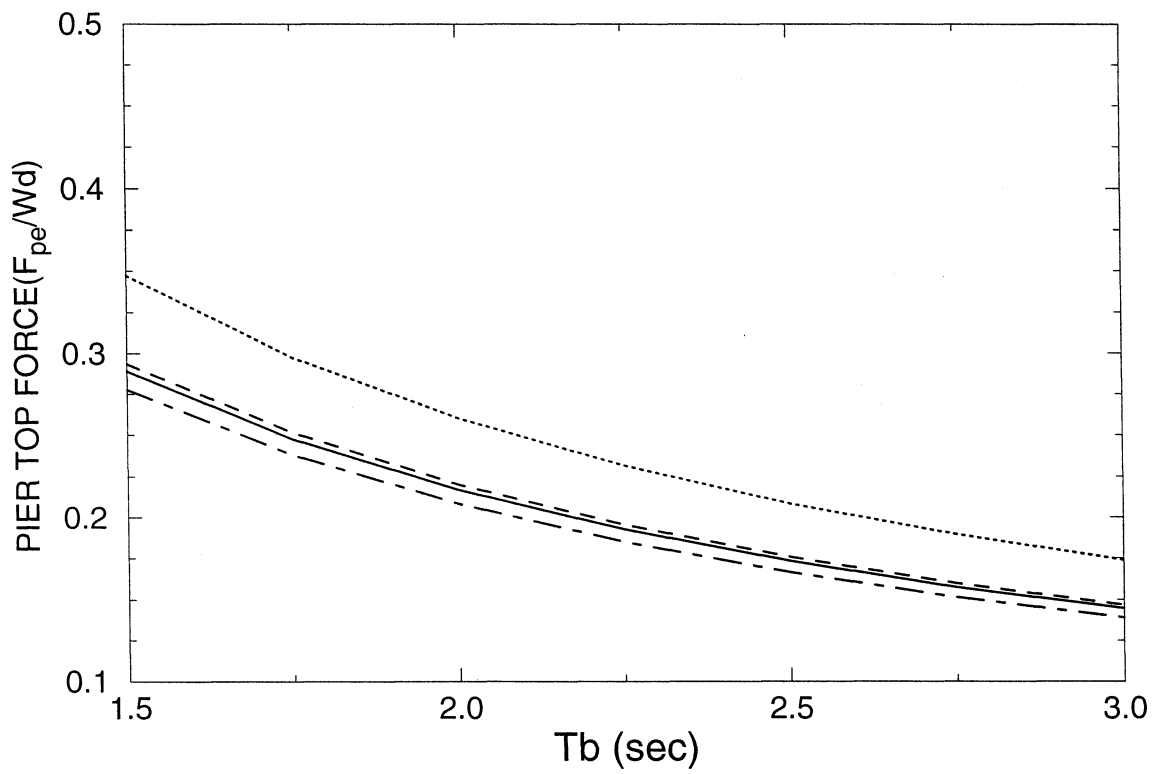
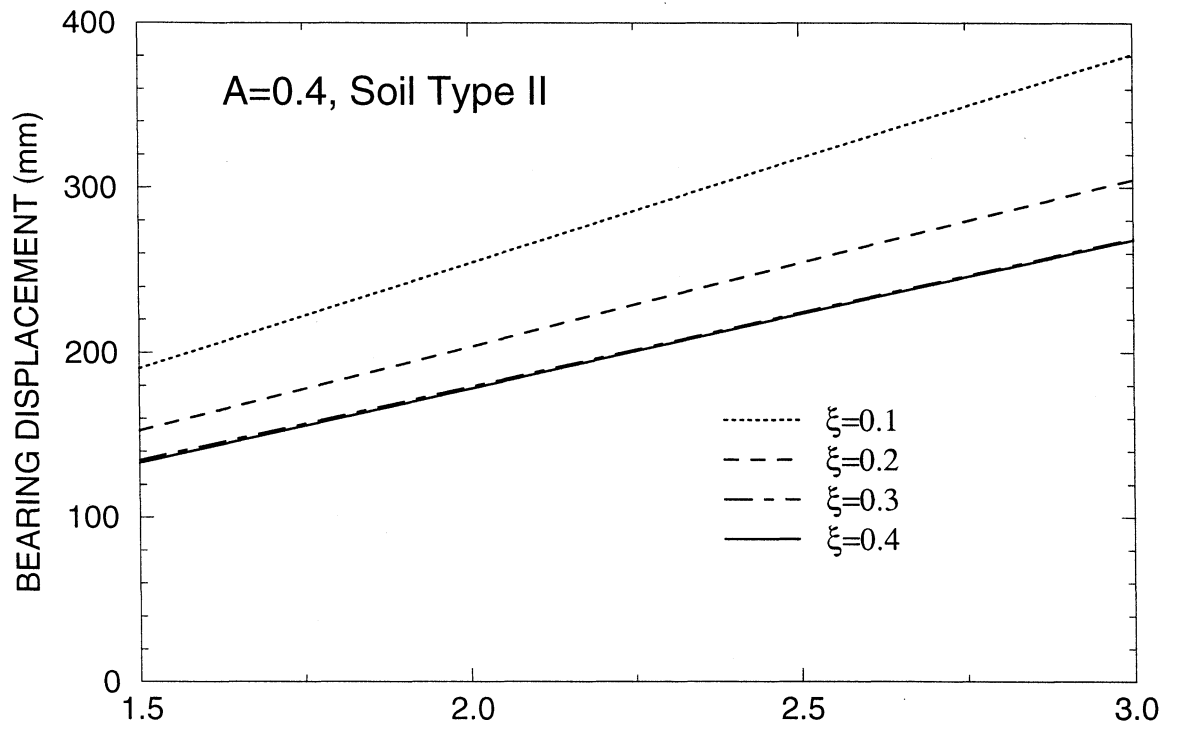
Wd/Wp=10, Tp=0.25 s, AASHTO UNIFORM LOAD METHOD
LINEAR ELASTIC/VISCOUS ISOLATION SYSTEM



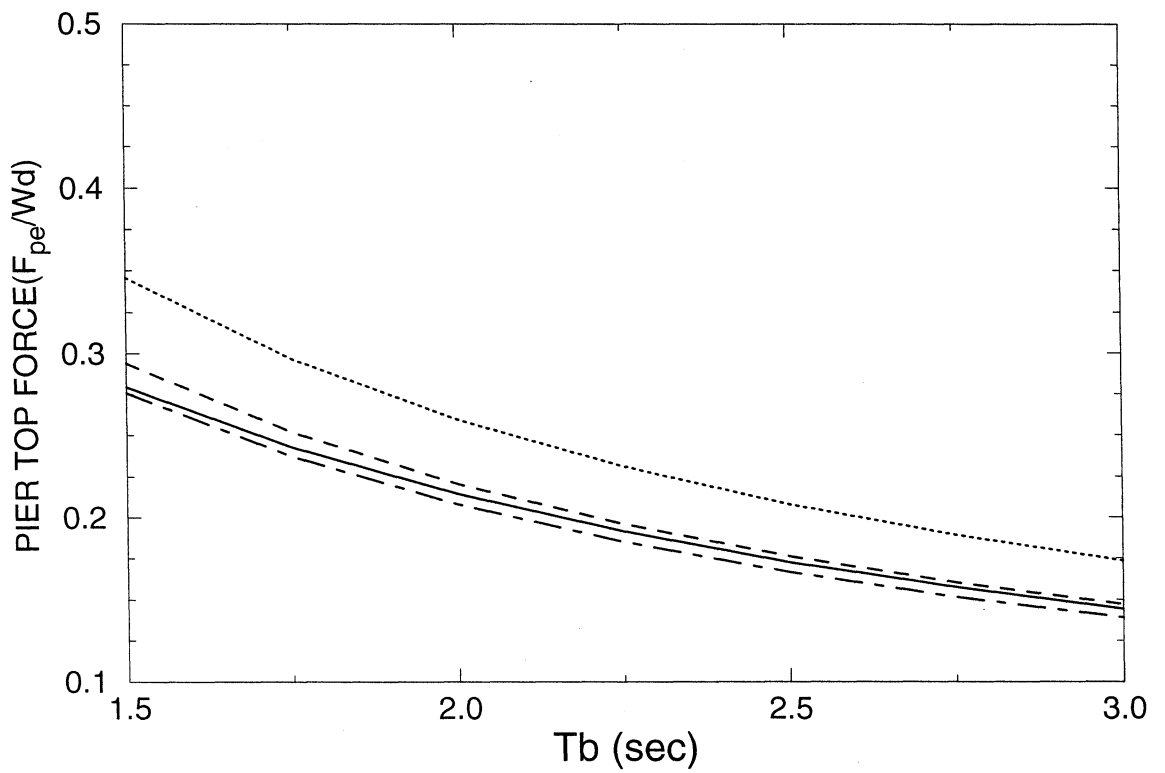
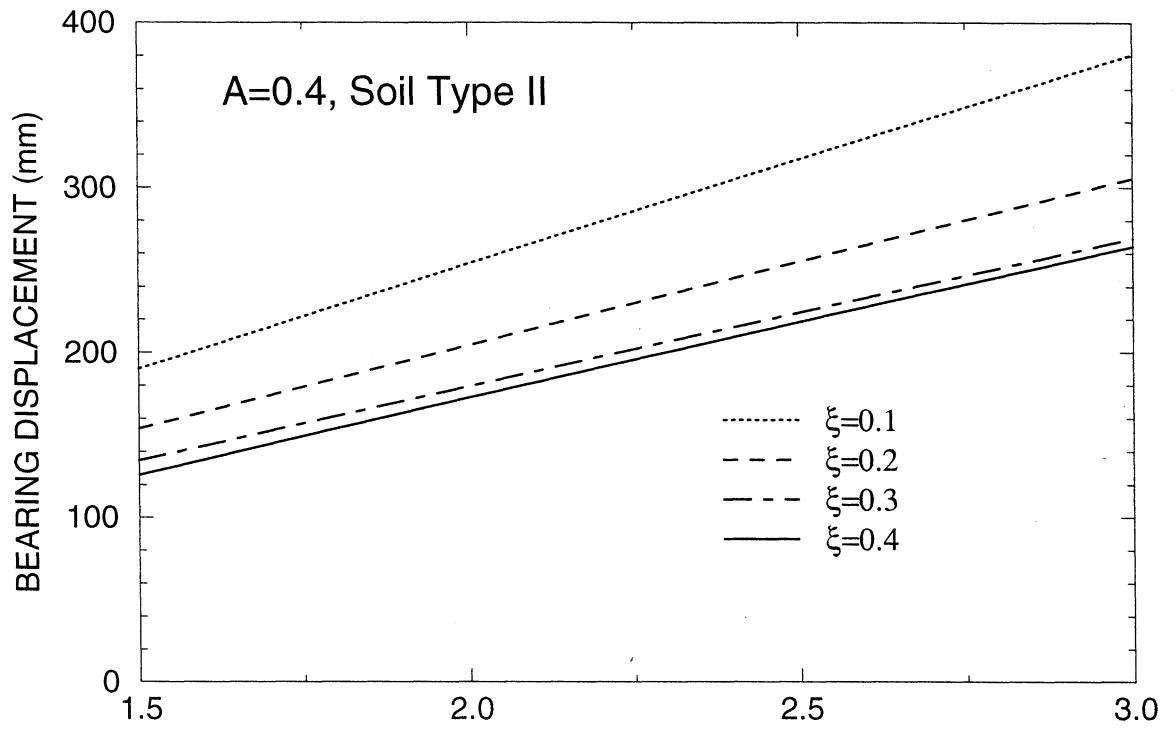
Wd/Wp=10, Tp=0.5 s, AASHTO UNIFORM LOAD METHOD
LINEAR ELASTIC/VISCOUS ISOLATION SYSTEM



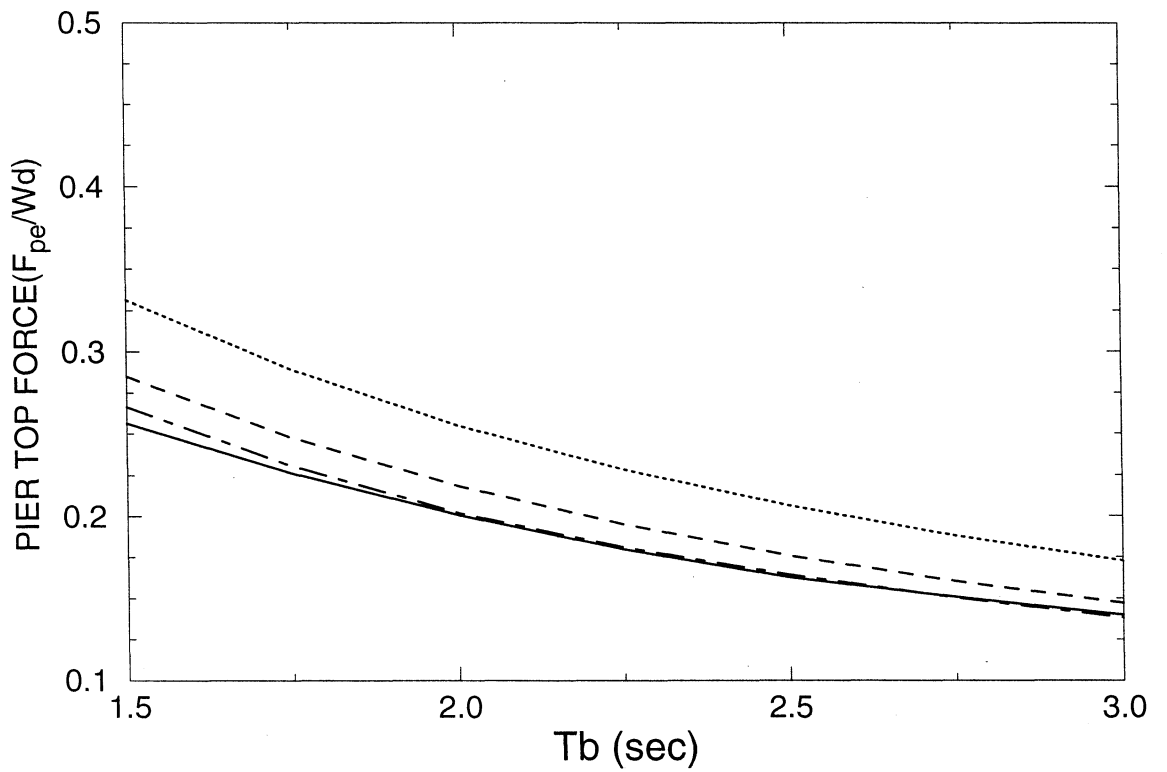
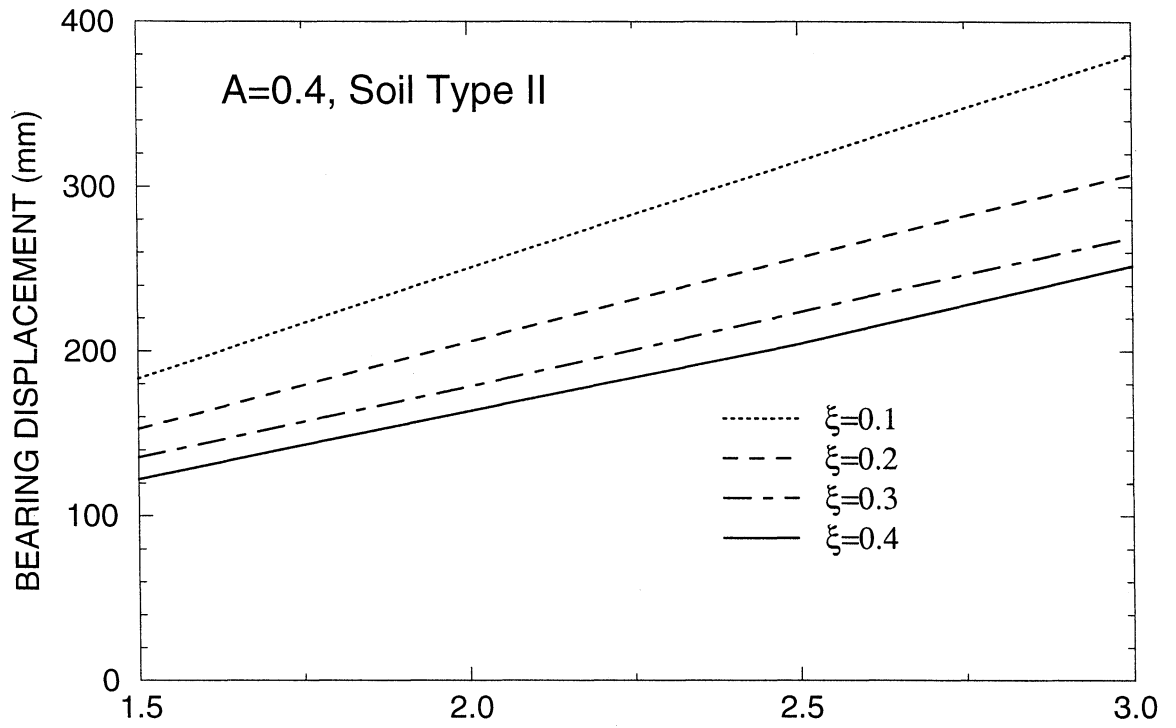
Wd/Wp=5, Tp=0.1 s, AASHTO UNIFORM LOAD METHOD
LINEAR ELASTIC/VISCOUS ISOLATION SYSTEM



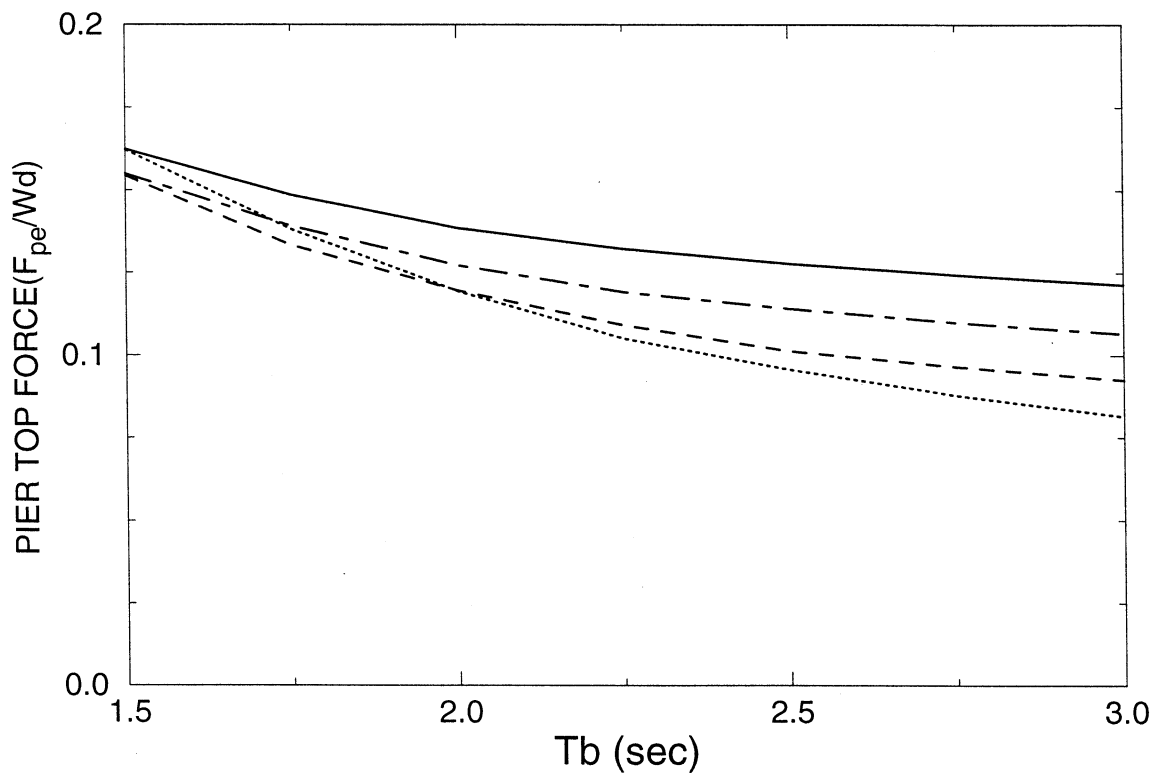
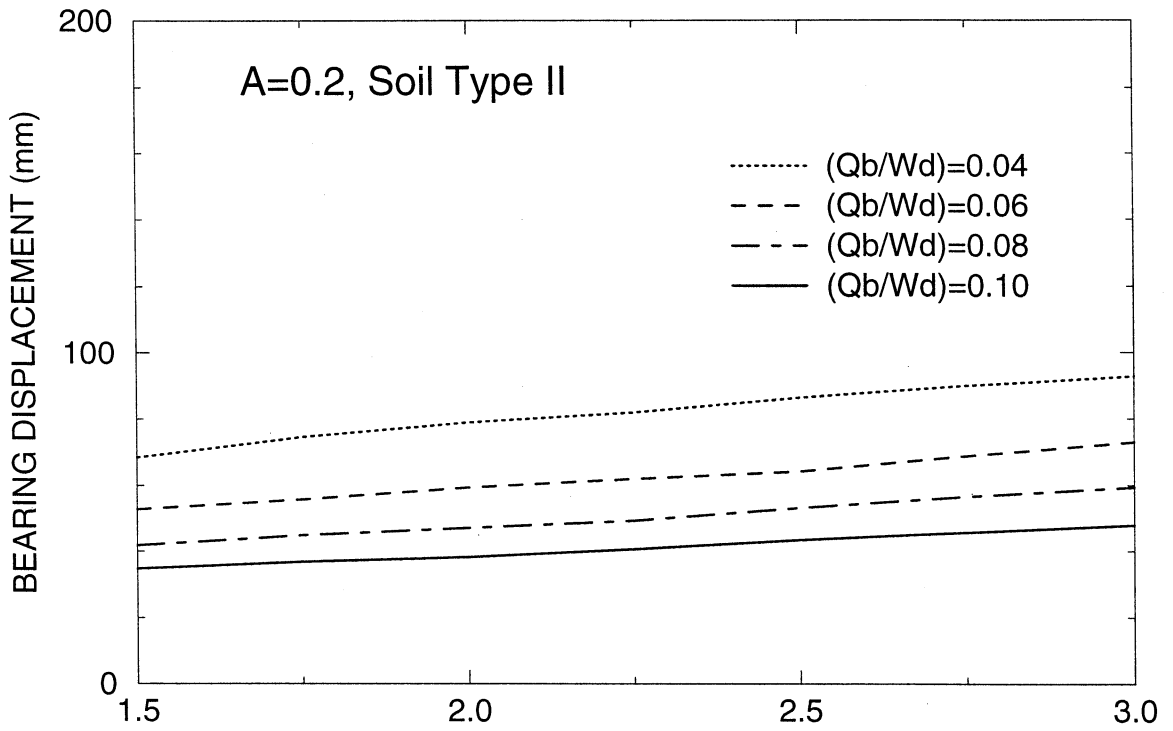
Wd/Wp=5, Tp=0.25 s, AASHTO UNIFORM LOAD METHOD
LINEAR ELASTIC/VISCOUS ISOLATION SYSTEM



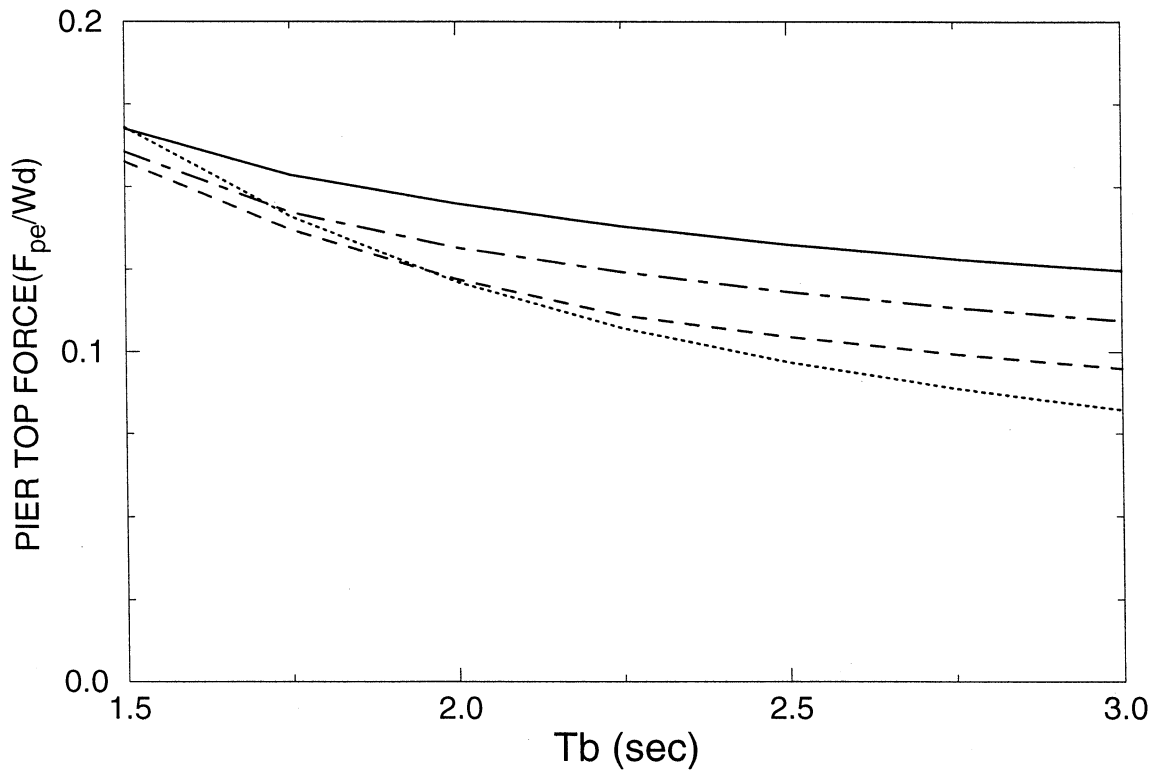
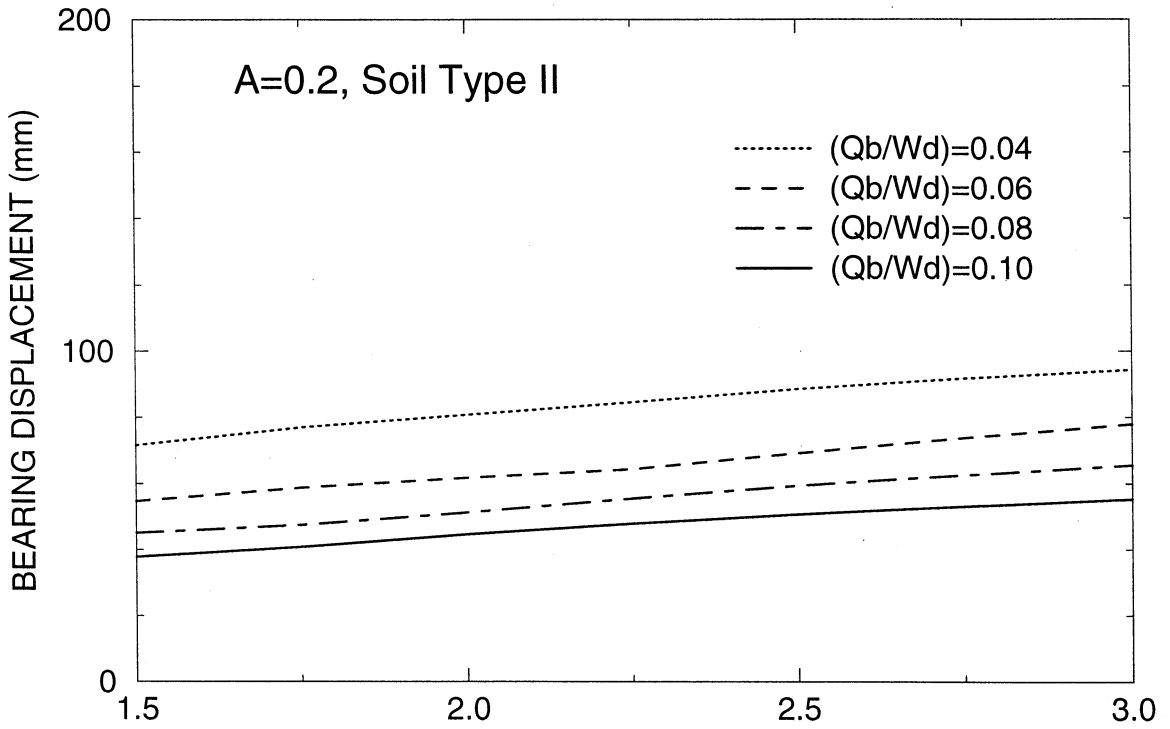
Wd/Wp=5, Tp=0.5 s, AASHTO UNIFORM LOAD METHOD
LINEAR ELASTIC/VISCOUS ISOLATION SYSTEM



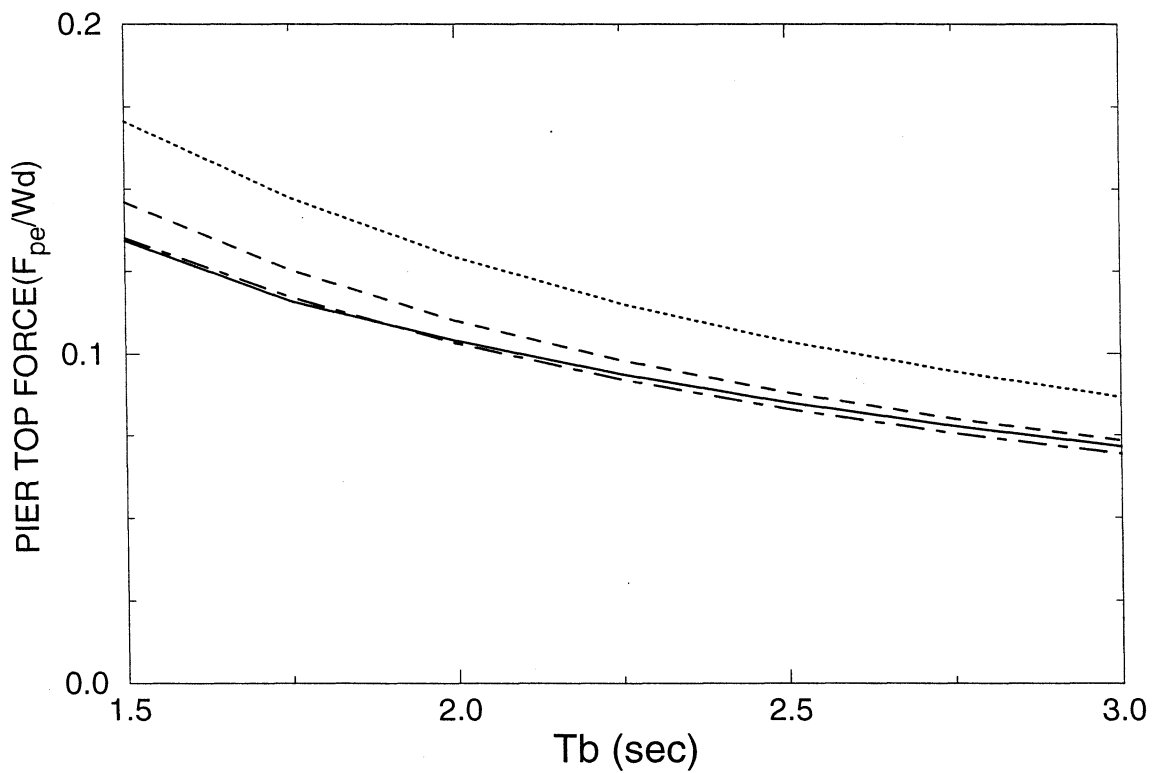
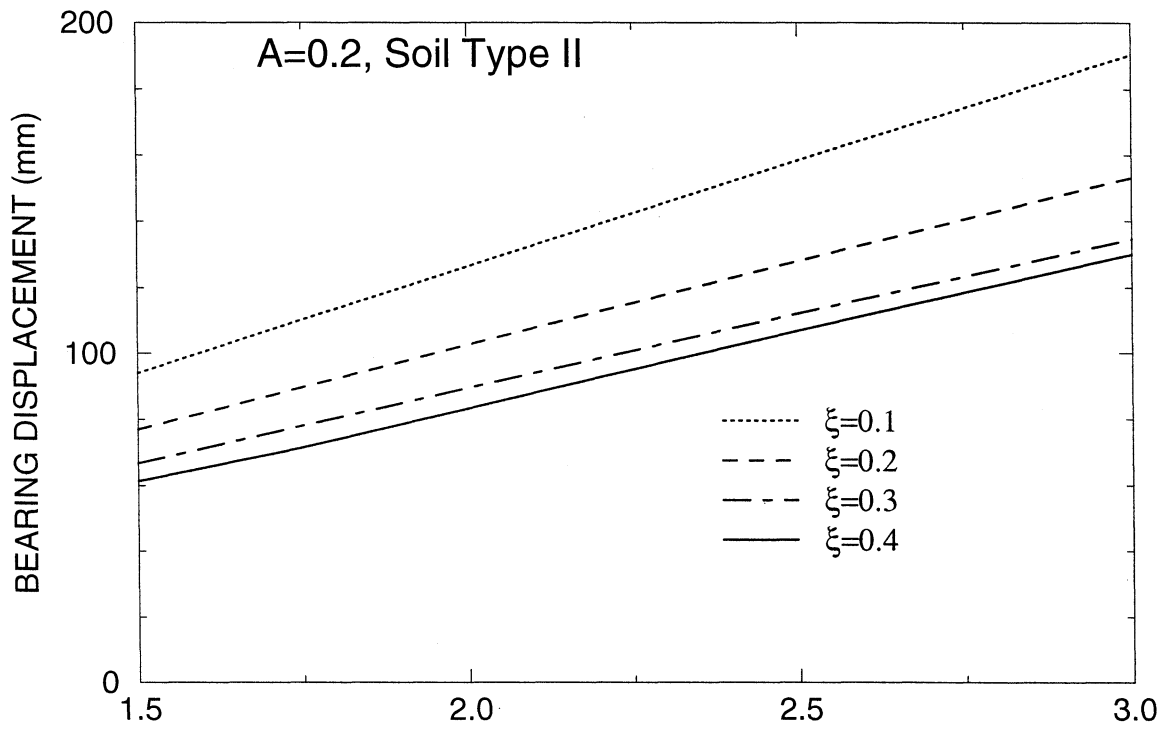
Wd/Wp=10, Tp=0.25 s, AASHTO UNIFORM LOAD METHOD
BILINEAR HYSTERETIC OR SLIDING ISOLATION SYSTEM



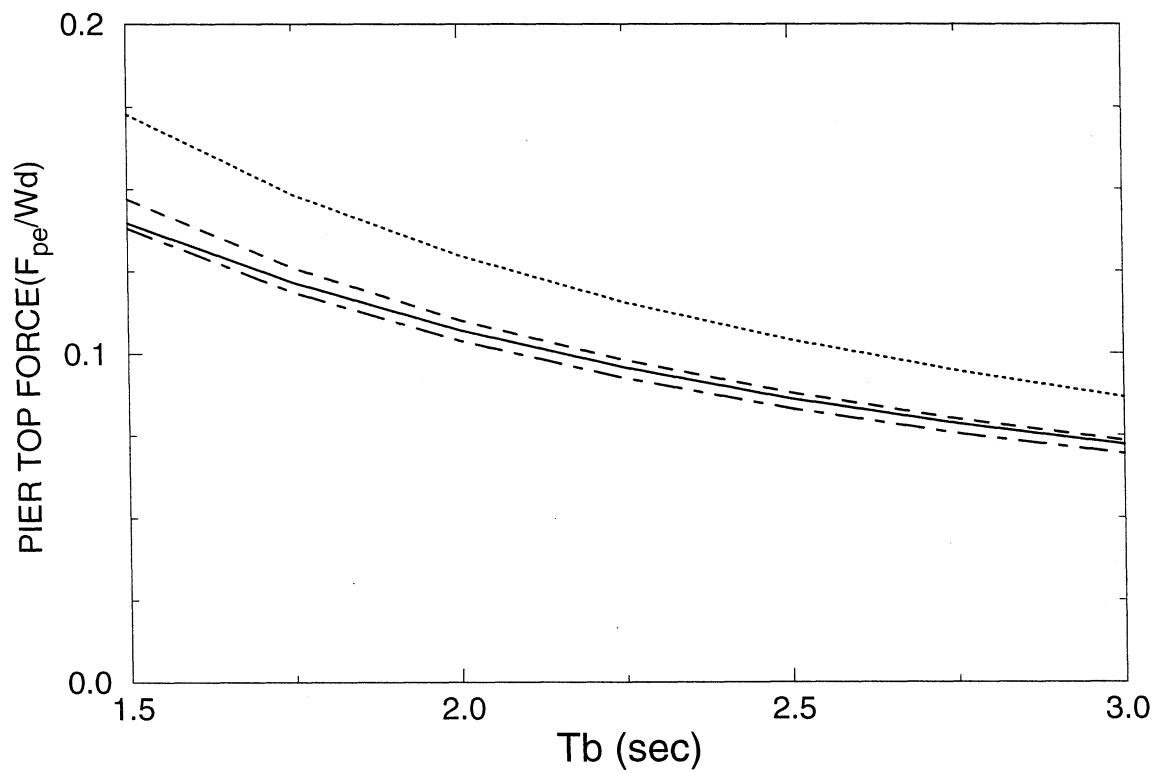
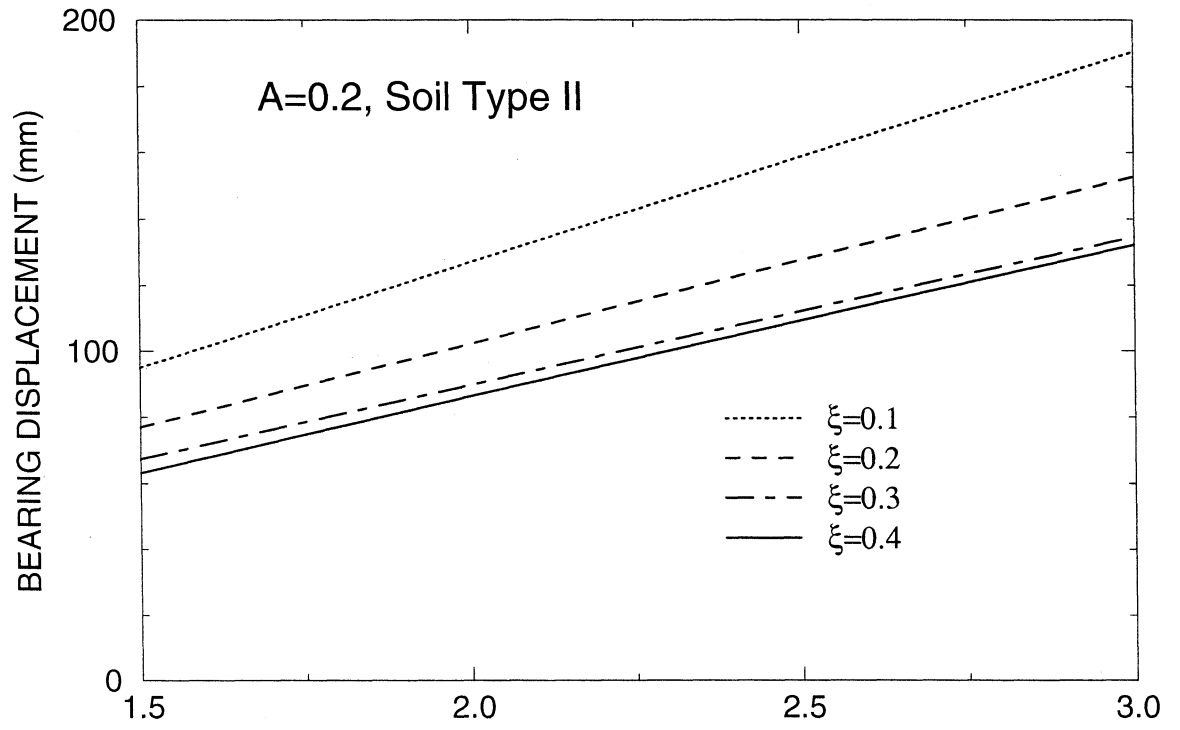
Wd/Wp=5, Tp=0.25 s, AASHTO UNIFORM LOAD METHOD
BILINEAR HYSTERETIC OR SLIDING ISOLATION SYSTEM



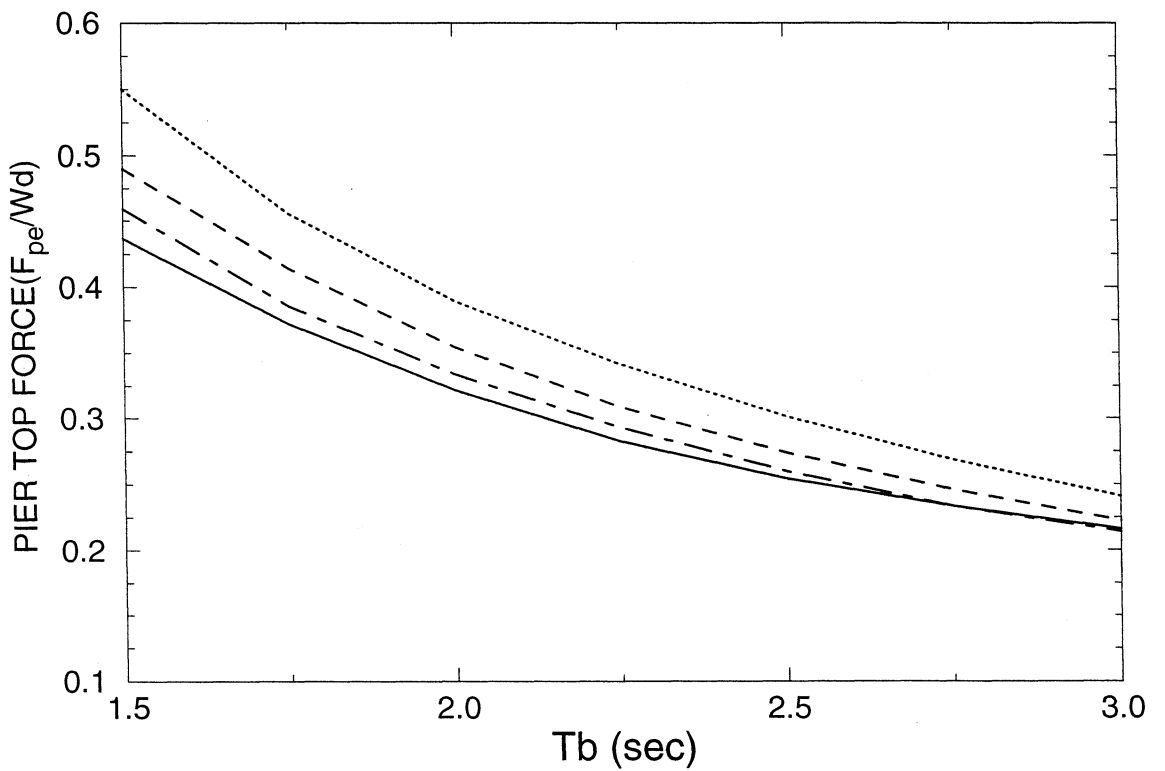
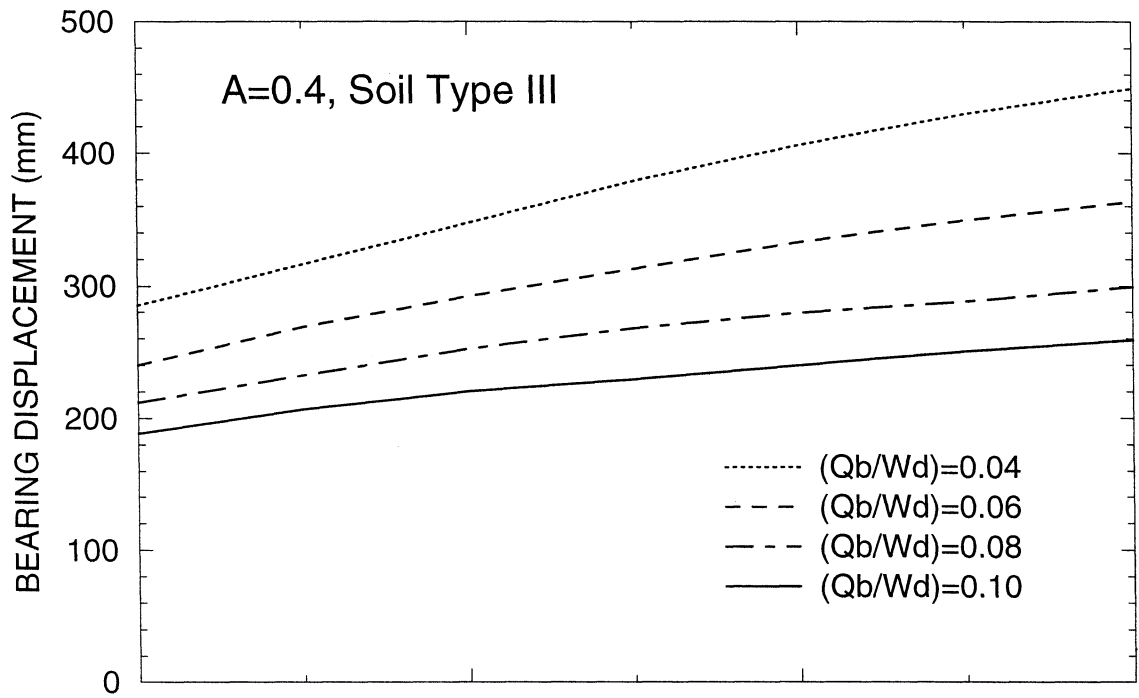
Wd/Wp=10, Tp=0.25 s, AASHTO UNIFORM LOAD METHOD
LINEAR ELASTIC/VISCOUS ISOLATION SYSTEM



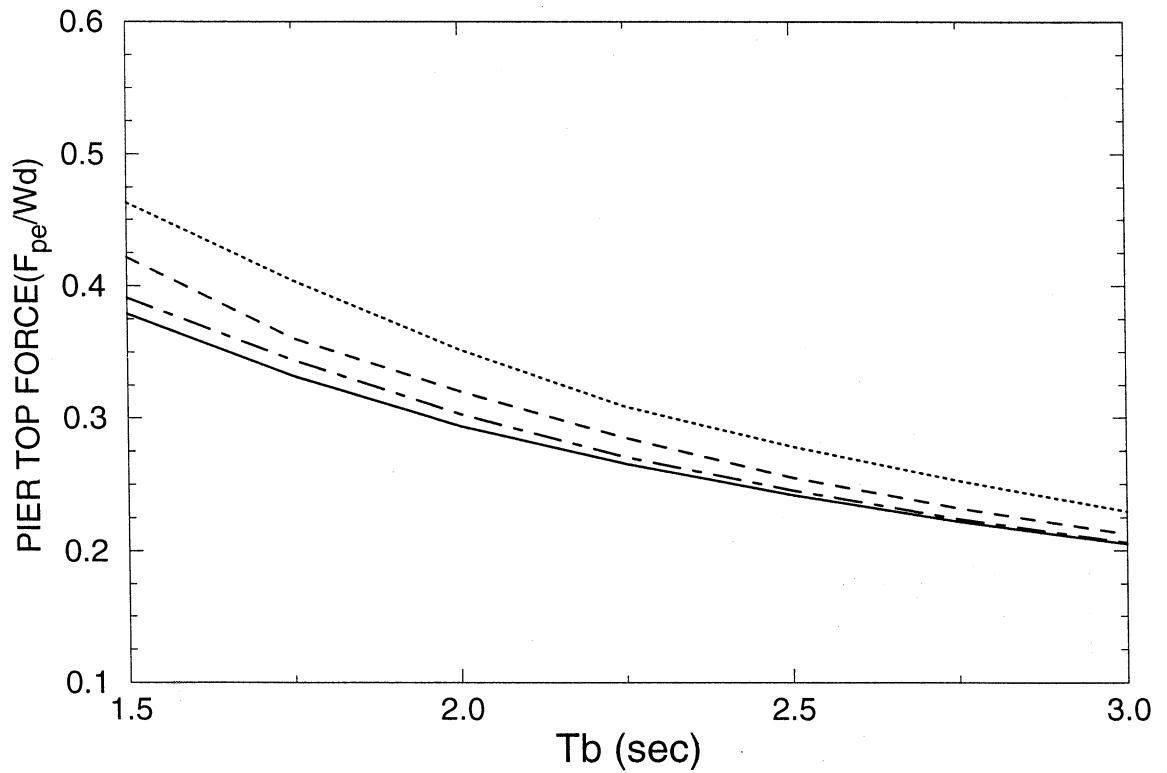
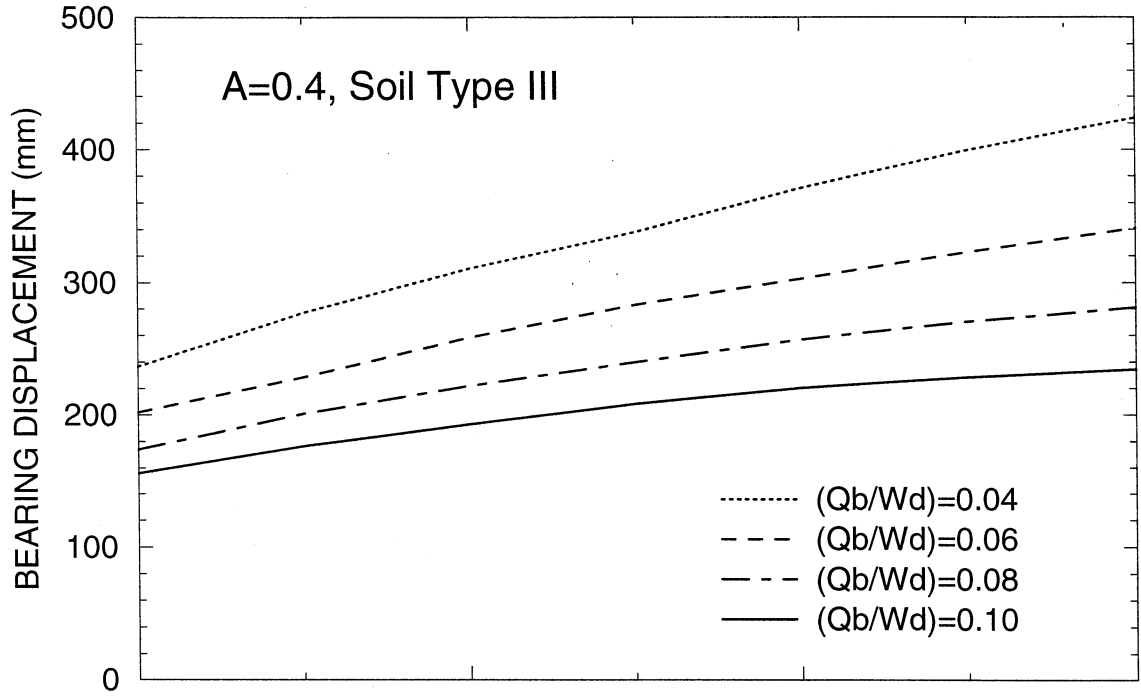
Wd/Wp=5, Tp=0.25 s, AASHTO UNIFORM LOAD METHOD
LINEAR ELASTIC/VISCOUS ISOLATION SYSTEM



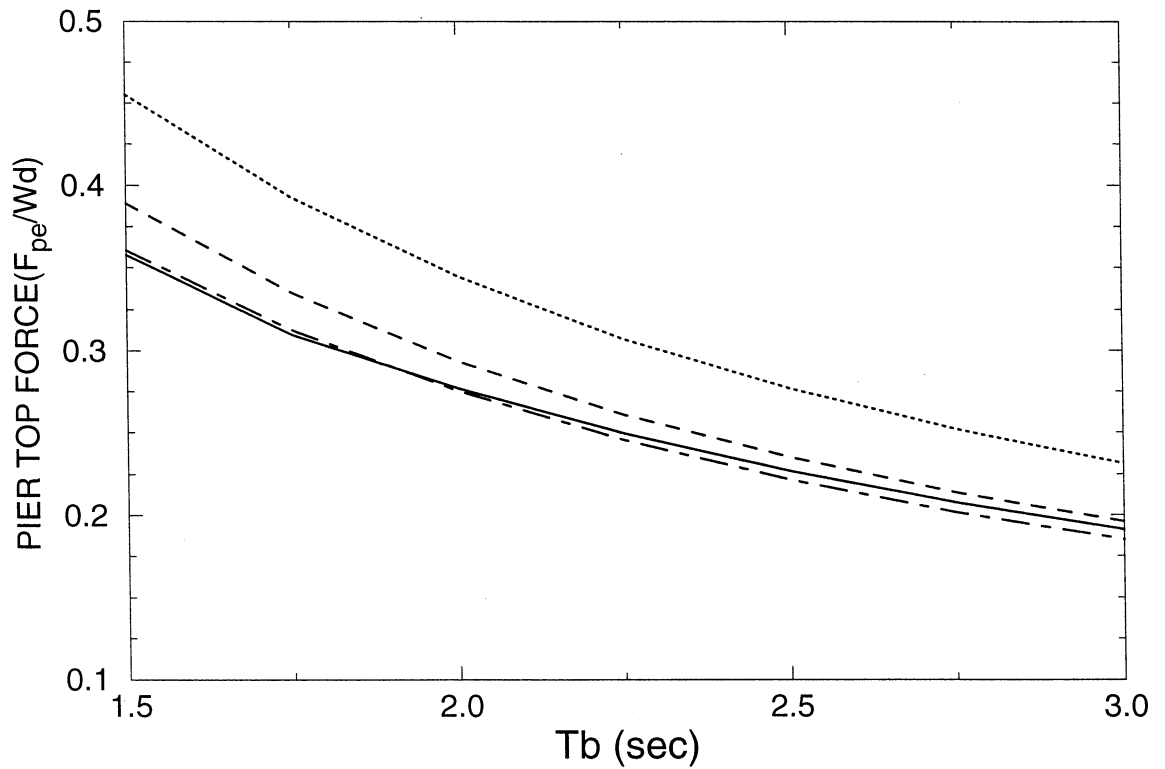
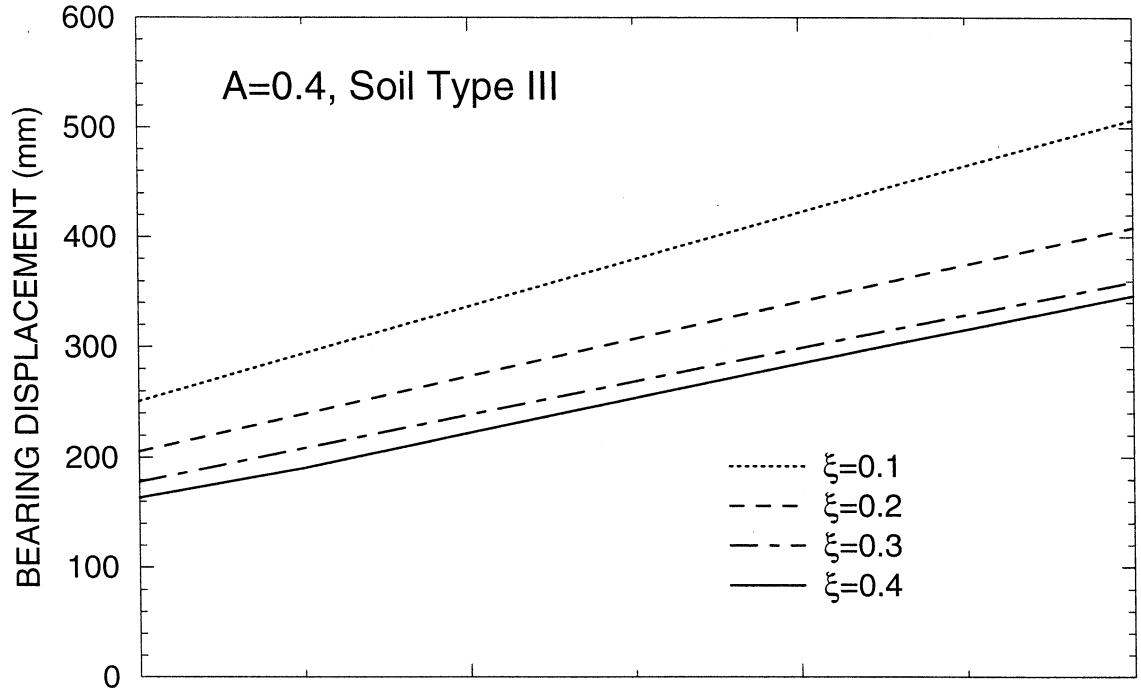
Wd/Wp=10, Tp=0.25 s, AASHTO UNIFORM LOAD METHOD
BILINEAR HYSTERETIC OR SLIDING ISOATION SYSTEM



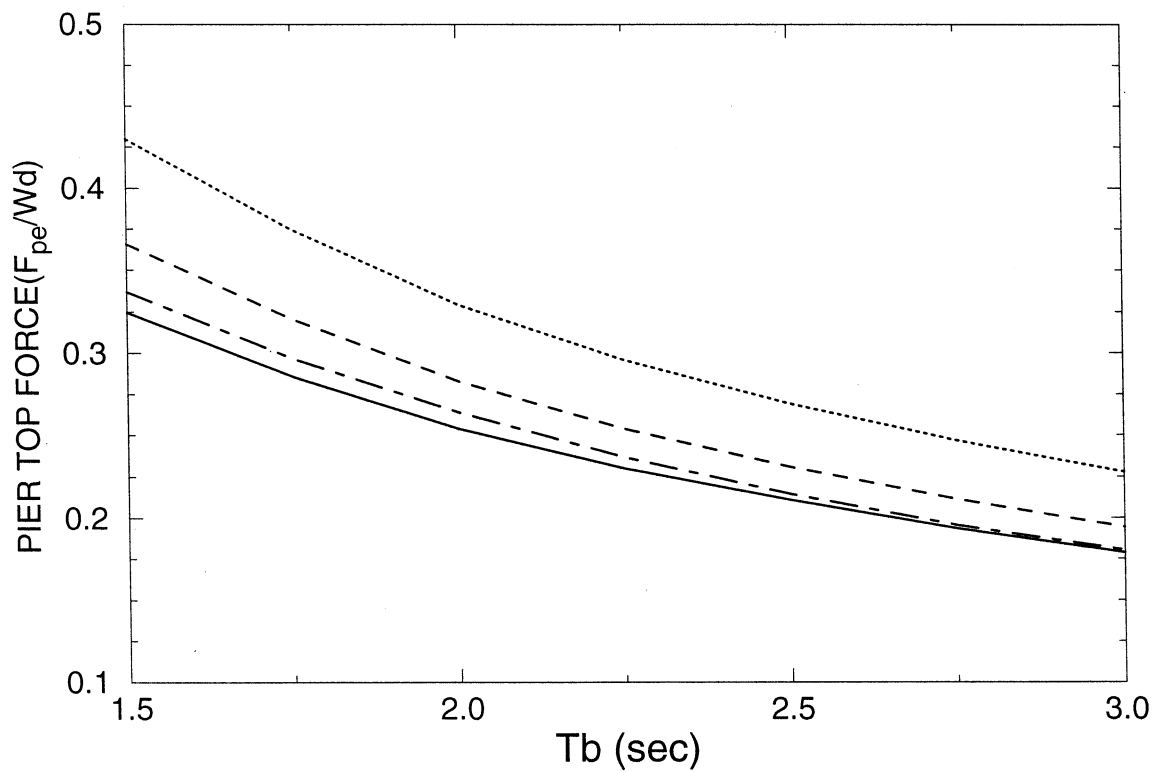
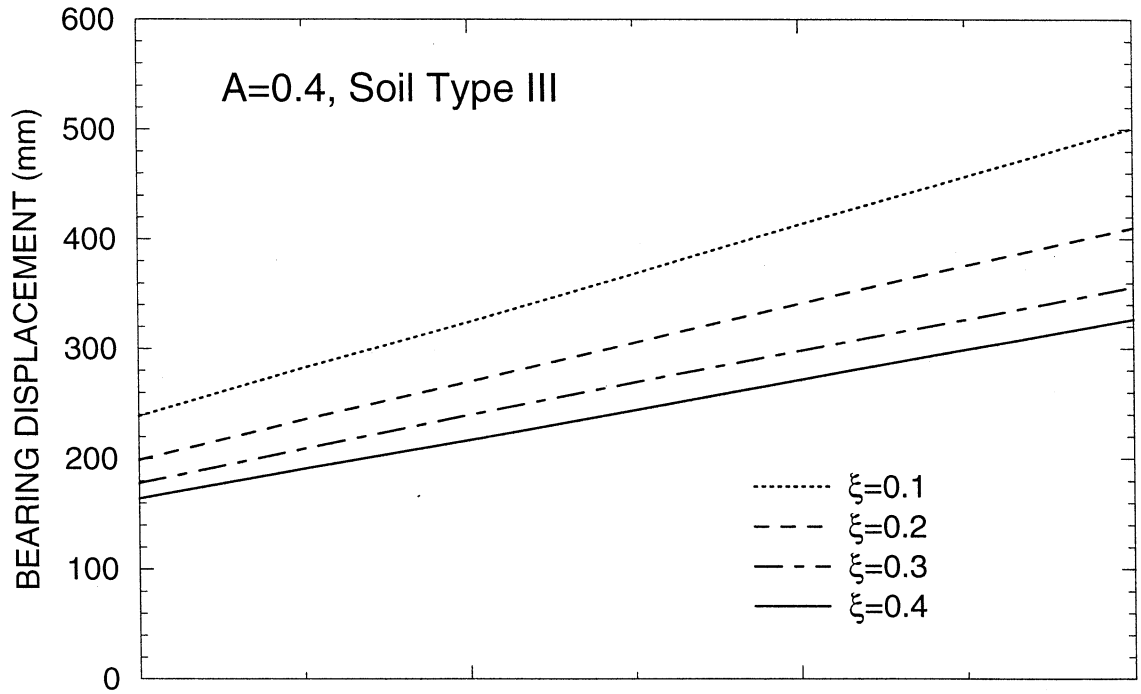
Wd/Wp=10, Tp=0.5 s, AASHTO UNIFORM LOAD METHOD
BILINEAR HYSTERETIC OR SLIDING ISOLATION SYSTEM



Wd/Wp=10, Tp=0.25 s, AASHTO UNIFORM LOAD METHOD
LINEAR ELASTIC/VISCOUS ISOLATION SYSTEM



Wd/Wp=10, Tp=0.5 s, AASHTO UNIFORM LOAD METHOD
LINEAR ELASTIC/VISCOUS ISOLATION SYSTEM

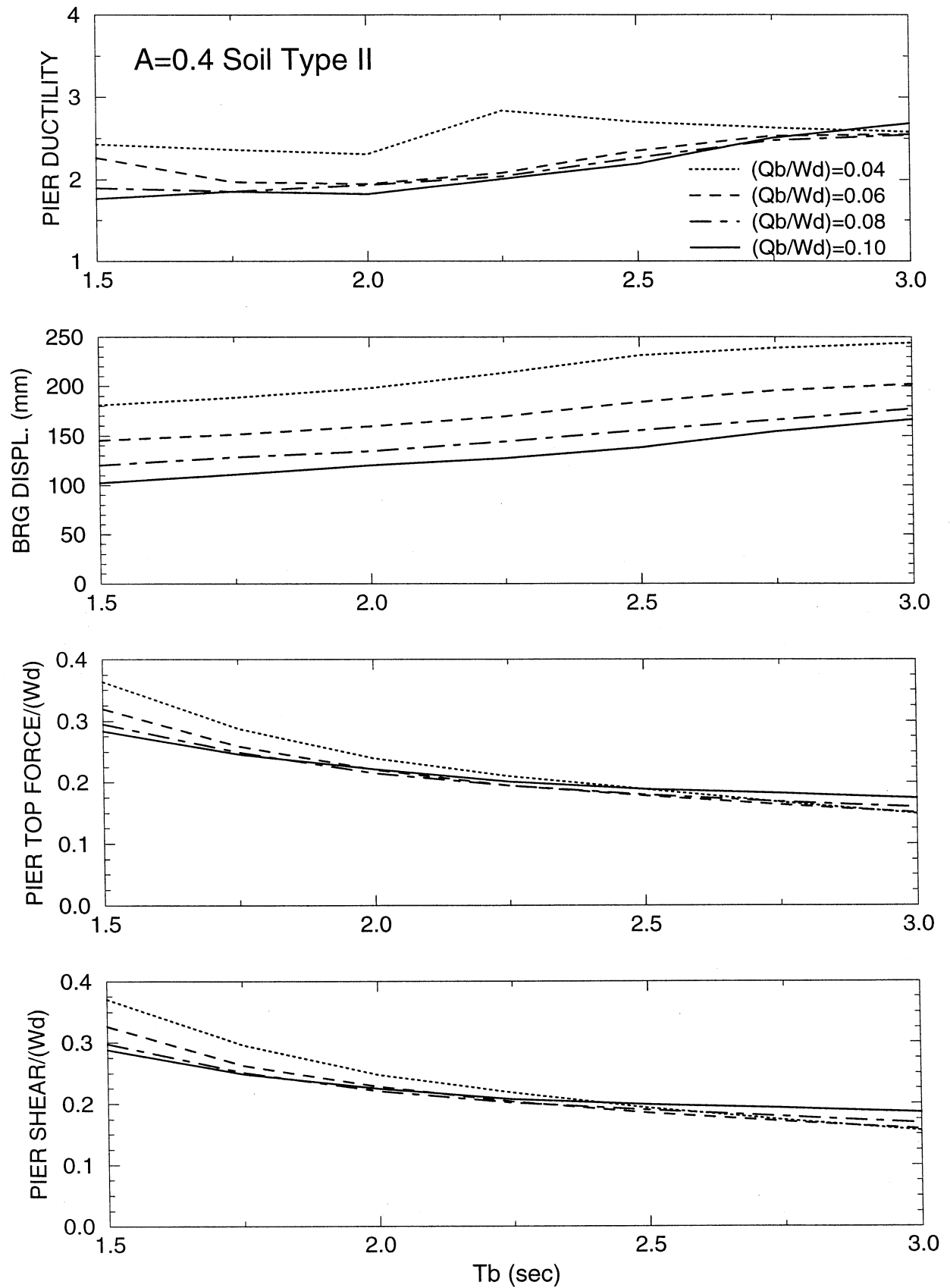


APPENDIX E

**RESULTS OF NONLINEAR DYNAMIC ANALYSIS OF SEISMIC-ISOLATED
BRIDGE WITH PERFECT BILINEAR HYSTERETIC PIER
AND BILINEAR HYSTERETIC ISOLATION SYSTEM
FOR AASHTO, A=0.4, SOIL PROFILE TYPE II INPUT**

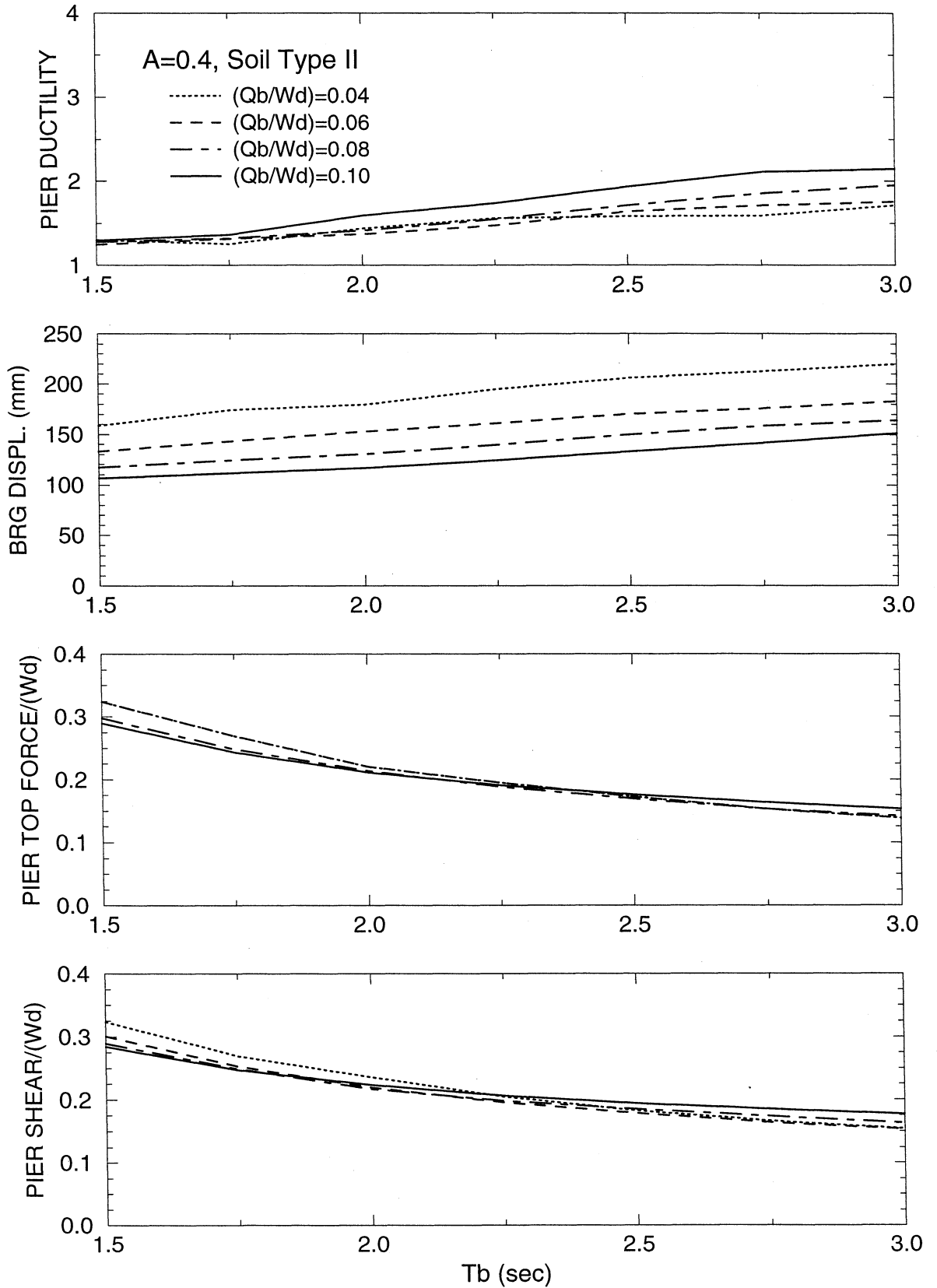
$W_d/W_p=10, T_p=0.1s, R_\mu=1.0, \alpha=0.05$

BILINEAR HYSTERETIC PIER, BILINEAR HYSTERETIC ISOLATION SYSTEM



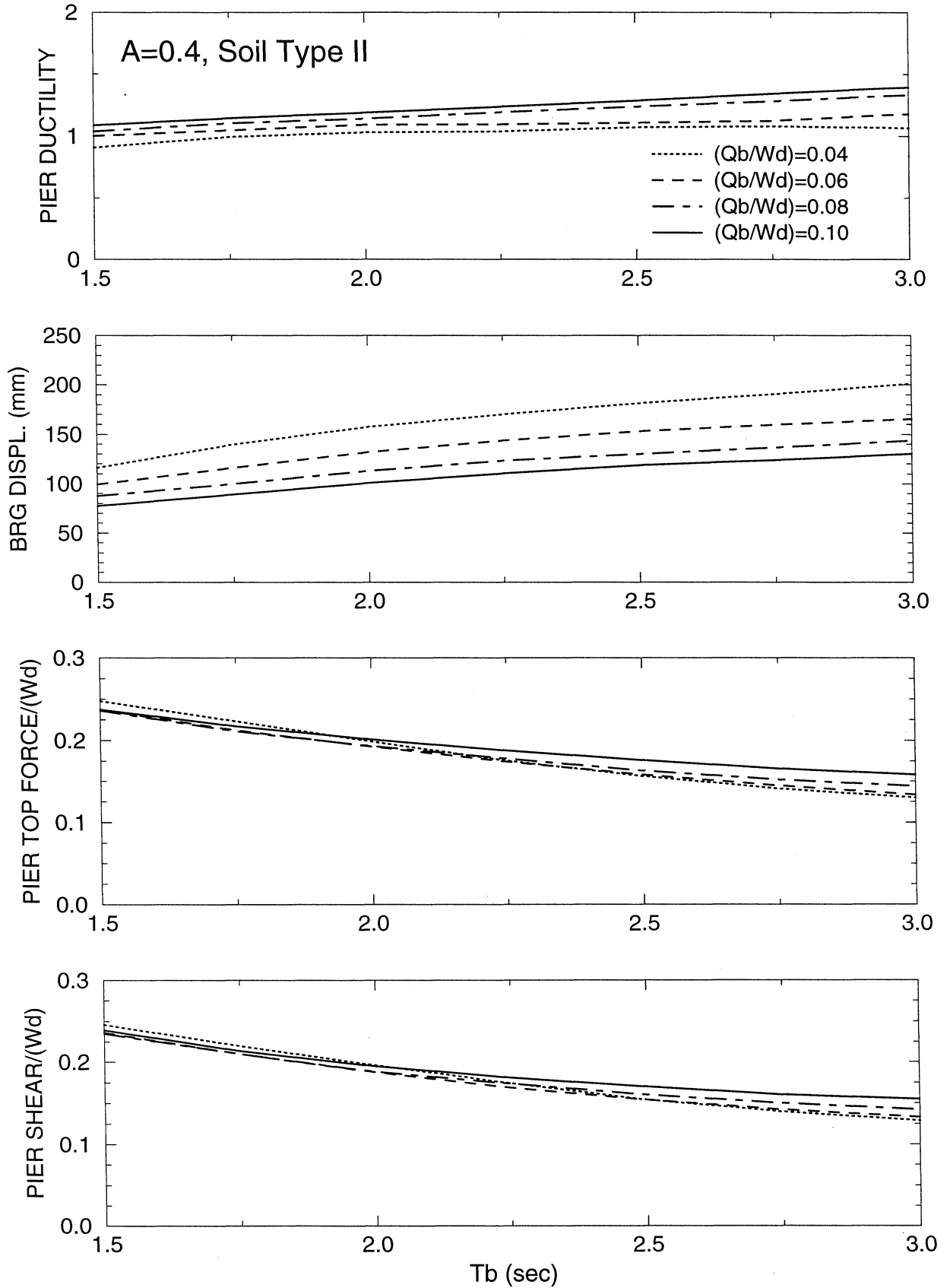
$W_d/W_p=10, T_p=0.25s, R_{\mu}=1.0, \alpha=0.05$

BILINEAR HYSTERETIC PIER, BILINEAR HYSTERETIC ISOLATION SYSTEM



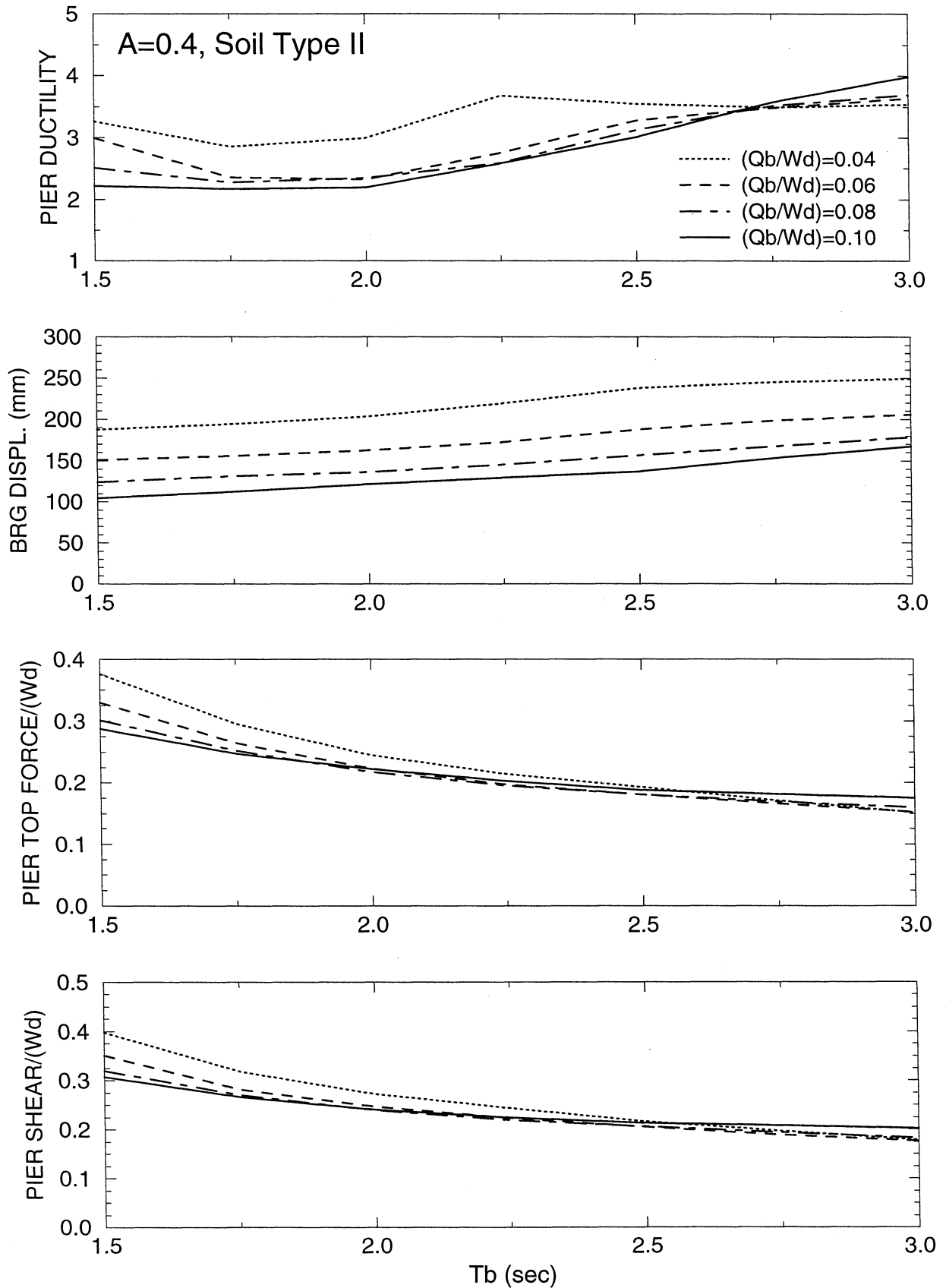
$W_d/W_p=10, T_p=0.5 \text{ s}, R_\mu=1.0, \alpha=0.05$

BILINEAR HYSTERETIC PIER, BILINEAR HYSTERETIC ISOLATION SYSTEM



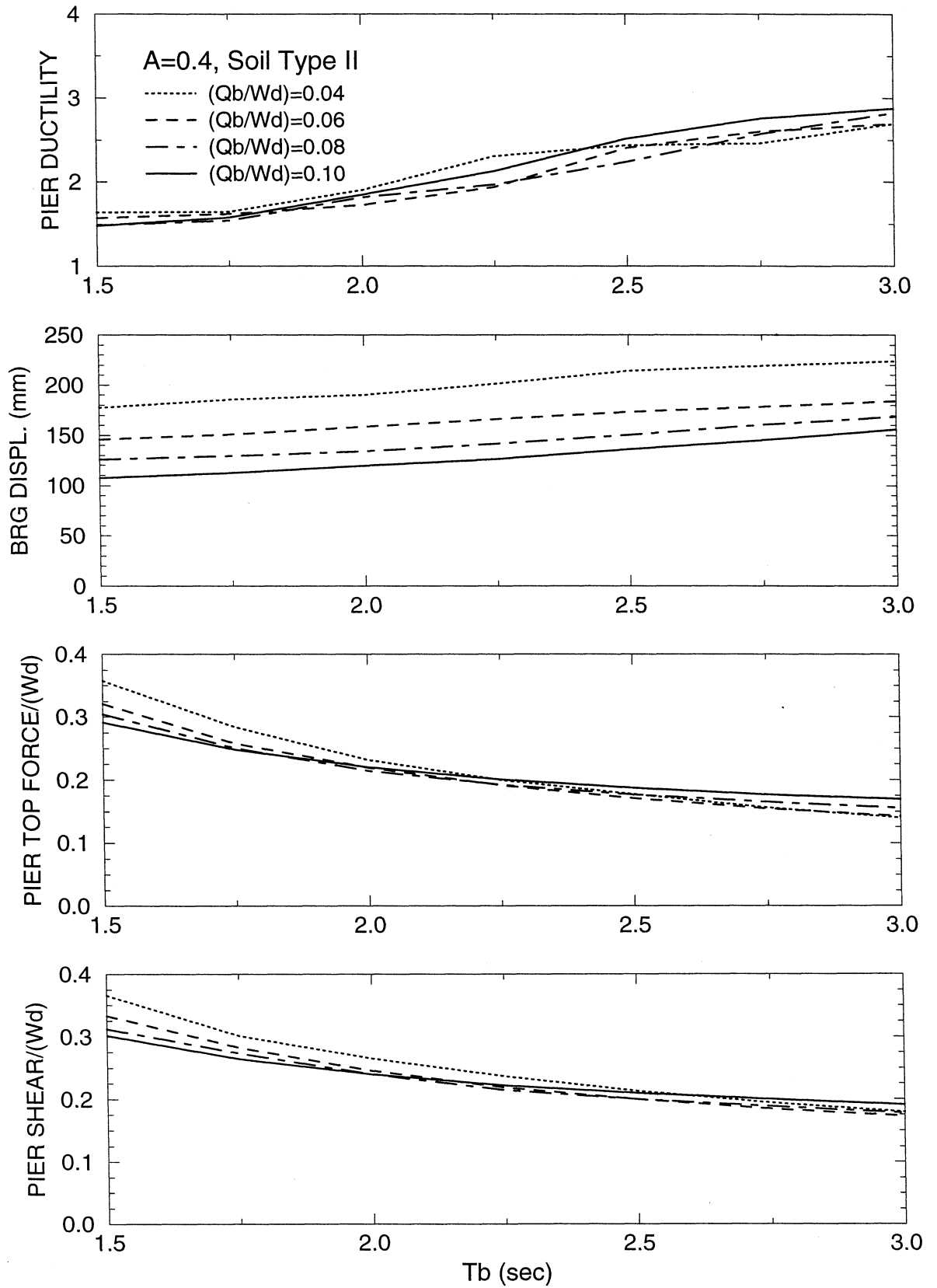
$W_d/W_p=5, T_p=0.1 \text{ s}, R_{\mu}=1.0, \alpha=0.05$

BILINEAR HYSTERETIC PIER, BILINEAR HYSTERETIC ISOLATION SYSTEM



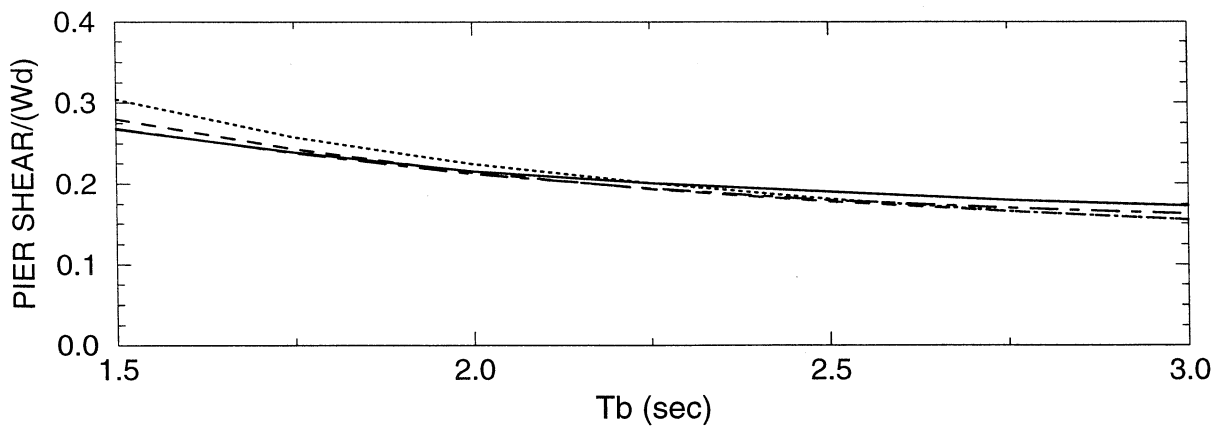
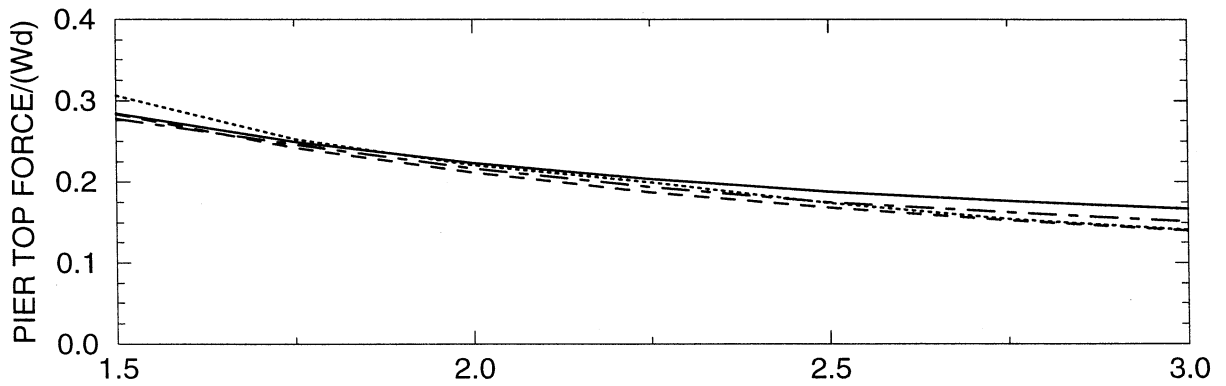
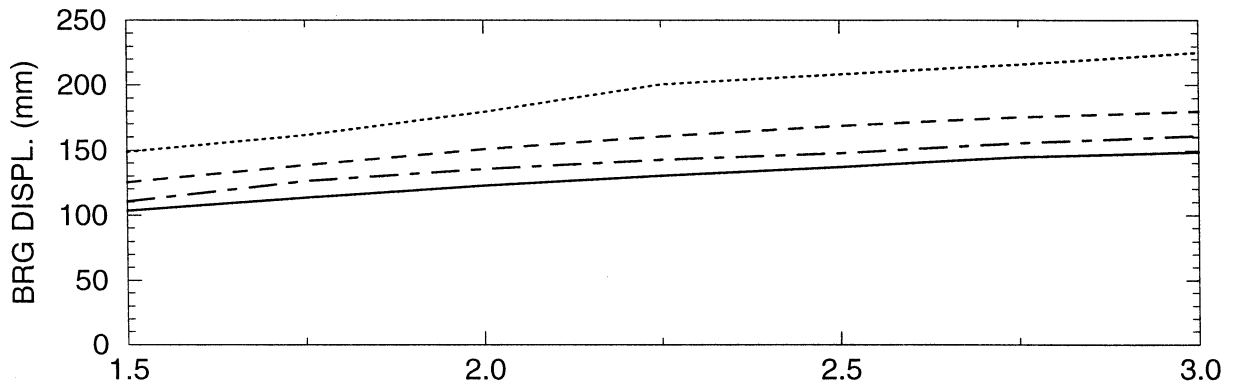
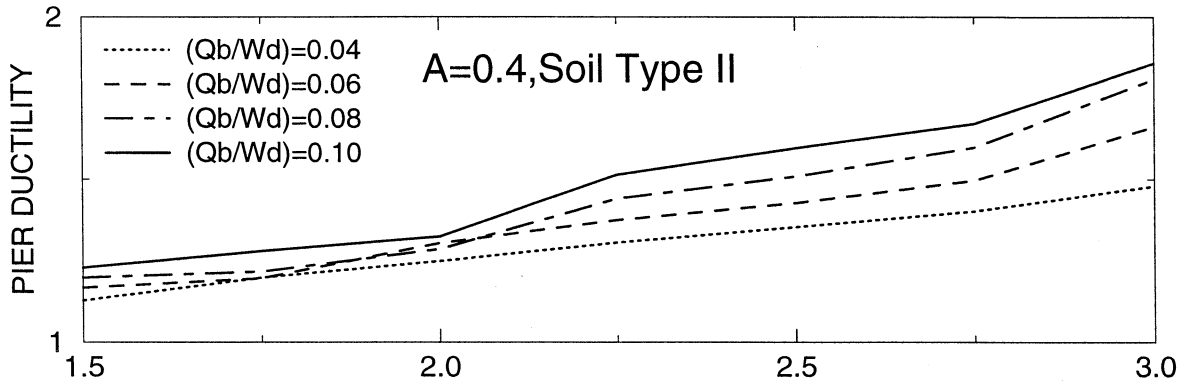
$W_d/W_p=5, T_p=0.25 \text{ s}, R_{\mu}=1.0, \alpha=0.05$

BILINEAR HYSTERETIC PIER, BILINEAR HYSTERETIC ISOLATION SYSTEM



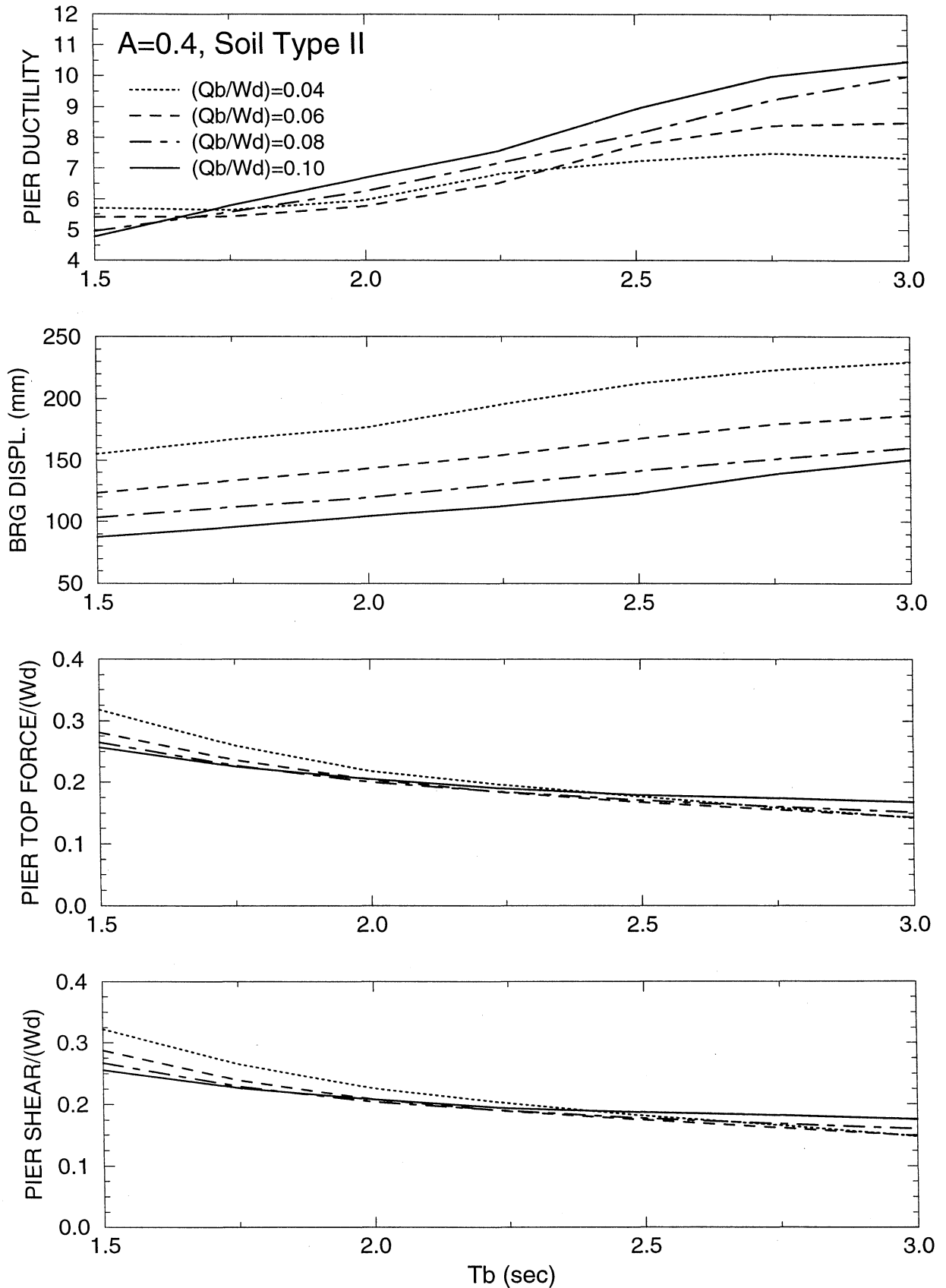
$W_d/W_p=5, T_p=0.5 \text{ s}, R_{\mu}=1.0, \alpha=0.05$

BILINEAR HYSTERETIC PIER, BILINEAR HYSTERETIC ISOLATION SYSTEM



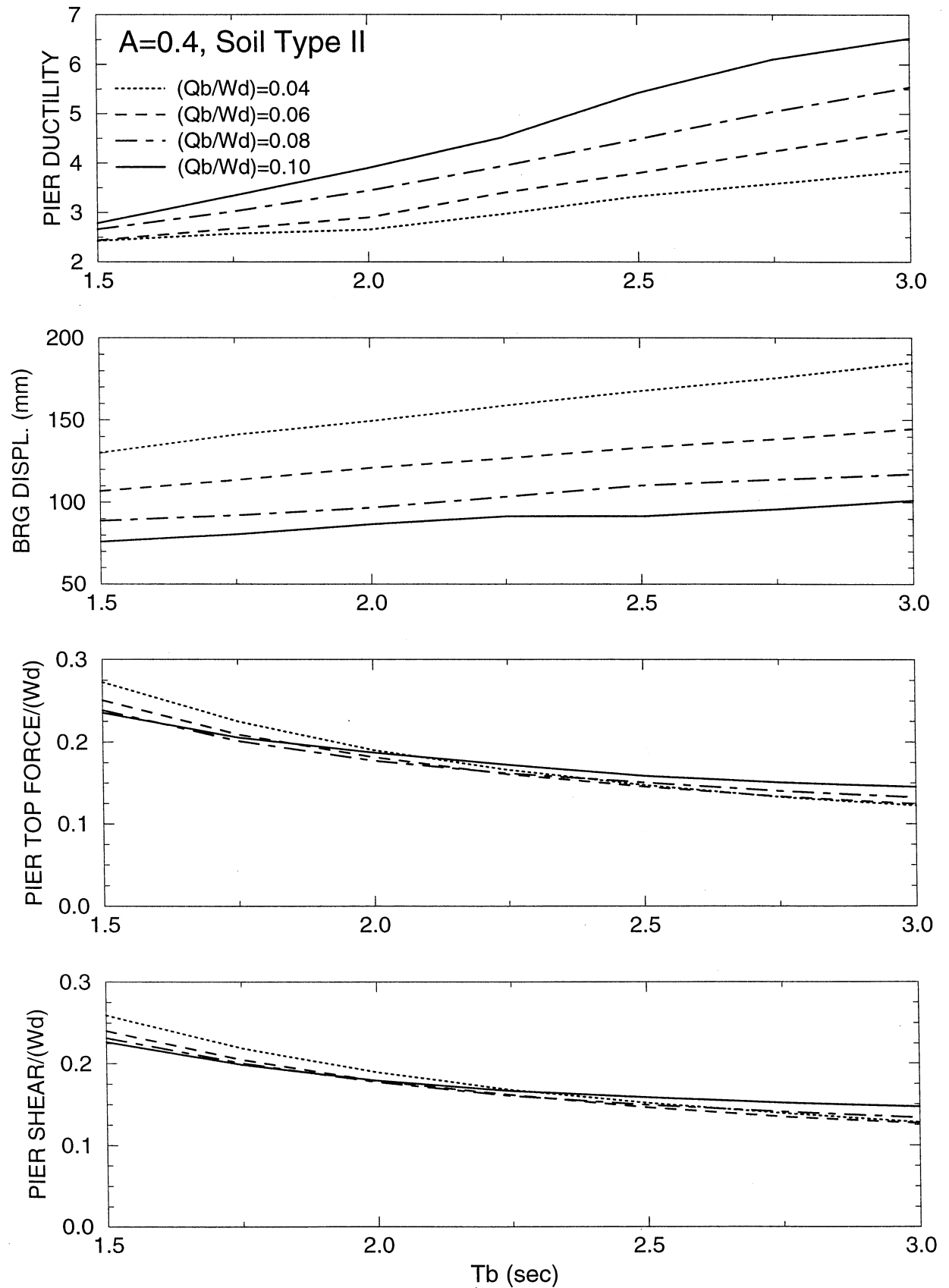
$W_d/W_p=10, T_p=0.1s, R=1.5, \alpha=0.05$

BILINEAR HYSTERETIC PIER, BILINEAR HYSTERETIC ISOLATION SYSTEM



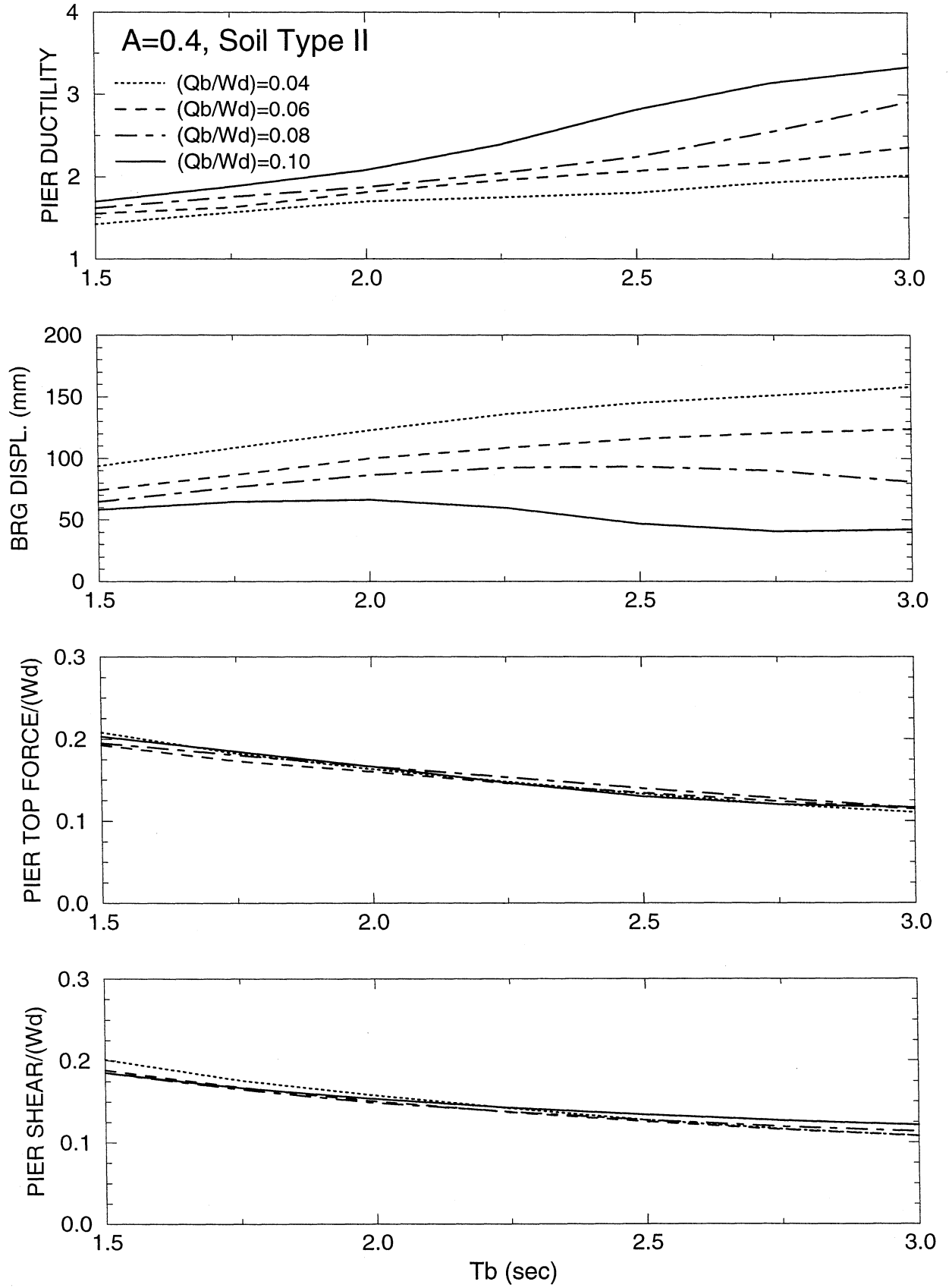
Wd/Wp=10, Tp=0.25s, R=1.5, $\alpha=0.05$

BILINEAR HYSTERETIC PIER, BILINEAR HYSTERETIC ISOLATION SYSTEM



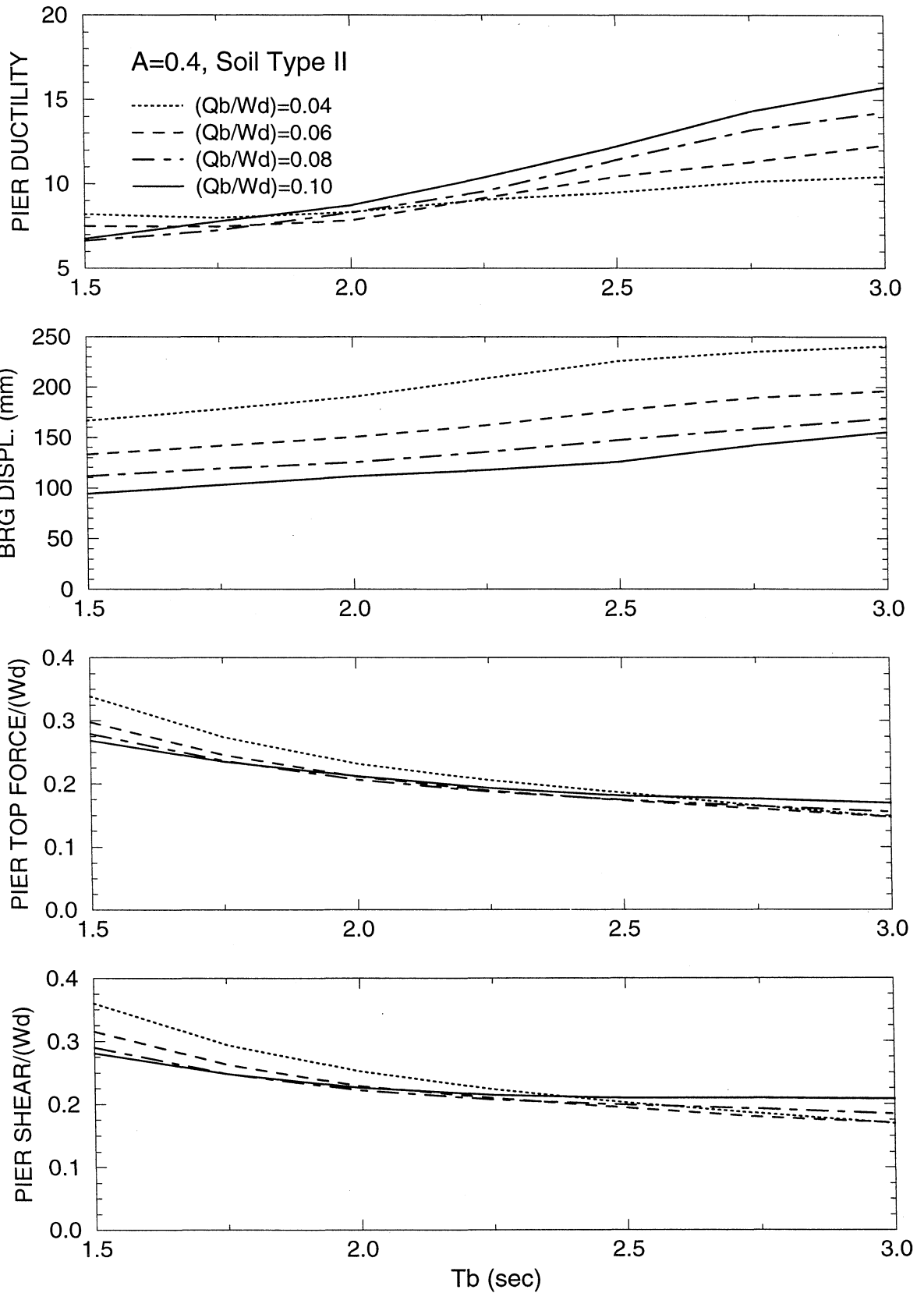
$W_d/W_p=10, T_p=0.5 \text{ s}, R_{\mu}=1.5, \alpha=0.05$

BILINEAR HYSTERETIC PIER, BILINEAR HYSTERETIC ISOLATION SYSTEM



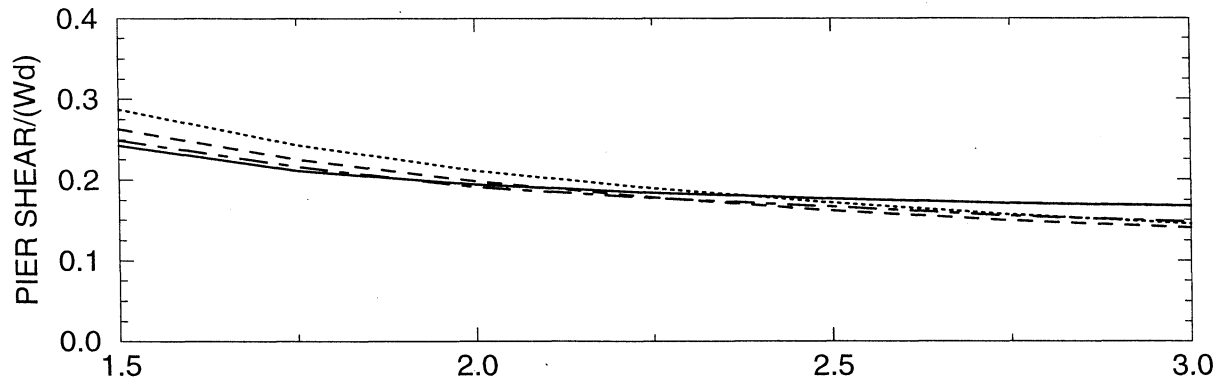
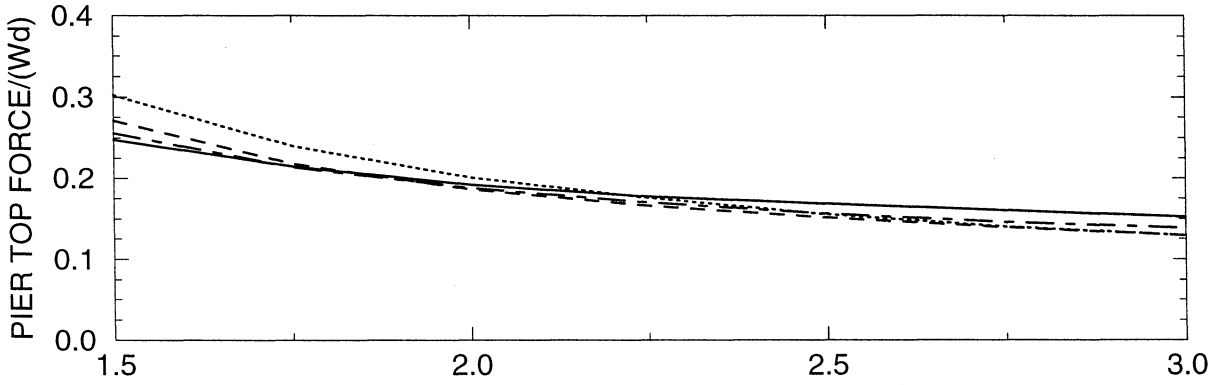
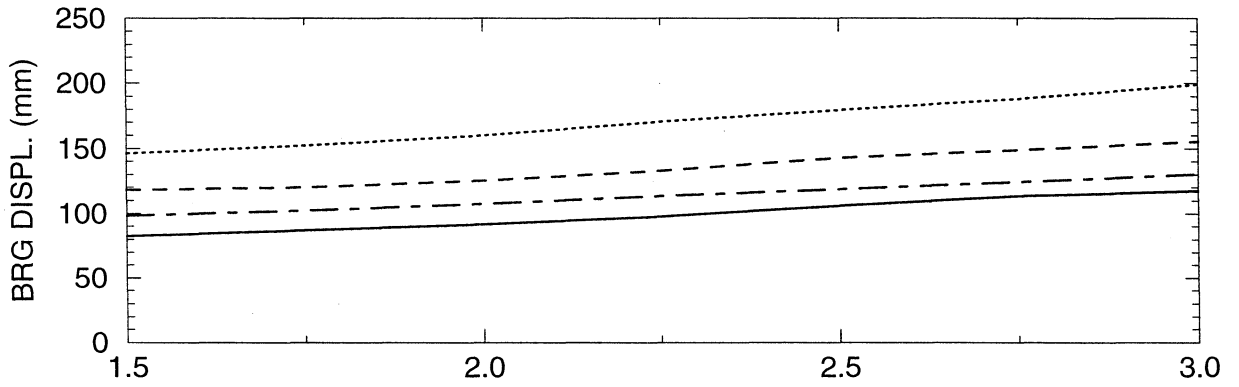
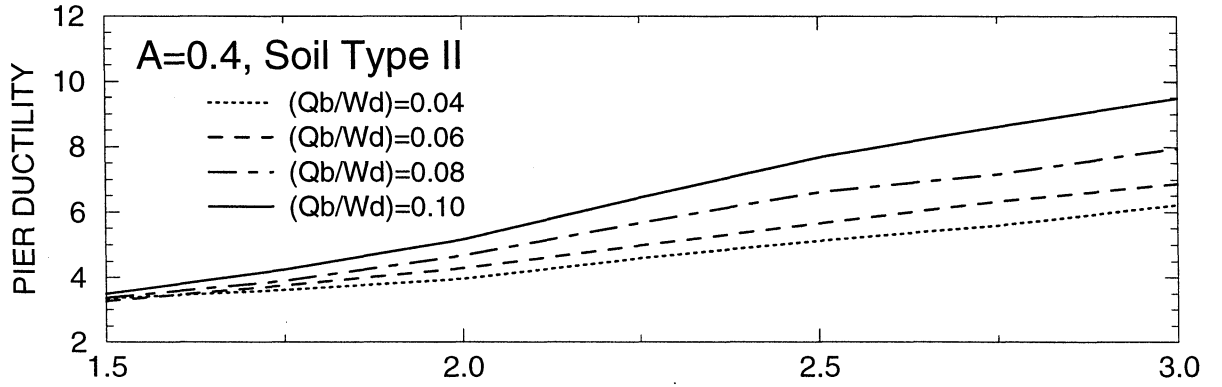
$W_d/W_p=5, T_p=0.1 \text{ s}, R_\mu=1.5, \alpha=0.05$

BILINEAR HYSTERETIC PIER, BILINEAR HYSTERETIC ISOLATION SYSTEM



$W_d/W_p=5, T_p=0.25 \text{ s}, R_\mu=1.5, \alpha=0.05$

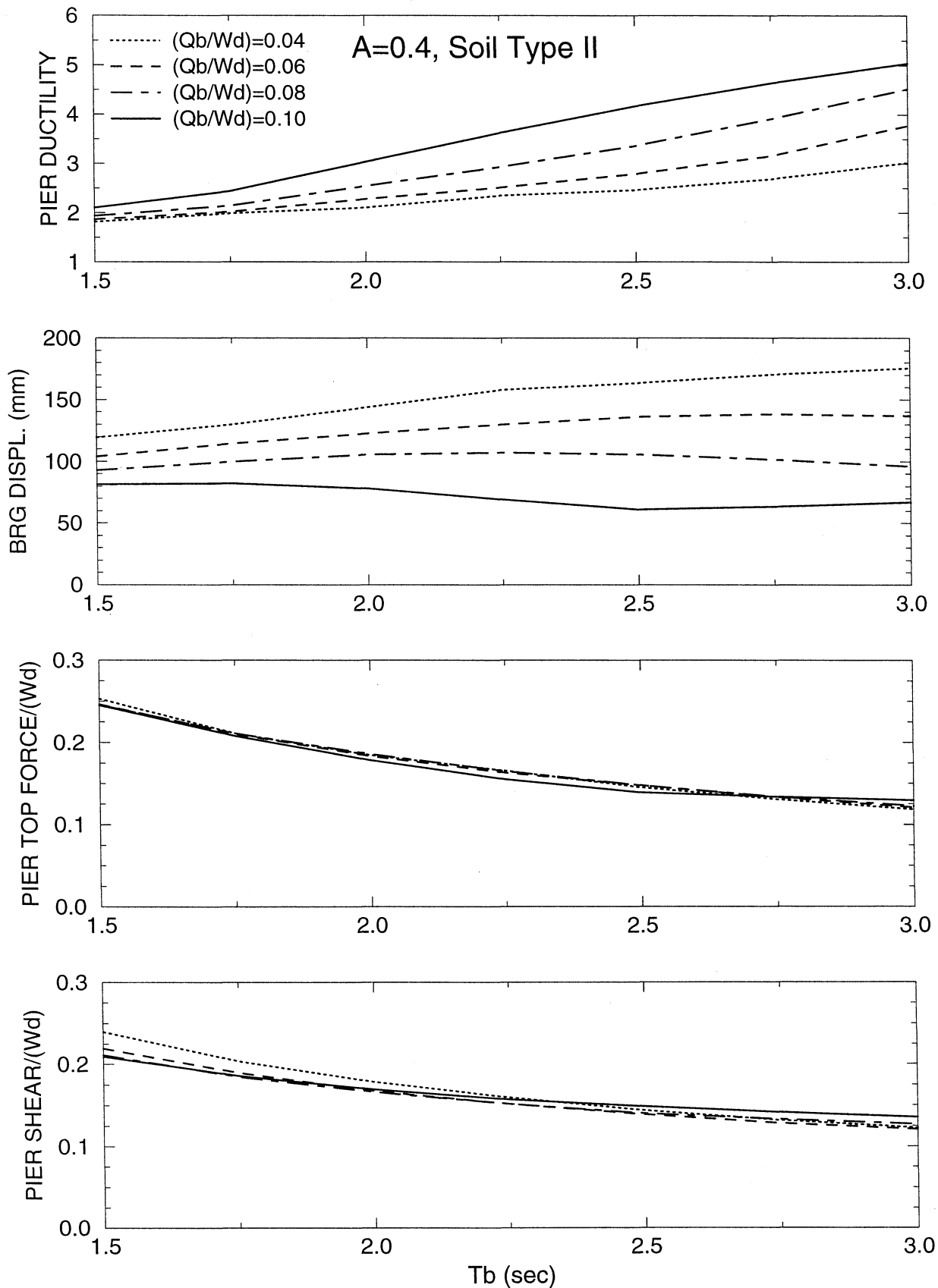
BILINEAR HYSTERETIC PIER, BILINEAR HYSTERETIC ISOLATION SYSTEM



Tb (sec)

$W_d/W_p=5$, $T_p=0.5$ s, $R_\mu=1.5$, $\alpha=0.05$

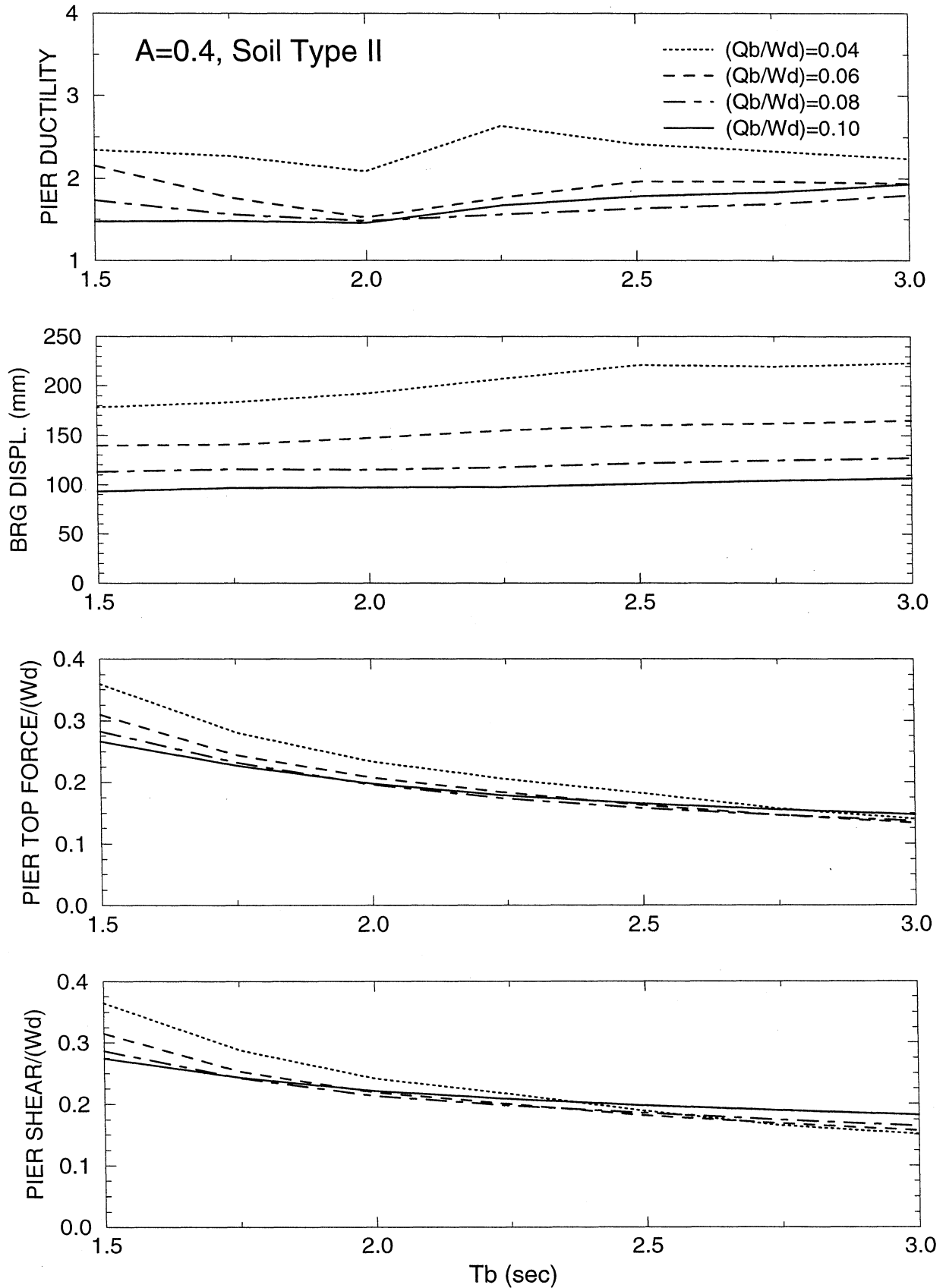
BILINEAR HYSTERETIC PIER, BILINEAR HYSTERETIC ISOLATION SYSTEM



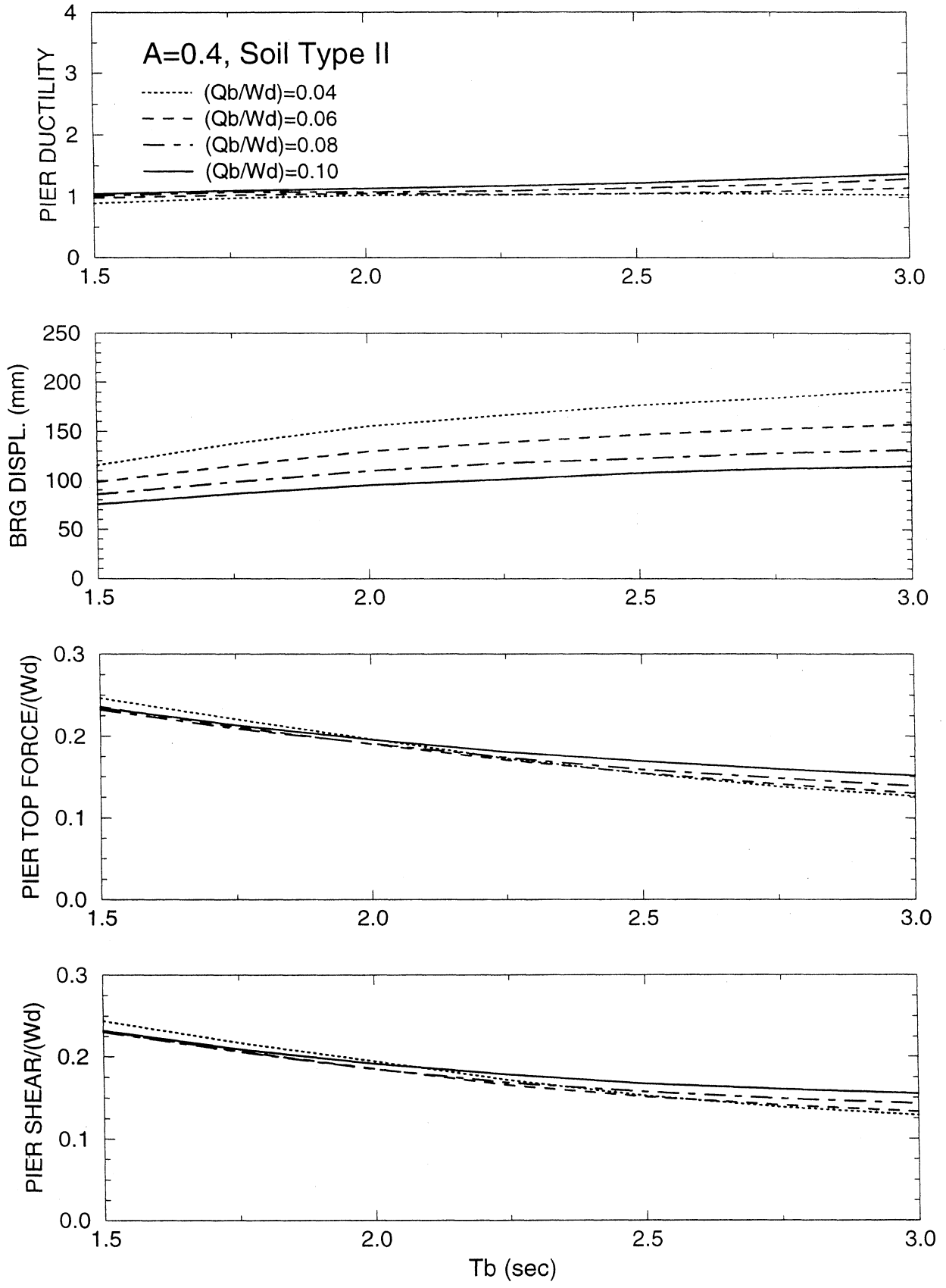
APPENDIX F

**RESULTS OF NONLINEAR DYNAMIC ANALYSIS OF SEISMIC-ISOLATED
BRIDGE WITH PERFECT BILINEAR HYSTERETIC PIER
AND SLIDING ISOLATION SYSTEM
FOR AASHTO, A=0.4, SOIL PROFILE TYPE II INPUT**

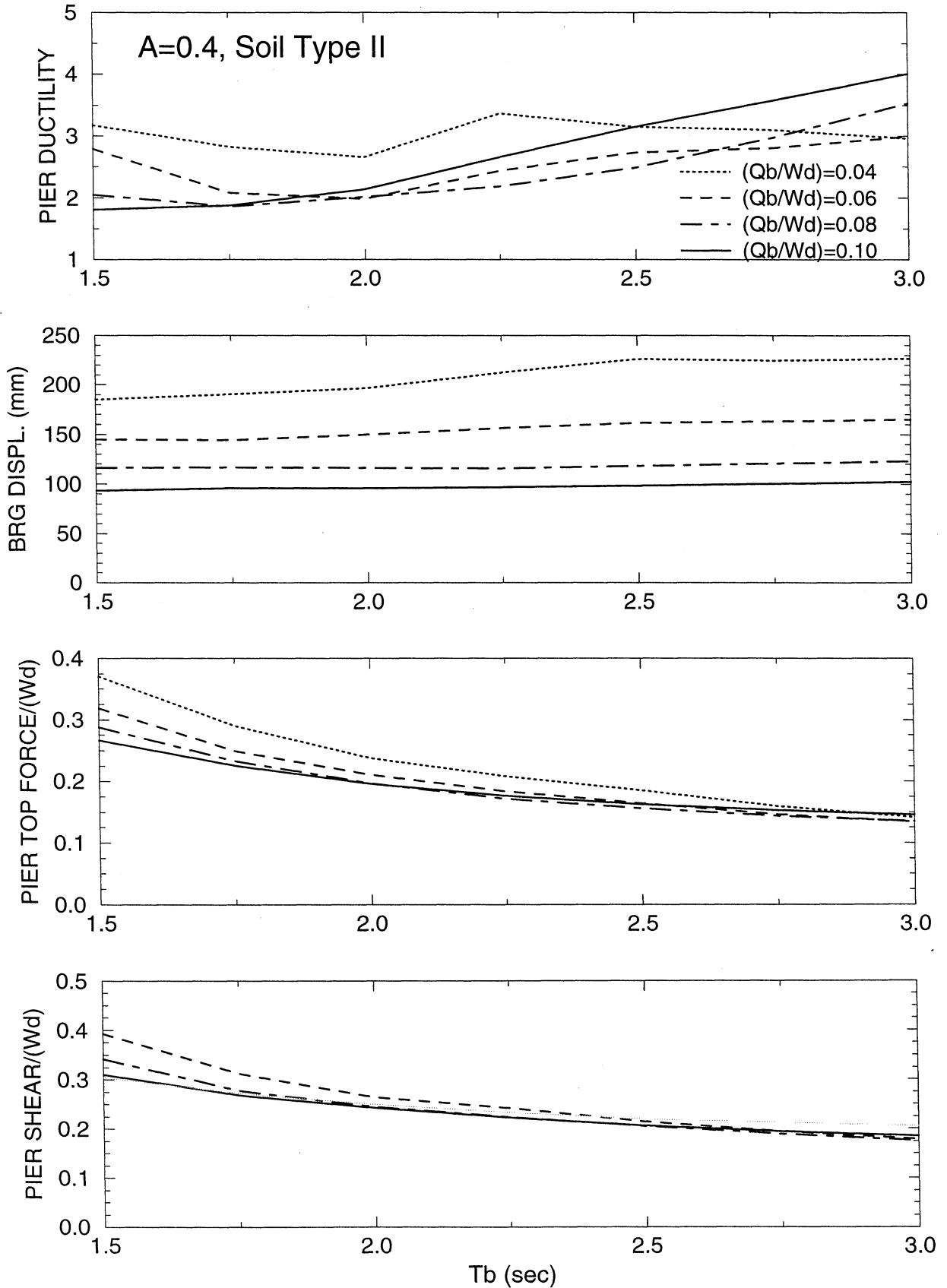
$W_d/W_p=10, T_p=0.1 \text{ s}, R_\mu=1.0, \alpha=0.05$
 BILINEAR HYSTERETIC PIER, SLIDING ISOLATION SYSTEM



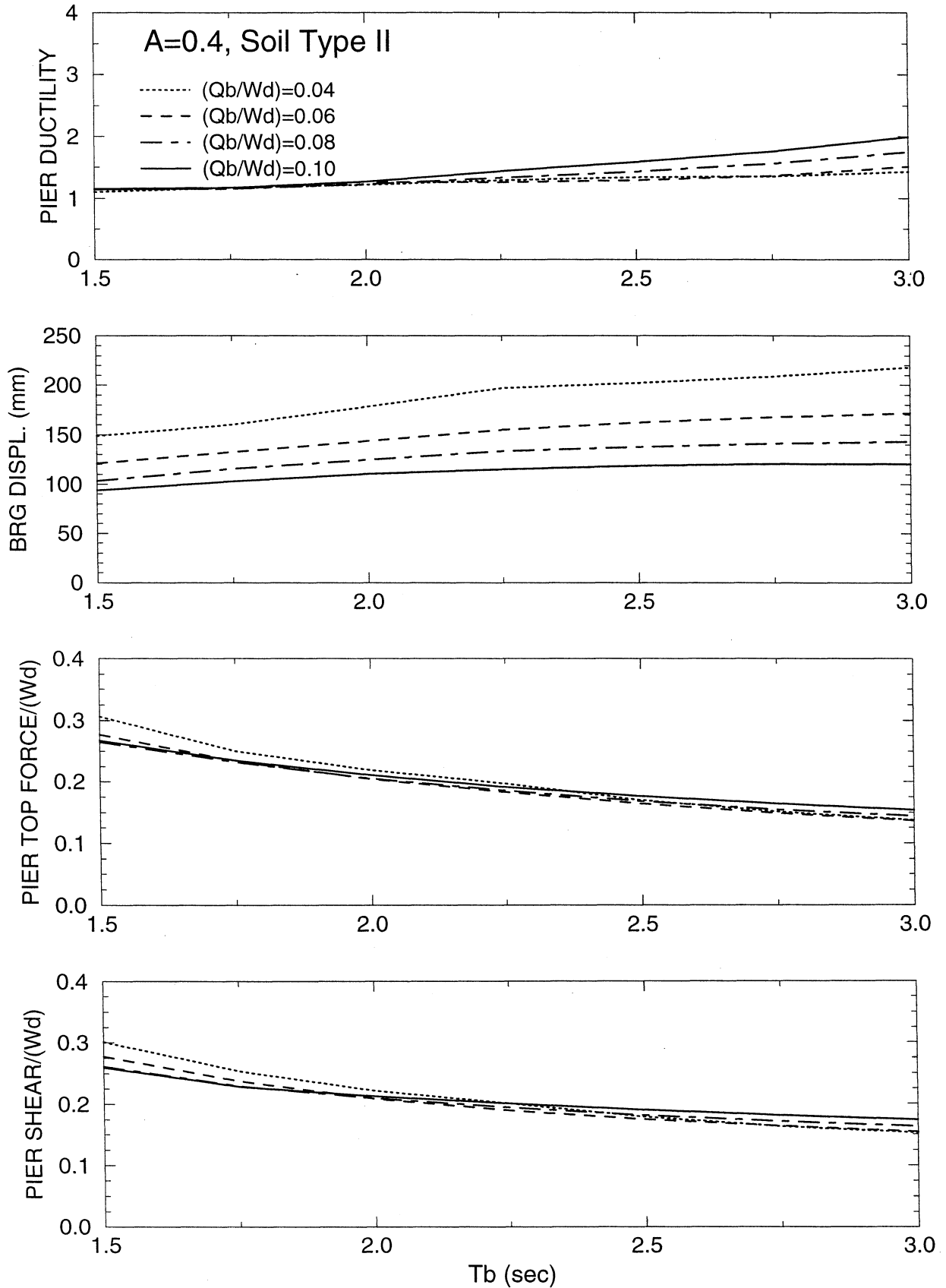
$W_d/W_p=10, T_p=0.5 \text{ s}, R_{\mu}=1.0, \alpha=0.05$
 BILINEAR HYSTERETIC PIER, SLIDING ISOLATION SYSTEM



$W_d/W_p=5, T_p=0.1 \text{ s}, R_\mu=1.0, \alpha=0.05$
 BILINEAR HYSTERETIC PIER, SLIDING ISOLATION SYSTEM

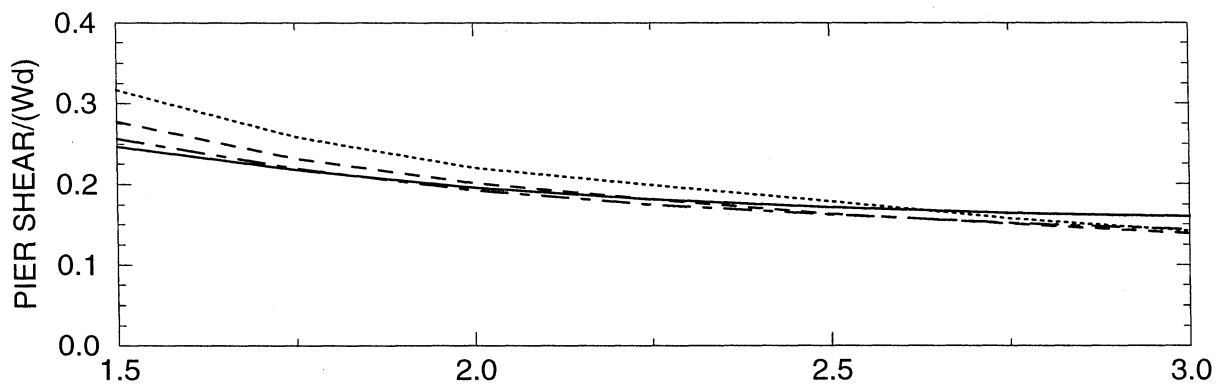
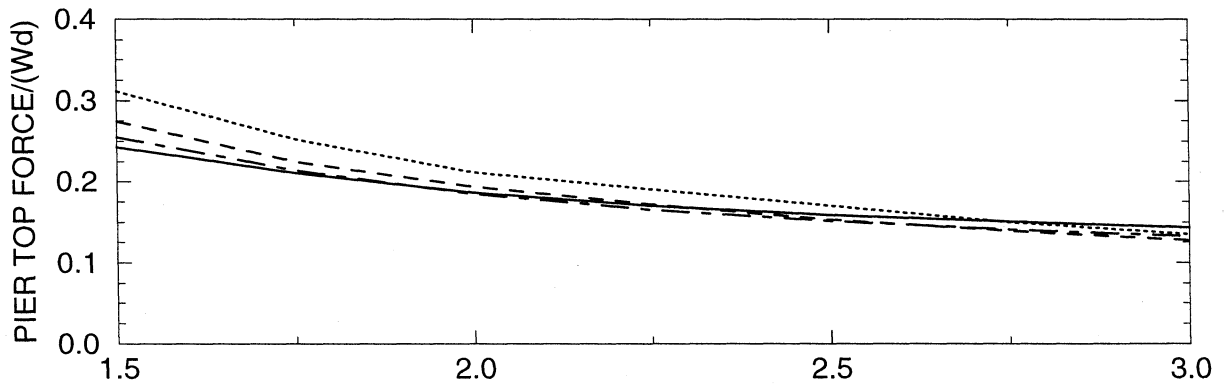
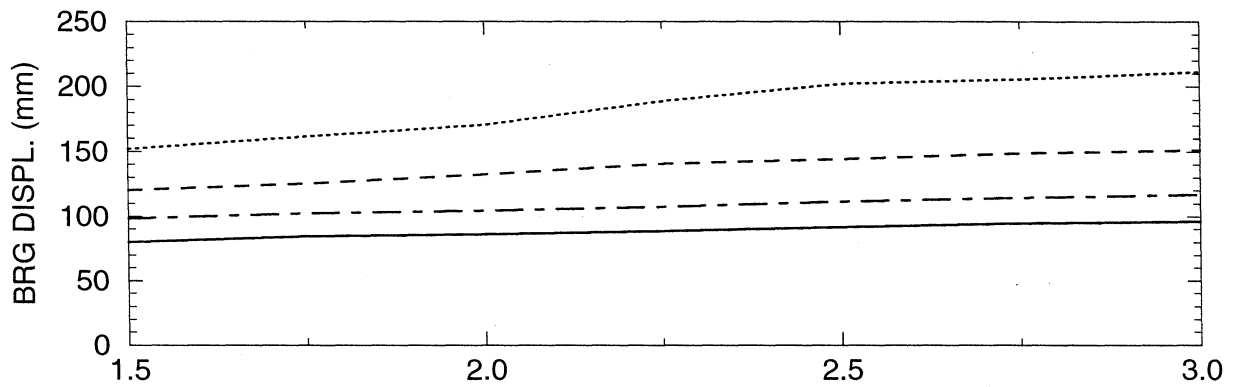
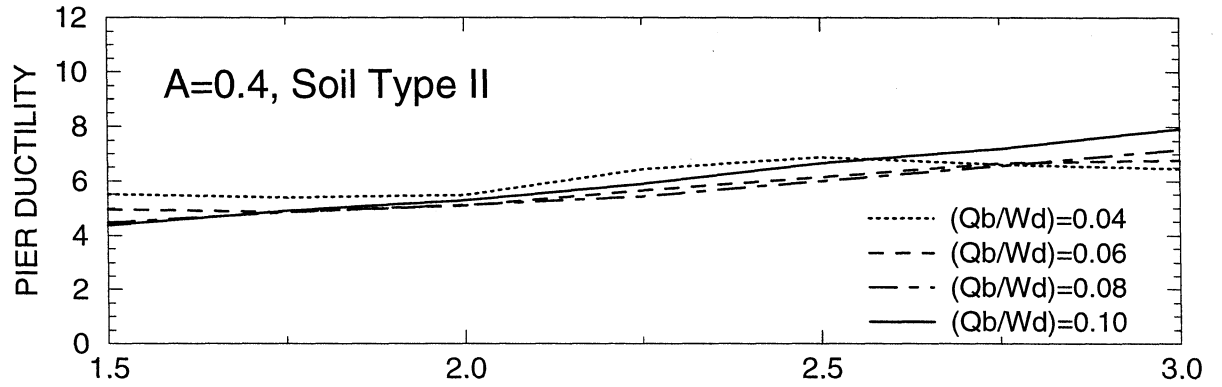


$W_d/W_p=5, T_p=0.5 \text{ s}, R_\mu=1.0, \alpha=0.05$
 BILINEAR HYSTERETIC PIER, SLIDING ISOLATION SYSTEM



Wd/Wp=10, Tp=0.1 s, $R_{\mu}=1.5$, $\alpha=0.05$

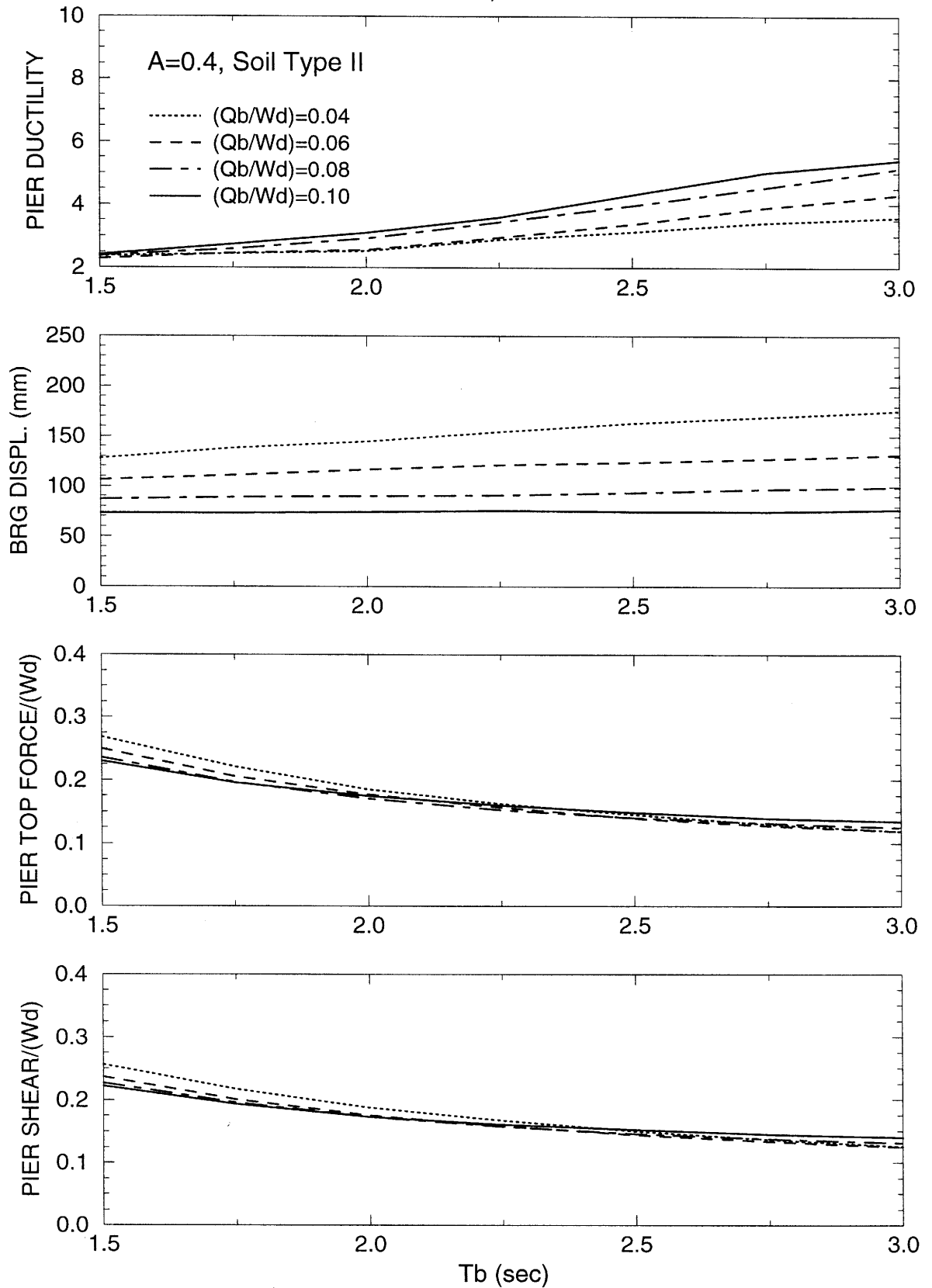
BILINEAR HYSTERETIC PIER, SLIDING ISOLATION SYSTEM



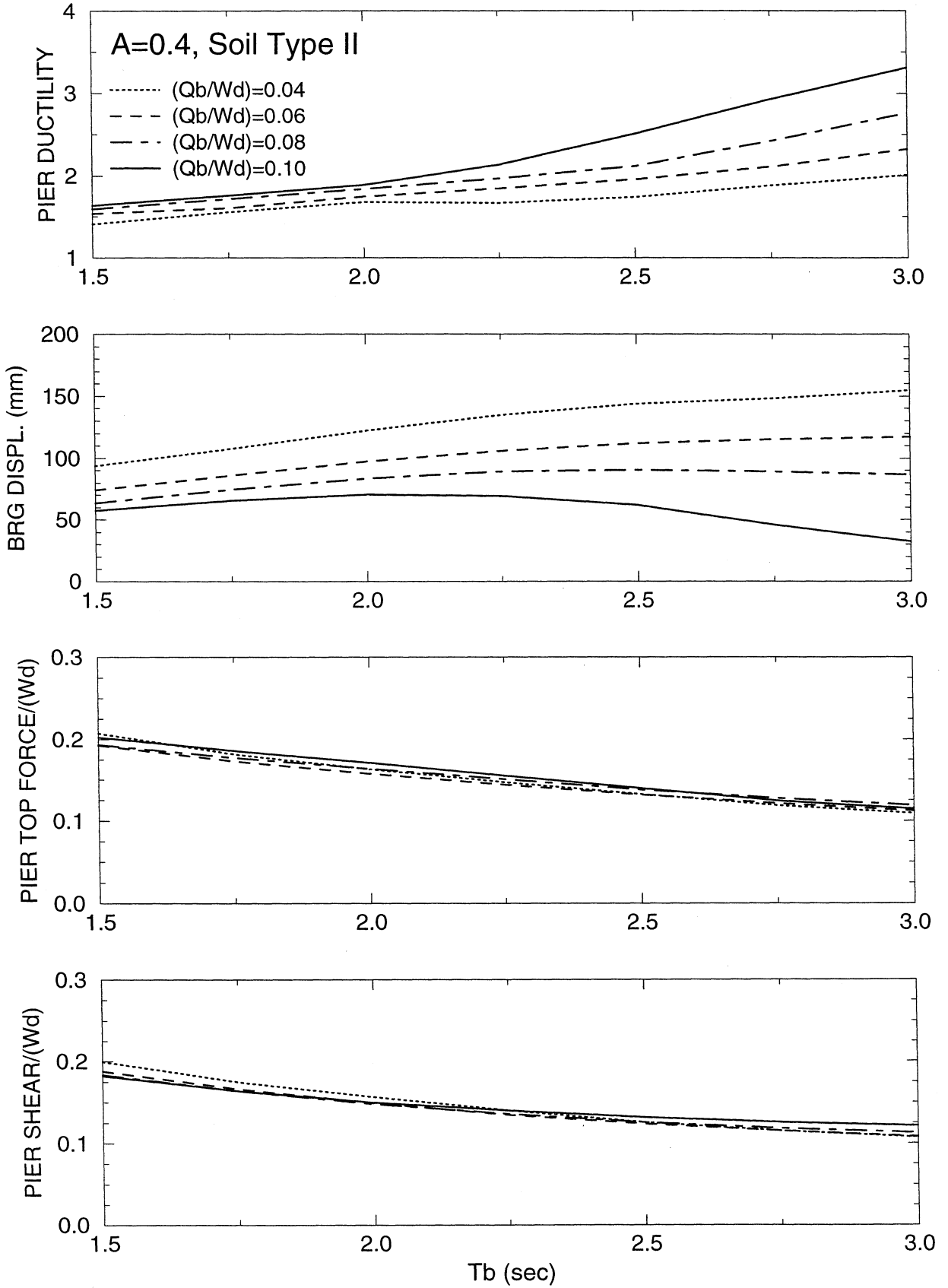
Tb (sec)

$W_d/W_p=10$, $T_p=0.25$ s, $R_\mu=1.5$, $\alpha=0.05$

BILINEAR HYSTERETIC PIER, SLIDING ISOLATION SYSTEM

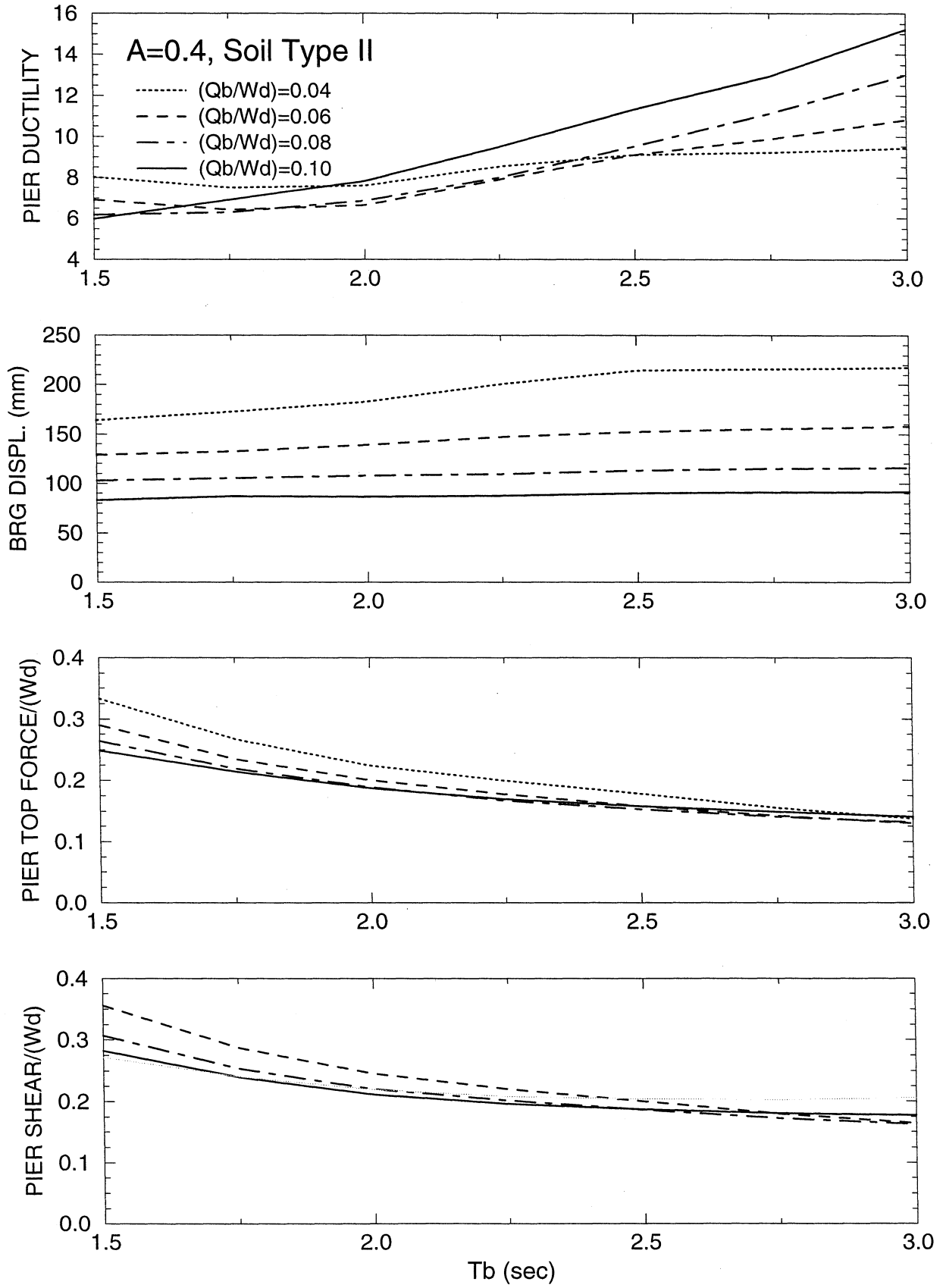


$W_d/W_p=10, T_p=0.5 \text{ s}, R_\mu=1.5, \alpha=0.05$
 BILINEAR HYSTERETIC PIER, SLIDING ISOLATION SYSTEM

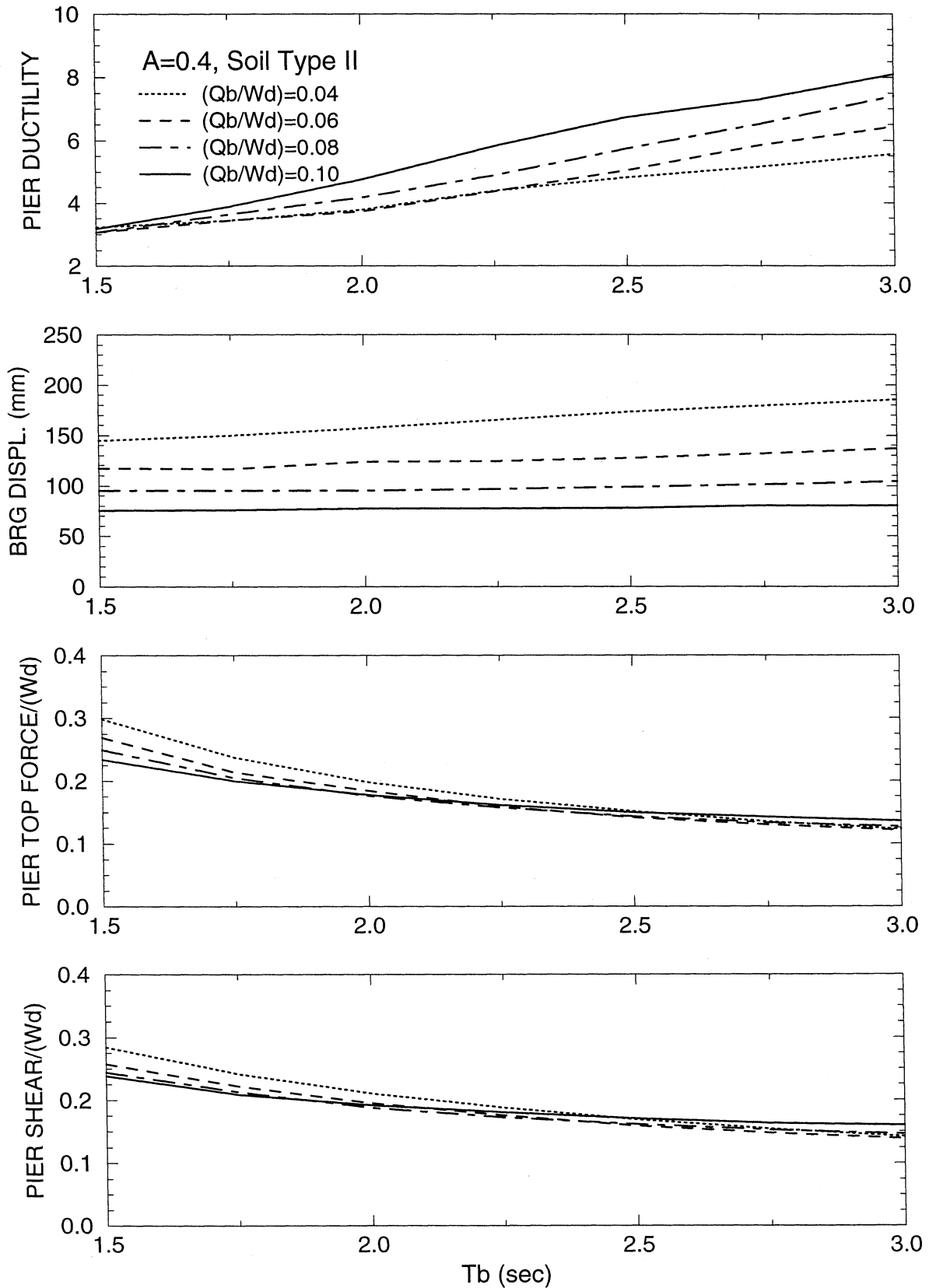


$W_d/W_p=5, T_p=0.1 \text{ s}, R_{\mu}=1.5, \alpha=0.05$

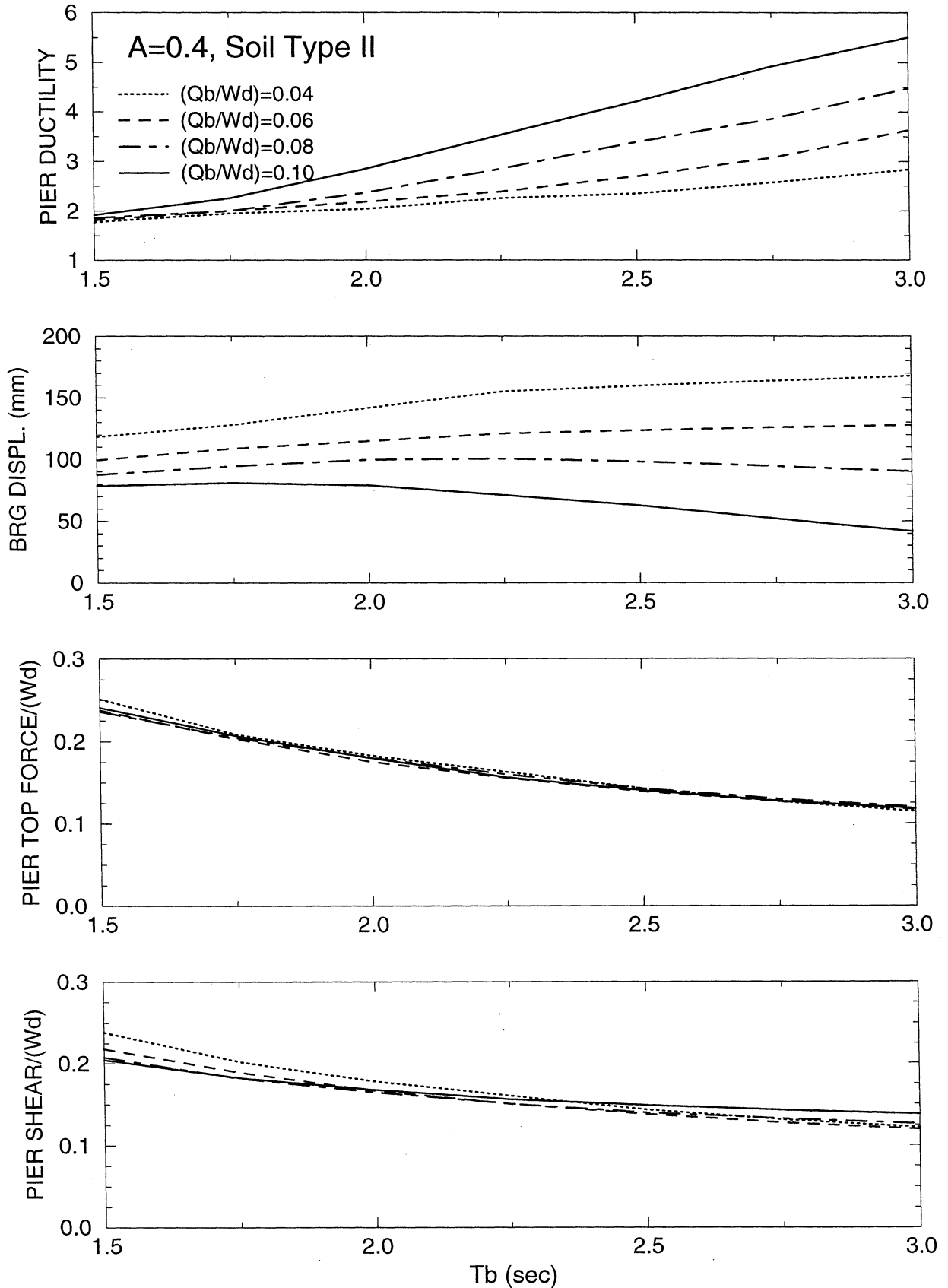
BILINEAR HYSTERETIC PIER, SLIDING ISOLATION SYSTEM



$W_d/W_p=5, T_p=0.25 \text{ s}, R_{\mu}=1.5, \alpha=0.05$
BILINEAR HYSTERETIC PIER, SLIDING ISOLATION SYSTEM



$W_d/W_p=5, T_p=0.5 \text{ s}, R_\mu=1.5, \alpha=0.05$
 BILINEAR HYSTERETIC PIER, SLIDING ISOLATION SYSTEM

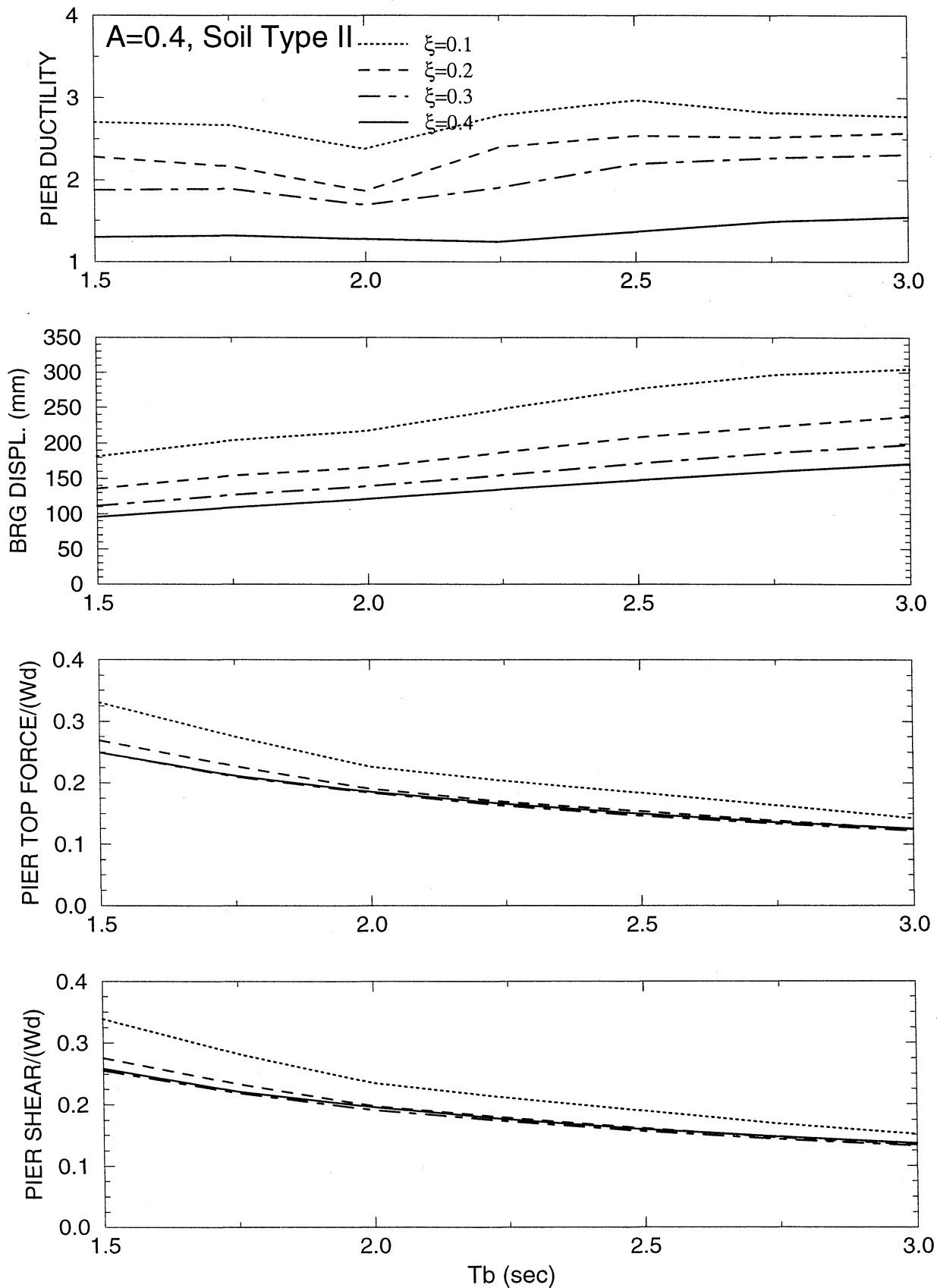


APPENDIX G

**RESULTS OF NONLINEAR DYNAMIC ANALYSIS OF SEISMIC-ISOLATED
BRIDGE WITH PERFECT BILINEAR HYSTERETIC PIER
AND LINEAR ELASTIC/VISCOUS ISOLATION SYSTEM
FOR AASHTO, A=0.4, SOIL PROFILE TYPE II INPUT**

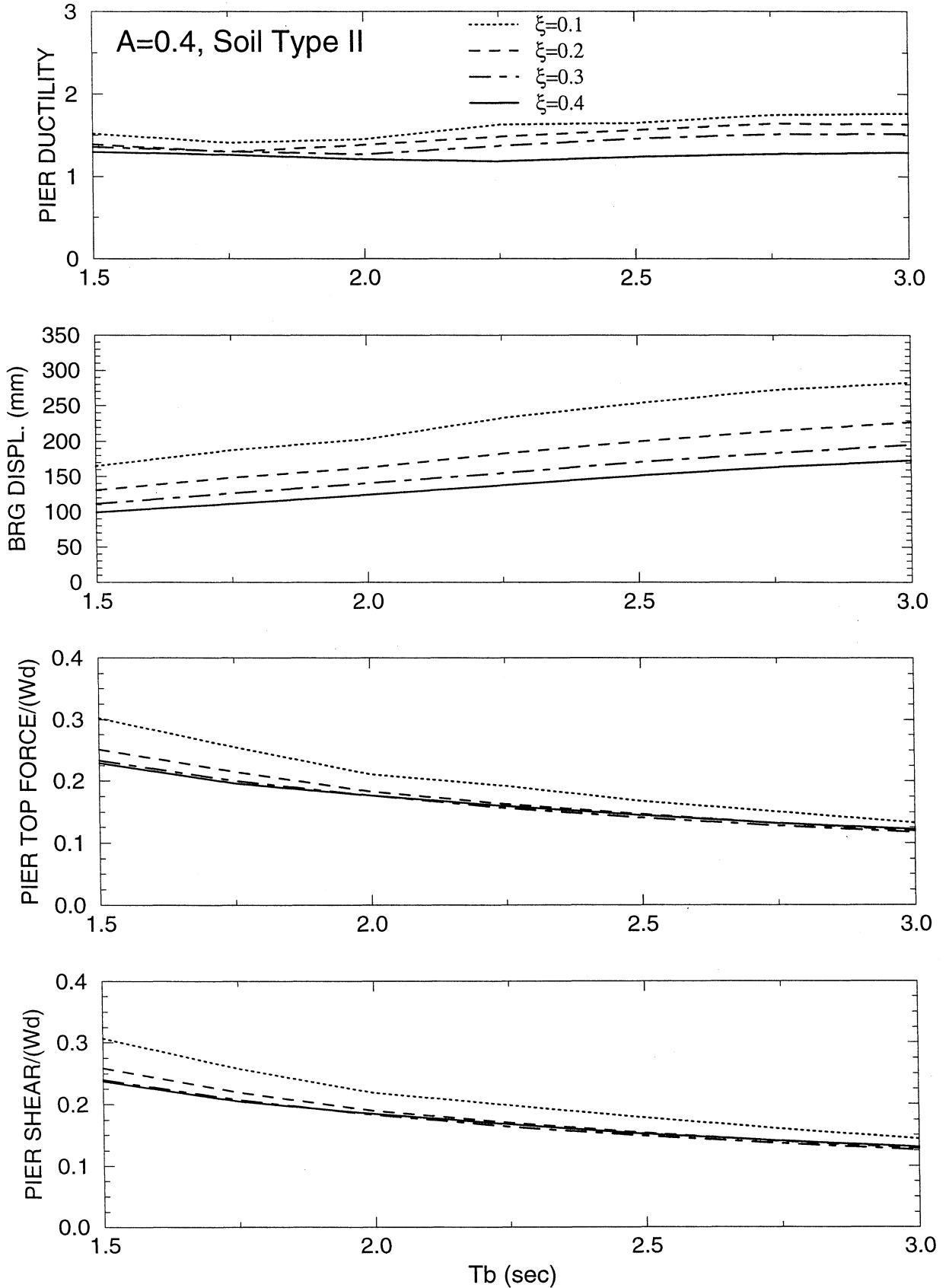
$W_d/W_p=10, T_p=0.1 \text{ s}, R_\mu=1.0, \alpha=0.05$

BILINEAR HYSTERETIC PIER, LINEAR ELASTIC/VISCOUS ISOLATION SYSTEM



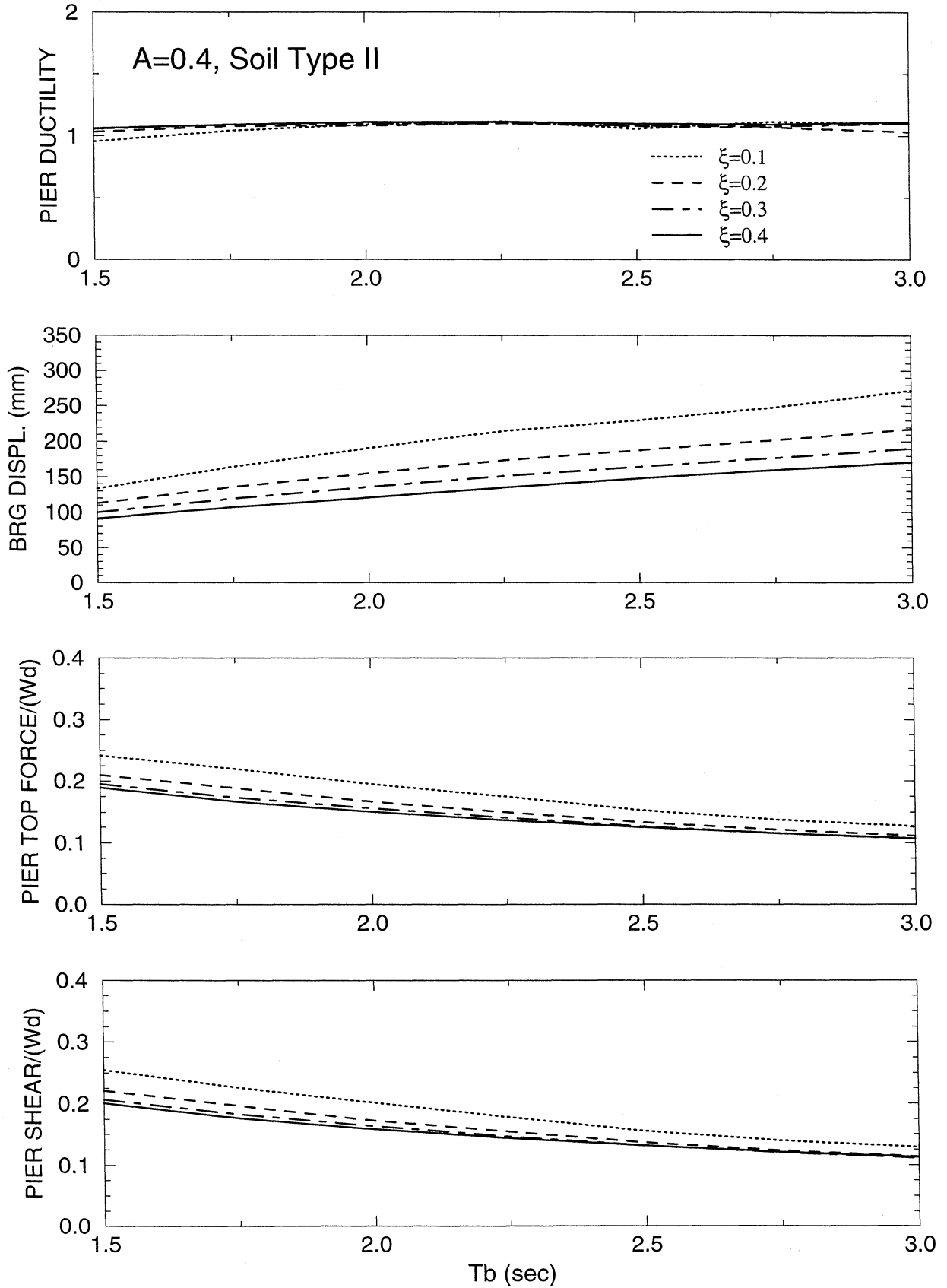
$W_d/W_p=10, T_p=0.25 \text{ s}, R_\mu=1.0, \alpha=0.05$

BILINEAR HYSTERETIC PIER, LINEAR ELASTIC/VISCOUS ISOLATION SYSTEM



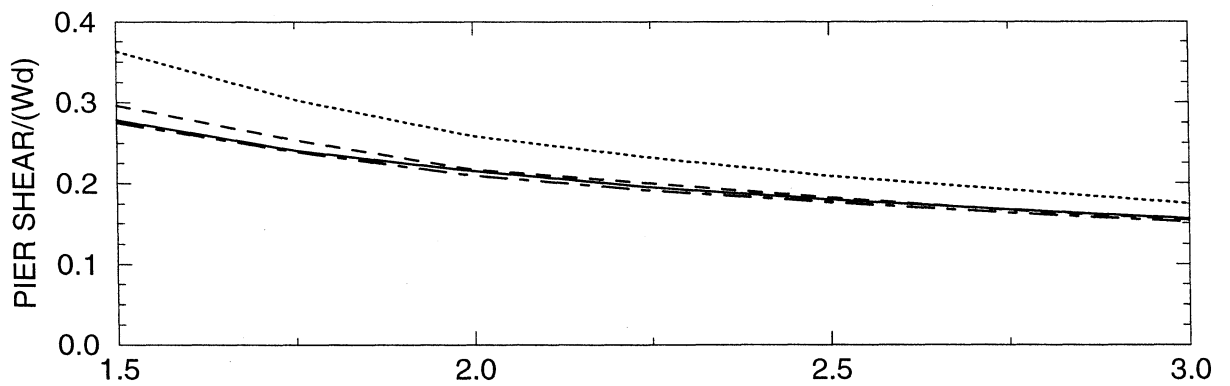
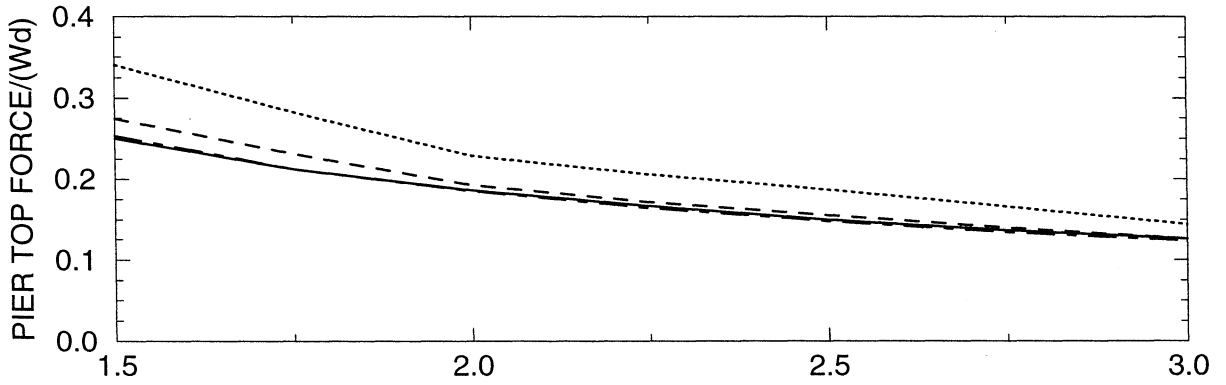
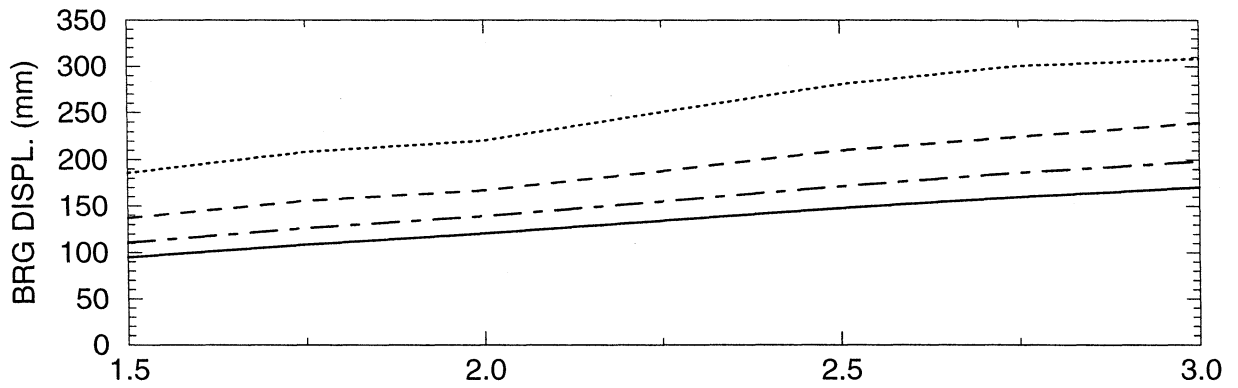
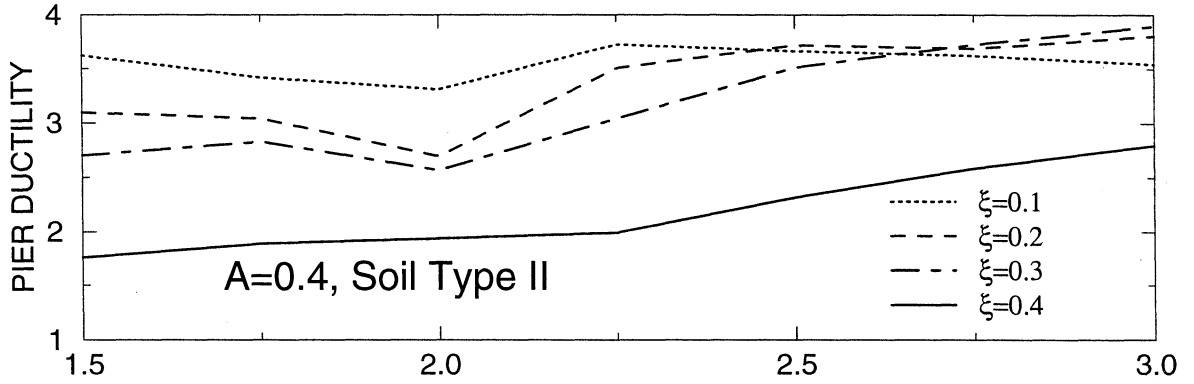
$W_d/W_p=10$, $T_p=0.5$ s, $R_\mu=1.0$, $\alpha=0.05$

BILINEAR HYSTERETIC PIER, LINEAR ELASTIC/VISCOUS ISOLATION SYSTEM



$W_d/W_p=5, T_p=0.1 \text{ s}, R_\mu=1.0, \alpha=0.05$

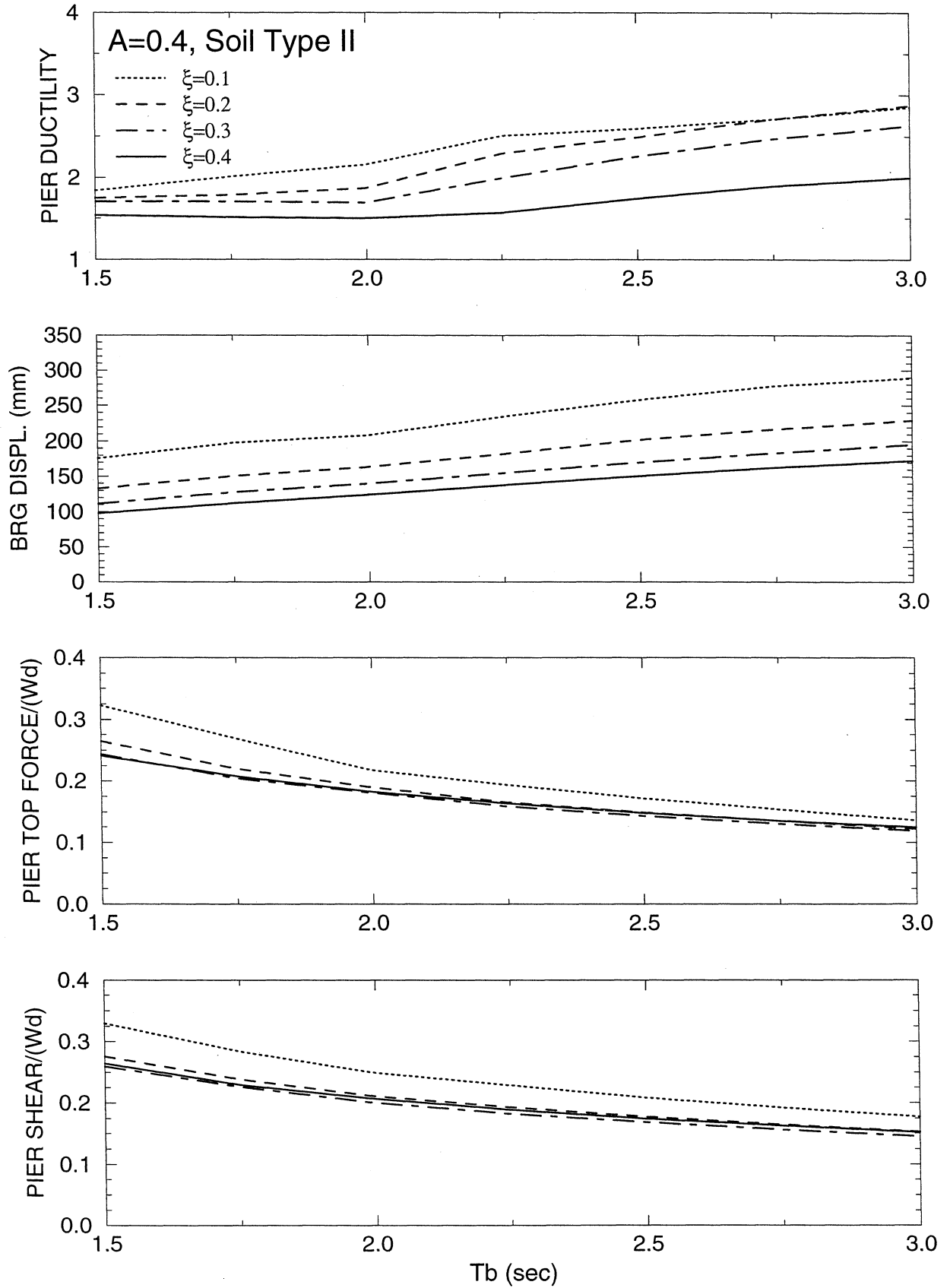
BILINEAR HYSTERETIC PIER, LINEAR ELASTIC/VISCOUS ISOLATION SYSTEM



$T_b \text{ (sec)}$

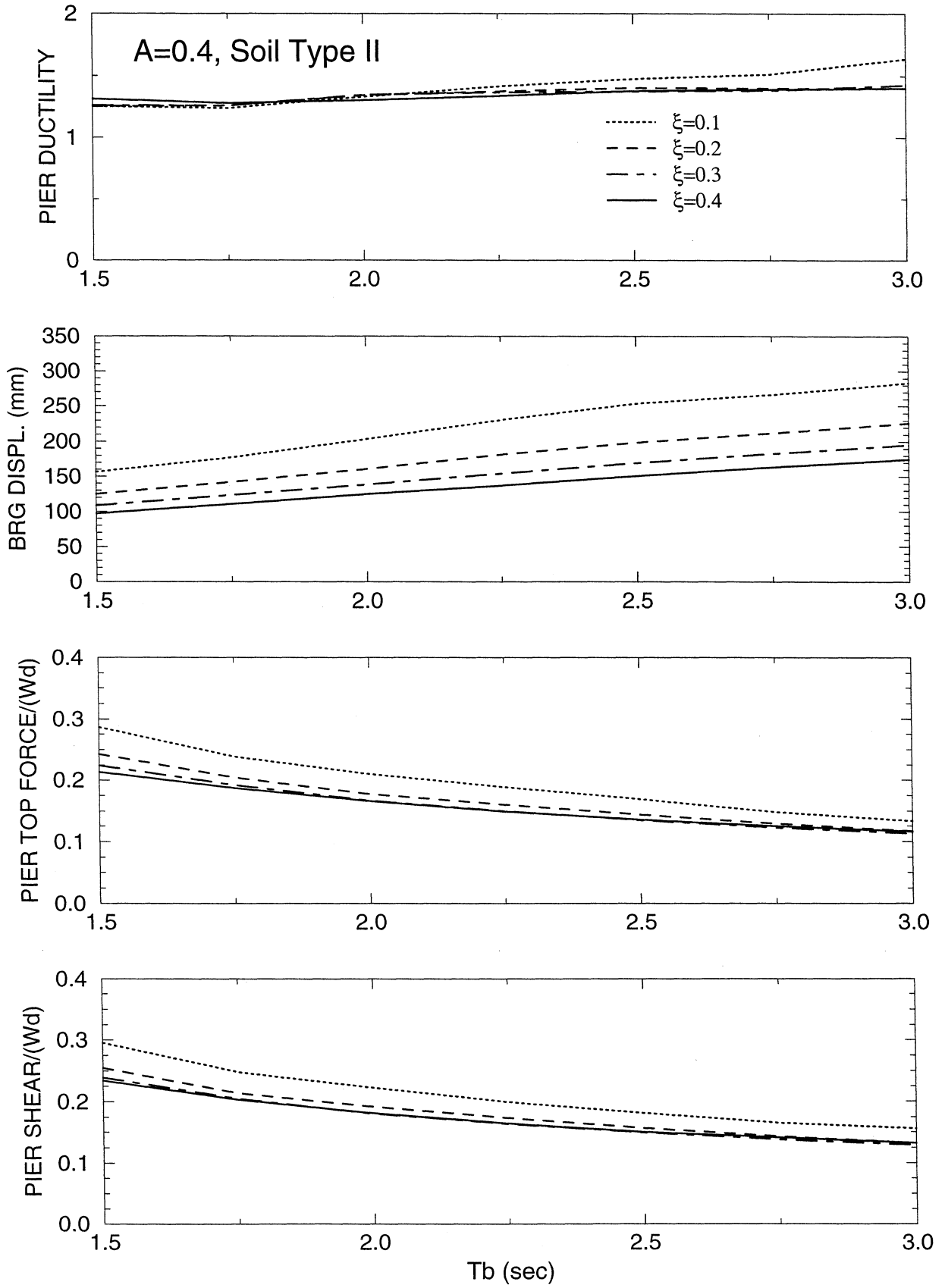
$W_d/W_p=5, T_p=0.25 \text{ s}, R_\mu=1.0, \alpha=0.05$

BILINEAR HYSTERETIC PIER, LINEAR ELASTIC/VISCOUS ISOLATION SYSTEM



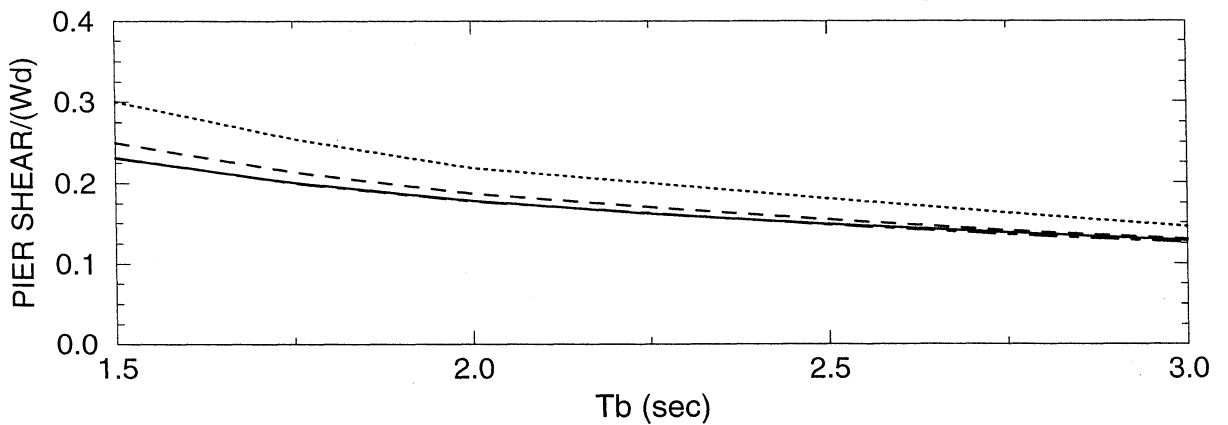
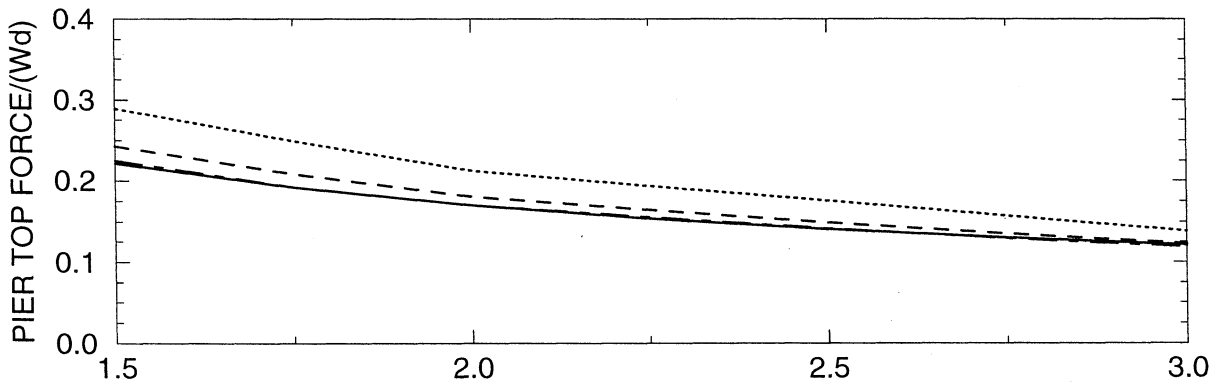
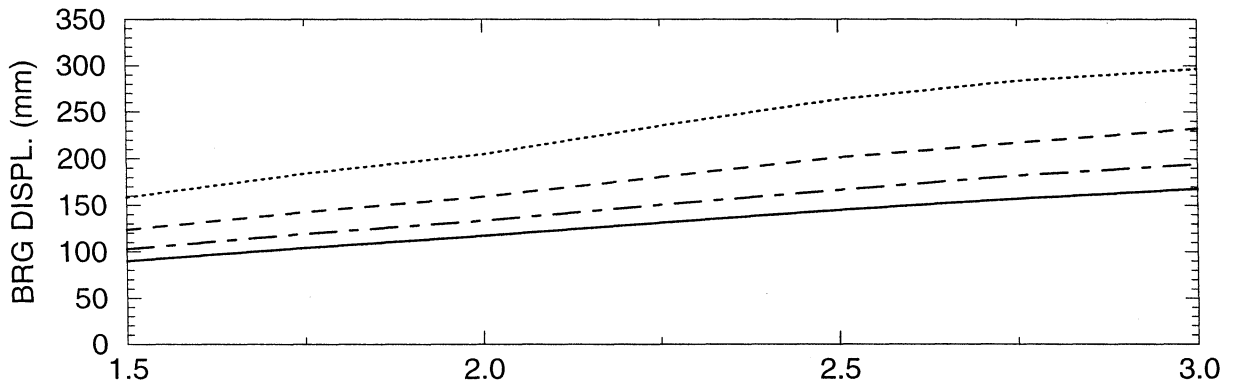
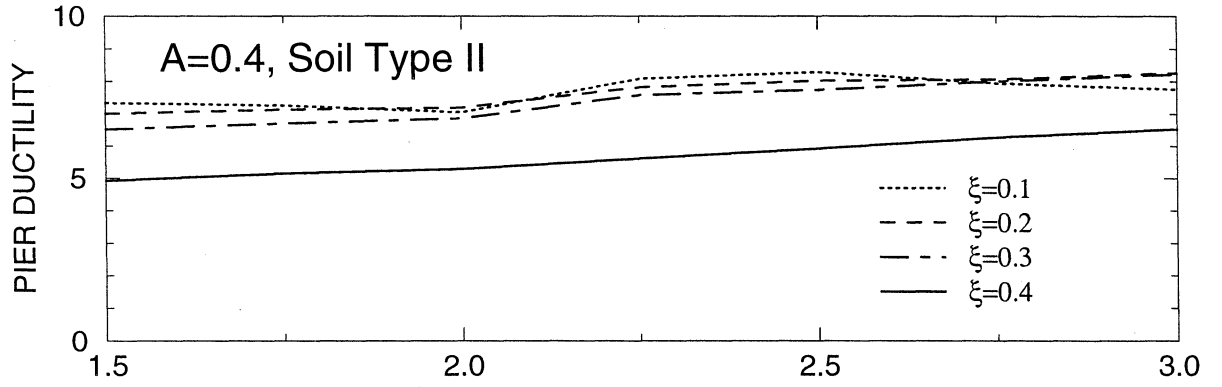
$W_d/W_p=5, T_p=0.5 \text{ s}, R_\mu=1.0, \alpha=0.05$

BILINEAR HYSTERETIC PIER, LINEAR ELASTIC/VISCOUS ISOLATION SYSTEM



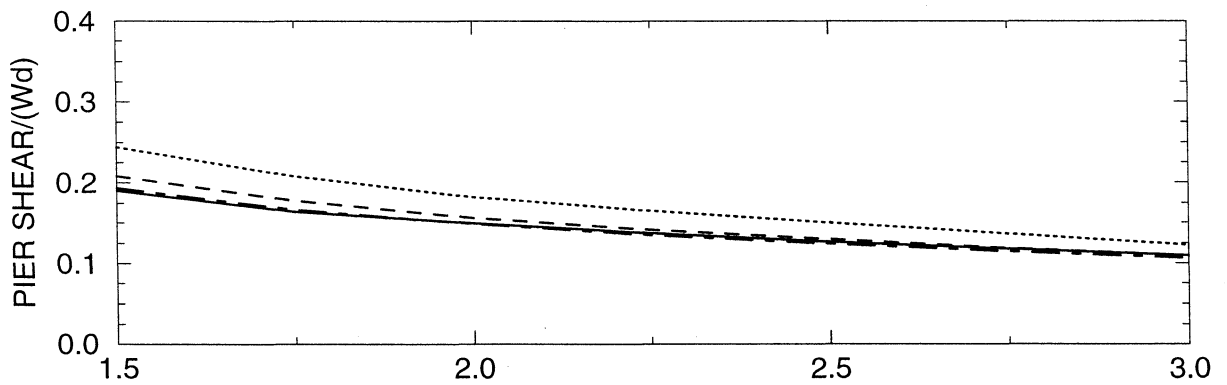
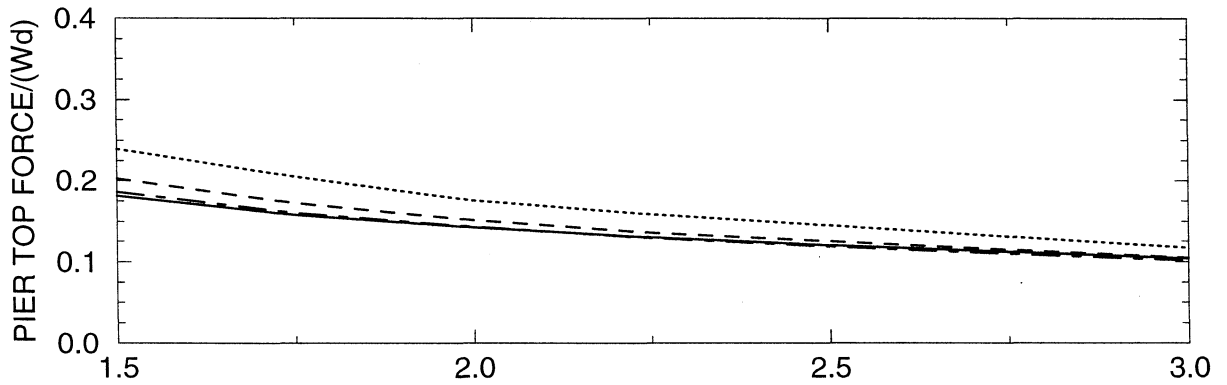
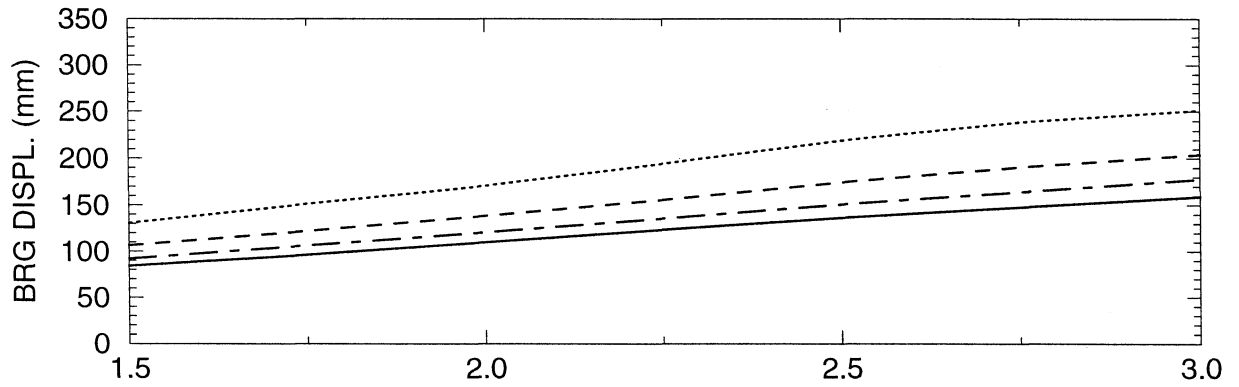
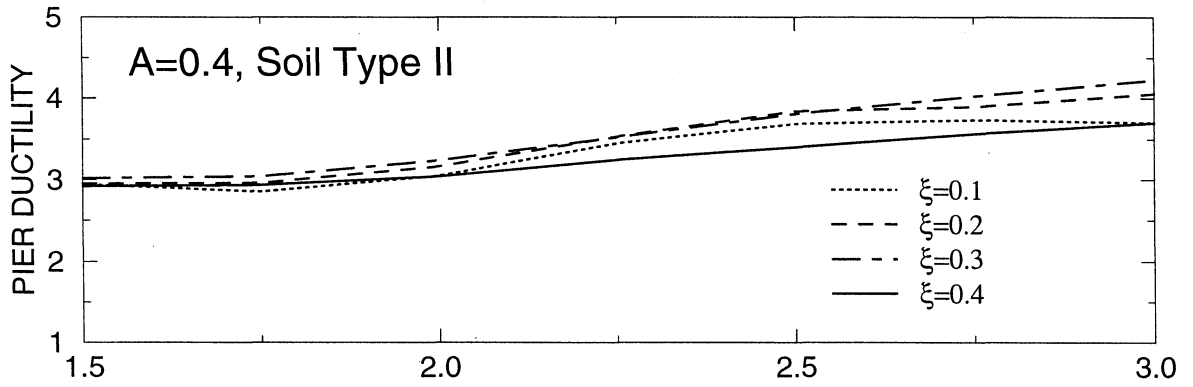
$W_d/W_p=10, T_p=0.1 \text{ s}, R_\mu=1.5, \alpha=0.05$

BILINEAR HYSTERETIC PIER, LINEAR ELASTIC/VISCOUS ISOLATION SYSTEM



$W_d/W_p=10$, $T_p=0.25$ s, $R_\mu=1.5$, $\alpha=0.05$

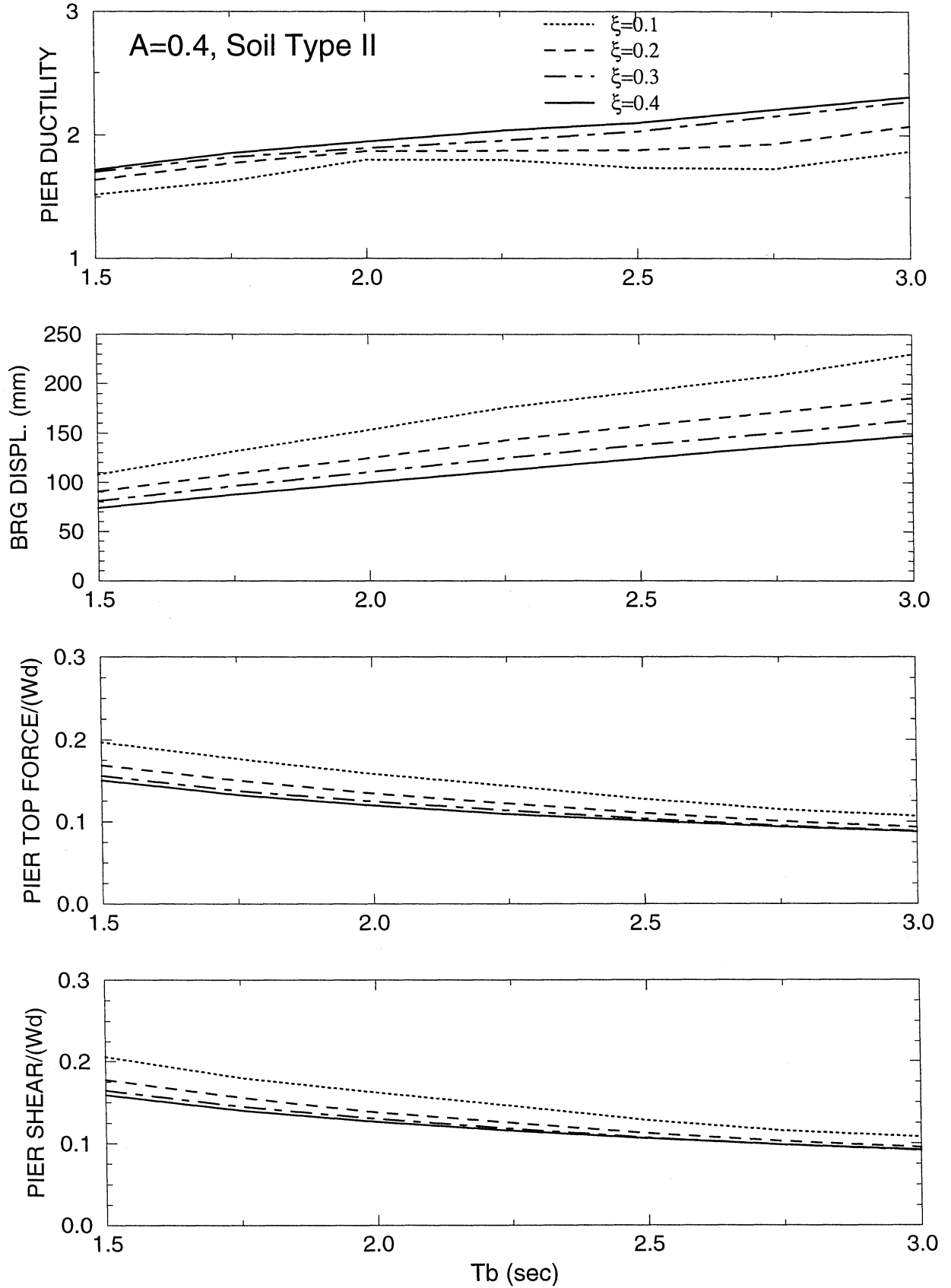
BILINEAR HYSTERETIC PIER, LINEAR ELASTIC/VISCOUS ISOLATION SYSTEM



Tb (sec)

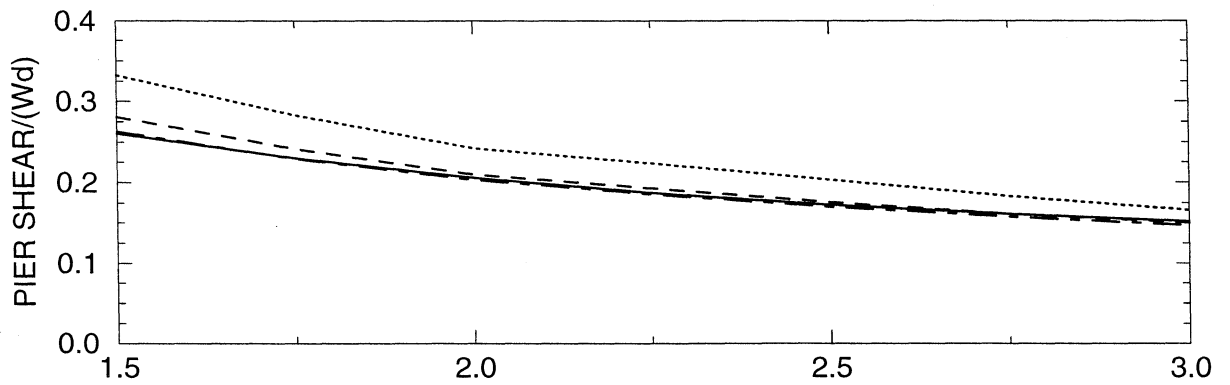
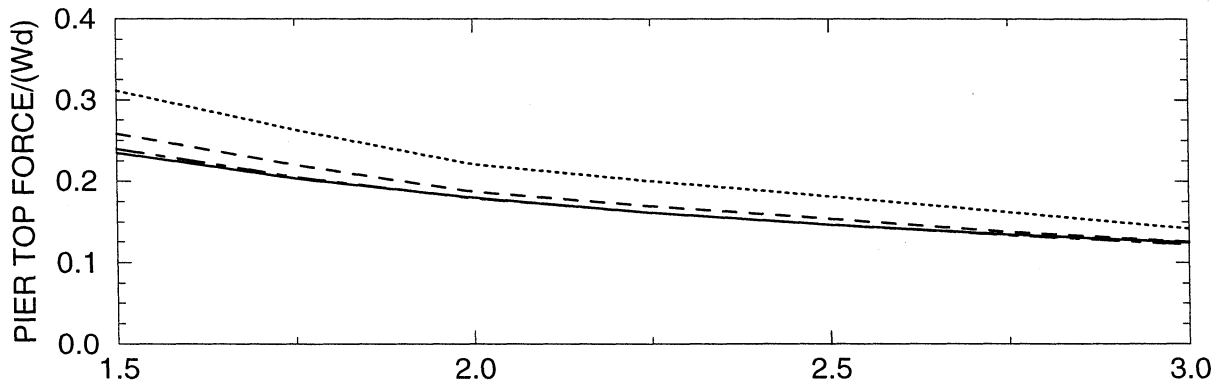
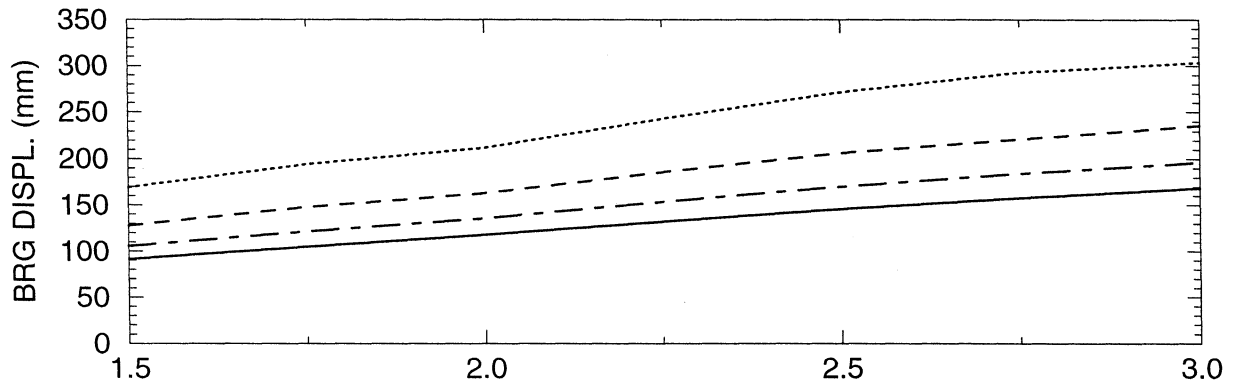
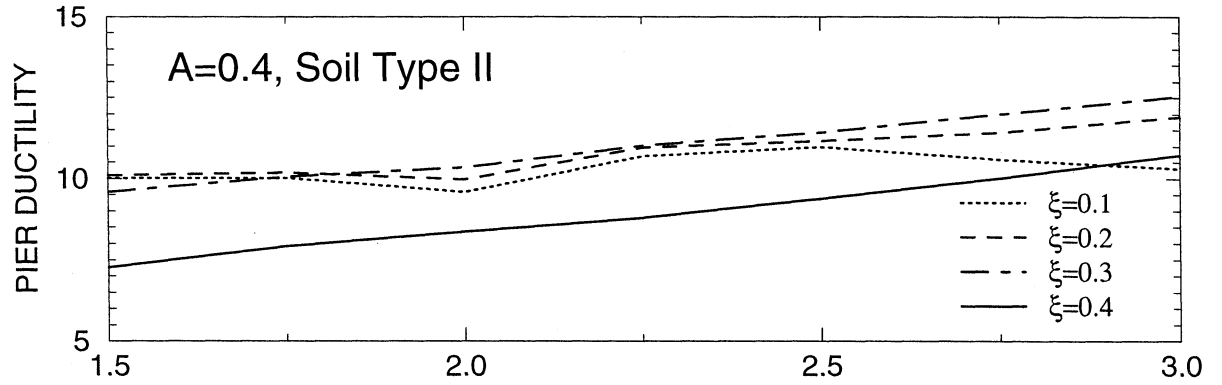
$W_d/W_p=10, T_p=0.5 \text{ s}, R_\mu=1.5, \alpha=0.05$

BILINEAR HYSTERETIC PIER, LINEAR ELASTIC/VISCOUS ISOLATION SYSTEM



$W_d/W_p=5, T_p=0.1s, R_{\mu}=1.5, \alpha=0.05$

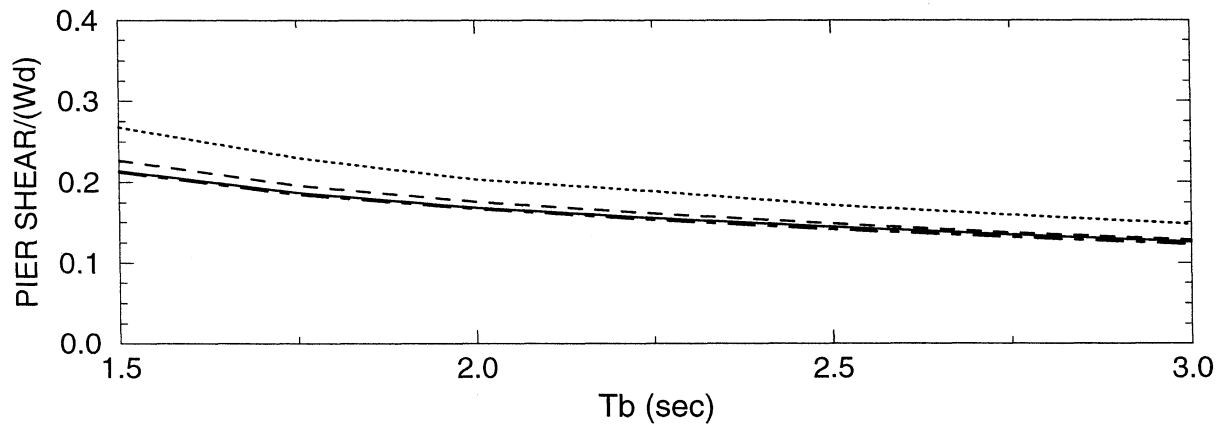
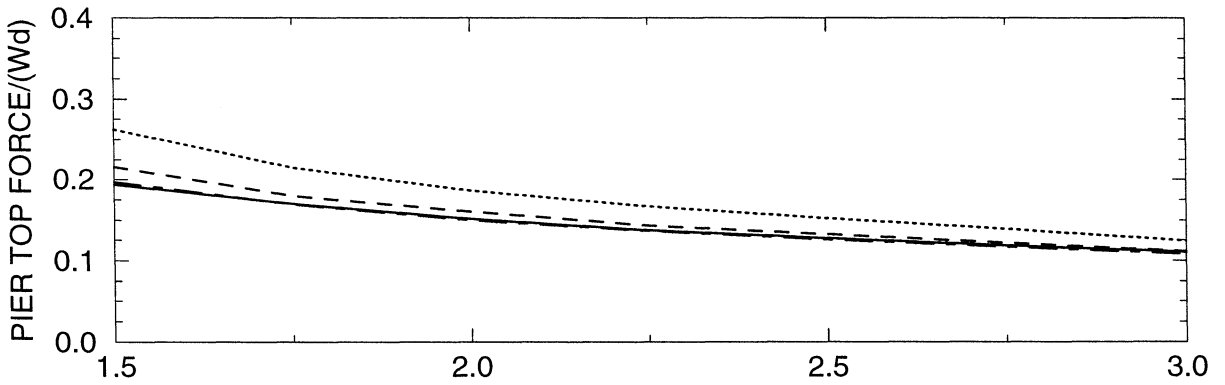
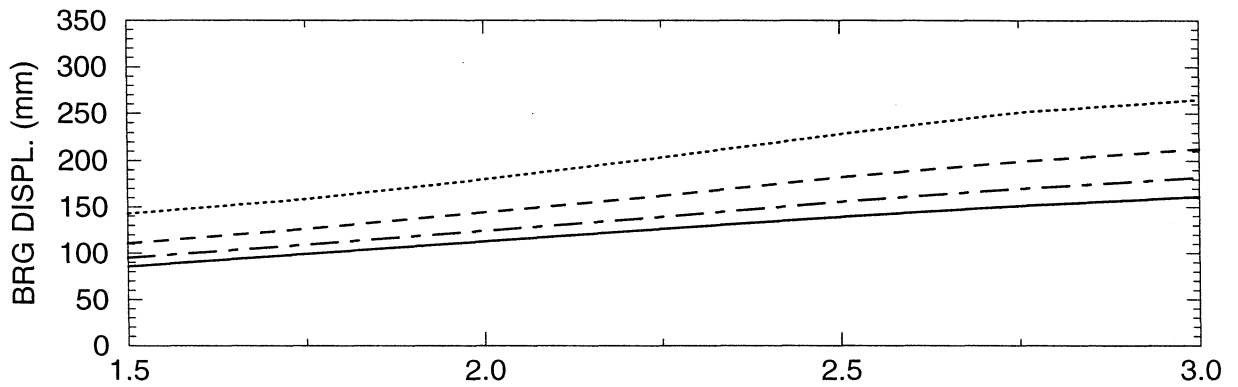
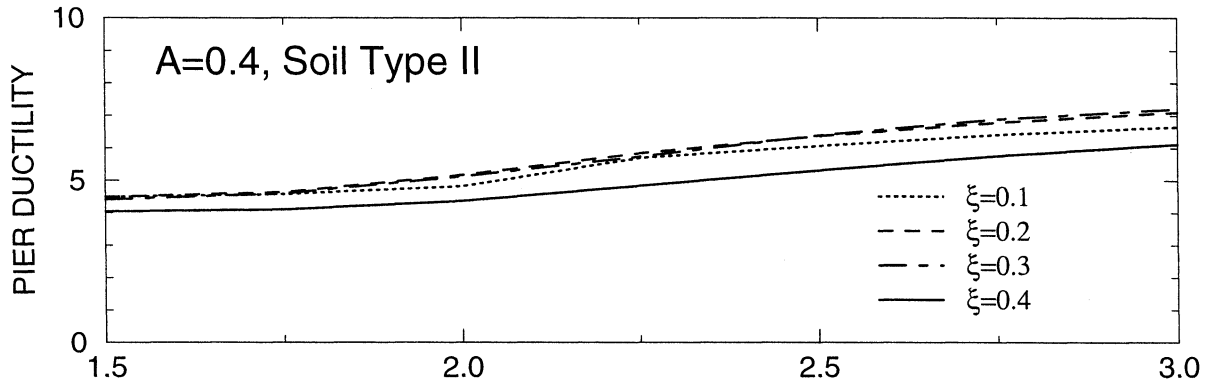
BILINEAR HYSTERETIC PIER, LINEAR ELASTIC/VISCOUS ISOLATION SYSTEM



Tb (sec)

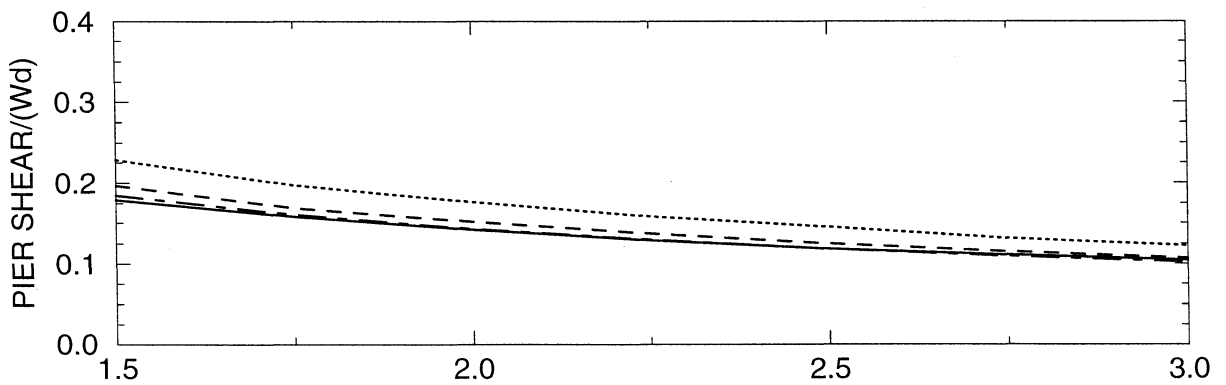
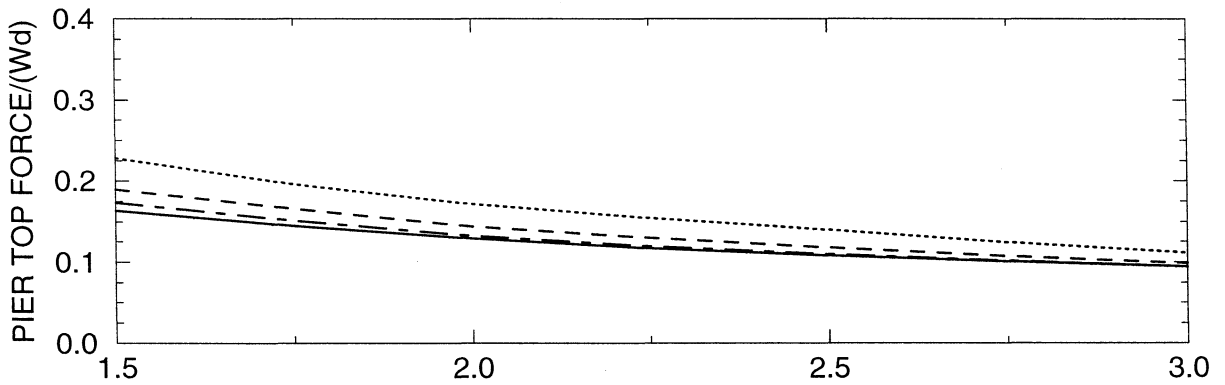
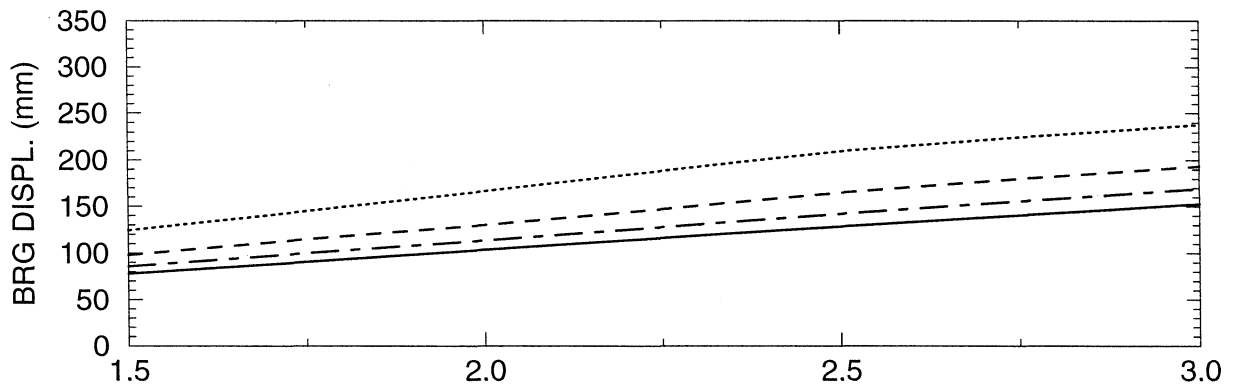
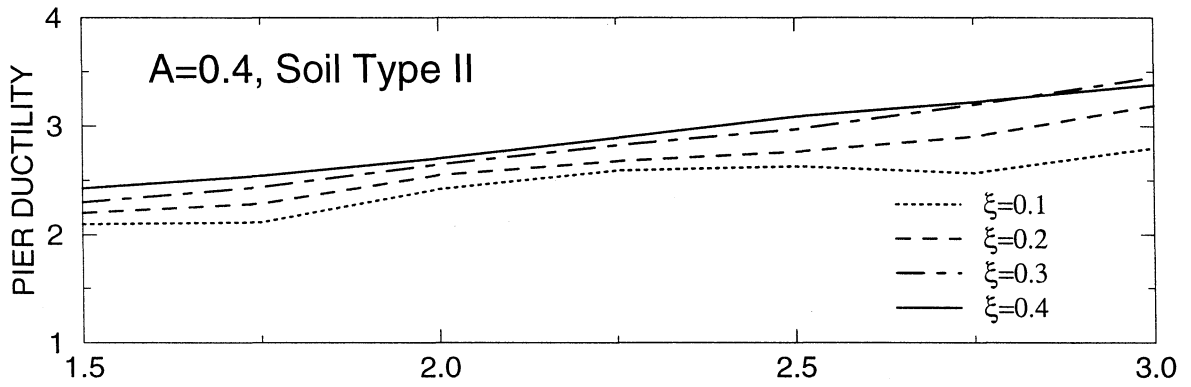
$W_d/W_p=5, T_p=0.25 \text{ s}, R_\mu=1.5, \alpha=0.05$

BILINEAR HYSTERETIC PIER, LINEAR ELASTIC/VISCOUS ISOLATION SYSTEM



$W_d/W_p=5, T_p=0.5 \text{ s}, R_\mu=1.5, \alpha=0.05$

BILINEAR HYSTERETIC PIER, LINEAR ELASTIC/VISCOUS ISOLATION SYSTEM



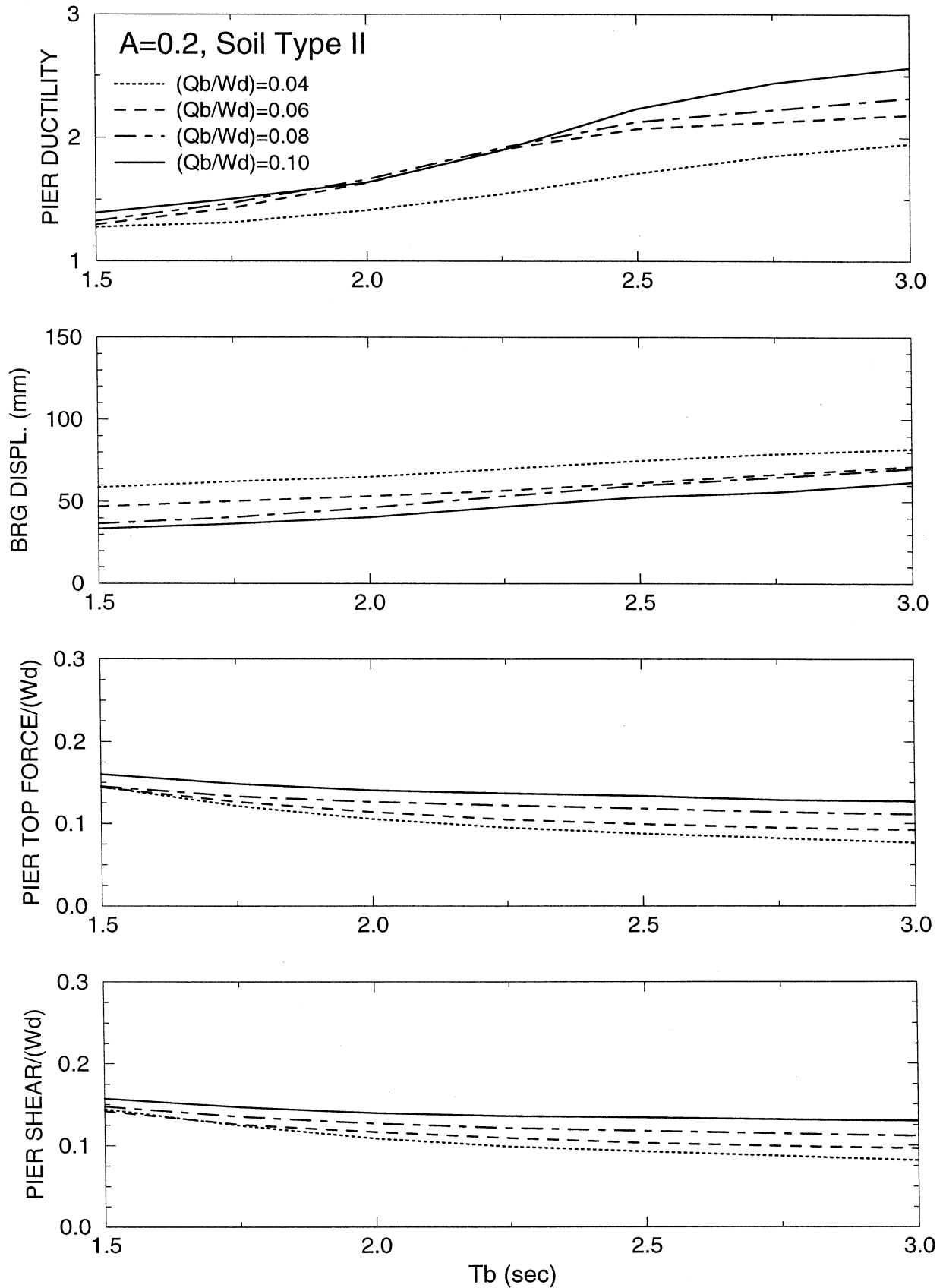
Tb (sec)

APPENDIX H

RESULTS OF NONLINEAR DYNAMIC ANALYSIS OF SEISMIC-ISOLATED BRIDGE WITH PERFECT BILINEAR HYSTERETIC PIER AND BILINEAR HYSTERETIC ISOLATION SYSTEM FOR AASHTO, A=0.2, SOIL PROFILE TYPE II INPUT

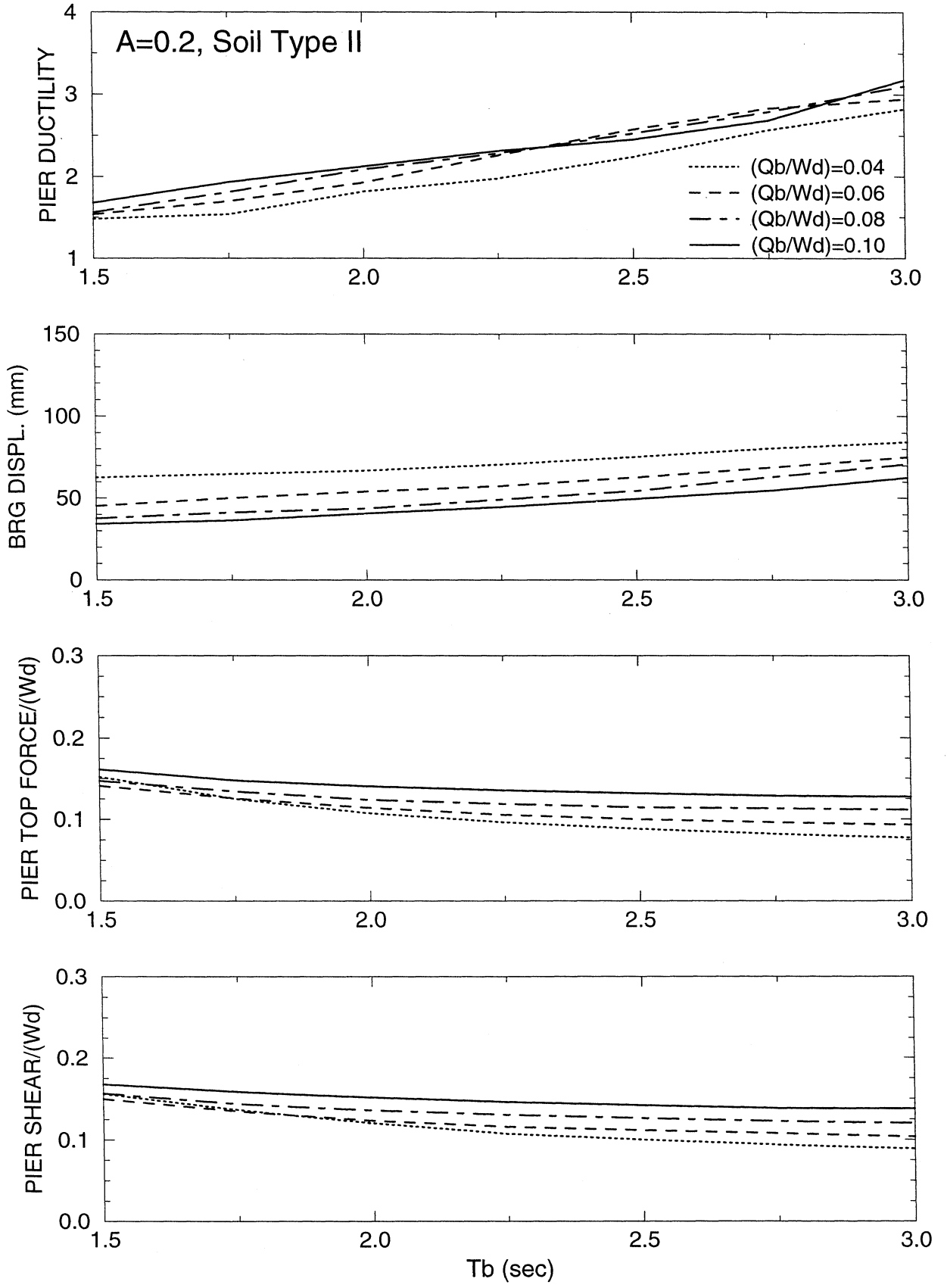
$W_d/W_p=10, T_p=0.25 \text{ s}, R_\mu=1.0, \alpha=0.05$

BILINEAR HYSTERETIC PIER, BILINEAR HYSTERETIC ISOLATION SYSTEM

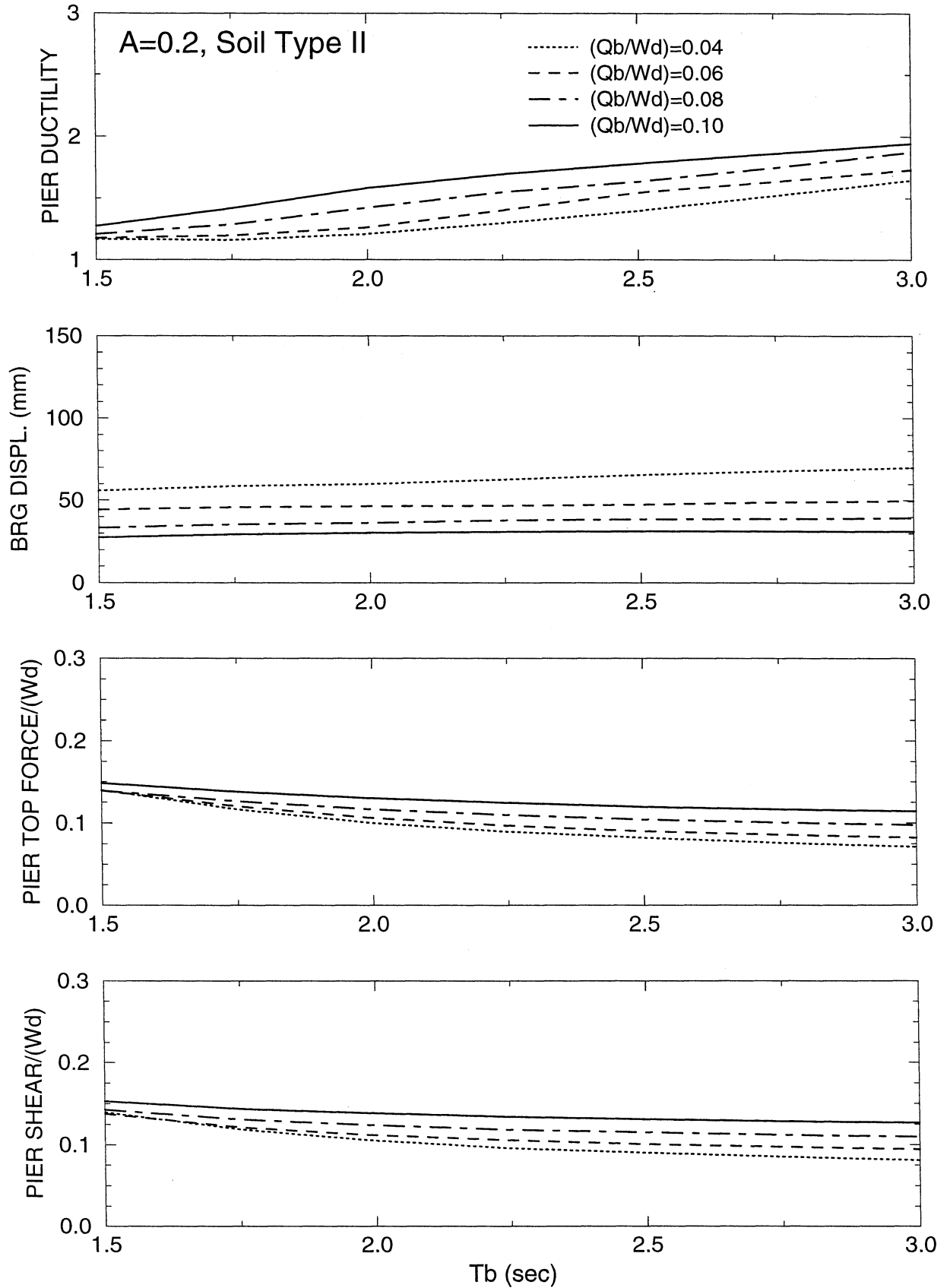


$W_d/W_p=5$, $T_p=0.25$ s, $R_\mu=1.0$, $\alpha=0.05$

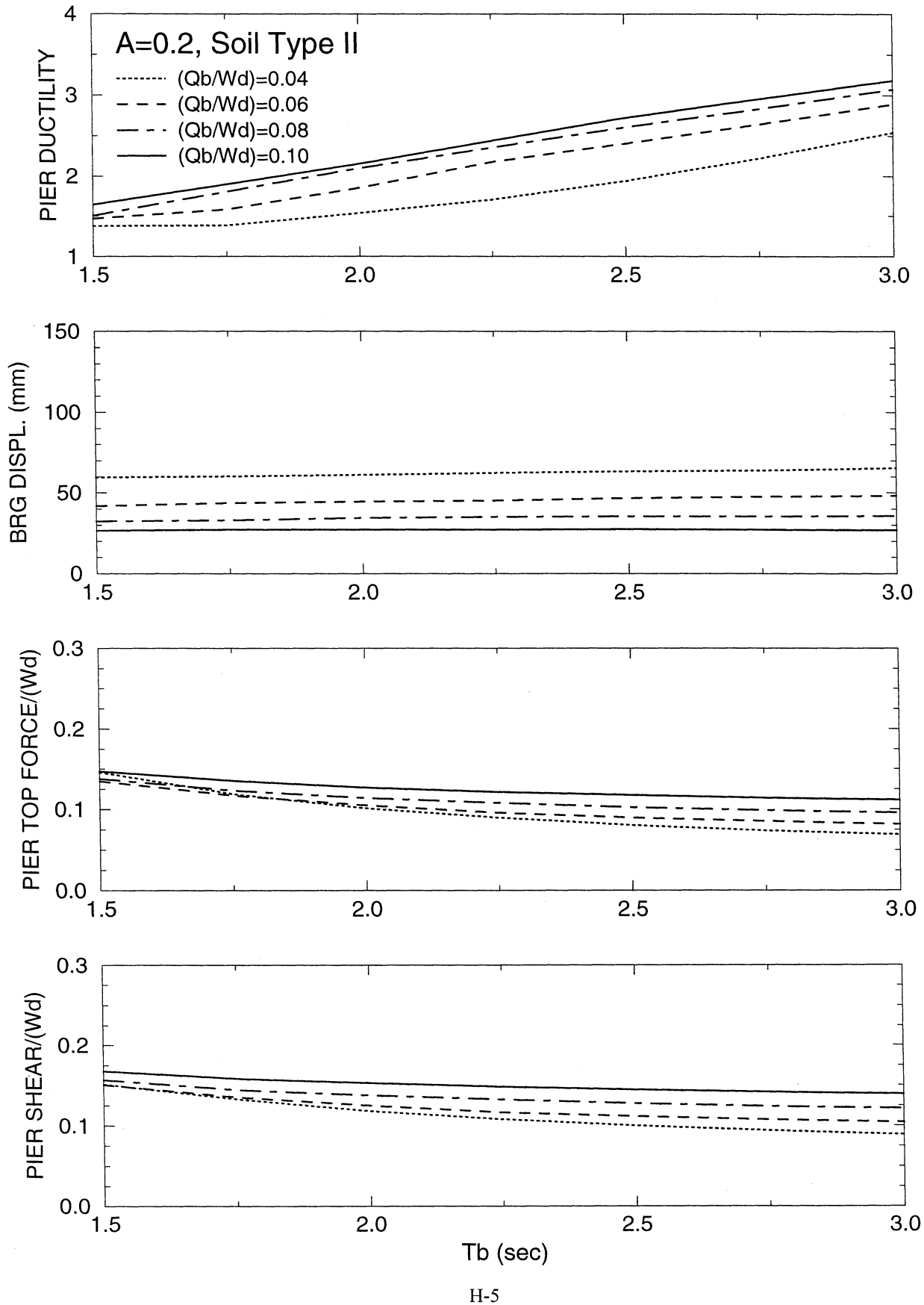
BILINEAR HYSTERETIC PIER, BILINEAR HYSTERETIC ISOLATION SYSTEM



Wd/Wp=10, Tp=0.25 s, R_μ=1.0, α=0.05
BILINEAR HYSTERETIC PIER, SLIDING ISOLATION SYSTEM

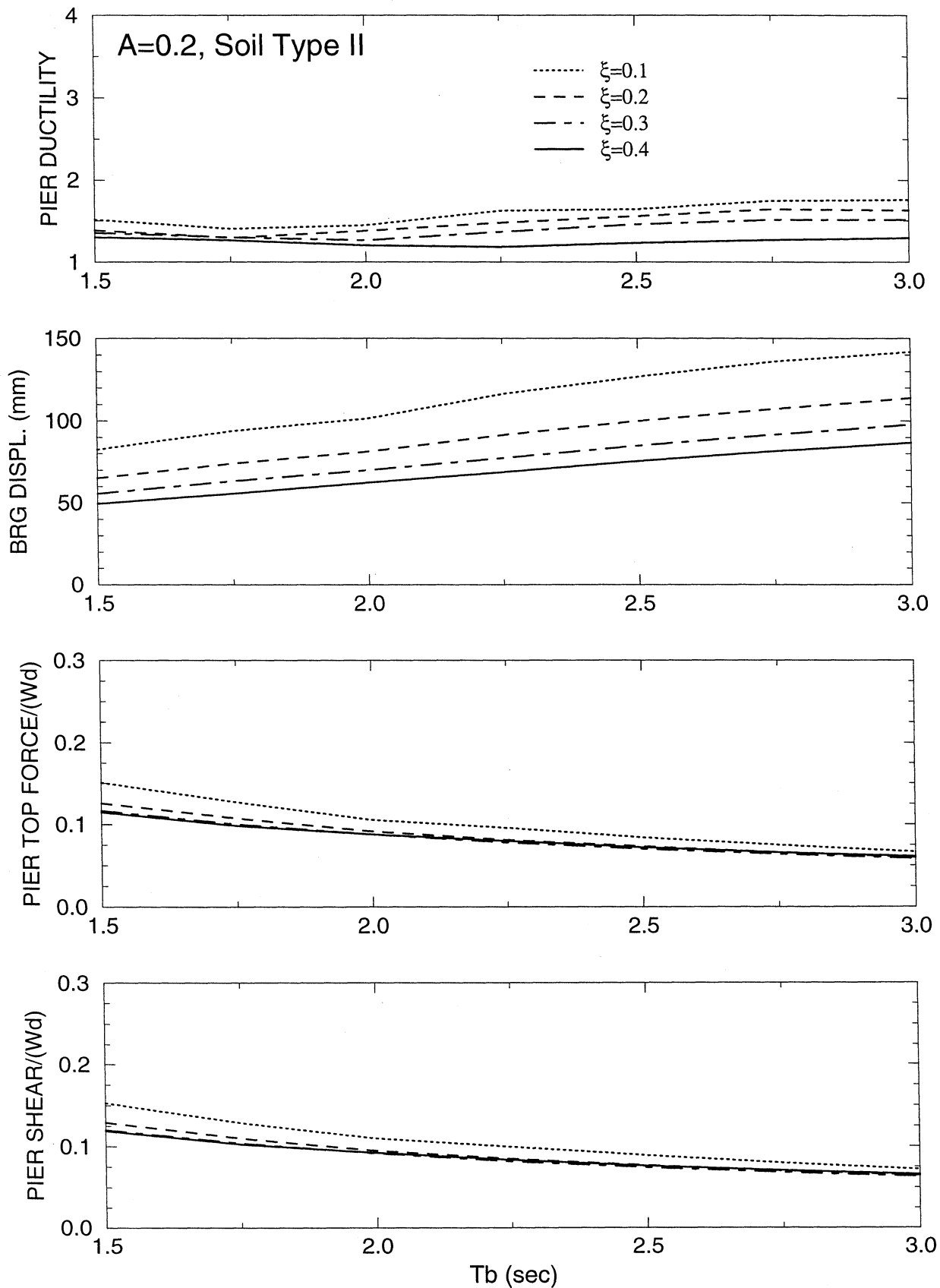


Wd/Wp=5, Tp=0.25 s, R_μ=1.0, α=0.05
BILINEAR HYSTERETIC PIER, SLIDING ISOLATION SYSTEM



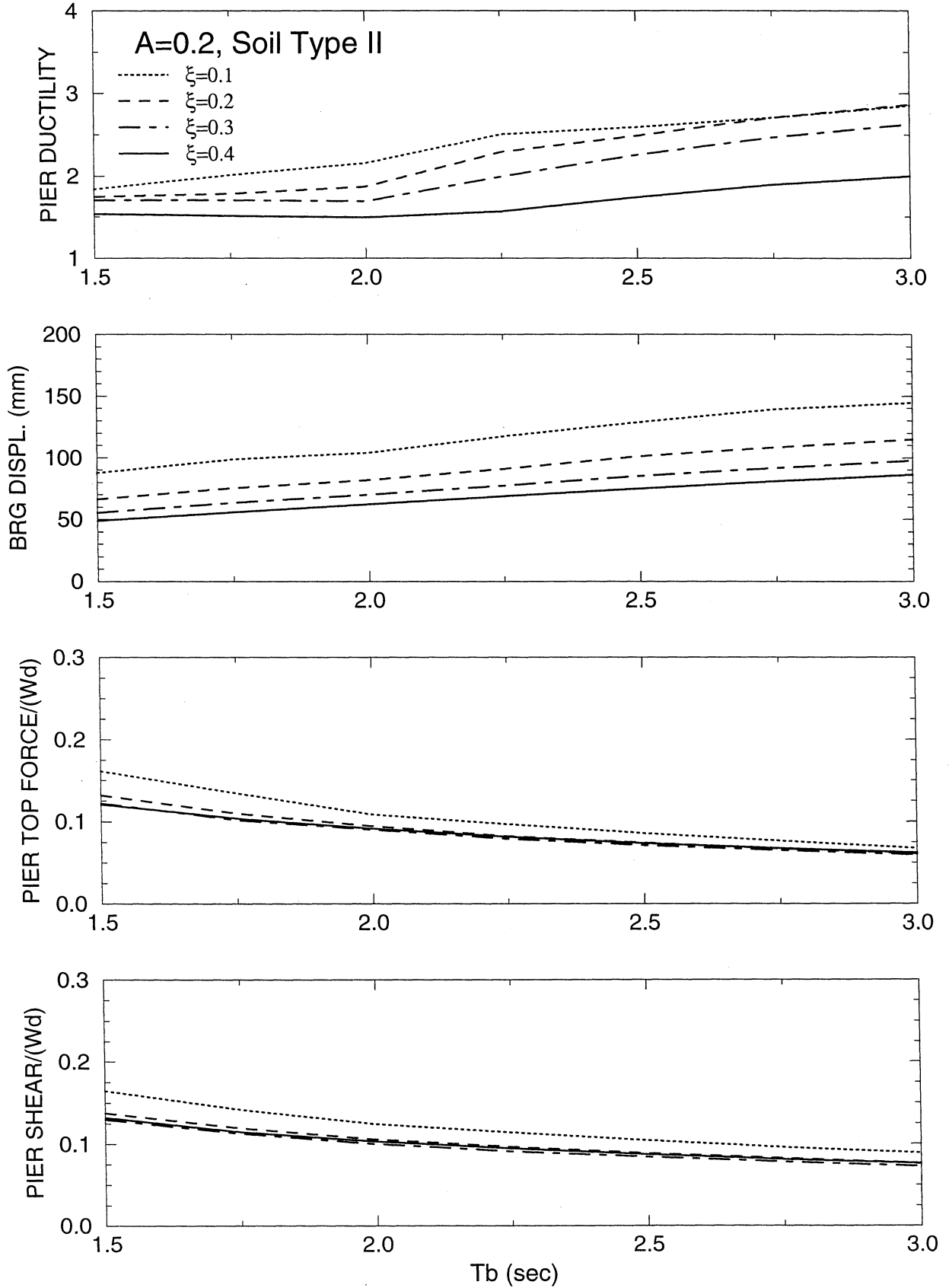
$W_d/W_p=10$, $T_p=0.25$ s, $R_{\mu}=1.0$, $\alpha=0.05$

BILINEAR HYSTERETIC PIER, LINEAR ELASTIC/VISCOUS ISOLATION SYSTEM



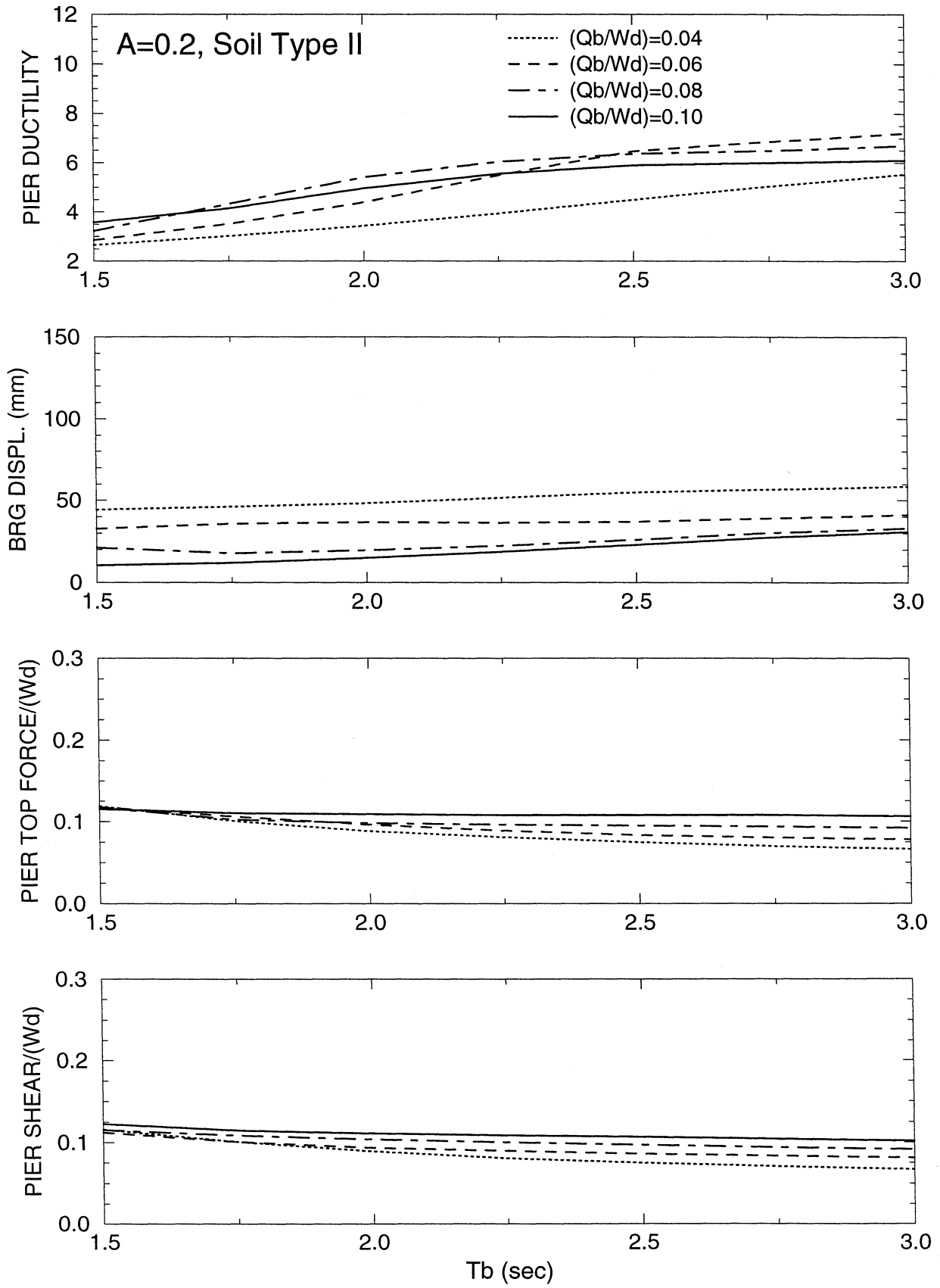
$W_d/W_p=5, T_p=0.25 \text{ s}, R_\mu=1.0, \alpha=0.05$

BILINEAR HYSTERETIC PIER, LINEAR ELASTIC/VISCOUS ISOLATION SYSTEM



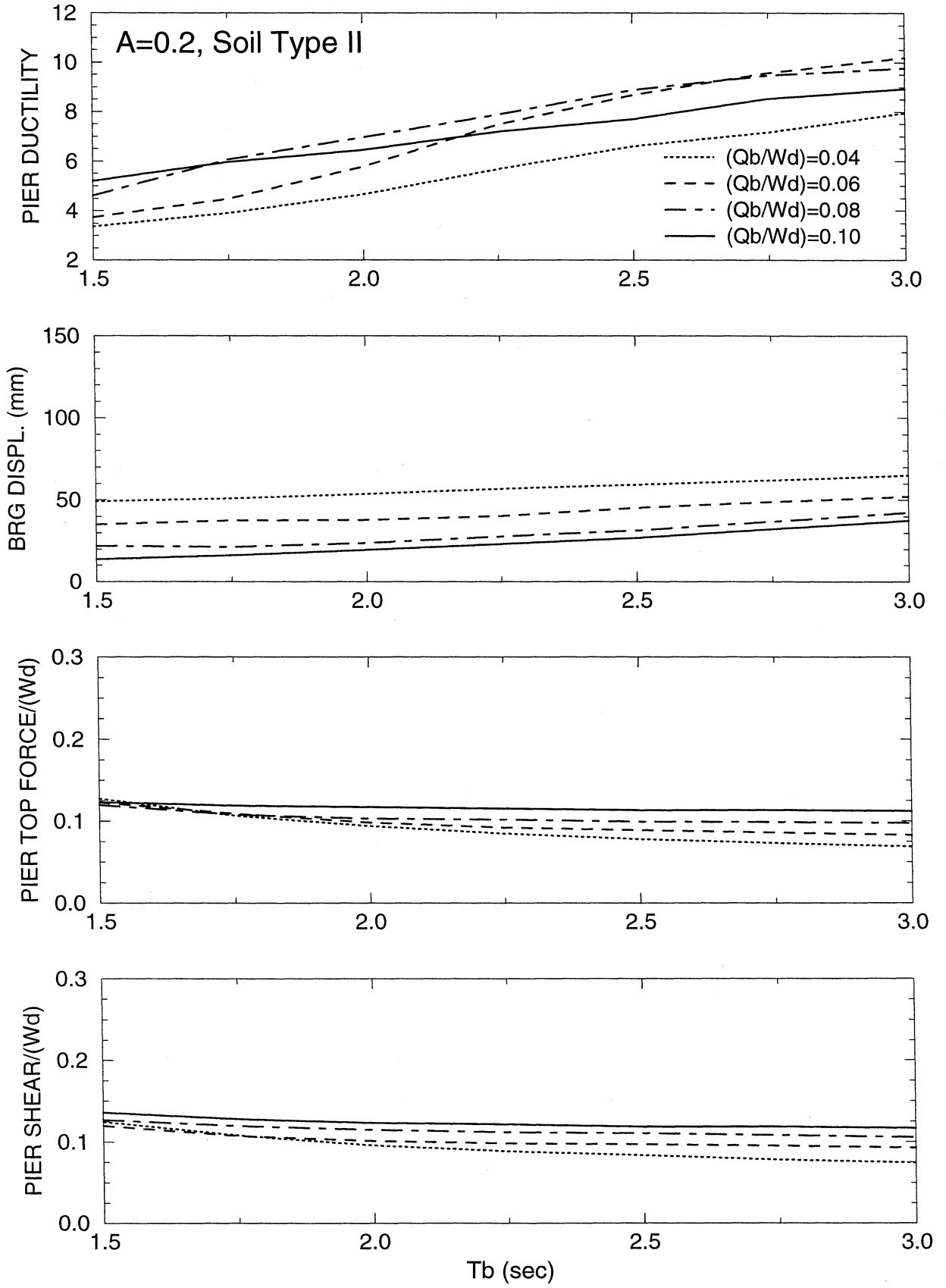
$W_d/W_p=10$, $T_p=0.25$ s, $R_{\mu}=1.5$, $\alpha=0.05$

BILINEAR HYSTERETIC PIER, BILINEAR HYSTERETIC ISOLATION SYSTEM

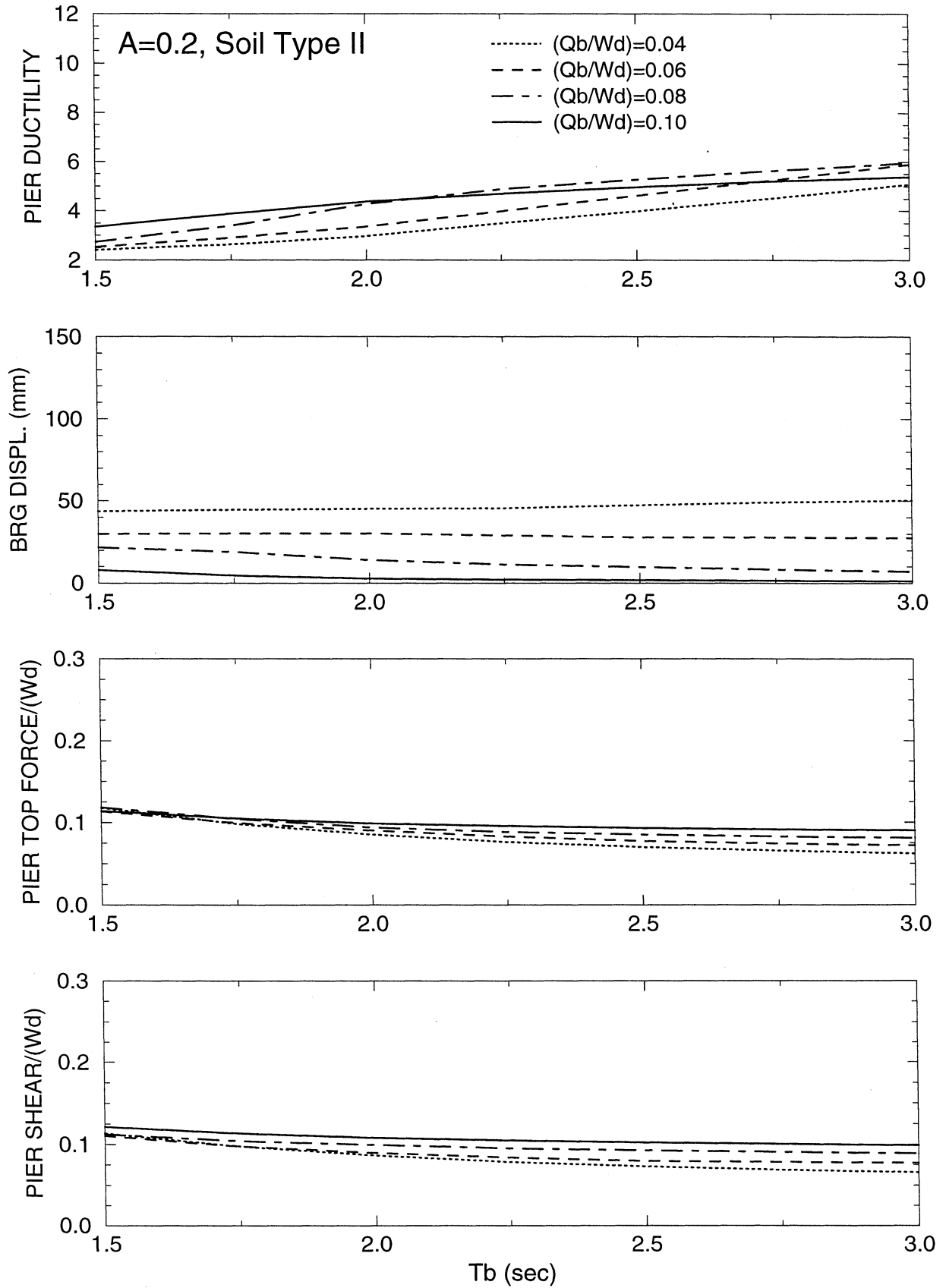


$W_d/W_p=5$, $T_p=0.25$ s, $R_{\mu}=1.5$, $\alpha=0.05$

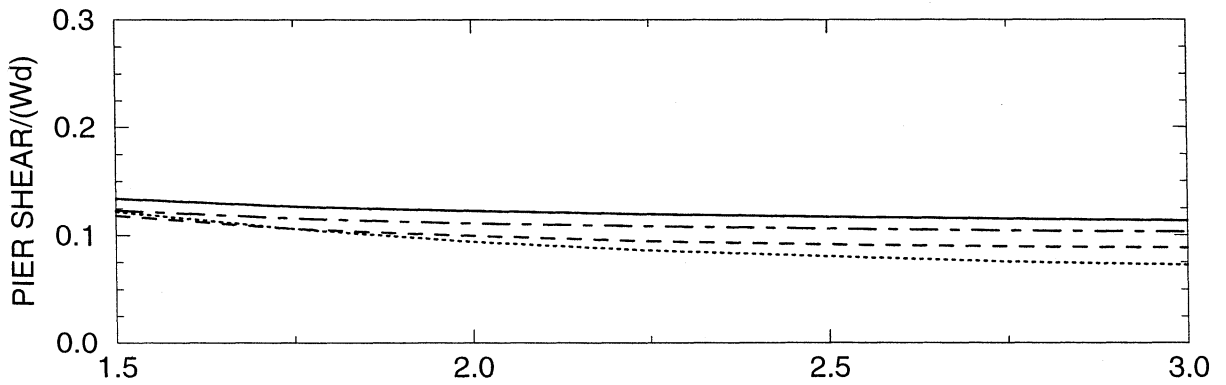
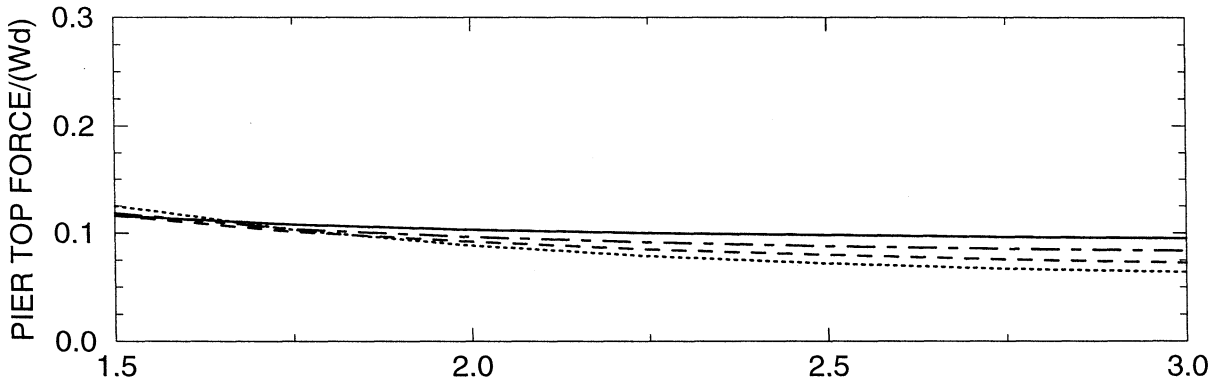
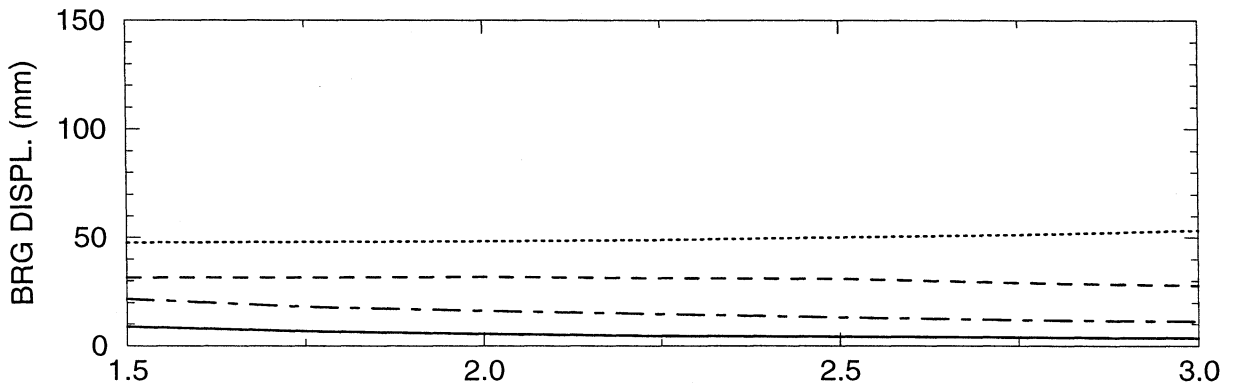
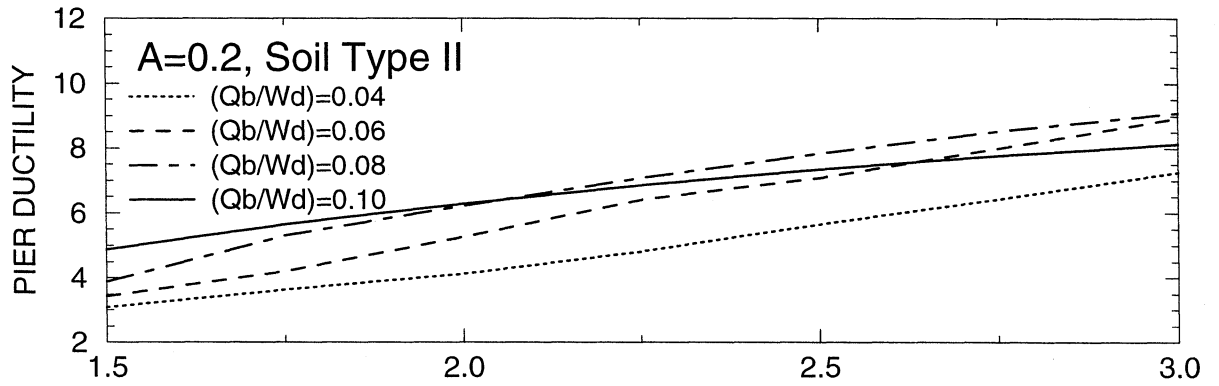
BILINEAR HYSTERETIC PIER, BILINEAR HYSTERETIC ISOLATION SYSTEM



$W_d/W_p=10, T_p=0.25 \text{ s}, R_\mu=1.5, \alpha=0.05$
BILINEAR HYSTERETIC PIER, SLIDING ISOLATION SYSTEM



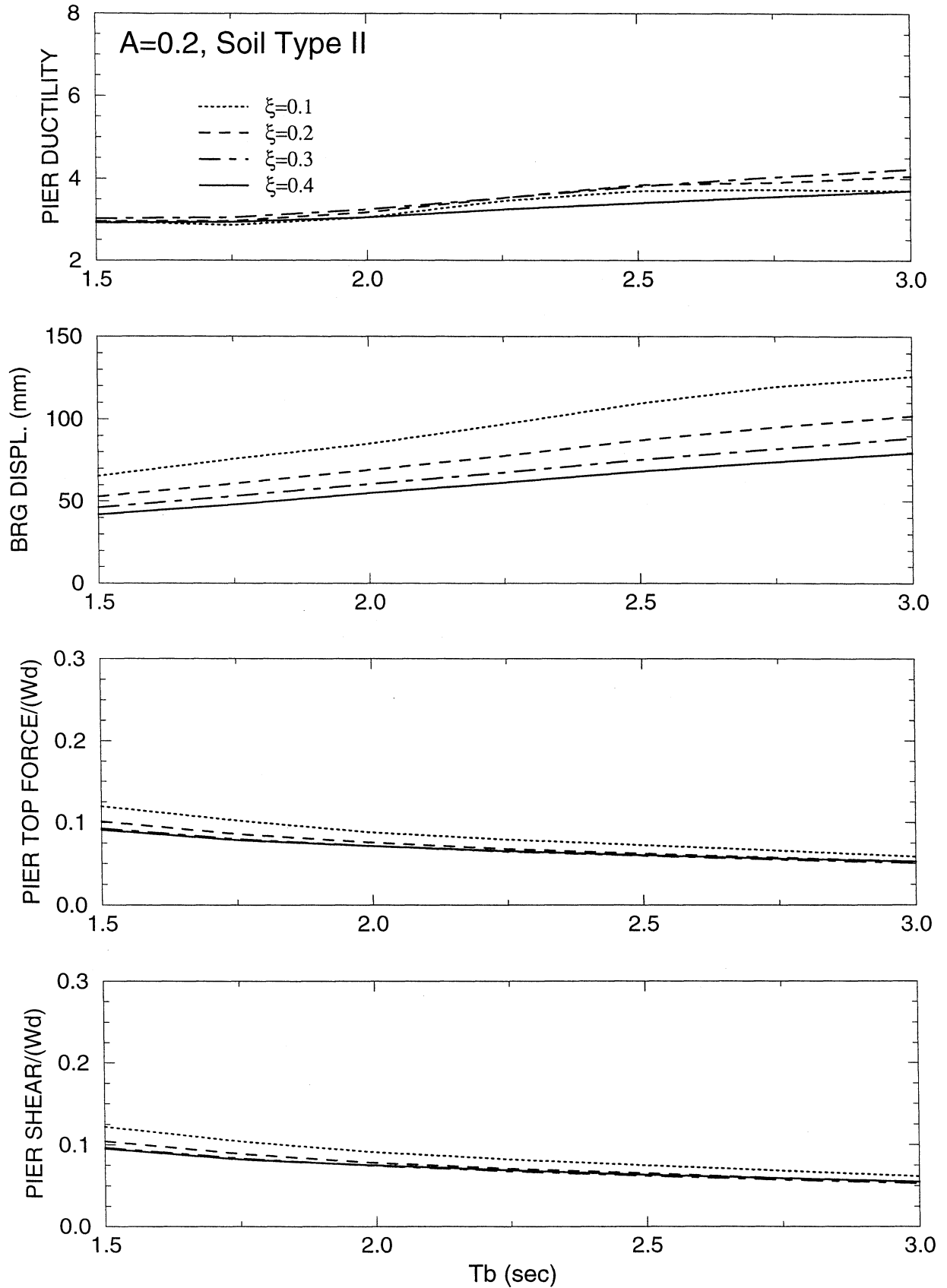
$W_d/W_p=5, T_p=0.25 \text{ s}, R_\mu=1.5, \alpha=0.05$
 BILINEAR HYSTERETIC PIER, SLIDING ISOLATION SYSTEM



T_b (sec)

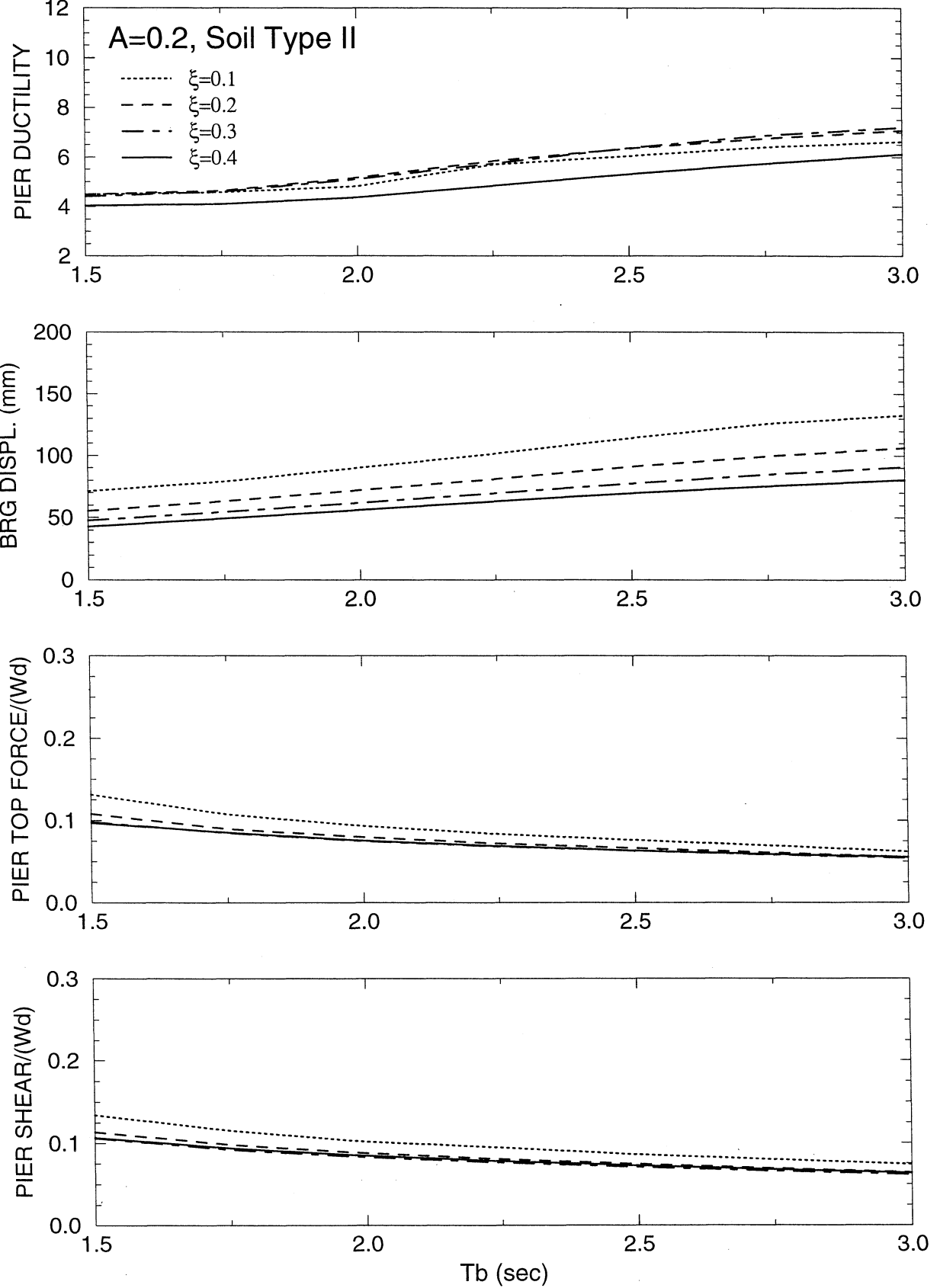
$W_d/W_p=10, T_p=0.25 \text{ s}, R_\mu=1.5, \alpha=0.05$

BILINEAR HYSTERETIC PIER, LINEAR ELASTIC/VISCOUS ISOLATION SYSTEM



$W_d/W_p=5, T_p=0.25 \text{ s}, R_{\mu}=1.5, \alpha=0.05$

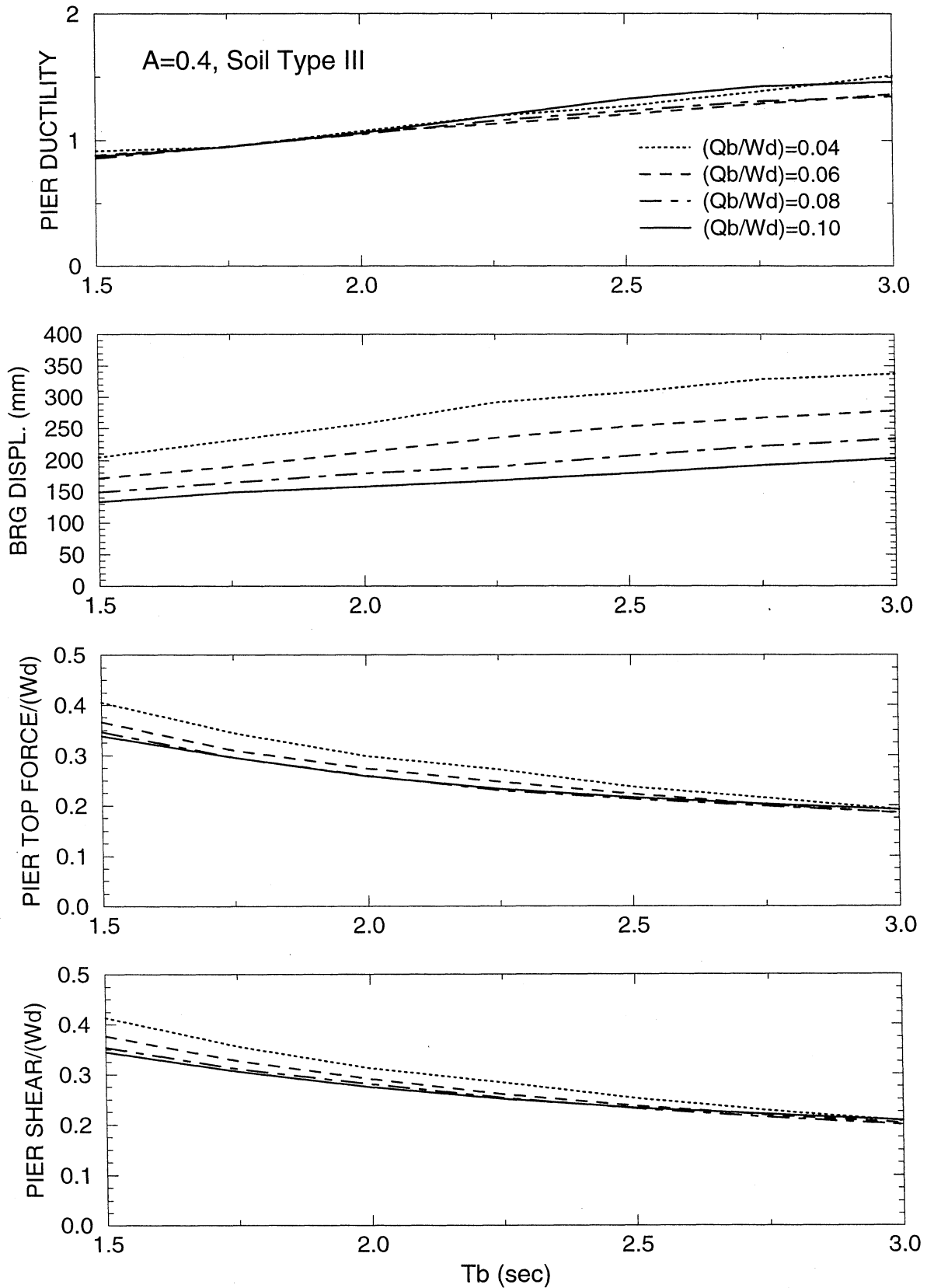
BILINEAR HYSTERETIC PIER, LINEAR ELASTIC/VISCOUS ISOLATION SYSTEM



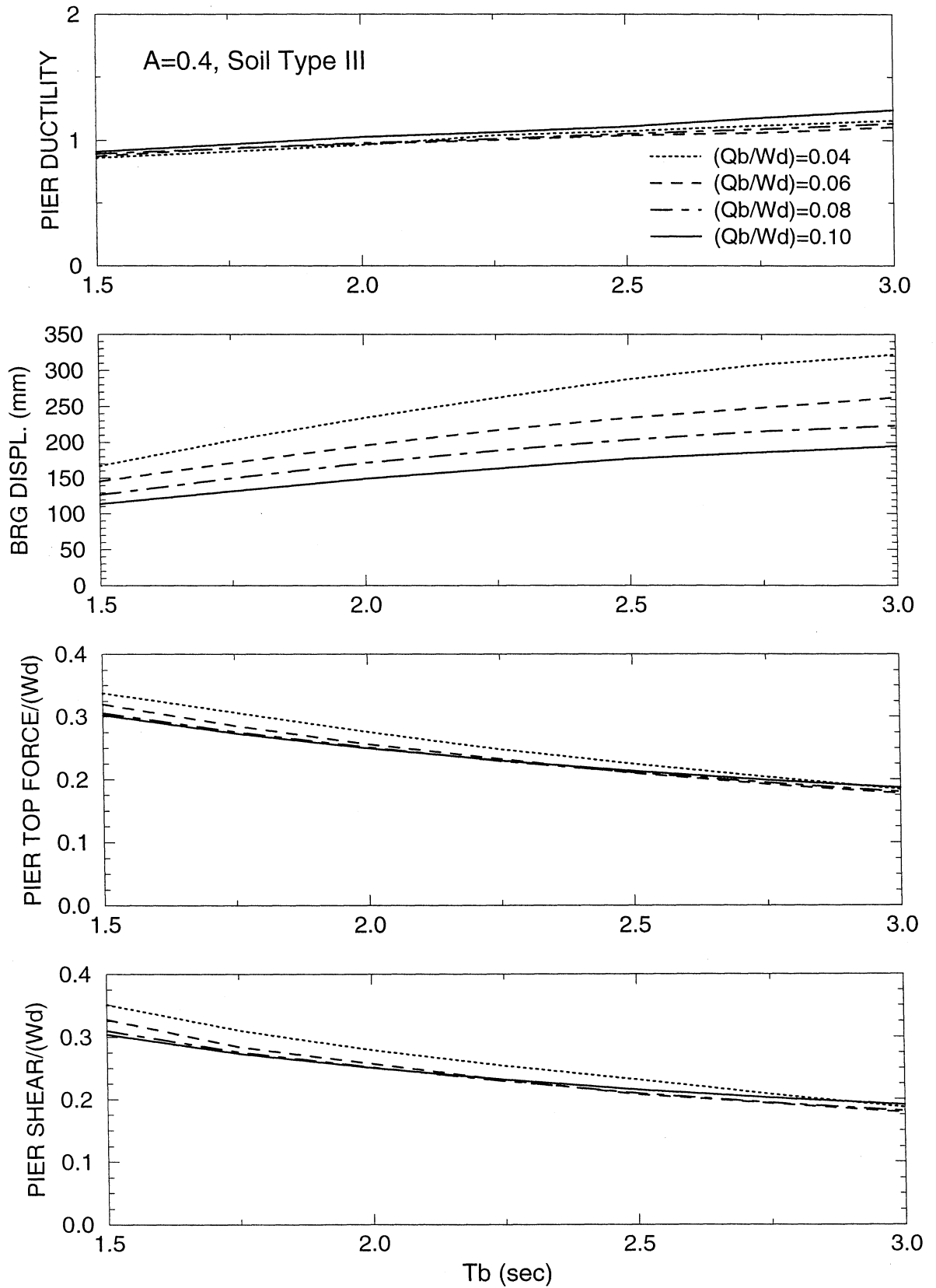
APPENDIX I

**RESULTS OF NONLINEAR DYNAMIC ANALYSIS OF SEISMIC-ISOLATED
BRIDGE WITH PERFECT BILINEAR HYSTERETIC PIER
AND BILINEAR HYSTERETIC ISOLATION SYSTEM
FOR AASHTO, A=0.4, SOIL PROFILE TYPE III INPUT**

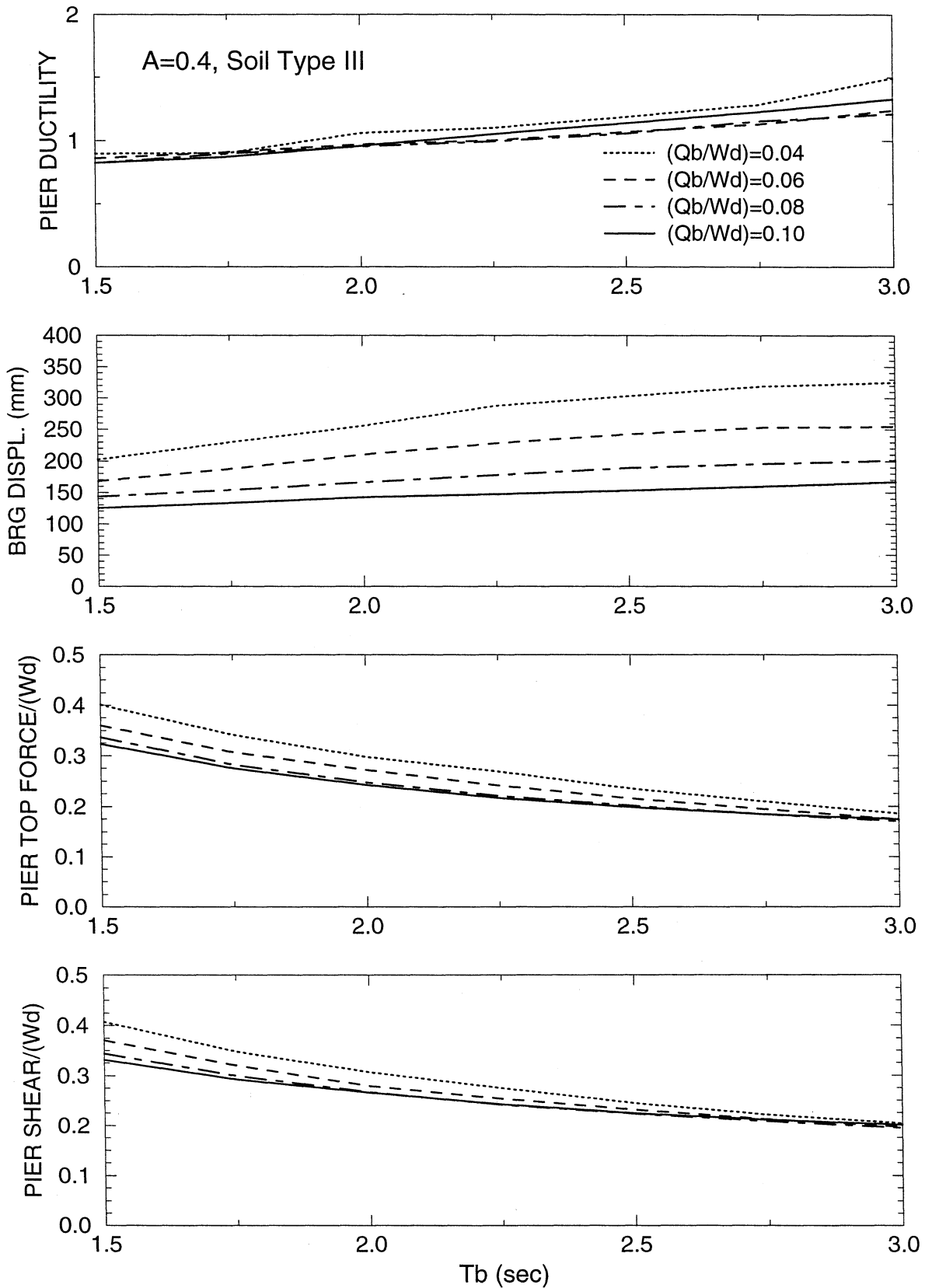
$W_d/W_p=10, T_p=0.25 \text{ s}, R_{\mu}=1.0, \alpha=0.05$
 BILINEAR HYSTERETIC PIER, BILINEAR HYSTERETIC ISOLATION SYSTEM



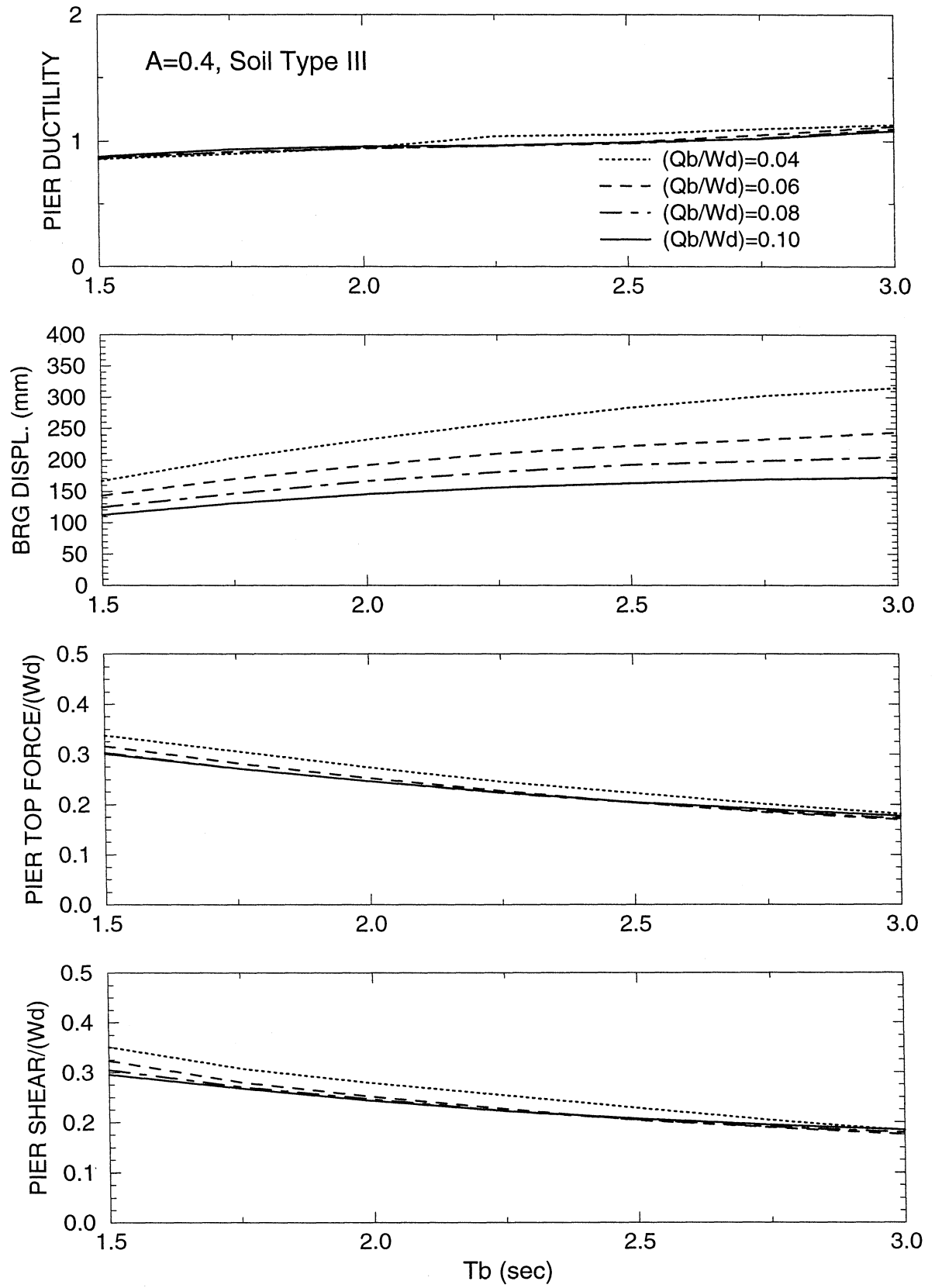
$W_d/W_p=10, T_p=0.5 \text{ s}, R_{\mu}=1.0, \alpha=0.05$
 BILINEAR HYSTERETIC PIER, BILINEAR HYSTERETIC ISOLATION SYSTEM



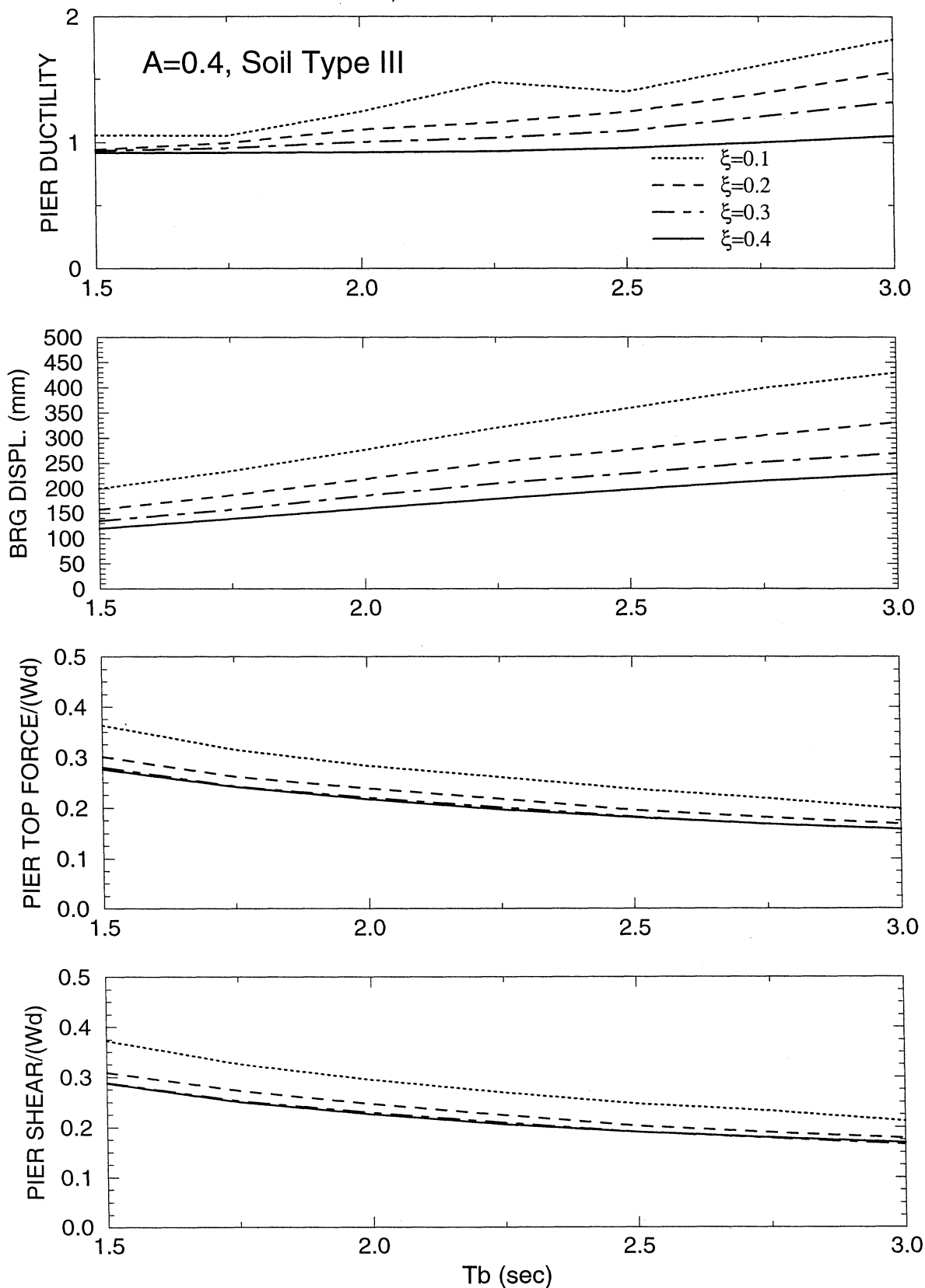
$W_d/W_p=10, T_p=0.25 \text{ s}, R_\mu=1.0, \alpha=0.05$
 BILINEAR HYSTERETIC PIER, SLIDING ISOLATION SYSTEM



$W_d/W_p=10, T_p=0.5 \text{ s}, R_{\mu}=1.0, \alpha=0.05$
 BILINEAR HYSTERETIC PIER, SLIDING ISOLATION SYSTEM



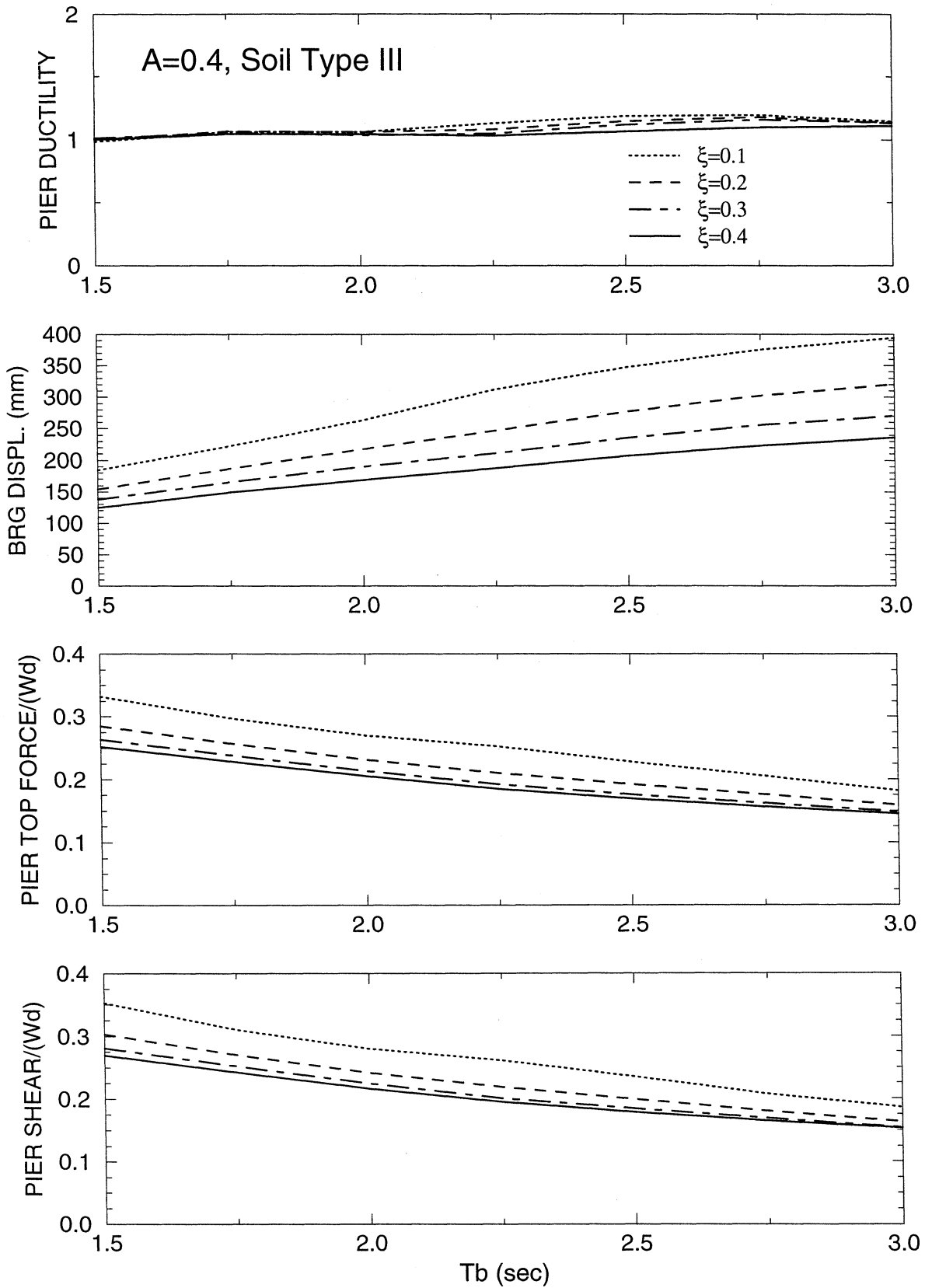
$W_d/W_p=10, T_p=0.25 \text{ s}, R_\mu=1.0, \alpha=0.05$
 BILINEAR HYSTERETIC PIER, LINEAR ELASTIC/VISCOUS ISOLATION SYSTEM



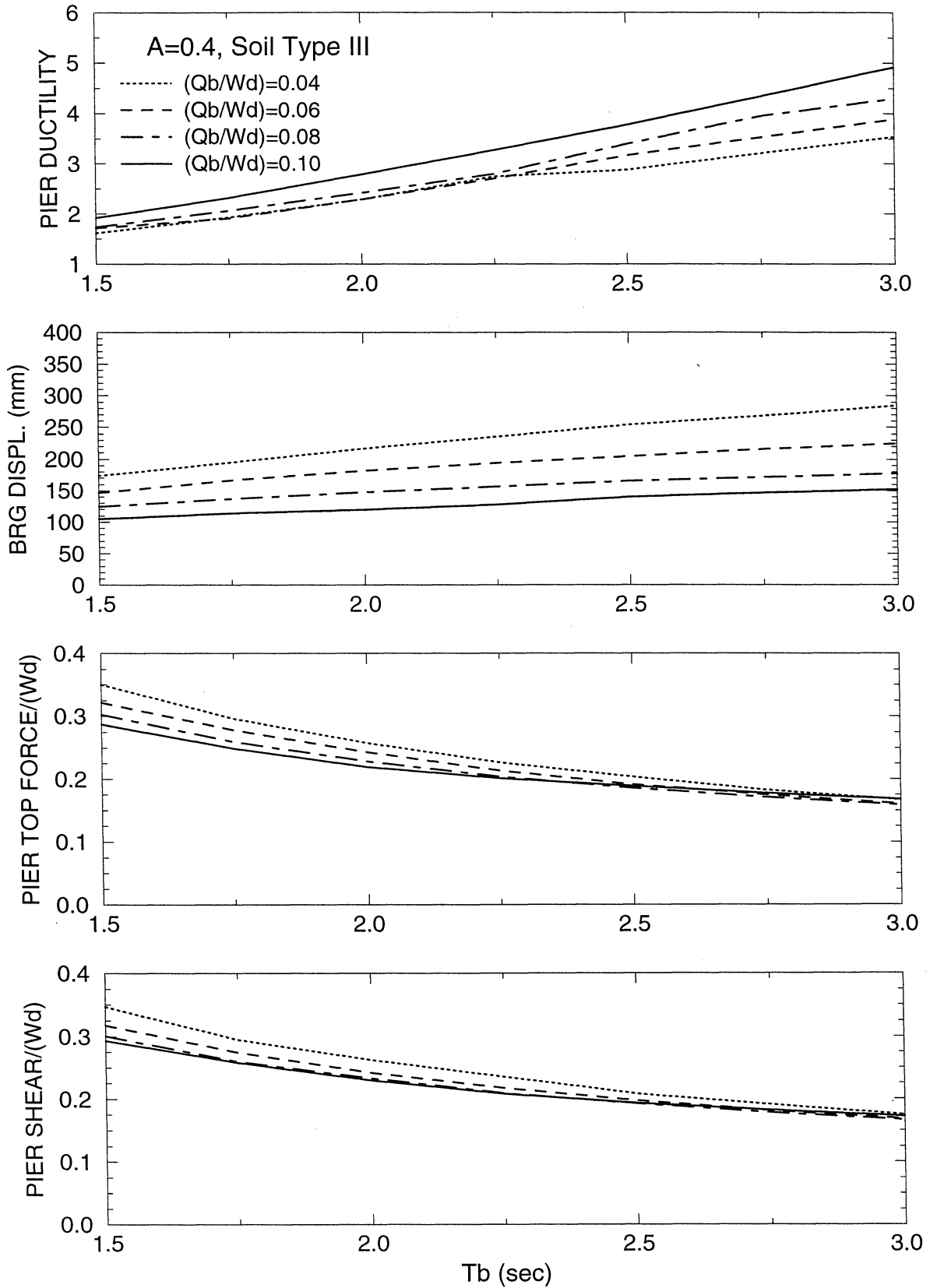
$W_d/W_p=10, T_p=0.5 \text{ s}, R_\mu=1.0, \alpha=0.05$

BILINEAR HYSTERETIC PIER, LINEAR ELASTIC/VISCOUS ISOLATION SYSTEM

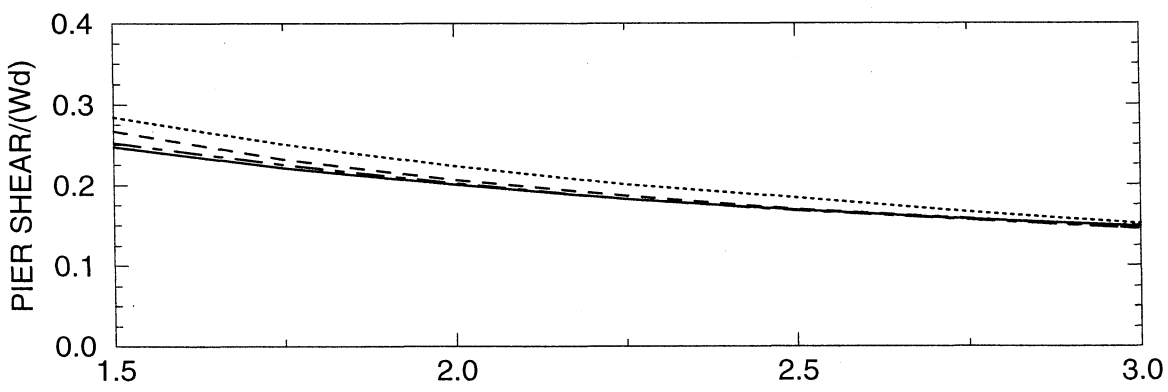
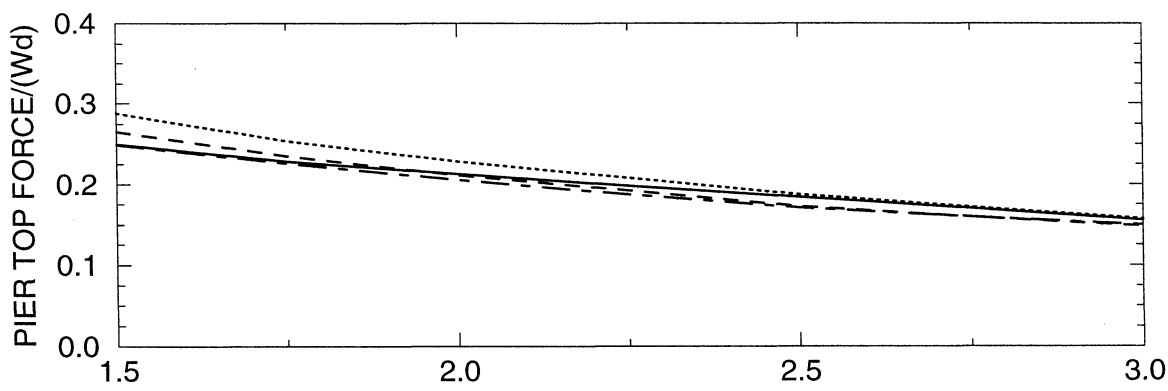
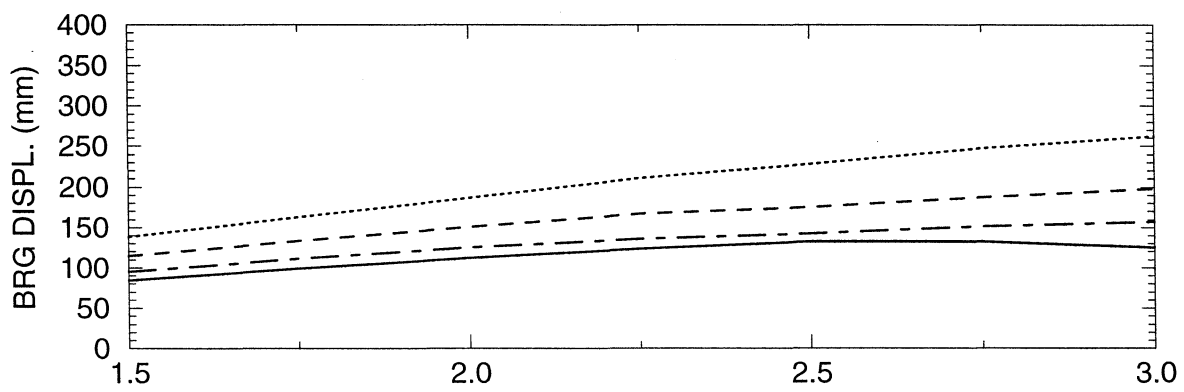
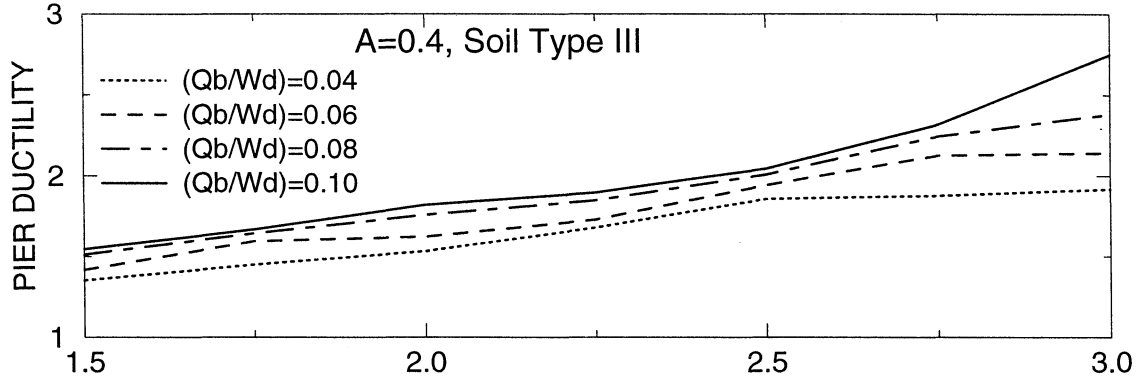
$A=0.4, \text{ Soil Type III}$



$W_d/W_p=10, T_p=0.25 \text{ s}, R_\mu=1.5, \alpha=0.05$
 BILINEAR HYSTERETIC PIER, BILINEAR HYSTERETIC ISOLATION SYSTEM

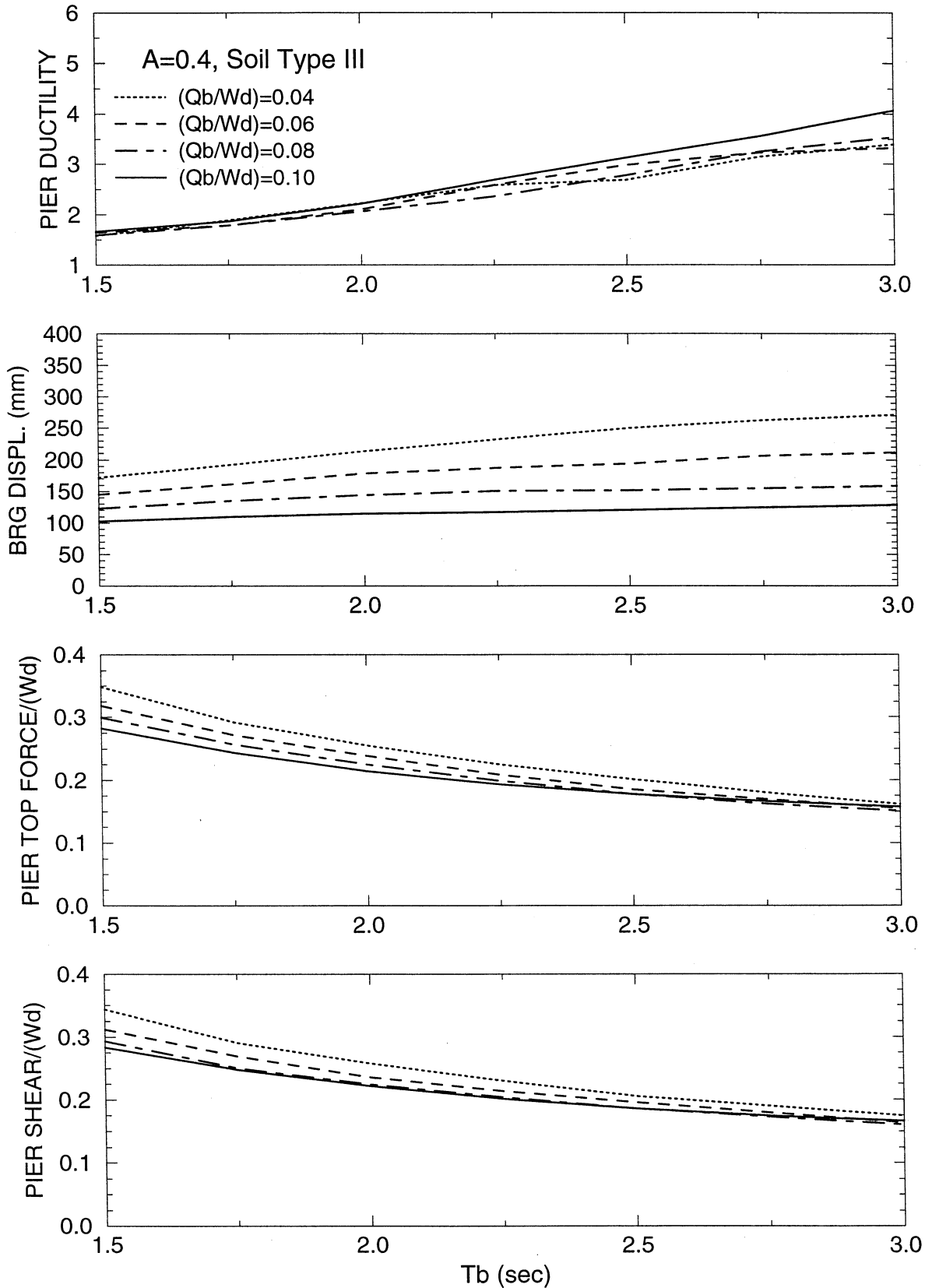


$W_d/W_p=10, T_p=0.5 \text{ s}, R_\mu=1.5, \alpha=0.05$
 BILINEAR HYSTERETIC PIER, BILINEAR HYSTERETIC ISOLATION SYSTEM

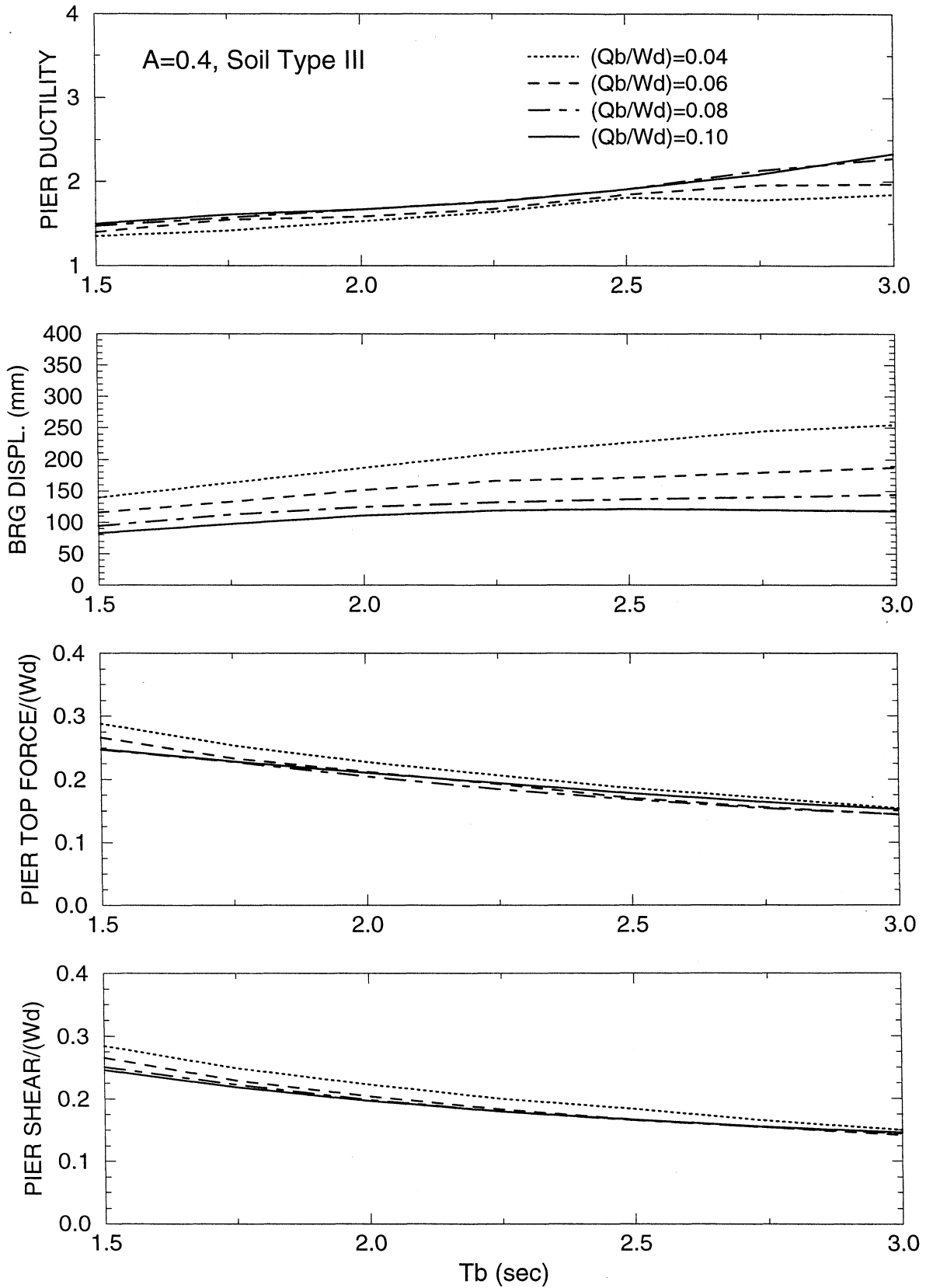


Tb (sec)

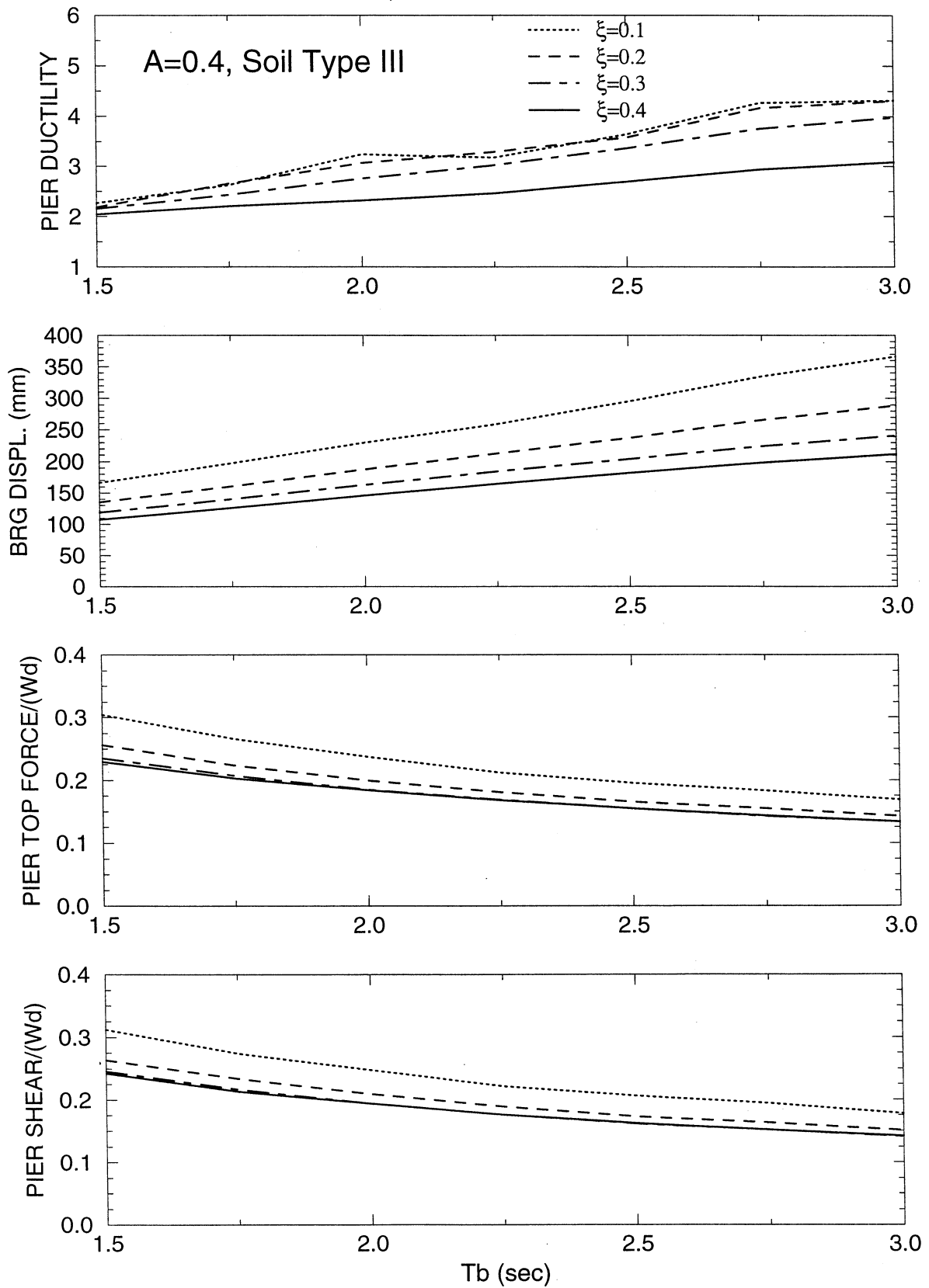
$W_d/W_p=10, T_p=0.25 \text{ s}, R_\mu=1.5, \alpha=0.05$
 BILINEAR HYSTERETIC PIER, SLIDING ISOLATION SYSTEM



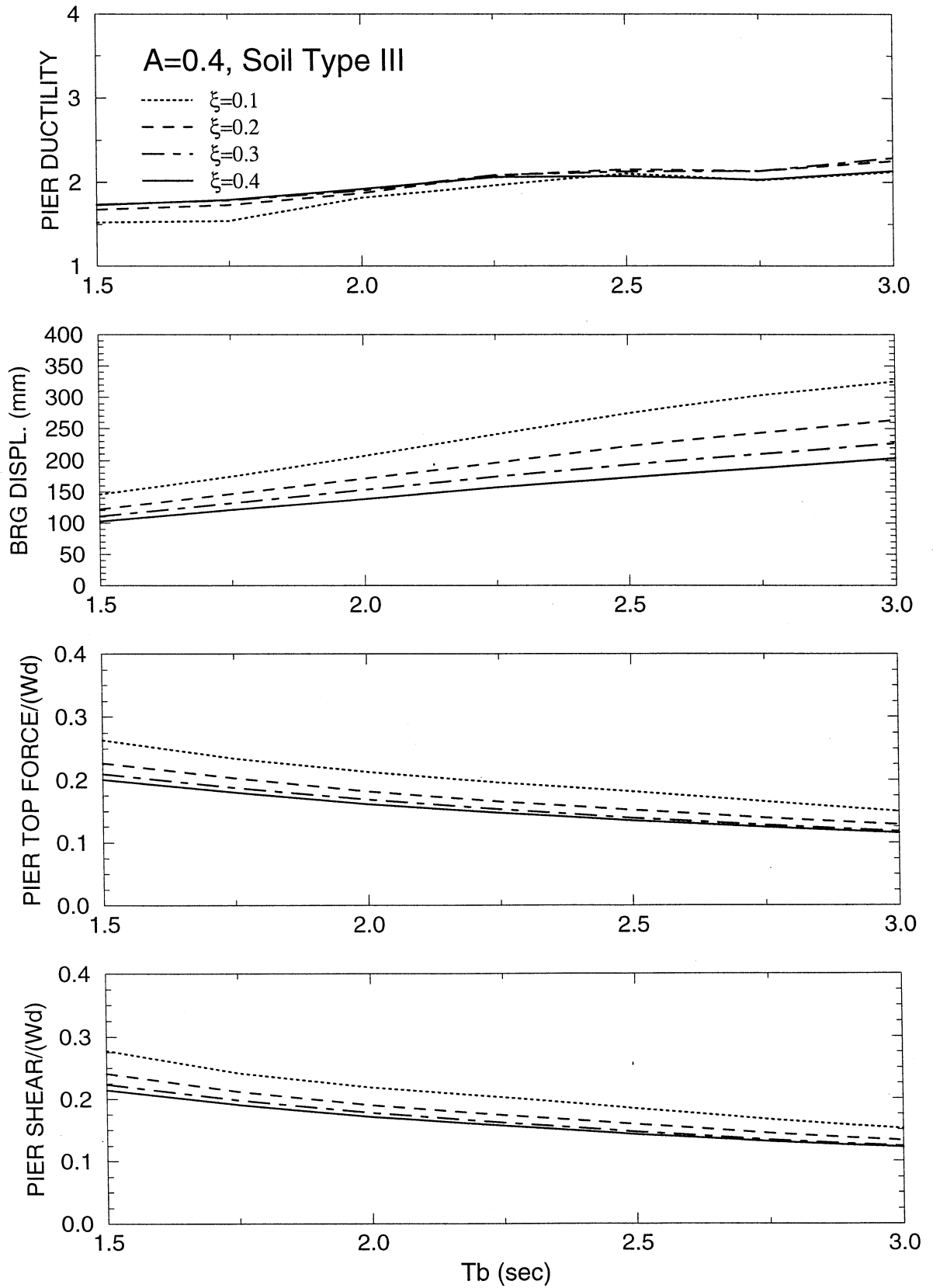
$W_d/W_p=10, T_p=0.5 \text{ s}, R_{\mu}=1.5, \alpha=0.05$
 BILINEAR HYSTERETIC PIER, SLIDING ISOLATION SYSTEM



$W_d/W_p=10, T_p=0.25 \text{ s}, R_\mu=1.5, \alpha=0.05$
 BILINEAR HYSTERETIC PIER, LINEAR ELASTIC/VISCOUS ISOLATION SYSTEM



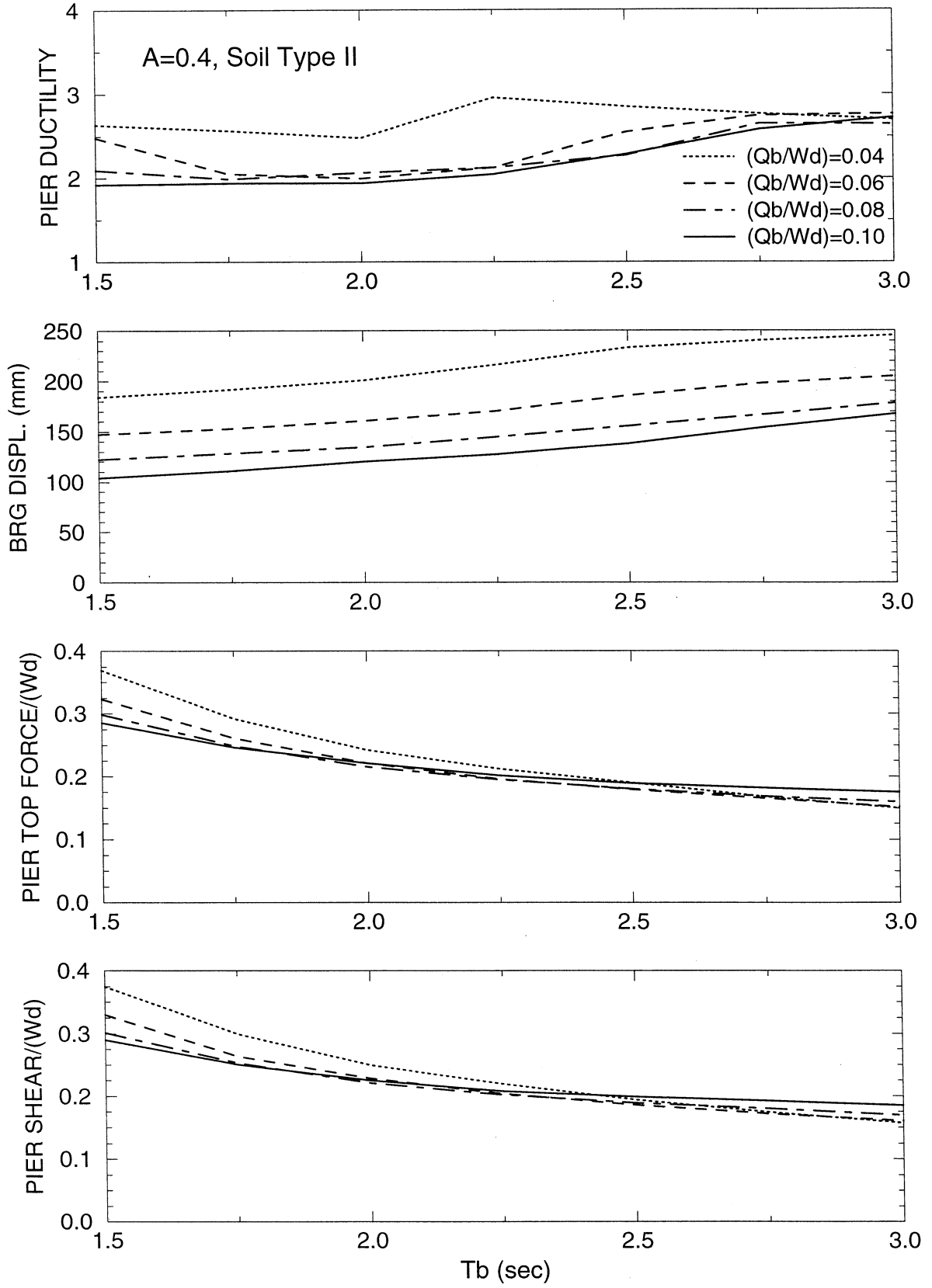
$W_d/W_p=10, T_p=0.5 \text{ s}, R_\mu=1.5, \alpha=0.05$
 BILINEAR HYSTERETIC PIER, LINEAR ELASTIC/VISCOUS ISOLATION SYSTEM



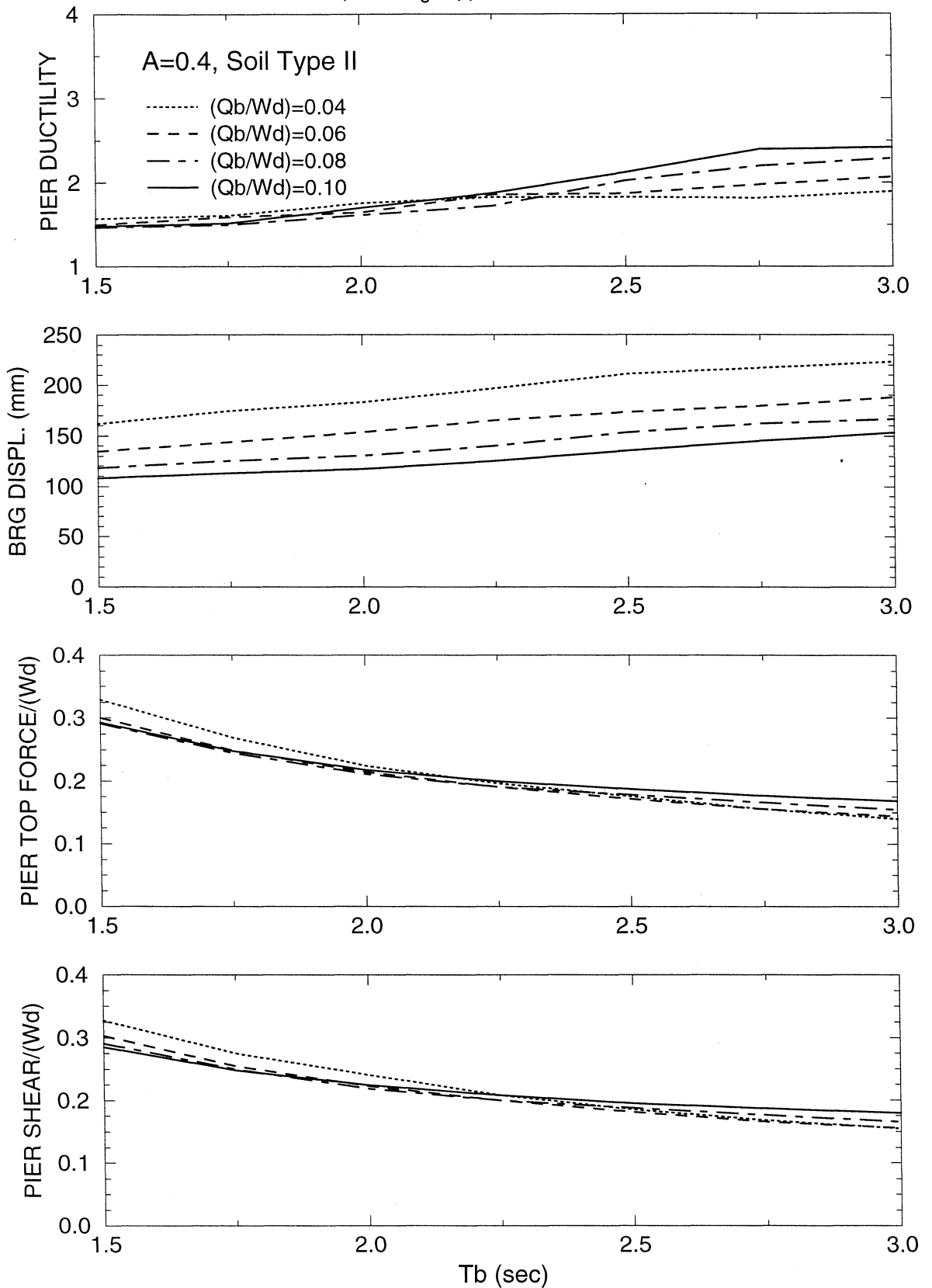
APPENDIX J

**RESULTS OF NONLINEAR DYNAMIC ANALYSIS OF SEISMIC-ISOLATED
BRIDGE WITH PINCHED HYSTERETIC PIER AND
BILINEAR HYSTERETIC ISOLATION SYSTEM FOR
AASHTO, A=0.4, SOIL PROFILE TYPE II INPUT**

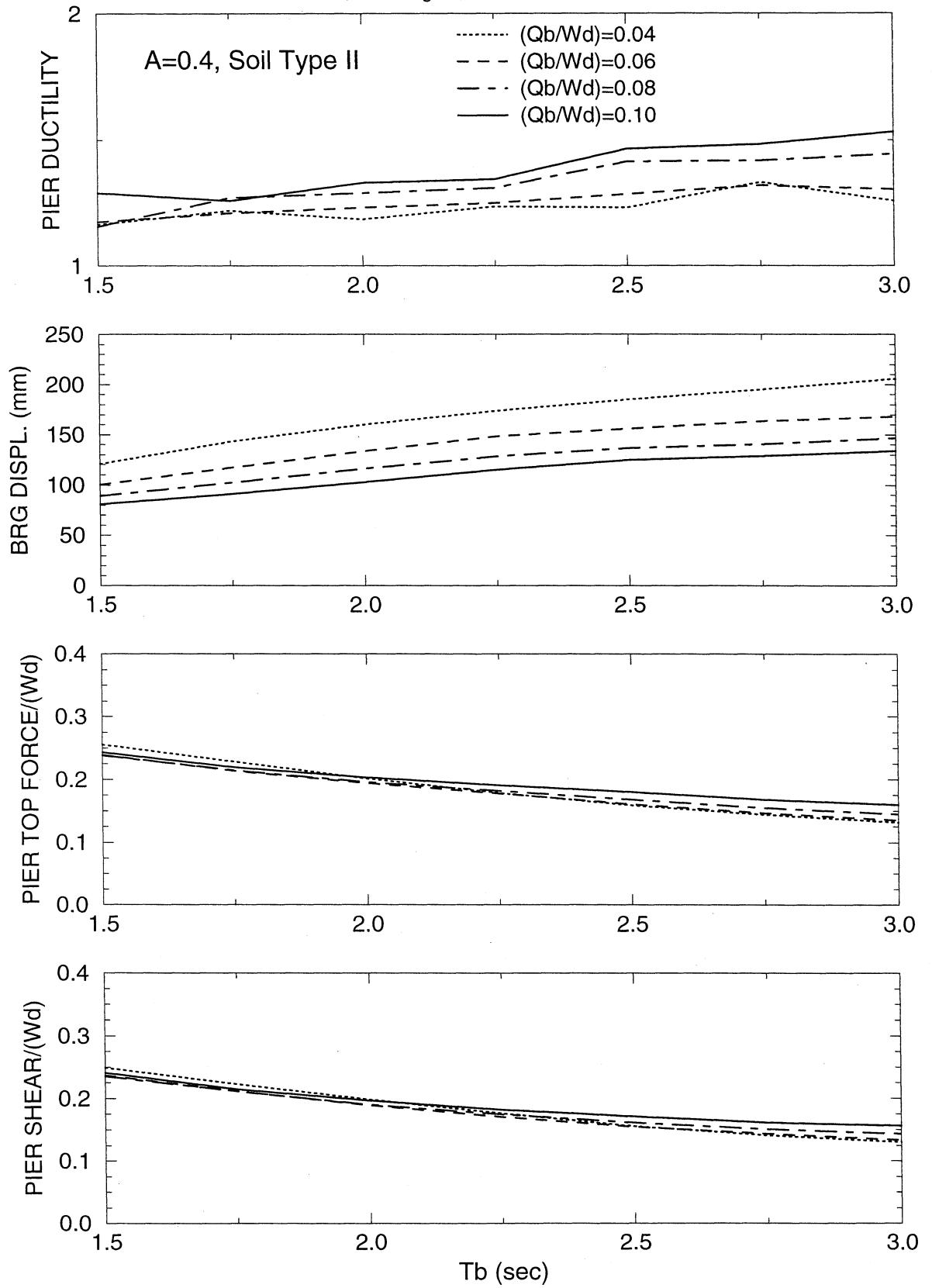
Wd/Wp=10, Tp=0.1 s, R_μ=1.0, α=0.05
 PINCHED HYST. PIER (σ=0.2, a_g=Yp), BILINEAR HYST. ISOLATION SYSTEM



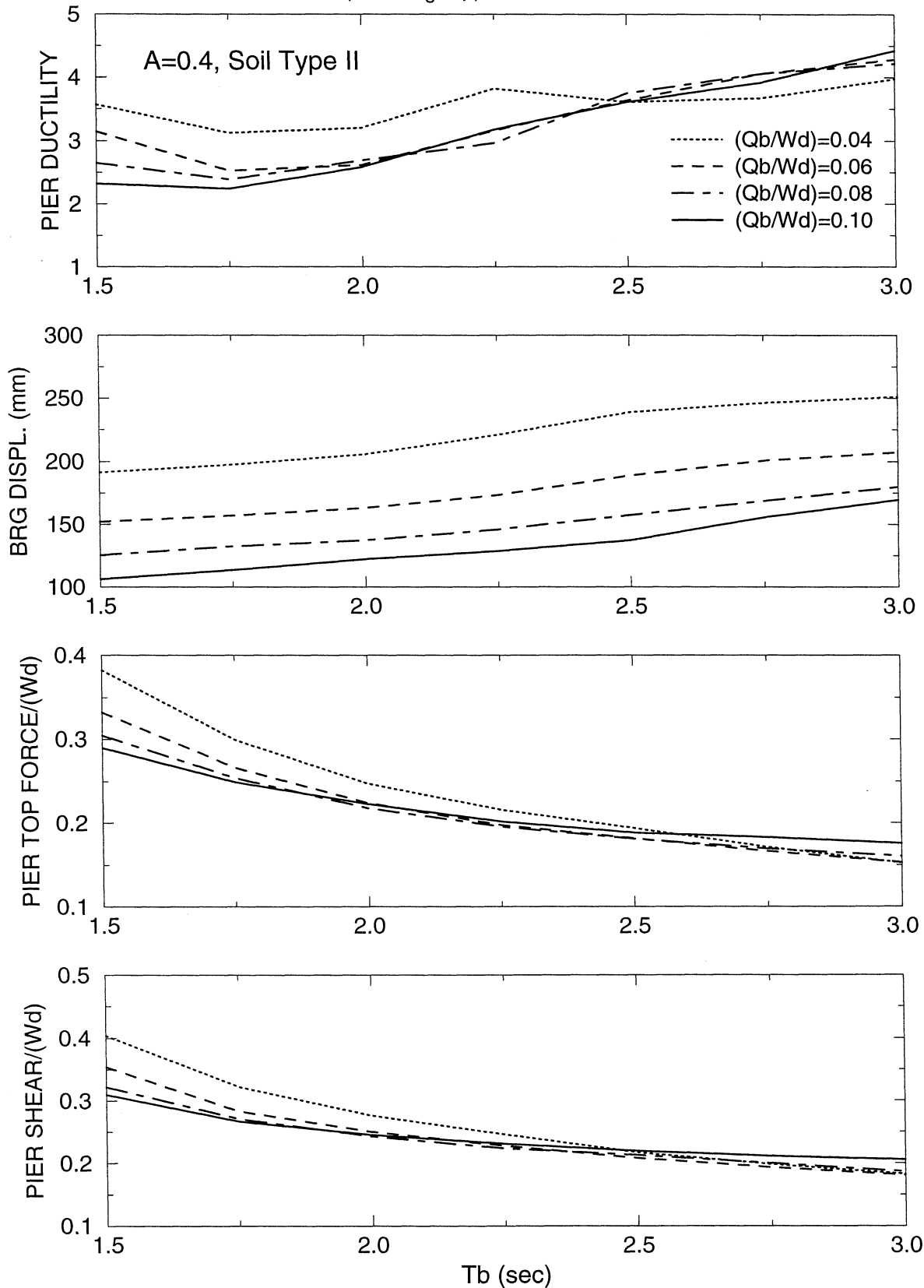
$W_d/W_p=10, T_p=0.25 \text{ s}, R_\mu=1.0, \alpha=0.05$
 PINCHED HYST. PIER ($\sigma=0.2, a_s=Y_p$), BILINEAR HYST. ISOLATION SYSTEM



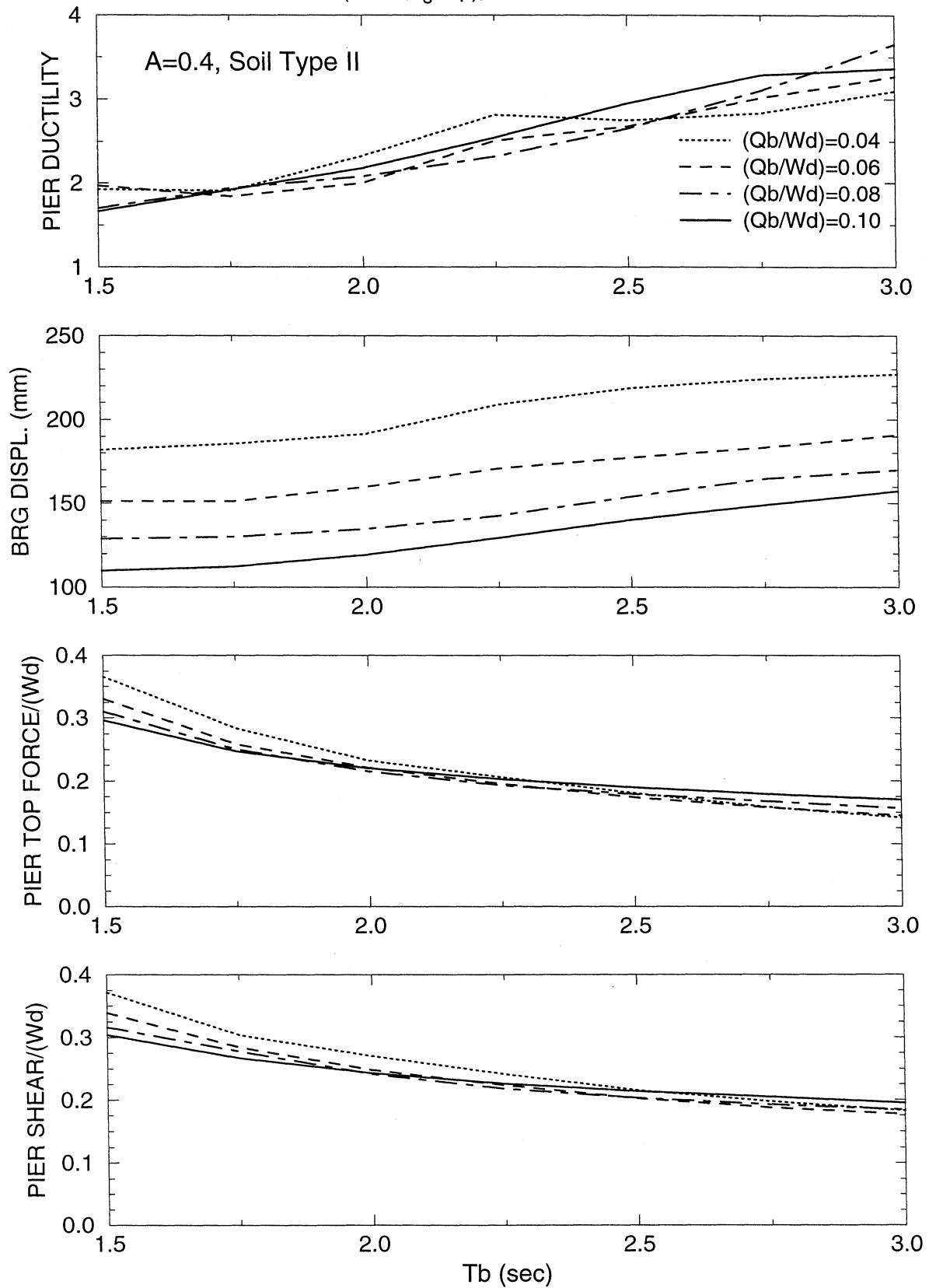
$W_d/W_p=10, T_p=0.5 \text{ s}, R_{\mu}=1.0, \alpha=0.05$
 PINCHED HYST. PIER ($\sigma=0.2, a_s=Y_p$), BILINEAR HYST. ISOLATION SYSTEM



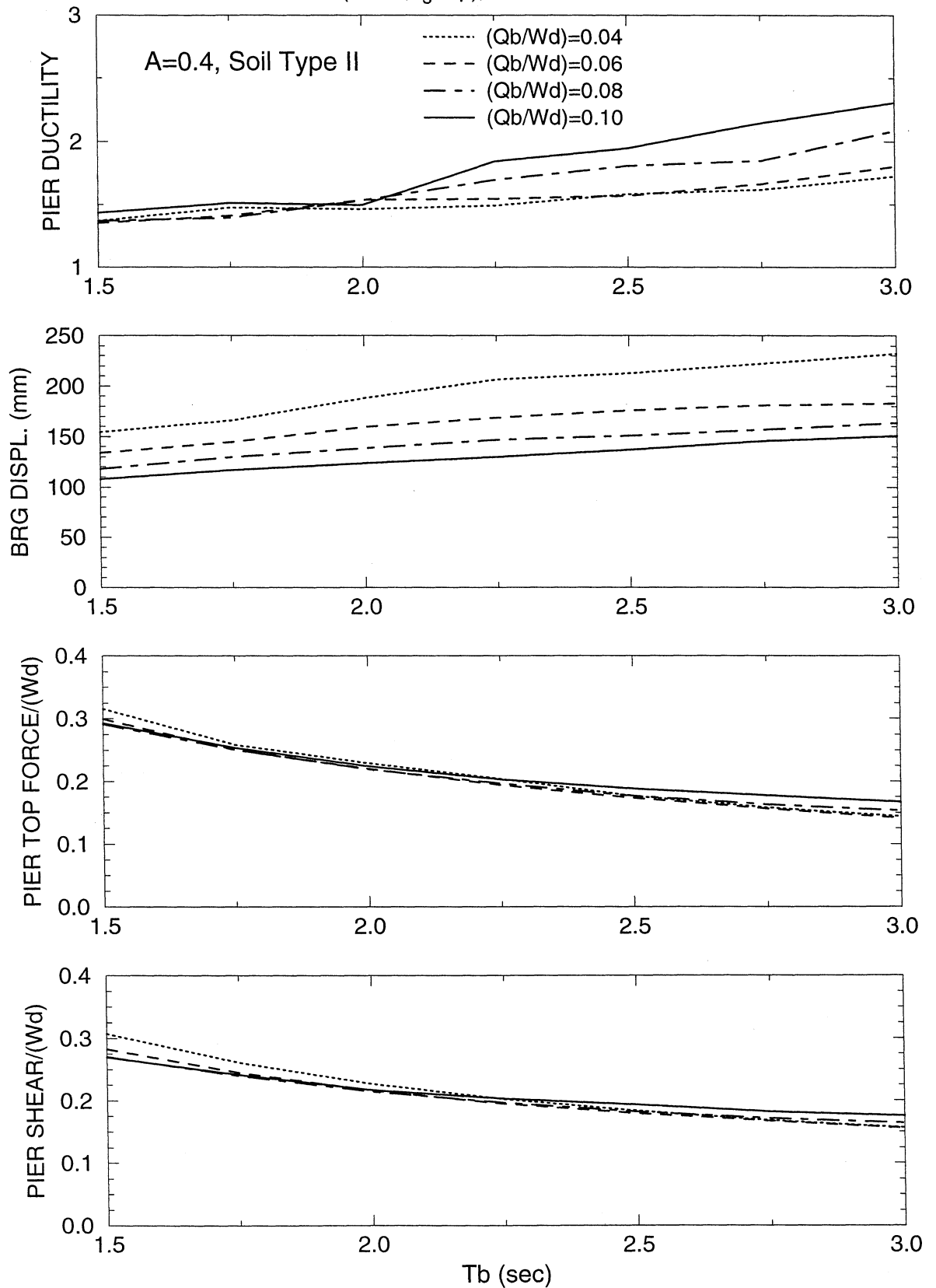
Wd/Wp=5, Tp=0.1 s, $R_{\mu}=1.0$, $\alpha=0.05$
 PINCHED HYST. PIER ($\sigma=0.2, a_s=Y_p$), BILINEAR HYST. ISOLATION SYSTEM



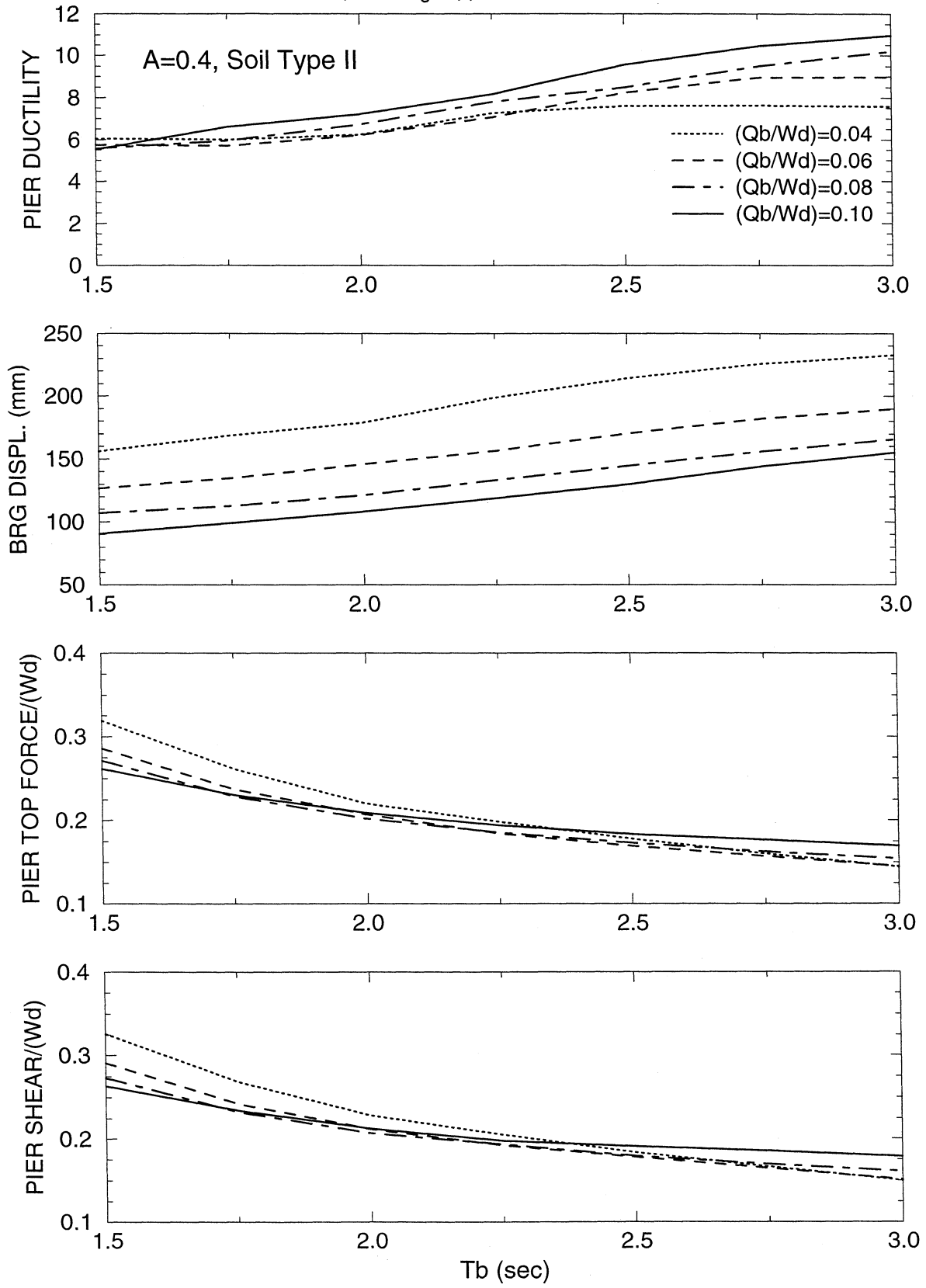
$W_d/W_p=5, T_p=0.25 \text{ s}, R_{\mu}=1.0, \alpha=0.05$
 PINCHED HYST. PIER ($\sigma=0.2, a_s=Y_p$), BILINEAR HYST. ISOLATION SYSTEM



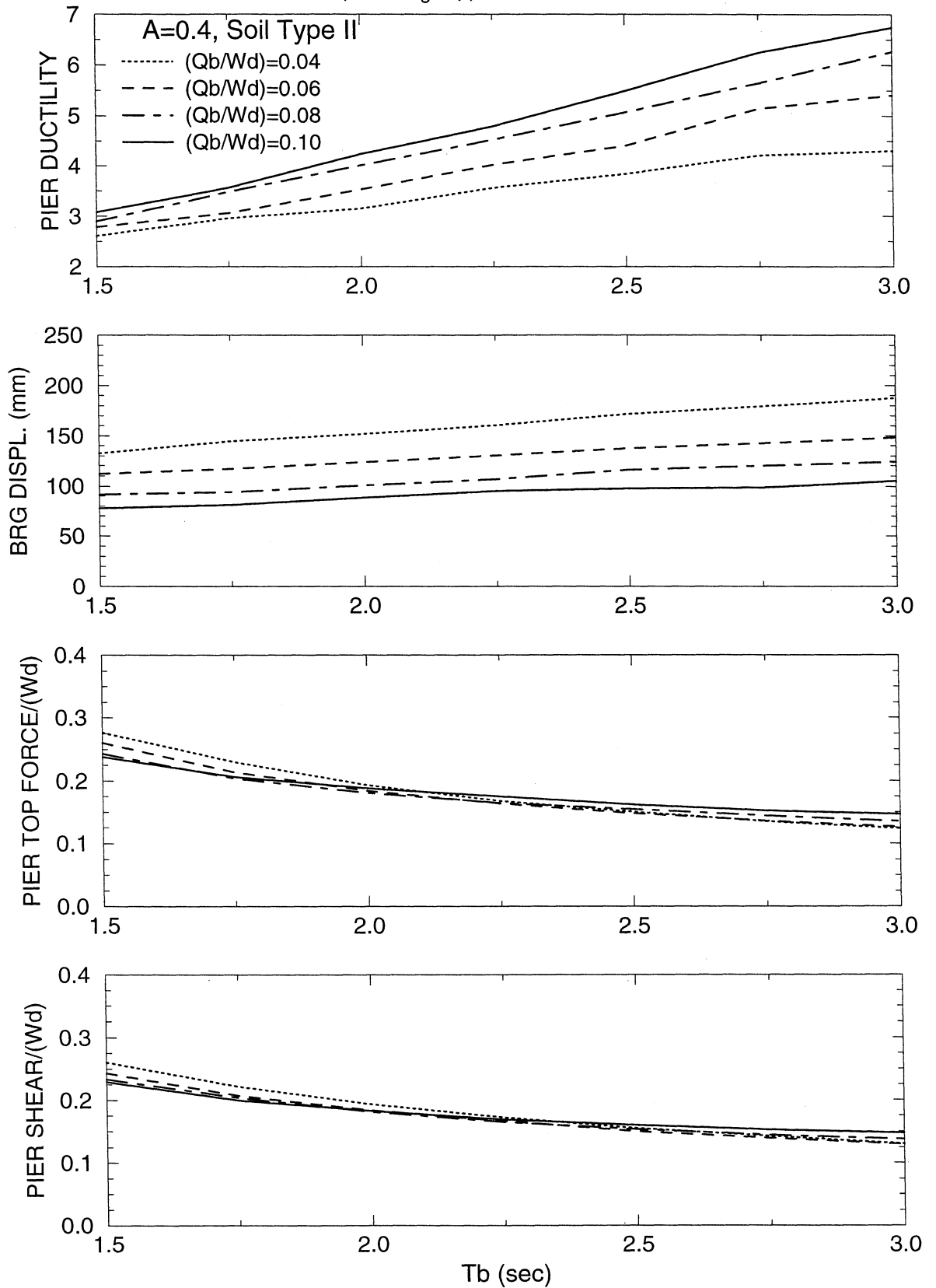
$W_d/W_p=5, T_p=0.5 \text{ s}, R_\mu=1.0, \alpha=0.05$
 PINCHED HYST. PIER ($\sigma=0.2, a_s=Y_p$), BILINEAR HYST. ISOLATION SYSTEM



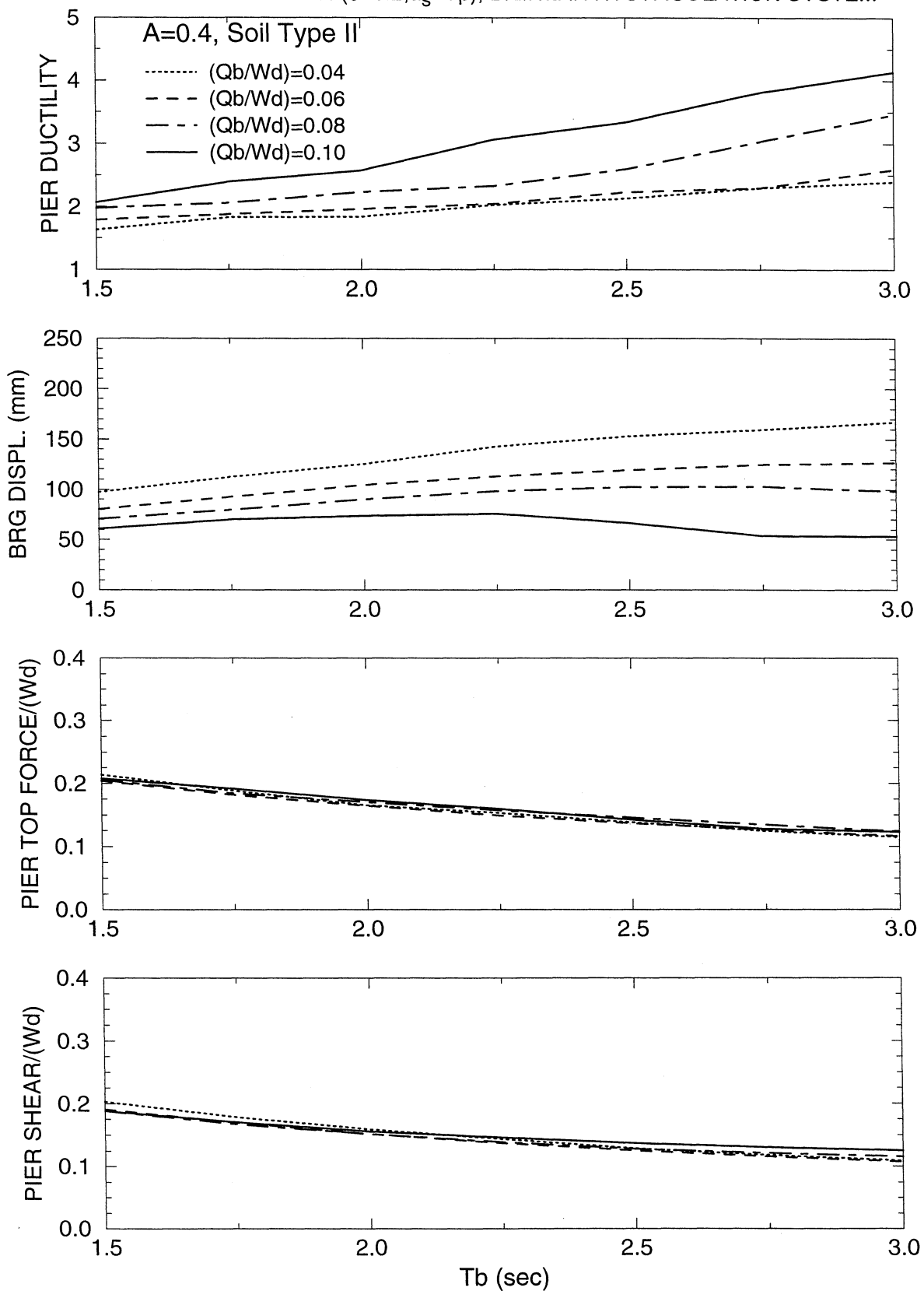
$W_d/W_p=10, T_p=0.1 \text{ s}, R_{\mu}=1.5, \alpha=0.05$
 PINCHED HYST. PIER ($\sigma=0.2, a_s=Y_p$), BILINEAR HYST. ISOLATION SYSTEM



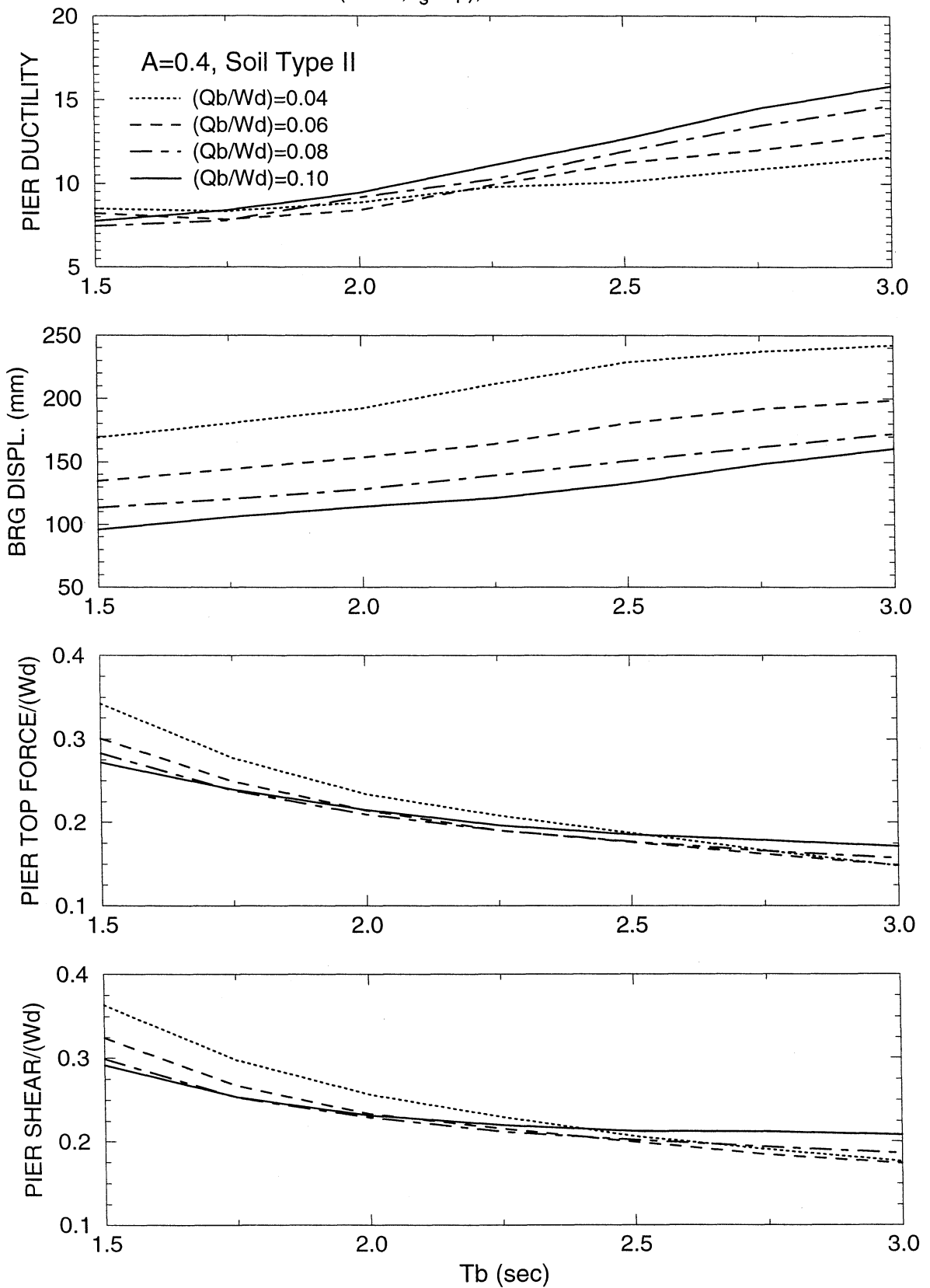
Wd/Wp=10, Tp=0.25 s, R_μ=1.5, α=0.05
 PINCHED HYST. PIER (σ=0.2, a_s=Y_p), BILINEAR HYST. ISOLATION SYSTEM



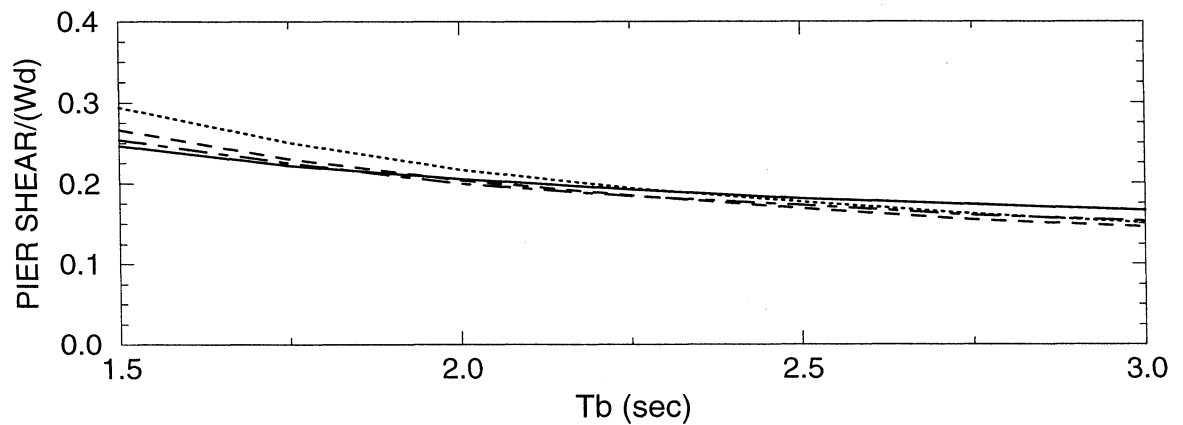
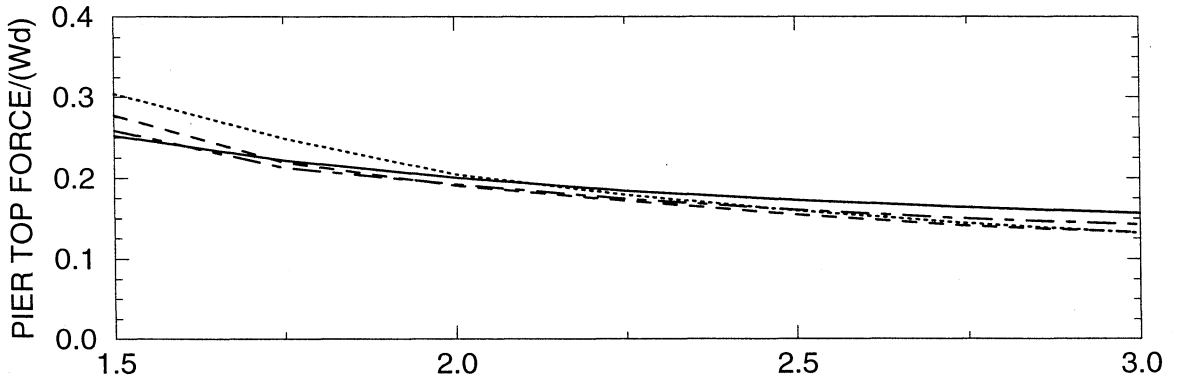
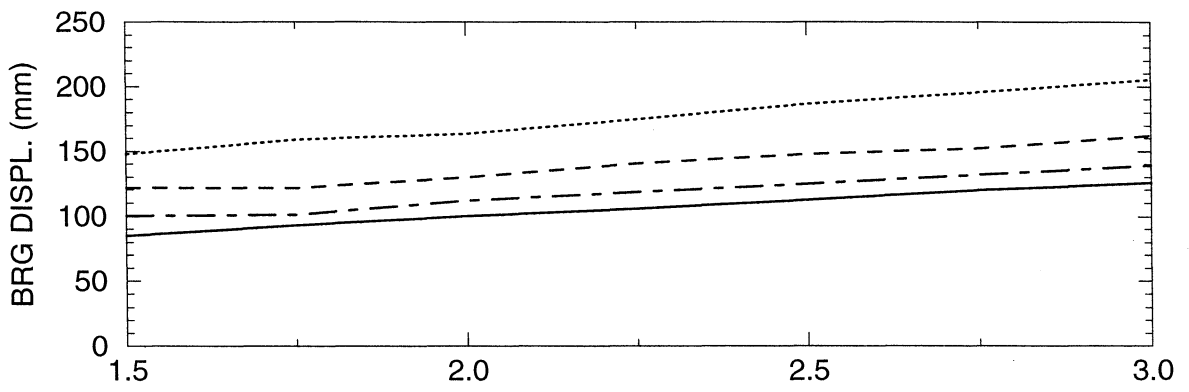
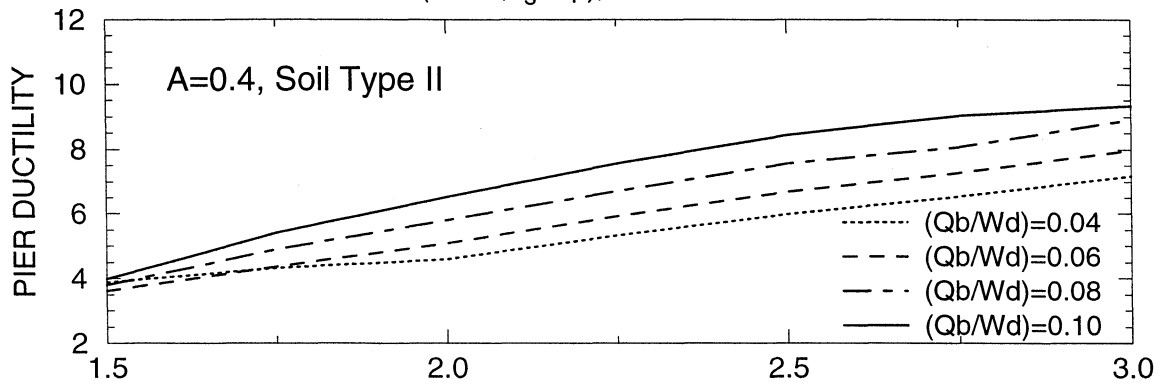
(Wd/Wp)=10, Tp=0.5 s, $R_{\mu}=1.5$, $\alpha=0.05$
 PINCHED HYST. PIER ($\sigma=0.2, a_s=Y_p$), BILINEAR HYST. ISOLATION SYSTEM



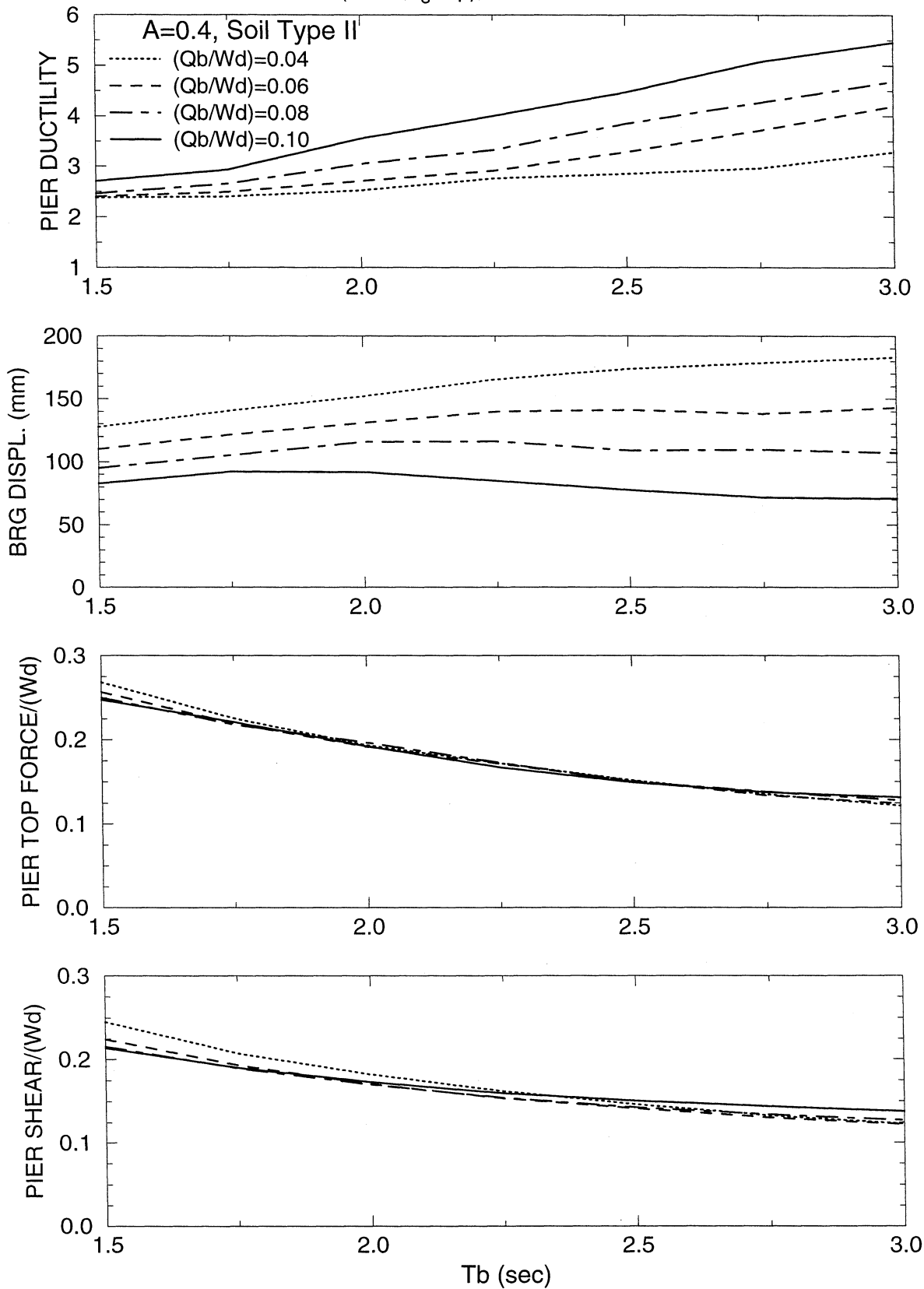
$W_d/W_p=5, T_p=0.1 \text{ s}, R_\mu=1.5, \alpha=0.05$
 PINCHED HYST. PIER ($\sigma=0.2, a_s=Y_p$), BILINEAR HYST. ISOLATION SYSTEM



$W_d/W_p=5, T_p=0.25 \text{ s}, R_{\mu}=1.5, \alpha=0.05$
 PINCHED HYST. PIER ($\sigma=0.2, a_s=Y_p$), BILINEAR HYST. ISOLATION SYSTEM



$W_d/W_p=5, T_p=0.5 \text{ s}, R_{\mu}=1.5, \alpha=0.05$
 PINCHED HYST. PIER ($\sigma=0.2, a_s=Y_p$), BILINEAR HYST. ISOLATION SYSTEM





MULTIDISCIPLINARY CENTER FOR EARTHQUAKE ENGINEERING RESEARCH

A National Center of Excellence in Advanced Technology Applications

University at Buffalo, State University of New York
Red Jacket Quadrangle ■ Buffalo, New York 14261-0025
Phone: 716/645-3391 ■ Fax: 716/645-3399
E-mail: mceer@acsu.buffalo.edu ■ WWW Site: <http://mceer.buffalo.edu>



University at Buffalo *The State University of New York*

ISSN 1520-295X